

“I am among those who think that science has great beauty. A scientist in his laboratory is not only a technician: he is also a child placed before natural phenomena which impress him like a fairy tale.”

— *Marie Curie (1867—1934)*

He that spared not his own Son, but delivered him up for us all, how shall he not with him also freely give us all things?

Romans 8:32

University of Alberta

**Rhenium-Osmium Geochronology of Low-Level Sulfide Minerals from
Hydrothermal Ore Deposits - Applications, Limitations, and Implications**

by

Ryan Michael Morelli



A thesis submitted to the Faculty of Graduate Studies and Research
in partial fulfillment of the requirements for the degree of

Doctor of Philosophy

Department of Earth and Atmospheric Sciences

**Edmonton, Alberta
Spring 2008**



Library and
Archives Canada

Published Heritage
Branch

395 Wellington Street
Ottawa ON K1A 0N4
Canada

Bibliothèque et
Archives Canada

Direction du
Patrimoine de l'édition

395, rue Wellington
Ottawa ON K1A 0N4
Canada

Your file *Votre référence*
ISBN: 978-0-494-45571-5
Our file *Notre référence*
ISBN: 978-0-494-45571-5

NOTICE:

The author has granted a non-exclusive license allowing Library and Archives Canada to reproduce, publish, archive, preserve, conserve, communicate to the public by telecommunication or on the Internet, loan, distribute and sell theses worldwide, for commercial or non-commercial purposes, in microform, paper, electronic and/or any other formats.

The author retains copyright ownership and moral rights in this thesis. Neither the thesis nor substantial extracts from it may be printed or otherwise reproduced without the author's permission.

AVIS:

L'auteur a accordé une licence non exclusive permettant à la Bibliothèque et Archives Canada de reproduire, publier, archiver, sauvegarder, conserver, transmettre au public par télécommunication ou par l'Internet, prêter, distribuer et vendre des thèses partout dans le monde, à des fins commerciales ou autres, sur support microforme, papier, électronique et/ou autres formats.

L'auteur conserve la propriété du droit d'auteur et des droits moraux qui protègent cette thèse. Ni la thèse ni des extraits substantiels de celle-ci ne doivent être imprimés ou autrement reproduits sans son autorisation.

In compliance with the Canadian Privacy Act some supporting forms may have been removed from this thesis.

Conformément à la loi canadienne sur la protection de la vie privée, quelques formulaires secondaires ont été enlevés de cette thèse.

While these forms may be included in the document page count, their removal does not represent any loss of content from the thesis.

Bien que ces formulaires aient inclus dans la pagination, il n'y aura aucun contenu manquant.

■+■
Canada

Abstract

Rhenium-osmium geochronology of common sulfide minerals is a technique that offers a theoretical means of directly dating many hydrothermal ore deposits in Earth's crust. In practice, however, the successful application of this technique has historically been impeded by major analytical challenges. This PhD thesis utilizes recent analytical developments that, for the first time, permit precise and accurate isotopic measurements of the low concentrations of rhenium and osmium typical of most crustal sulfide minerals. The objective of this study is to further develop this technique for mainstream application, and to assess the strengths and limitations of the technique with different sulfide minerals. To accomplish this, measurement of rhenium-osmium isotopic compositions have been performed for common sulfide minerals, including arsenopyrite, pyrite, pyrrhotite, chalcopyrite, sphalerite, and gersdorffite, from multiple gold and base metal deposits in worldclass ore districts globally, and through geologic time. By comparison of determined rhenium-osmium results to existing geochronologic constraints for the deposits, and considering the thermal histories of the host terranes, a more comprehensive understanding of the utility of this technique has been achieved. The results of this study indicate that, using proper sampling, analytical, and data reduction protocols, both arsenopyrite and pyrite are very reliable chronometers of ore-forming hydrothermal events. Demonstrably accurate and relatively precise (better than 1.5%) rhenium-osmium mineralization ages have been determined for important orogenic gold deposits using arsenopyrite (Homestake, South Dakota; Muruntau, Uzbekistan) and for orogenic gold (Con, Northwest Territories) and volcanogenic massive sulfide (Trout Lake and Sherritt Gordon, Manitoba) deposits using pyrite. For these minerals, apparent

minimum closure temperatures of 400°C for arsenopyrite and possibly as high as 675°C for pyrite can be inferred. Both the rhenium-osmium mineralization ages and initial Os isotopic compositions of these sulfides can be used to provide crucial petrogenetic information regarding ore genesis. In contrast, spurious rhenium-osmium results from coexisting pyrrhotite and sphalerite demonstrate that these minerals are readily disturbed during low temperature, post-crystallization thermal events, and are poor choices for rhenium-osmium geochronology. Results for chalcopyrite from the Konuto Lake volcanogenic massive sulfide deposit, Saskatchewan, are less conclusive, but suggest that chalcopyrite rhenium-osmium isotopic compositions may be reset at metamorphic temperatures of less than ~ 500°C.

*This thesis is dedicated with love to my wife, Lia,
and to my sons, Vincent, Angelo, and Noel.
We did it together.*

Acknowledgements

Looking back on the past four and a half years, it is evident to me that there are many people without whom this PhD thesis could never have been completed, and then there are those few that it was completed in spite of. Now that the work is done, I am grateful to have this opportunity to acknowledge the former, and to forget the latter.

First and foremost, I thank my wonderful wife, Lia, and my three incredible sons, Vincent, Angelo, and Noel, for their unconditional love and support throughout my graduate studies and always. I am extremely blessed to have such a wonderful family, and am so thankful that we can share in this accomplishment together. I love you!!

I would like to express deepest gratitude to my supervisor, Dr. Robert Creaser, for giving me an opportunity to work with and learn from one of the best in the business. I am extremely fortunate to have worked with a scientist who not only strives to provide his students with the best possible academic foundation, but who also understands and provides support through the personal tribulations that go along with graduate student life. Though I would not have it any other way, raising a young family during the course of my MSc and PhD studies has been an especially challenging experience - there is absolutely no way Lia and I could have done it without the exemplary supervisory support I've received over the past six years. Thank you, Rob, for everything.

In retrospect, it can sometimes seem as if the successful completion of a PhD study involves an endless cycle of frustration, infrequently interrupted by 'blips' of promise and excitement that fuel motivation. Between these fleeting moments of renewed enthusiasm, the love and support of others was crucial for keeping me focused and for calming the day-to-day storms of life. For providing such a stable base of love and support, now and always, I thank my parents and my brother and sister - the comfort in knowing that there are people who are always there for you is indescribable, and I know how truly fortunate I am to have such a loving family. I am also blessed to have the Stolte family in my life; for your continued love, guidance, and encouragement, I am profoundly thankful.

My time at the U of A was enhanced by the wonderful EAS faculty, staff, and students. It has been a pleasure getting to know all of you, and each of you has positively affected my experience in some way. Though too numerous to mention in detail, there are a few people that are particularly deserving of acknowledgement. Thank you to the professors that have sat on my PhD committees, namely Larry Heaman, Sarah Gleeson, Martyn Unsworth, Tom Chacko, and Richard Tosdal (UBC), for your fairness and guidance. Martin Sharp, Bob Luth, Ed Jackson, and Philippe Erdmer are thanked for their proficient service as Graduate Studies Associate Chairs. Rob Stefaniuk, Diane Caird, Sergei Matveev, George Braybrook, Mark Labbe, and Don Resultay are gratefully acknowledged for providing technical expertise of various types. Kim Arndt, Kathy Sanderson, and Marsha Boyd provided valuable service as graduate program administrators over the course of my studies.

On a more personal note, there were many people in the department with whom I've had the privilege of becoming close friends with over the past few years. These include my lab RIF cohorts, past and present: Dave Selby, Tony Simonetti, Kelly Nixon, Stacey Hagen, Gayle Hatchard, Jaime Donnelly, Jason Cameron, Guangcheng Chen, and Judy Schultz. I would particularly like to thank my 'Re-Os colleague' and great friend,

Brian Kendall – we've been on this ride together from start to finish, and there's not another person I'd rather have along. I know you are destined for (and deserve) great things!! Apart from the lab, I was able to get to know so many terrific people – many undergrad students that added some excitement to things, fellow grad students that I could bounce ideas off of and unwind with at the end of a long week, and professors that provided some great perspective....thank you to all of you. To my closest friends – Trevor and Nicole MacHattie, Rajeev Nair, Yvon and Caroline Lemieux, Russell Hartlaub, Hilary Corlett, and Shannon and Steve Zurevinski – thank you for always being there for Lia and I. We are so happy and fortunate to have had the opportunity to get to know all of you, and are hopeful that we can remain great friends for many years to come.

There are several scientists around the world that directly contributed in some capacity to the success of my PhD work. In no particular order, these include Reimar Seltmann, Fin Stuart, Hendrick Falck, Scott Cairns, Andreas Mueller, Gary Beakhouse, Chris Bell, Christian Böhm, Kelly Gilmore, Al Bailes, Trosten Graupner, Andrew Locock, and staff members at the Royal Ontario Museum. It was also a great pleasure to get to know Holly Stein, Judith Hannah, Aaron Zimmerman, Richard Markey, and Juliana Charão Marques, on both a professional and personal basis, through their visits to the U of A and encounters at various conferences.

Several organizations provided financial support to my graduate work, and are gratefully acknowledged. These include NSERC, Alberta Ingenuity, the University of Alberta, the U of A Department of Earth and Atmospheric Sciences, the U of A Institute for Geophysical Research, the U of A Faculty of Graduate Studies, and Research, and the Society of Economic Geologists. Completion of my PhD research would not have been possible without this support. I would especially like to thank the Hibbs and Cumming families for establishing scholarships in memory of Dr. Roy Dean Hibbs and Dr. George L. Cumming, respectively. I was fortunate to receive each of these awards during the course of my graduate studies, and truly appreciate these honours.

I would like to thank Bill Nickerson, Dr. John Rosie, and Dr. Laura Leclaire, as well as Rhian and Diane Thornhill, for helping my family and I get through some difficult times over the past year. Finally, I would like to thank Gary Delaney and the geologists and staff at Saskatchewan Energy and Resources for their support as I begin the next chapter of my life.....

Table of Contents

Chapter 1: Introduction	1
1.1. Background.....	1
1.2. The Re-Os System: History and Applications.....	3
1.3. Traditional Methods for Dating Ore Formation.....	4
1.4. Re-Os Geochronology of Molybdenite.....	8
1.5. Re-Os Geochronology of Low-Level Sulfide Minerals: What We Know	10
1.6. Objectives of This Study.....	12
1.7. References.....	14
Chapter 2: Analytical Considerations and Methodology.....	23
2.1. Analytical Challenges Inherent to the Re-Os system	23
2.2. Re-Os Sampling Protocol	27
2.3. Re-Os Analytical Protocol	29
2.4. Re-Os Procedural Blanks.....	33
2.5. Re-Os Spike Solutions and Low-Level Sulfides	35
2.6. Error Propagation for Re-Os Analyses of Low-Level Sulfides	36
2.7. Conclusions.....	38
2.8. References.....	39
Chapter 3: Re-Os Low Level Sulfide Geochronology of Archean Orogenic Gold Deposits: A Feasibility Study	44
3.1. Introduction.....	44
3.2. Deposit Geology and Age Constraints on Mineralization.....	46
3.3 Sampling and Mineral Separation.....	54
3.4 Results.....	57
3.5. Discussion.....	61
3.6 Conclusions.....	75
3.7. References.....	76
Chapter 4: Re-Os Sulfide Geochronology of Post-Archean Orogenic Gold Deposits, and Implications for Deposit Genesis:	85
4.1 Re-Os geochronology of arsenopyrite and pyrrhotite - a case study from the Paleoproterozoic Homestake Orogenic Au deposit, Black Hills, South Dakota 	85
4.1.1. Introduction.....	85
4.1.2. Regional and Deposit Geology	86
4.1.3. Proposed Models for and Timing of Gold Mineralization.....	91
4.1.4. Sample Locality and Description.....	93
4.1.5. Sample Separation and Analytical Procedures	94
4.1.6. Results.....	96
4.1.7. Discussion.....	101
4.1.8. References.....	116

4.2 Age and source constraints for the giant Muruntau gold deposit, Uzbekistan, from coupled Re-Os-He isotopes in arsenopyrite	122
4.2.1. Introduction.....	122
4.2.2. Kal'makyr and Muruntau: Geology and Existing Geochronology.....	124
4.2.3. Re-Os Results.....	129
4.2.4. Discussion.....	135
4.2.5. References.....	154
4.3 Conclusions.....	163
Chapter 5: Generation of a World Class Volcanogenic Massive Sulfide Camp: Constraints from Re-Os Geochronology of Paleoproterotic Sulfides of the Flin Flon and Kisseynew Domains, Trans-Hudson Orogen	166
5.1. Introduction.....	166
5.2. Geology.....	167
5.3. Sampling Protocol.....	172
5.4. Results.....	174
5.5. Discussion.....	182
5.6. Conclusions.....	192
5.7. References.....	193
Chapter 6: Thesis Conclusions	201
Appendix 1: Thesis Collection List.....	208

List of Tables

Table 2.1 Re-Os data showing possible effects of drill bit contamination on the composition of Muruntau arsenopyrite sample 9824.....	30
Table 3.1 Re-Os data for sulfides from select Archean orogenic gold deposits	58
Table 4.1.1 Re-Os isotopic data for Homestake arsenopyrite and pyrrhotite	99
Table 4.1.2 U-Pb isotopic data for Harney Peak granite monazite	102
Table 4.2.1 Re-Os isotopic data for Kal'makyr molybdenite.....	130
Table 4.2.2 Re-Os and He isotopic data for Muruntau arsenopyrite.....	132
Table 4.2.3 Existing Os isotopic data for sulfides from orogenic gold deposits.....	143
Table 4.2.4 Rare earth element data for arsenopyrite/pyrite from Muruntau and other orogenic gold deposits worldwide	150
Table 5.1 Re-Os isotopic data for VMS-hosted sulfides in the northern Trans-Hudson Orogen.....	176

List of Figures:

Figure 2.1: Isochron diagram showing effects of drill bit contamination on arsenopyrite Re-Os compositions	31
Figure 3.1: Location of sampled Archean orogenic gold deposits	47
Figure 3.2 Geology of the Uchi Subprovince, Ontario, with location of the Red Lake gold deposit.....	49
Figure 3.3 General geology of the Eastern Goldfields, Australia, with location of the Golden Mile gold deposit	51
Figure 3.4 General geology of the Yellowknife greenstone belt, Northwest Territories, with location of the Con gold deposit	53
Figure 3.5 Photomicrographs of Archean sulfide samples used for Re-Os isotopic analysis.....	56
Figure 3.6 Results of linear regression of Re-Os analyses of Red Lake arsenopyrite and gersdorffite	59
Figure 3.7 Results of linear regression of Re-Os analyses of Golden Mile arsenopyrite	60
Figure 3.8 Re-Os pyrite isochron from the Con Deposit	62
Figure 3.9 Re concentration of orogenic gold deposit-derived arsenopyrite and pyrite through time	64
Figure 3.10 Chronological evolution of the Yellowknife greenstone belt, with proposed models for orogenic gold mineralization.	73
Figure 4.1.1 General geology of the Black Hills Uplift.....	88
Figure 4.1.2 Geology of the Lead window.....	90
Figure 4.1.3 Cross section of the Homestake deposit	92
Figure 4.1.4 Photo/photomicrograph of Homestake sulfide sample HMO20.....	95
Figure 4.1.5 Photomicrograph of Harney Peak granite monazite samples	97
Figure 4.1.6 Re-Os arsenopyrite, pyrrhotite isochron diagrams	100
Figure 4.1.7 U-Pb isotopic data from laser ablation analyses of monazite from the Harney Peak granite	103

Figure 4.1.8 Photomicrograph of Homestake sulfide sample HMO20.....	109
Figure 4.1.9 Magmatic zoning in monazite crystal 9B-1.....	111
Figure 4.1.10 Electron microprobe photomicrographs of Harney Peak granite monazite sample 9B-3.....	113
Figure 4.2.1 Subdivisions of the Tien Shan Orogen, with deposit locations.....	123
Figure 4.2.2 Geology of the Kal'makyr deposit, Middle Tien Shan Orogen, Uzbekistan.....	125
Figure 4.2.3 Geology of the Muruntau gold deposit.....	127
Figure 4.2.4 Re-Os isochron for Kal'makyr molybdenite.....	131
Figure 4.2.5 Re-Os isochrons for Muruntau arsenopyrite.....	134
Figure 4.2.6 Comparison of Re-Os arsenopyrite isochron ages to existing ages for Muruntau gold mineralization.....	137
Figure 4.2.7 Comparison of Os_i from arsenopyrite to terrestrial Os reservoirs that may have contributed Os to the Muruntau hydrothermal system.....	139
Figure 4.2.8 Evolution of Os isotopic compositions in potential metal source reservoirs to orogenic gold deposits over time.....	145
Figure 4.2.9 Schematic cross section of an active continental margin showing possible fluid/metal sources.....	148
Figure 4.2.10 Chondrite-normalized rare earth element patterns for sulfides from Muruntau and other global examples of orogenic gold deposits.....	152
Figure 4.2.11 Chondrite-normalized rare earth element ratios for sulfides from Muruntau and other global examples of orogenic gold deposits.....	153
Figure 5.1 Lithotectonic Domains of the Reindeer Zone, with detailed geology of the Flin Flon and Kiseynew Domains.....	168
Figure 5.2 Sample photos of sulfides used for Re-Os analysis in this study.....	175
Figure 5.3 Regression of Re-Os isotopic data from Trout Lake sulfides.....	178
Figure 5.4 Results of linear regression of Re-Os isotopic analyses of Konuto Lake chalcopyrite.....	179

Figure 5.5 Linear regression of Re-Os isotopic analyses of pyrite from the Harmin deposit.....	180
Figure 5.6 Re-Os isochron from analyses of the Sherritt Gordon deposit.....	181
Figure 5.7 Synthesis of Re-Os sulfide geochronology for VMS mineralization at the Trout Lake, Konuto Lake, Harmin, and Sherritt Gordon deposits, with reference to existing geochronology in the Flin Flon and Kisseynew Domains	187

List of Symbols/Abbreviations

A = amps

a = annum (year)

atm = atmospheres

b.y. = billion years

cm = centimetres

eV = electron volts

fg = femtograms

Fm = formation

fmol = femtomoles

g/t = grams/metric ton (tonne)

Ga = giga annum (billions of years before present)

Gt = billion tonnes

ID-TIMS = isotope dilution – thermal ionization mass spectrometry

kbar = kilobars

kg = kilograms

km = kilometers

kV = kilovolts

L = litres

LLHR = low-level highly radiogenic

m = metres

Ma = mega annum (millions of years before present)

mg = milligrams

ml = millilitres

mm = millimeters

Moz = million ounces

ms = milliseconds

MSWD = Mean Square of Weighted Deviates

m.y. = million years

N = normal (weight of solute per litre of solution; g/dm^3)

ng = nanograms

NTIMS = negative thermal ionization mass spectrometry

OGD = orogenic gold deposit

$^{187}\text{Os}^*$ = radiogenic osmium (i.e. produced by *in situ* radioactive decay of ^{187}Os)

Os_i = initial $^{187}\text{Os}/^{188}\text{Os}$ ratio

Os_{IC} = blank $^{187}\text{Os}/^{188}\text{Os}$ composition

P = pressure

pg = picograms

ppb = parts per billion (ng/g)

ppm = parts per million ($\mu\text{g}/\text{g}$)

ppt = parts per trillion (pg/g)

REE = rare earth elements

s = seconds

σ (sigma) = standard deviation

SE = standard error

SHRIMP = Sensitive High Resolution Ion Microprobe

t = (tonnes), metric tons

T = temperature

THO = Trans-Hudson Orogen

μl = microlitres

μm = micrometres / microns

VMS = volcanogenic massive sulfide deposit

1. Introduction

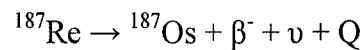
1.1. Background

In the early 1900's, Ernest Rutherford made the first age determination on a natural specimen using radioactive isotopes (see Dalrymple, 2004). Though the methodology was crude and the determined age highly inaccurate, this development would prove to be a revolutionary development in the Earth sciences. Since this first measurement, the ability of scientists to measure the absolute ages of rocks and minerals through isotopic analysis has arguably become the most powerful analytical tool available for advancing our understanding of Earth history. There are several decay systems in common usage, all based on the radioactive decay of a parent isotope within a mineral to a stable daughter product (e.g. ^{238}U - ^{206}Pb and ^{235}U - ^{207}Pb , ^{87}Rb - ^{87}Sr , ^{40}K - ^{40}Ar / ^{40}Ca , ^{147}Sm - ^{143}Nd , ^{176}Lu - ^{176}Hf). To be an effective chronometer, any individual technique must meet a specific set of criteria (Faure, 1991). These include: (a) certainty that the measured parent isotopic composition of the mineral reflects that which was present during crystallization of the mineral, and that the isotopic composition of the daughter reflect changes due only to radioactive decay (i.e. no fractionation of isotopes during mineral crystallization), (b) confidence that the parent and daughter isotopic composition have remained undisturbed since the event which is being dated (c) precise determination of the system half-life, (d) accurate analytical data, and (e) assurance that the measured isotopic compositions did not result from mixing of multiple sources.

In recent history, geochronologic techniques that meet these criteria have been used to determine the absolute timing of a diversity of geologic events, ranging from the origin of extra-terrestrial bodies, to terrestrial magmatism, metamorphism, and deformation, and even to processes as discrete as biologically induced carbonate precipitation. Despite the overall success of geochronology as a field, some significant geologic events remain 'undateable' using common techniques. Such shortcomings are mainly a consequence of the physical properties of the parent isotope, in that partitioning of these elements into specific rocks and minerals is dictated by the atomic characteristics of the parent element. The preponderance of conventionally used radioisotope systems are characterized by parents with a strong affinity for oxygen (i.e. are 'lithophile' elements), which therefore segregate preferentially into silicate mineral phases upon high

temperature differentiation of the Earth. Although clearly advantageous when considering the dominance of silicate minerals in the Earth's mantle and crust, this trait is also the source of our inability to date mantle and crustal processes involving non-lithophile elements and/or low temperature processes.

Over the past half-century, intermittent effort was directed towards analytical development of the rhenium-osmium (Re-Os) system, with the hope that it could address these deficiencies. This technique is based on the spontaneous beta decay of radioactive ^{187}Re to stable ^{187}Os over a half-life of ~ 42 b.y., according to the reaction:



where β^- is a beta particle, ν is an antineutrino, and Q is released energy. The Re-Os system has been specifically targeted for such applications due to the unique geochemical properties of both the parent and daughter isotopes compared to the other commonly used systems. Re is a transition metal that has a strong affinity for Fe (i.e. it is 'siderophile'), whereas Os is a platinum group element (PGE) with a strong affinity for Fe and S (i.e. is 'siderophile-chalcophile'). These characteristics require that both elements partition preferentially from magmas and fluids into crystallizing metal alloys or sulfide minerals. Consequently, both Re and Os were largely sequestered into the core during primordial differentiation of the Earth, resulting in generally low concentrations of Re and Os in both the mantle and crust. Furthermore, both elements are known to be highly sensitive to redox conditions during surficial processes, and will partition into organic matter (i.e. are 'organophile') deposited under strongly reducing conditions. In combination, these characteristics theoretically allow the application of the Re-Os chronometer to specific geochronologic problems that can not be investigated by other chronometers.

Another important characteristic of the Re-Os system is the relative difference in the compatibilities of the parent and daughter elements in mantle minerals, and their consequent fractionation during mantle partial melting and magma producing events. Os is very compatible in the structures of important mantle phases (e.g. sulfide minerals, metal alloys, chromite, olivine) compared to Re, which is incompatible in these components. Significant Re-Os fractionation occurs during partial melting of the mantle,

with Re being concentrated in the melt phase and Os remaining in the residue. Consequently, the Os isotopic evolution of mantle and crustal reservoirs evolve at greatly different rates, and this characteristic makes the Re-Os system an extremely sensitive tracer of relative crustal and mantle inputs during generation of a mineral or rock. This information is preserved as the initial Os isotope ratio (Os_i) from the y-intercept value of an $^{187}Re/^{188}Os$ vs. $^{187}Os/^{188}Os$ isochron diagram.

1.2. The Re-Os System: History and Applications

Despite the enormous potential of the Re-Os technique for both age and source determination of an exclusive group of rocks and minerals, its practical use was hindered for decades by a unique set of analytical obstacles (see Chapter 2). These factors prevented the widespread use of the Re-Os system as a geological dating or tracing tool for most of the 20th century, and limited its utility to studies of natural specimens with very high Re and Os concentrations that did not require sensitive measurement techniques. This was the case until the mid 1990's, when newly developed analytical techniques eliminated some of these problems. Important advances included an improved knowledge of the ^{187}Re decay constant (Smoliar et al., 1996; Selby et al. 2007), recognition that sensitive Re and Os isotopic analysis could be performed through generation of negative ion beams in a conventional thermal ionization mass spectrometer (Creaser et al., 1991; Völkening et al., 1991) and use of an alternative sample dissolution techniques utilizing a sealed glass vessel (Creaser et al., 1993; Shirey and Walker, 1995). These developments together initiated a resurgence of investigation into the applications of the Re-Os radioisotope system by a select number of research groups globally, and it was soon evident that this 'new' technique held potential to revolutionize our understanding of many geologic processes.

Since the mid-1990's, Re-Os geochronology has been successfully applied to diverse geological problems that reflect the unique geochemical properties of the system, including dating of iron meteorites (e.g. Shen et al., 1996; Smoliar et al., 1996), mantle xenoliths (e.g. Pearson et al., 1995), diamond-hosted sulfide inclusions (e.g. Pearson et al., 1998), organic-rich sedimentary rocks (e.g. Cohen et al., 1999; Creaser et al., 2002; Kendall et al., 2004), and emplacement of hydrocarbons (Selby and Creaser, 2005).

Additionally, Os isotopic compositions of various materials have been used to geochemically trace such events as the evolution of the solar system (Walker et al., 2002), terrestrial differentiation (Brandon et al., 2003), mantle evolution (Meisel et al., 1999; Bennett et al., 2002), meteorite impact events (Hart et al., 2002), and seawater evolution (Peucker-Ehrenbrink et al., 1995).

Another promising application of the Re-Os system, and the focus of this study, is geochronology of ore deposit formation by Re-Os dating of sulfide minerals. The inability to directly date ore forming-events is a long-standing problem for understanding ore genesis, and stems largely from the paucity of minerals in ore deposits that are datable using conventional, silicate-based chronometers that are also demonstrably cogenetic with the ore. This impediment restricts comprehensive genetic modeling of the ore-forming processes, and can lead to misunderstanding of the true ore-forming event(s) in some cases. Re-Os sulfide geochronology is a technique that promises to permanently circumvent this problem, since sulfide minerals typically either have a direct cogenetic origin with ore, or constitute the ore itself.

1.3. Traditional Methods for Dating Ore Formation

The formation of different types of ore deposits through time reflects an intrinsic link with terrestrial crustal evolution, resulting from the operation of specific tectonic events at particular times during a Wilson cycle (i.e. the tectonic stages during the lifespan of an ocean basin). This phenomenon, recognizable from at least the Neoproterozoic (~2700 Ma), is demonstrated by the observed association between temporal distributions of specific ore deposit types with rocks produced in specific geodynamic settings (Barley and Groves, 1992; Kerrich et al., 2000; Groves et al., 2005). Put another way, the temporal distribution of several ore deposit types throughout much of Earth history was controlled by the period of the supercontinent cycle during which they formed.

The hypothesized link between tectonism and ore deposition makes the ability to routinely date ore deposit formation an important development, the implications of which are far reaching from both an academic and economic point of view. This would definitively clarify models for ore-deposit formation by providing an unambiguous temporal link between the timing of ore generation to specific geologic events. Further,

for deposit types with a known origin, age determination of ore will also serve to date the tectonothermal event (e.g. magmatism, metamorphism, etc.) that caused its development, and temporally constrain the tectonic history of the host terrane. From an economic perspective, dating of ore provides an important exploration criterion, as potential host rocks and appropriate structures can be more accurately targeted

Interestingly, one of Rutherford's first attempts at geochronology was performed on the uranium-rich ore mineral, uraninite (UO_2), due to its high uranium concentrations and consequent ease of measurement. However, the ability to directly date ore minerals has been an unusual circumstance, and ore deposit chronology has traditionally relied on age determination of rocks showing specific crosscutting relationships with ore, or dating of hydrothermal 'gangue' minerals (i.e. non-metallic minerals interpreted to be cogenetic with the ore). Dating of rocks that crosscut or are crosscut by ore can often provide accurate age brackets for the timing of mineralization, but minimum and maximum ages determined in this manner may not precisely resolve deposit genesis. Geochronology of gangue minerals can be an effective technique, but is limited by the confidence with which a cogenetic relationship to the ore itself can be established, and by the robustness of the chronometer itself under hydrothermal conditions. Richards and Noble (1998) provide a comprehensive review of techniques applicable to ore deposit geochronology, and a brief discussion is provided below.

A popular method for dating formation of ore deposits has been the K-Ar (and variant $^{40}\text{Ar}/^{39}\text{Ar}$) technique, specifically using hydrothermal muscovite and biotite. Despite its widespread use, this technique has significant drawbacks for use as an ore chronometer. Consideration of temperature and/or pressure conditions of the deposit and its host rocks during and after its formation is critical when using the K-Ar mica technique because the Ar daughter product can diffuse readily from some minerals. The result of this is a relatively low closure temperature for the K-Ar / Ar-Ar chronometers ($\sim 300^\circ\text{C}$ for biotite, $\sim 350^\circ\text{C}$ for muscovite), a fundamental limitation of this technique for use with many ore deposits. This restriction is evident from studies in which the Ar-Ar mica chronometer yields erroneously young mineralization ages for higher temperature ore-forming events that have reasonably well-bracketed ages derived from more robust chronometers (e.g. Homestake deposit, Dahl et al., 1999).

The Rb-Sr and Sm-Nd systems have also received attention as ore deposit chronometers. Rb-Sr dating of combinations of hydrothermal minerals, including mica, amphibole, carbonate, sulfate, and fluorite, has been attempted due to the large ranges in Rb/Sr ratios of the different minerals, resulting in sufficient spread along the constructed isochron. Another novel approach has been Rb-Sr dating of fluid inclusions and their host minerals, including quartz, sphalerite, and pyrite (e.g. Shepherd and Darbyshire, 1981; Christensen et al., 1995; Pettke and Diamond, 1996). Likewise, Sm-Nd geochronology of hydrothermal fluoride, tungstate, and U-Th-bearing oxide minerals is theoretically feasible due to the characteristically elevated rare earth element concentrations in these minerals. In practice, however, the utility of both systems for dating ore events has been limited, at best, due to the imprecision of calculated ages, uncertain paragenetic relationships between dated and ore minerals, and mobility issues. In short, Rb-Sr and Sm-Nd dating of hydrothermal minerals has not received widespread acceptance as a reliable technique for dating ore-forming events.

An emerging technique that shows good potential for yielding reliable ore mineralization ages is U-Th-Pb dating of hydrothermal silicate and phosphate minerals (Vielreicher et al., 2003). These U-Th-Pb chronometers, including zircon (ZrSiO_4), monazite ((Ce, La, Th) PO_4), and xenotime (YPO_4), can be analyzed by either *in situ* SHRIMP or conventional ID-TIMS techniques and appear promising because of their relatively high closure temperatures, estimated to exceed 600°C. However, like other techniques based on non-metallic minerals, this method carries the disadvantage of utilizing minerals that can have an ambiguous relationship to ore minerals. Other problems have also prevented the mainstream application of this technique, such as the paucity of required mineral phases in many hydrothermal ore deposits, low U concentrations, uncertainty of initial Pb compositions, excess ^{206}Pb in some monazites, and/or the potential of isotopic resetting of fine-grained monazite and (possibly) xenotime at temperatures > 400°C due to dissolution and recrystallization (Teufel and Heinrich, 1997). Unsatisfactory resolution of these complications is apparent in some preliminary applications of these chronometers, for which significantly different U-Pb ages were determined for 'cogenetic' zircon and monazite taken from the same

hydrothermal gold deposits in northern Australia (cf. Şener et al., 2005, and Rasmussen et al., 2006).

The U-Pb radioisotope system, based on the decay of ^{235}U to ^{207}Pb and ^{238}U to ^{206}Pb , has also been used to investigate the age of ore deposits. Analysis of uranium-rich ore minerals (e.g. uraninite; UO_2) can directly yield concordant U-Pb ages or discordant upper intercept ages, due to the high concentrations of radiogenic Pb and negligible common Pb contents (e.g. Richards et al., 1988). Minerals that meet these criteria are, unfortunately, rare in the majority of ore deposit types, and the technique is therefore not commonly used for ore deposit dating.

The U-Pb technique is more commonly applied to dating of ore-related minerals through 'common Pb' isotopic techniques. Such techniques are based on knowledge of the Pb isotopic evolution of the geochemical reservoir(s) from which the ore-forming system was isolated. Assuming that the Pb isotopic composition of an ore system is known at the time of formation (i.e. using established Pb isotopic growth models; e.g. Stacey and Kramers (1975) two-stage model), then the present-day Pb isotopic composition of Pb-rich, U-deficient ore minerals (e.g. galena; PbS) can be related to a unique composition along the growth curve that corresponds to a hypothetical mineralization age. This technique is referred to as Pb Model Age determination. If other cogenetic sulfide minerals are present that do contain small amounts of U, 'secondary Pb-Pb isochron' construction is possible, whereby the growth of radiogenic ^{207}Pb and ^{206}Pb is recorded by the slope of the line that connects the points along the isochron to the 'initial' Pb isotopic composition of the ore system, as recorded in the galena. Spread along the isochron can be generated either through analysis of different ore minerals characterized by different U/Pb ratios or, in the absence of these components, by measurement of sequential leachates from individual minerals (e.g. Cummings et al., 1982; Richards et al., 1988; Frei and Pettke, 1996). The upside of common Pb dating techniques for ore deposit dating is that, because Pb is a chalcophile element, isotopic analyses and age calculations can be performed directly on ore-related sulfide minerals. However, though conceptually sound, this technique suffers from its own set of limitations, including the potential for mobility of Pb, and isotopic mixing of Pb in analyzed minerals from

multiple sources. Such factors would lead to the determination of erroneous and imprecise Pb-Pb ages for ore mineralization.

It is clear from the preceding discussion that no technique is currently capable of routinely providing reliable dates for hydrothermal ore mineralization. This explains the anticipation of economic geologists for development of the Re-Os technique, due to its potential for providing a robust technique for dating sulfide minerals with a direct cogenetic relationship to ore in most deposit types. As previously discussed, however, the use of this technique has long been hampered by analytical obstacles, and has only recently been developed to a point where its overall utility can be meaningfully assessed.

1.4. Re-Os Geochronology of Molybdenite

Initial attempts at Re-Os geochronology of crustal sulfide minerals focused on the mineral molybdenite (MoS_2), due to the high (ppm to percent) Re contents of this mineral, resulting from the similar geochemical behaviour of Re and Mo in hydrothermal fluids. Molybdenite is an extremely useful chronometer because the amount of common Os incorporated into the mineral at formation is negligible relative to the proportion of Os produced strictly by decay of ^{187}Re (i.e. $^{187}\text{Os}^*$). This means that all molybdenite is characterized by extremely high Re/Os ratios, and thus yield Re-Os Model Ages from a single analysis that assume no initial Os in the sample. This eliminates the need for isochron construction, requiring only knowledge of the present day (PD) ^{187}Re and ^{187}Os contents:

$$^{187}\text{O}_{\text{SPD}} = ^{187}\text{Re}_{\text{PD}} * (e^{\lambda t} - 1)$$

where λ = the ^{187}Re decay constant and t = time since formation of the molybdenite. A comprehensive overview of the utility and history of the Re-Os molybdenite chronometer is provided by Stein et al. (1998a) and Stein et al. (2001); some of the more important points are discussed below.

The first documented attempt at Re-Os isotopic analysis of molybdenite was by Hirt et al. (1963), who performed isotopic analysis of OsO_4 from several molybdenites by gas source mass spectrometry in order to constrain the half-life of the ^{187}Re - ^{187}Os decay

system. This study, of limited success due to analytical issues, remained the only attempt at molybdenite geochronology until the early 1980's, when Luck and Allegre (1982) explored Re-Os geochronology of Precambrian molybdenites by secondary ionization mass spectrometry (SIMS). They achieved reasonable levels of precision, and calculated Model Ages for some molybdenites that were consistent with age constraints on mineralization provided by other techniques. However, other molybdenites yielded geologically impossible (> 4.5 Ga) Re-Os ages. The authors attributed this to susceptibility of the Re-Os molybdenite chronometer to isotopic disturbance by post-crystallization metamorphic and/or hydrothermal affects.

Other research groups reached a similar conclusion over the next 10 – 15 years (e.g. Ishihara et al., 1989; McCandless et al., 1993; Santosh et al., 1994; Suzuki et al., 1996), leading to the widespread belief that the chronometer was readily disturbed by metamorphic, hydrothermal, and/or supergene processes, and was largely unreliable. This conclusion was ultimately challenged by subsequent studies that obtained demonstrably accurate Re-Os molybdenite ages (Stein et al., 1997, 1998a; Selby and Creaser, 2001a, 2001b; Selby et al., 2002), and conclusively showed that intracrystal decoupling of Re and Os in molybdenite could explain the anomalous ages determined in previous studies (Stein et al., 1998a, 2003; Selby and Creaser, 2004). The result of these studies is that, through employment of a stringent sampling and analytical protocol, the Re-Os molybdenite chronometer can be extremely reliable, even surviving intense deformation and granulite facies metamorphism (Bingen and Stein, 2003).

The Re-Os molybdenite chronometer is now more widely accepted as a reliable and robust option for dating hydrothermal ore mineralization. Although this represents a major advancement for ore-deposit studies, particularly those on porphyry intrusion-related deposits in which molybdenite is a common mineral, the paucity of molybdenite in most mineral deposits limits the application of the technique. This limitation provides the impetus for investigation of Re-Os geochronology in other sulfide minerals with a more common occurrence in ore deposits. However, such sulfide minerals are characterized by much lower Re (and $^{187}\text{Os}^*$) concentrations than molybdenite, making analysis of these 'low-level' sulfides (Stein et al., 2000) a much more challenging endeavor and requiring more rigorous scrutiny of analytical protocols and generated data.

1.5. Re-Os Geochronology of Low-Level Sulfide Minerals: What We Know

Preliminary studies attempting to date hydrothermal ore mineralization using the Re-Os low-level sulfide technique first appeared in the late 1990's, and it was immediately evident that the application was not straightforward. In one of the earliest examples, Freydier et al. (1997) analyzed the Re-Os isotopic compositions of pyrite (FeS_2), chalcopyrite (CuFeS_2), sphalerite (ZnS), and bornite (Cu_5FeS_4) from a base metal porphyry deposit in Chile. The sulfides contained very low Re contents (mainly < 5 ppb) but detectable common Os contents, resulting in much lower Re/Os ratios than molybdenite. The detection of common Os in the samples required construction of a Re-Os isochron, so that the initial Os isotopic compositions of the sulfides could be accounted for according to the linear equation:

$$\left(\frac{{}^{187}\text{Os}}{{}^{188}\text{Os}}\right)_M = \left(\frac{{}^{187}\text{Os}}{{}^{188}\text{Os}}\right)_I + \left(\frac{{}^{187}\text{Re}}{{}^{188}\text{Os}}\right)_M (e^{\lambda t} - 1)$$

where M indicates a measured isotopic ratio, I indicates the initial ${}^{187}\text{Os}/{}^{188}\text{Os}$ ratio (Os_i), λ = the ${}^{187}\text{Re}$ decay constant, and t = time.

The conclusion of this study, based on poorly defined Re-Os 'errorchrons' and their y-intercept values (i.e. Os_i), was the inferred definition of a Re-Os mineralization age of between 90 – 100 Ma and recognition of a mantle Os source for the deposit. The unconvincing results of this study served primarily to reveal the infancy of the technique. Interestingly, a coauthor of this paper interpreted a predominately crustal Os source for the deposit using the same data (Ruiz et al., 1997).

Stein et al. (1998b) also had limited success in producing meaningful Re-Os mineralization ages through the combined analysis of cogenetic molybdenite and pyrite from two Archean Au-Mo prospects in Finland. Although molybdenite produced a Re-Os mineralization age of ca. 2780 Ma, three pyrite Re-Os analyses yielded widely variable and imprecise Model Ages ranging between 2710 and 2830 Ma, and a 3-point ${}^{187}\text{Re}$ – ${}^{187}\text{Os}$ 'isochron' of ca. 2607 Ma. Although the authors did not report common Os contents and were not explicit as to how the pyrite Model Ages were calculated, they

provided bold interpretations of the significance of the pyrite Re-Os data. They concluded that the 2780 Ma molybdenite Re-Os age recorded the timing of molybdenite and pyrite growth, whereas millimeter-scale resetting of the Re-Os pyrite chronometer occurred due to a ca. 2650 Ma metamorphic event.

A seminal paper on low-level Re-Os sulfide geochronology was published shortly thereafter by the same research group (Stein et al., 2000), which provided a thorough description of the Re-Os isotopic systematics of, and appropriate data treatment for, such sulfides. The term ‘low-level highly radiogenic’ (LLHR) sulfides was coined to describe the observation that the Re-Os isotopic compositions of many sulfide minerals, presumed to be crustally-derived, were similar to that characteristic of molybdenite, but at much lower concentrations. The main finding was that Model Age calculation was deemed appropriate for any sulfide mineral with a $^{187}\text{Re}/^{188}\text{Os}$ ratio $> \sim 5000$, with the assumption that common Os present in the mineral is effectively negligible. The authors also stressed the significance of the highly correlated errors inherent to LLHR samples that result from the large uncertainty in the measurement of (predominantly blank) ^{188}Os , which is the denominator on both axes of the traditional $^{187}\text{Re}/^{188}\text{Os}$ vs. $^{187}\text{Os}/^{188}\text{Os}$ isochron diagram. To avoid these highly correlated uncertainties, Stein et al. (2000) suggest plotting ^{187}Re vs. $^{187}\text{Os}^*$ concentrations of each sample for definition of an isochron. They applied these criteria to LLHR pyrite samples from the Harnäs gold deposit, Sweden, to determine the timing of gold mineralization. The pyrite Re and $^{187}\text{Os}^*$ contents ranged between 1 – 5 ppb and 12 – 35 ppt respectively, with common Os contents as low as 2 - 3 ppt for some samples. The pyrite analyses yielded two distinct mean Model Ages: one at ca. 998 ± 23 Ma (5 analyses of 3 samples), and another at 616 ± 40 Ma (4 analyses of 1 sample). Linear regression of these two groups of analyses yielded two broadly corresponding ^{187}Re vs. ^{187}Os isochron ages, interpreted to reflect two separate mineralizing events. This interpretation is difficult to critically assess, however, due to a lack of reliable independent geochronological constraints for gold mineralization in the region.

Another early application of the Re-Os low-level sulfide technique studied the gold ores of the Witwatersrand basin, southern Africa (Kirk et al., 2001, 2002). These two studies report analyses of both pyrite and gold from one of the deposits in the basin (Vaal Reef), and determined both traditional Re-Os isochron ages and Re-Os model ages

from these data. The Model Ages, termed 'rhenium depletion ages' (T_{RD}), are calculated based on the assumed depletion of Re in the sample upon its segregation from the mantle and is determined from the point of the intersection between a line with a horizontal trajectory from the sample with a calculated mantle Os evolution curve on a plot of $^{187}\text{Os}/^{188}\text{Os}$ vs. time (see Shirey and Walker, 1998). The calculated Vaal Reef pyrite and gold Model Ages ranged from 2.9 to 3.5 Ga, in relatively good agreement with the determined Model 1 isochron age of ~ 3016 Ma for combined pyrite ($n = 3$) and gold ($n = 5$). Based on these data, an Os_i of ~ 0.1079 was also defined. A long-standing controversy on the origin of the Witwatersrand ore is whether it had a hydrothermal origin at ca. 2.7 to 2.4 Ga, or whether it has a placer origin, physically transported from an older source terrane with an assumed age of > 2.9 Ga. According to the authors, these new Re-Os ages and Os_i effectively resolved this century-old debate by showing that the ore formed at ca. 3.0 Ga during a major crust-forming event, and therefore must have been transported to the basin as detritus. These studies are widely cited as conclusive evidence by proponents of the detrital model for ore formation; however, in detail interpretation of the Re-Os data is not straightforward due to issues that will be addressed in this study.

1.6. Objectives of This Study

Although not a comprehensive account of all published Re-Os dating and tracing studies on low level sulfides to date, the above discussion provides an indication of the current status of the technique. The determination of Model 1¹ Re-Os isochron ages, Model Ages, and/or initial Os ratios by some researchers is encouraging, but there clearly exists an insufficient understanding among specialists of the actual utility of the technique in terms of its overall reliability. This is a result of several factors, including (i) nonstandardization of interlaboratory analytical methodologies and treatment of uncertainties, (ii) an absence of studies demonstrating the accuracy of the technique in comparison to independent age constraints from reliable chronometers, and (iii) a lack of knowledge of the blocking temperatures of the different low level sulfide minerals, as well as gold.

¹ from the algorithm of York (1968), assumes that the assigned errors are the only reason for scattering of data points from the straight regression line.

With these inadequacies in mind, the primary goal of this PhD study is to answer the question: “*Can the Re-Os low-level sulfide technique routinely yield accurate and precise mineralization ages for hydrothermal ore deposits*”? Further goals are to better understand limitations of the technique by determining the usefulness of individual sulfide minerals as Re-Os chronometers, to constrain the effective closure temperatures of various sulfide minerals, and to investigate any temporal limitations of the technique, as well as advancing analytical methodologies.

This study specifically focuses on two ore deposit types: (i) orogenic gold deposits (OGD), ranging from Late Archean to Late Paleozoic in age, and (ii) volcanogenic massive sulfide (VMS) deposits. The general characteristics of these deposit types are provided throughout the text, but the reasoning for this selection is noted here. Both OGD and VMS deposits are economically important sources of their contained metals, are well represented globally and temporally, and are well studied, sometimes with reasonably well-constrained mineralization ages (for VMS), yet their genesis (esp. OGD) is not wholly understood at present. This combination of factors makes these ore deposits ideal candidates for examination using Re-Os geochronology of low-level sulfides.

The research presented here builds on an earlier stage of this graduate research (Morelli, 2003), in which the accuracy of the Re-Os pyrite chronometer was demonstrated for the low temperature, sediment-hosted Red Dog Zn-Pb deposit, Alaska (Morelli et al., 2004), and precise Re-Os Model Ages and isochron ages were determined for arsenopyrite from the Meguma gold deposits, Nova Scotia, Canada (Morelli et al., 2005). The approach taken in this study is to perform Re-Os isotopic analysis on sulfides from OGD and VMS deposits mainly with existing, well-constrained mineralization ages to evaluate the accuracy of determined Re-Os ages. Where successful, the technique is then applied to sulfides from ore deposits with an unknown age. In this way, the reliability of the Re-Os low level sulfide ages can be determined, as can the reliability of other geochronological techniques routinely used in ore deposit studies. The significance of Os_i ratios from the sulfides is also examined, and is used along with other tracing techniques to interpret the origin of ore components for different deposits.

1.7. References

Barley, M.E., and Groves, D.I., 1992, Supercontinental cycles and the distribution of metal deposits through time: *Geology*, v. 20, p. 291-294.

Bennett, V.C., Nutman, A.P., Esat, T.M., 2002, Constraints on mantle evolution from $^{187}\text{Os}/^{188}\text{Os}$ isotopic compositions of Archean ultramafic rocks from southern West Greenland (3.8 Ga) and Western Australia (3.46 Ga): *Geochimica et Cosmochimica Acta*, v. 66, p.2615-2630.

Bingen, B., and Stein, H.J., 2003, Molybdenite Re-Os dating of biotite dehydration melting in the Rogaland high-temperature granulites, S Norway: *Earth and Planetary Science Letters*, v. 208, p. 181 - 195.

Brandon, A.D., Walker, R.J., Puchtel, I.S., Becker, H., Humayun, M., and Revillon, S., 2003, *Earth and Planetary Science Letters*, v. 206, p. 411-426.

Christensen, J.M., Halliday, A.N., Leigh, K.E., Randell, R.N., and Kesler, S.E., 1995, Direct dating of sulfides by Rb-Sr: A critical test using the Polaris Mississippi Valleytype Zn-Pb deposit: *Geochimica et Cosmochimica Acta*, v. 79, p. 5191-5197.

Cohen, A.S., Coe, A.L., Bartlett, J.M., and Hawkesworth, C.J., 1999, Precise Re-Os ages of organic-rich mudrocks and the Os isotope composition of Jurassic seawater: *Earth and Planetary Science Letters*, v. 167, p. 159-173.

Creaser, R.A., Sannigrahi, P., Chacko, T., and Selby, D., 2002, Further evaluation of the Re-Os geochronometer in organic-rich sedimentary rocks: a test of hydrocarbon maturation effects in the Exshaw Formation, Western Canada Sedimentary Basin: *Geochimica et Cosmochimica Acta*, v. 66, p. 3441-3452.

Creaser, R.A., Papanastassiou, D.A., and Wasserburg, G.J., 1993, Rhenium-osmium isotopic systematics of group IIA and group IVA iron meteorites [abs.]: 24th Lunar and Planetary Science Conference, Houston, Texas, Abstracts, p. 339-340.

Creaser, R.A., Papanastassiou, D.A., and Wasserburg, G.J., 1991, Negative thermal ion mass spectrometry of osmium, rhenium and iridium: *Geochimica et Cosmochimica Acta*, v. 55, p. 397 – 401.

Cumming, G.L., Eckstrand, O.R., and Peredery, W.V., 1982, Geochronologic interpretations of Pb isotope ratios in nickel sulfides of the Thompson belt, Manitoba: *Canadian Journal of Earth Sciences*, v. 19, p. 2306-2324.

Dahl, P.S., Holm, D.K., Gardner, E.T., Hubacher, F.A., and Foland, K.A., New constraints on the timing of Early Proterozoic tectonism in the Black Hills (South Dakota), with implications for docking of the Wyoming province with Laurentia: *GSA Bulletin*, v. 111, p. 1335 – 1349.

Dalrymple, G.B., 2004, *Ancient Earth, Ancient Skies: The Age of Earth and its Cosmic Surroundings*, Stanford University Press, Connecticut, USA, 247 p.

Faure, G., 1991, *Principles and Applications of Geochemistry*, 2nd Edition, Macmillan Publishing Company, New York, USA, 626 p.

Frei, R. and Pettke, T., 1996, Mono-sample Pb-Pb dating of pyrrhotite and tourmaline: Proterozoic vs. Archean intracratonic gold mineralization in Zimbabwe: *Geology*, v. 24, p. 823-826.

Freydier, C., Ruiz, J., Chesley, J., McCandless, T., and Munizaga, F., 1997, Re-Os isotope systematics of sulfides from felsic igneous rocks: application to base metal porphyry mineralization in Chile: v. 25, p. 775 – 778.

Groves, D.I., Condie, K.C., Goldfarb, R.J., Hronsky, J.M.A., and Vielreicher, R.M., 2005, Secular changes in global tectonic processes and their influence on the temporal distribution of gold-bearing mineral deposits: *Economic Geology*, v. 100, p. 203-224.

Hart, R.J., Cloete, Iain McDonald, Carlson, R.W., Marco A. G. Andreoli, 2002, Siderophile-rich inclusions from the Morokweng impact melt sheet, South Africa: possible fragments of a chondritic meteorite: *Earth and Planetary Science Letters*, v. 198, p.49-62.

Hirt, B., Tilton, G.R., Herr, W., and Hoffmeister, W., 1963, The half life of ^{187}Re , *in*: Geiss, J. and Goldberg, E. [eds.], *Earth Science Meteoritics*, North Holland Publications, p. 273-280.

Ishihara, S., Shibata, K., and Uchiumi, S., 1989, K-Ar age of molybdenum mineralization in the east-central Kitakami mountains, northern Honshu, Japan: comparison with the Re-Os age: *Geochemical Journal*, v. 23, p. 85-89.

Kendall, B.S., Creaser, R.A., Ross, G.M., and Selby, D., 2004, Constraints on the timing of Marinoan “snowball Earth” glaciation by ^{187}Re - ^{187}Os dating of a Neoproterozoic, post-glacial black shale in western Canada: *Earth and Planetary Science Letters*, v. 222, p. 729-740.

Kerrick, R., Goldfarb, R., Groves, D.I., and Garwin, S., 2000, The geodynamics of world-class gold deposits: characteristics, space-time distribution, and origins, *in*: Hagemann, S.G. and Brown, P.E [Eds.], *Gold in 2000*, SEG Reviews, Society of Economic Geologists, v. 10, p. 195 – 233.

Kirk, J., Ruiz, J., Chesley, J., Tittley, Walshe, J., and England, G., 2002, A major Archean gold- and crust-forming event in the Kaapvaal craton, South Africa: *Science*, v. 297, p. 1856 – 1858.

Kirk, J., Ruiz, J., Chesley, J., Titley, and Walshe, J., 2001, A detrital model for the origin of gold and sulfides in the Witwatersrand basin based on Re-Os isotopes: *Geochimica et Cosmochimica Acta*, v. 65, p. 2149 – 2159.

Luck, J.M., and Allegre, C.J., 1982, The study of molybdenites through the $^{187}\text{Re} - ^{187}\text{Os}$ chronometer: *Earth and Planetary Science Letters*, v. 61, p. 291 – 296.

McCandless, T.E., Ruiz, J., and Campbell, A.R., 1993, Rhenium behavior in molybdenite in hypogene and near surface environments: implications for Re-Os geochronometry: *Geochimica et Cosmochimica Acta*, v. 57, p. 889-905.

Meisel, T., Walker, R.J., Irving, A.J., and Lorand, J.P., 1999, Osmium isotopic compositions of mantle xenoliths: A global perspective: *Geochimica et Cosmochimica Acta*, v. 65, p. 1311-1323.

Morelli, R.M., 2003, Evaluation of rhenium-osmium geochronology of pyrite, sphalerite, and arsenopyrite: examples from the Red Dog Zn-Pb-Ag deposit, Alaska, and the Meguma Group Gold Deposits, Nova Scotia: unpublished M.Sc. Thesis, University of Alberta, 78p.

Morelli, R.M., Creaser, R.A., Selby, D., Kontak, D.J., and Horne, R.J., 2005, Rhenium-osmium geochronology of arsenopyrite in Meguma Group gold deposits, Meguma Terrane, Nova Scotia, Canada; evidence for multiple gold-mineralizing events: *Economic Geology*, v. 100, p. 1229 – 1242.

Morelli, R.M., Creaser, R.A., Selby, D., Kelley, K.D., Leach, D.L., and King, A.R., 2004, Re-Os Sulfide Geochronology of the Red Dog Sediment-Hosted Zn-Pb-Ag Deposit, Brooks Range, Alaska: *Economic Geology*, v. 99, p. 1569 – 1576.

Pearson, D.G, Shirey, S.B., Harris, J.W., and Carlson, R.W., 1998, Sulphide inclusions in diamonds from the Koffiefontein kimberlite, S Africa; constraints on diamond ages and mantle Re-Os systematics: *Earth and Planetary Science Letters*, v. 160, p. 311-326.

Pearson, D.G., Carlson, R.W., Shirey, S.B., Boyd, F.R., and Nixon, P.H., 1995, Stabilisation of Archaean lithospheric mantle; a Re-Os isotope study of peridotite xenoliths from the Kaapvaal Craton: *Earth and Planetary Science Letters*, v. 134, p. 341-357.

Pettke, T. and Diamond, L., 1996, Rb-Sr dating of sphalerite based on fluid inclusion-host mineral isochrones: a clarification of why it works: *Economic Geology*, v. 91, p. 951-956.

Peucker-Ehrenbrink, B., Ravizza, G., and Hoffman, A.W., 1995, The marine $^{187}\text{Os}/^{186}\text{Os}$ record of the past 80 million years: *Earth and Planetary Science Letters*, v. 130, p. 155-167.

Rasmussen, B., Sheppard, S., and Fletcher, I.R., 2006, Testing ore deposit models using in situ U-Pb geochronology of hydrothermal monazite: Paleoproterozoic gold mineralization in northern Australia: *Geology*, v. 34, p. 77-80.

Richards, J.P., and Noble, S.R., 1998, Application of radiogenic isotope systems to the timing and origin of hydrothermal processes, in: (Richards, J.P., and Larson, P.B., Eds.) *Techniques in Hydrothermal Ore Deposits Geology, Reviews in Economic Geology, Society of Economic Geologists*, v. 10, p. 195 – 233.

Richards, J.P., Cumming, G.L., Krstic, D., Wagner, P., and Spooner, E.T.C., 1988, Pb isotopic constraints on the age of sulfide ore deposition and U-Pb age of late uraninite veining at the Musoshi stratiform copper deposit, Central African Copperbelt, Zaire: *Economic Geology*, v.83, p. 724-741.

Ruiz, J., Freydier, C., McCandless, T., Chesley, J., and Munizaga, F., 1997, Re-Os isotopic systematics of sulfides from base metal porphyry copper and manto-type mineralization in Chile: *International Geology Reviews*, v. 39, p. 317-324.

Santosh, M., Suzuki, K., and Masuda, A., 1994, Re-Os dating of molybdenites from southern India: implications for Pan-African metallogeny: *Journal of the Geological Society of India*, v. 43, p. 585-590.

Selby, D., and Creaser, R.A., 2005, Direct radiometric dating of hydrocarbon deposits using rhenium-osmium isotopes: *Science*, v. 308, p. 1293-1295.

Selby, D., and Creaser, R.A., 2004, Macroscale NTIMS and microscale LA-MC-ICP-MS Re-Os isotopic analysis of molybdenite: Testing spatial restrictions for reliable Re-Os age determinations, and implications for the decoupling of Re and Os within molybdenite: *Geochimica et Cosmochimica Acta*, v. 68, p. 3897 – 3908.

Selby, D., and Creaser, R.A., 2001b, Re-Os geochronology and systematics in molybdenite from the Endako porphyry molybdenum deposit, British Columbia, Canada: *Economic Geology*, v. 96, p. 197 – 204.

Selby, D., and Creaser, R.A., 2001a, Late and Mid Cretaceous mineralization in the northern Canadian Cordillera: constraints from Re-Os molybdenite dates: *Economic geology*, v. 96, p. 1461 – 1467.

Selby, D., Creaser, R.A., Stein, H.J., Markey, R.J., and Hannah, J.L., 2007, Assessment of the ^{187}Re decay constant by cross calibration of Re-Os molybdenite and U-Pb zircon chronometers in magmatic ore systems: *Geochimica et Cosmochimica Acta*, v. 71, 1999 – 2013.

Selby, D., Creaser, R.A., Hart, C.J.R., Rombach, C.S., Thompson, J.H., Smith, M.T., Bakke, A.A., and Goldfarb, R.J., 2002, Absolute timing of sulfide and gold

mineralization: a comparison of Re-Os molybdenite and Ar-Ar mica methods from the Tintina Gold Belt, Alaska: *Geology*, v. 30, p. 791 – 794.

Shen, J.J., Papanastassiou, D.A., Wasserburg, G.J., 1996, Precise Re-Os determinations and systematics of iron meteorites: *Geochimica et Cosmochimica Acta*, v. 60, p. 2887 – 2900.

Şener, A.K., Young, C., Groves, D.I., Krapez, B., and Fletcher, I.R., 2005, Major orogenic gold episode associated with Cordilleran-style tectonics related to the assembly of Paleoproterozoic Australia?: *Geology*, v. 33, p. 225-228.

Sheppherd, T.J. and Darbyshire, D.P.F., 1981, Fluid inclusion Rb-Sr isochrons for dating mineral deposits: *Nature*, v. 290, p. 578-579.

Shirey, S., B. and Walker, R.J., 1998, The Re-Os isotope system in cosmochemistry and high-temperature geochemistry: *Annual Review of Earth and Planetary Sciences*, v. 26, p. 423-500.

Shirey, S., B. and Walker, R.J., 1995, Carius tube digestion for low-blank rhenium-osmium analysis: *Analytical Chemistry*, v. 67, p. 2136 – 2141.

Smoliar, M.I., Walker, R.J., and Morgan, J.W., 1996, Re-Os ages of Group IIA, IIIA, IVA and IVB iron meteorites: *Science*, v. 271, p. 1099 – 1102.

Stein, H.J., Scherstén, A., Hannah, J.L., and Markey, R.J., 2003, Subgrain scale decoupling of Re and ¹⁸⁷Os and assessment of laser ablation ICP-MS spot dating in molybdenite: *Geochimica et Cosmochimica Acta*, v. 67, p. 3673 – 3686.

Stein, H.J., Markey, R.J., Morgan, J.W., Hannah, J.L., and Scherstén, A., 2001, The remarkable Re-Os chronometer in molybdenite: how and why it works: *Terra Nova*, v. 13, p. 479 – 486.

Stein, H.J., Morgan, J.W., and Scherstén, 2000, Re-Os dating of low-level highly radiogenic (LLHR) sulfides: the Hårnas gold deposit, Sweden, records continental-scale tectonic events: *Economic Geology*, v. 95, p. 1657-1671.

Stein, H.J., Morgan, J.W., Markey, R.J., and Hannah, J.L., 1998a, An introduction to Re-Os: what's in it for the mineral industry?: *Society of Economic Geologists Newsletter*, v. 32, p. 8 – 15.

Stein, H. J., Sundblad, K., Markey, R. J., Morgan, J. W., and Motuza, G., 1998b, Re-Os ages for Archean molybdenite and pyrite, Kuittila-Kivisuo, Finland and Proterozoic molybdenite, Kabeliai, Lithuania: testing the chronometer in a metamorphic and metasomatic setting, *Mineralium Deposita*, v. 33, p. 329 – 345.

Stein, H.J., Markey, R.J., Morgan, J.W., Du, A., and Sun, Y., 1997, Highly precise and accurate Re-Os ages for molybdenite from the east Qinling molybdenum belt, Shaanxi province, China: *Economic Geology*, v. 92, p. 827 – 835.

Suzuki, K., Shimizu, H., and Masuda, A., 1996, Re-Os dating of molybdenites from ore deposits in Japan: implication for the closure temperature of the Re-Os system for molybdenite and the cooling history of molybdenum ore deposits: *Geochimica et Cosmochimica Acta*, v. 60, p. 3151-3159.

Teufel, S., Heinrich, W., 1997, Partial resetting of the U-Pb isotope system in monazite through hydrothermal experiments: An SEM and U-Pb isotope study: *Chemical Geology*, v. 137, p. 273-281.

Vielreicher, N.M, Groves, D.I., Fletcher, I.R., McNaughton, N.J., and Rasmussen, B., 2003, Hydrothermal Monazite and Xenotime Geochronology: A new direction for precise dating of orogenic gold mineralization: *SEG Newsletter* 53, p. 1, 10-16.

Völkering, J., Walczyk, T., and Heumann, K., 1991, Osmium isotopic ratio determinations by negative thermal ionization mass spectrometry: *International Journal of Mass Spectrometry and Ion Physics*, v. 105, 147 – 159.

Walker, R.J., Horan, M.F., Morgan, J.W., Becker, H, Grossman, J.N., and Rubin, A.E., 2002, Comparative ^{187}Re - ^{187}Os systematics of chondrites; implications regarding early solar system processes: *Geochimica et Cosmochimica Acta*, v. 66, p. 4187-4201.

York, D., 1968, Least squares fitting of a straight line with correlated errors: *Earth and Planetary Science Letters*, v. 5, p. 320-324.

2. Analytical Considerations and Methodology

Though unique amongst geochronometers in its applications, the Re-Os technique also comes with distinct and inherent challenges; the elemental properties, characteristically low crustal Re-Os concentrations, and highly variable isotopic systematics in natural materials make this a uniquely challenging system to work with from an analytical standpoint. Such considerations are discussed in this chapter, including the developmental history of the Re-Os dating technique, current challenges of dating low-level sulfide minerals, and methodological advances made during the course of this study.

2.1. Analytical Challenges Inherent to the Re-Os system

Successful use of the Re-Os isotopic system was, until recently, stalled due to a collection of analytical challenges specific to this isotope system. A description of each of these issues, including its pertinent analytical history and its eventual resolution, are briefly described here.

The most obvious obstacle to successful application of the Re-Os chronometer is the low concentrations of Re and Os in the silicate Earth, a result of their siderophile (\pm chalcophile) geochemical characteristics. Because the majority of the budget of Re and Os is contained within the Earth's core, there is typically very low Re and Os contents in the majority of accessible terrestrial rocks and minerals. For example, estimates of Re and Os concentration in 'fertile mantle' are ~ 0.3 and 3 ppb, respectively (Meisel et al., 1996), whereas average continental crustal concentrations are only ~ 2 ppb Re and ~ 30 ppt Os (Sun et al., 2003; Peucker-Ehrenbrink and Jahn, 2001). This is not an issue for molybdenite, which concentrates Re from a hydrothermal fluid, but is very problematic for low-level sulfides. Typical Re contents for these minerals range between < 1 to 100 ppb, whereas Os concentrations are commonly at the low ppt level. The only foreseeable resolution to this issue is to continuously advance analytical protocols to maximize chemical yield and optimize instrument sensitivity, and thus to allow precise isotopic measurements of the smallest possible Re and Os quantities.

As discussed in section 1.1, a crucial requirement of any decay system used for geochronology is that the value of the decay constant (λ) is accurately and precisely

known. This has been problematic for the Re-Os system and the subject of numerous studies. Descriptions and results of previous attempts at ^{187}Re decay constant determination are reviewed by Selby et al. (2007). Prior to the mid-1990's, several values for $\lambda^{187}\text{Re}$ had been determined by direct counting experiments or by microcalorimetric determinations. Included in these studies was that of Lindner et al. (1989), whom determined a value of $1.64 \pm 0.05 \times 10^{-11} \text{ a}^{-1}$ based on measurement of radiogenic ^{187}Os produced by decay of known ^{187}Re contents in a Re-bearing solution. This value was widely cited in the literature, despite having a large associated uncertainty ($\pm 3\%$) that resulted from analytical issues associated with sample-spike equilibration, spike calibration problems, and low sensitivity and precision of quadrupole ICP-MS analysis. The work of Lindner et al (1989) was succeeded by the study of Smoliar et al. (1996), in which a value for $\lambda^{187}\text{Re}$ of $1.666 \times 10^{-11} \text{ a}^{-1}$ was calculated by using the slope from a Re-Os isochron of Group IIIA iron meteorites with an assumed age of 4558 Ma (derived from ^{53}Mn - ^{53}Cr dates on angrite meteorites to which they may be related). A significant result from this study was the low uncertainty ($\pm 0.31 \%$) associated with the value of $\lambda^{187}\text{Re}$, thereby providing a sufficiently precise value to allow Re-Os age determinations on other materials. Smoliar et al. (1996) stress that this reduced uncertainty applies only to those Re-Os isotopic analyses using the same Re-Os spike solution used to produce the Group IIIA meteorite isochron, due to possible systematic error in the spike calibration arising from the nonstoichiometry of the salt used to produce the Os standard. Independently, Selby et al. (2007) have determined, by cross-calibrating Re-Os molybdenite and U-Pb zircon chronometers derived from magmatic ore systems of varying ages, a $\lambda^{187}\text{Re}$ value of $1.6689 \pm 0.0031 \times 10^{-11} \text{ a}^{-1}$, indistinguishable from that of Smoliar et al. (1996) but with a marginally lower uncertainty of $< 0.2\%$. Thus, all Re-Os analyses processed using University of Alberta Re-Os spikes can take advantage of this reduced $\lambda^{187}\text{Re}$ uncertainty. However, the $\lambda^{187}\text{Re}$ value of Smoliar (1996) is used for age calculation throughout this thesis for consistency between results obtained prior to and following the Selby et al. (2007) study.

As indicated in the preceding discussion, accurate spike calibration is an issue that has been problematic for Re-Os geochronology. This problem arises due to the nonstoichiometry of the Os salt $((\text{NH}_4)_2\text{OsCl}_6$; ammonium hexachloro-osmate) used to

produce the gravimetric Os standard solution against which the Os spike (typically ^{190}Os) is calibrated at most Re-Os laboratories (Morgan et al., 1995). This nonstoichiometry introduces a systematic uncertainty that may be as high as $\pm 1.2\%$ to all determined Re-Os ages. Selby et al. (2007) document a solution to this problem. They found that heating pure $(\text{NH}_4)_2\text{OsCl}_6$ salt in a tube furnace at 500°C in 98% N_2 and under 2% H_2 gas causes reduction of the salt to pure metallic Os, from which the amount of Os in the salt can be accurately determined gravimetrically, thereby eliminating the nonstoichiometry issue altogether. This protocol has been implemented at the University of Alberta Radioisotope Facility for generation of our Os standard solution, to which all other Re-Os isotopic spike solutions are calibrated.

Perhaps the most significant challenge for Re-Os isotopic studies historically has been the inability to perform direct Re and Os isotopic analyses by conventional mass spectrometry techniques due to the atomic properties of these elements. Osmium (and to a lesser degree, Re) is a highly refractory metal with a correspondingly high ionization potential of ~ 8.7 eV, and is consequently not readily ionized to a positive species by standard thermo-ionization techniques. This characteristic results in extremely low yields and analytical precision, and has hindered routine isotopic analysis of Os in natural samples since the first attempt in the early 1960's by electron bombardment of gaseous OsO_4 (Hirt et al., 1963). Several other mass spectrometric techniques were subsequently applied to natural samples in attempts to overcome this problem, including secondary ionization (SIMS, Luck and Turekian, 1983), resonance ionization (RIMS, Walker and Fassett, 1986), and combinations of both techniques (Blum et al., 1990; England et al., 1992). Fehn et al. (1986) has also performed Re-Os isotopic analysis using accelerator mass spectrometry (AMS), and variations on the use of inductively coupled plasma mass spectrometry (ICP-MS) of Os has also been attempted (e.g. Lichte et al., 1986; Bazan, 1987). While variably improving achievable precision and decreasing the quantity of Os required for analysis, each of these techniques failed to obtain sufficiently precise results for the low (sub ng) Os concentrations characteristic of most natural specimens.

A major technological advance was made in the early 1990's, when it was discovered that ionization of Re and Os to a negative species was highly efficient, and that isotopic compositions of negatively charged Re and Os species could be made by

reversing the overall polarity of a standard thermal ionization mass spectrometer (Creaser et al., 1991; Völkening et al., 1991). Through analysis of ReO_4^- and OsO_3^- ions by negative thermal ionization mass spectrometry (NTIMS), it was determined that high precision (<5 %) Re and Os isotopic analysis of < 5 ng by Faraday collector and as little as 70 pg using a secondary electron multiplier was routinely attainable (Creaser et al., 1991). The implementation of this technique instantly improved the prognosis for use of the Re-Os system for dating and source tracing of natural samples, and remains unparalleled in sensitivity for Re-Os isotopic determinations. Recently, isotopic determinations of Re and Os by quadrupole (PQExcell) ICP-MS has been attempted (Yu et al., 2005). Notwithstanding the authors' claims, the ability of this technique to obtain accurate and precise Re and Os isotopic measurements has not been sufficiently demonstrated for low-level sulfide samples. In fact, the study reports an imprecise Re-Os arsenopyrite age (2316 ± 140 Ma) that is significantly older than the previously postulated Mesozoic age for mineralization. For this reason, this and other ICP-MS based spectrometric techniques are not recommended for use with this application, and only results derived from NTIMS Re-Os isotopic analyses will be considered further in this thesis.

Another major impediment to obtaining demonstrably reliable Re-Os isotopic results was rooted in a peculiar elemental property of Os. When subjected to high temperatures in an oxidizing environment, Os will convert to volatile OsO_4 (boiling point = 130°C at 1 atm). Thus, during high temperature acid digestion of a natural sample, escape of osmium from the digestion vessel will occur. This inhibits full equilibration of sample and spike Os, resulting in the measurement of misrepresentative isotopic compositions and calculation of erroneous ages.

A solution to this problem was introduced in the mid 1990's by application of samples used for Re-Os analysis to the 'Carius tube method' (Creaser et al., 1993; Shirey and Walker, 1995), a digestion technique originally developed over 100 years prior (Carius, 1865). The basis of this technique is the high temperature sample digestion within a sealed, thick-walled Pyrex tube, followed by tube opening only after its contents have been frozen (see section 2.4 for details). Through utilization of a sealed digestion vessel, this procedure effectively eliminates the escape of any OsO_4 during or after

sample dissolution, and ensures full equilibration of sample and spike Os by driving all Os to a terminal oxidation state (Os^{VIII}) and equilibrations fully in the gaseous phase.

2.2. Re-Os Sampling Protocol

Although the siderophile-chalcophile affinities of Re and Os make this system distinct among geochronometers, the same properties also introduce methodological complications that are unique to this system. An example is the sampling protocol for Re-Os analysis of sulfide minerals, for which extreme care must be taken to avoid contamination from sampling tools. Extraction of a sulfide specimen from its wall rock host should involve no direct contact between steel tools (e.g. hammer, chisel, etc.) and the desired mineral, but should instead be removed in such a manner that a sufficient proportion of the host material surrounding the sulfide is also extracted. This material provides an effective boundary between the tool and the sulfide, and eliminates the possibility of Re and/or Os input from the tool itself. If sawing of the sample is required to better isolate the sulfide fraction, all sawed surfaces should subsequently be ground using a non-metallic surface (e.g. a diamond-coated polisher) to ensure no residue from the saw blade remains on the sample. If required, the material should be roughly crushed by non-metallic tools (e.g. ceramic, agate) or, if metallic tools are necessary, both the tool and the sample should be wrapped in a protective covering to avoid direct contact. For this study, sulfide specimens that required crushing were wrapped in a polyethylene sample bag prior to being crushed with a hammer covered with duct tape. Individual crushed sulfide fragments were then picked out and crushed to a coarse powder ($\sim 0.5 - 1$ mm diameter) using an agate mortar and pestle. If extensive wall rock material remains after fine crushing, a full mineral separation is undertaken through methyl iodide density separation, FrantzTM magnetic separation using multiple settings, and, if necessary, hand-picking under a binocular microscope.

A technique that was initially used in this study, and has been reported for separation of molybdenite and other sulfide minerals in other studies, is sulfide extraction by means of an electric drill. In this study, a small DremelTM drill with a diamond-tipped drill bit (#7103) was used for some of the first Re-Os analyses performed. This technique is advantageous because it allows for extremely precise extraction of small sulfide grains

or specific portions of grains without the need for performing a full mineral separation procedure. However, comparison of results from both drilled and non-drilled aliquots of the same sample reveals contamination of the sample by the drill bit.

In one experiment, arsenopyrite (hardness = 5.5 - 6.0) and scheelite (hardness = 4.5 - 5.0) from the Golden Mile orogenic gold deposit, western Australia, were drilled to obtain ~ 50 mg of powder for Re concentration determinations by isotope dilution NTIMS. The drilled powders yielded Re concentrations of 133 ppb for arsenopyrite, and 720 ppb for scheelite. Such Re concentrations are atypically high for Archean gold-related hydrothermal minerals (see Chapter 3), so repeat analyses were performed on powders obtained from the same samples, but derived from chipping and crushing using agate tools rather than by drilling. These analyses yielded much more characteristic Re concentrations of 0.24 ppb for arsenopyrite, and 0.07 ppb for scheelite, thereby indicating a significant Re contribution from the drill bit.

In another experiment, repeat analysis of drilled and non-drilled aliquots of arsenopyrite sample 9824 from the Muruntau orogenic gold deposit, Uzbekistan, was performed. Sample 9824 yields a Model 1 Re-Os age of 288.6 ± 5.6 Ma (MSWD = 1.1) from five Re-Os analyses of non-drilled arsenopyrite, each characterized by $^{187}\text{Re}/^{188}\text{Os}$ ratios in excess of 16,500 (Chapter 4.2). Additionally, non-drilled analyses of sample 9824 combined with non-drilled analyses of related sample 18A from Muruntau yield a $^{187}\text{Os}/^{188}\text{Os}$ initial ratio of $ca. 0.37 \pm 0.27$ (chapter 4.2). These results are in stark contrast to determined isotopic compositions of analyses of 9824 obtained by drilling using a new drill bit. Figure 2.1a shows that nine drilled arsenopyrite analyses are characterized by $^{187}\text{Re}/^{188}\text{Os}$ ratios $< 7,000$, and yield a Model 3 Re-Os age of 283 ± 5 Ma (MSWD = 27) with an initial $^{187}\text{Os}/^{188}\text{Os}$ ratio of 0.14 ± 0.23 . This experiment indicates that drill-bit contamination of arsenopyrite displaces analyses towards the origin (i.e. less radiogenic Os compositions and lower Re/Os) and, in some cases, off the isochron to account for the increased scatter. To verify this effect, the tip of a #7103 drill bit was removed, dissolved and analyzed for Re-Os isotopic compositions and abundances, and found to contain relatively high Re and Os contents (Table 2.1). Mixing calculations between the drill bit and the uncontaminated 9824 arsenopyrite require an input of only 0.5 weight % drill bit contamination to explain the isotopic systematics of the contaminated arsenopyrite

(Figure 2.1b). From this figure, it is evident that even a small amount of contamination by the drill bit has a drastic effect on the measured isotopic composition of radiogenic sulfides. Because the most radiogenic point (9824-C2; pure arsenopyrite with no drill bit) controls the slope of the isochron, there is essentially no large effect from contamination on the calculated age. However, there is a very strong influence by the drill bit component on the determined initial Os ratio, with affected samples anchoring the mixing line near the y-axis at the composition of the drill bit (~ 0.14). These observations provide conclusive evidence that sampling with a drill, and potentially other steel tools, can contaminate and alter the Re-Os concentrations and isotopic compositions of sulfide samples, and should be avoided.

2.3. Re-Os Analytical Protocol

All Re-Os analyses of sulfide minerals reported in this study were performed by isotopic dilution of the sample with a mixed Re-Os spike solution of known composition, separation and chemical purification of Re and Os fractions, and analysis by negative thermal ionization mass spectrometry. The analytical protocol for this study follows that described by Selby and Creaser (2001a, b), with minor modifications. In detail, the crushed sulfide fractions were weighed and added, along with a known amount of mixed $^{185}\text{Re} + ^{190}\text{Os}$ spike solution, to a borosilicate Carius tube. Sulfide sample weights were limited to avoid the occurrence of the 'Claus reaction', whereby sample-derived Fe catalyzes the oxidization of sulfur to native sulfur, thus inhibiting the required oxidization of Os to OsO_4 (Frei et al., 1998). We have previously determined that, if this reaction occurs at all, it does not affect arsenopyrite samples with weights at least as high as 500 mg (Morelli et al., 2005). Accordingly, arsenopyrite sample weights for the present study were limited to a maximum of ~ 500 mg, whereas pyrite and pyrrhotite samples were limited to ~ 400 mg sample weights. Subsequent to the addition of sample and spike, 11 ml of inverse aqua regia (8 ml Fisher Scientific trace metal grade HNO_3 + 3 ml Seastar Chemicals 32-35% HCl) was added to the tube while it was immersed in a methanol + solid carbon dioxide slurry. The top of the tube was then sealed using a natural gas + oxygen torch with the contents still frozen, thereby inhibiting the release from the tube of any OsO_4 from the sample or spike. The sealed tube was allowed to thaw at room

Table 2.1: Re-Os elemental and isotopic data showing possible effects of drill bit contamination on the composition of Muruntau arsenopyrite sample 9824

	Re (ppb)	¹⁸⁷ Os* (ppt)	¹⁹² Os (ppt)	¹⁸⁷ Re/ ¹⁸⁸ Os
"pure" 9824	23.5	71	3	16536
drill bit	41	890	19735	4.13
<i>analyses:</i>				
9824a-1	15	45	18	1661
9824a-3	22	66	40	1085
9824a-4	21	61	116	359
9824b-1	19	54	112	329
9824b-2	38	111	13	5771
9824b-3	29	87	16	3500
9824c-2	20	60	29	1364
9824d-1	22	66	7	6379
9824 e-2	15	42	55	532

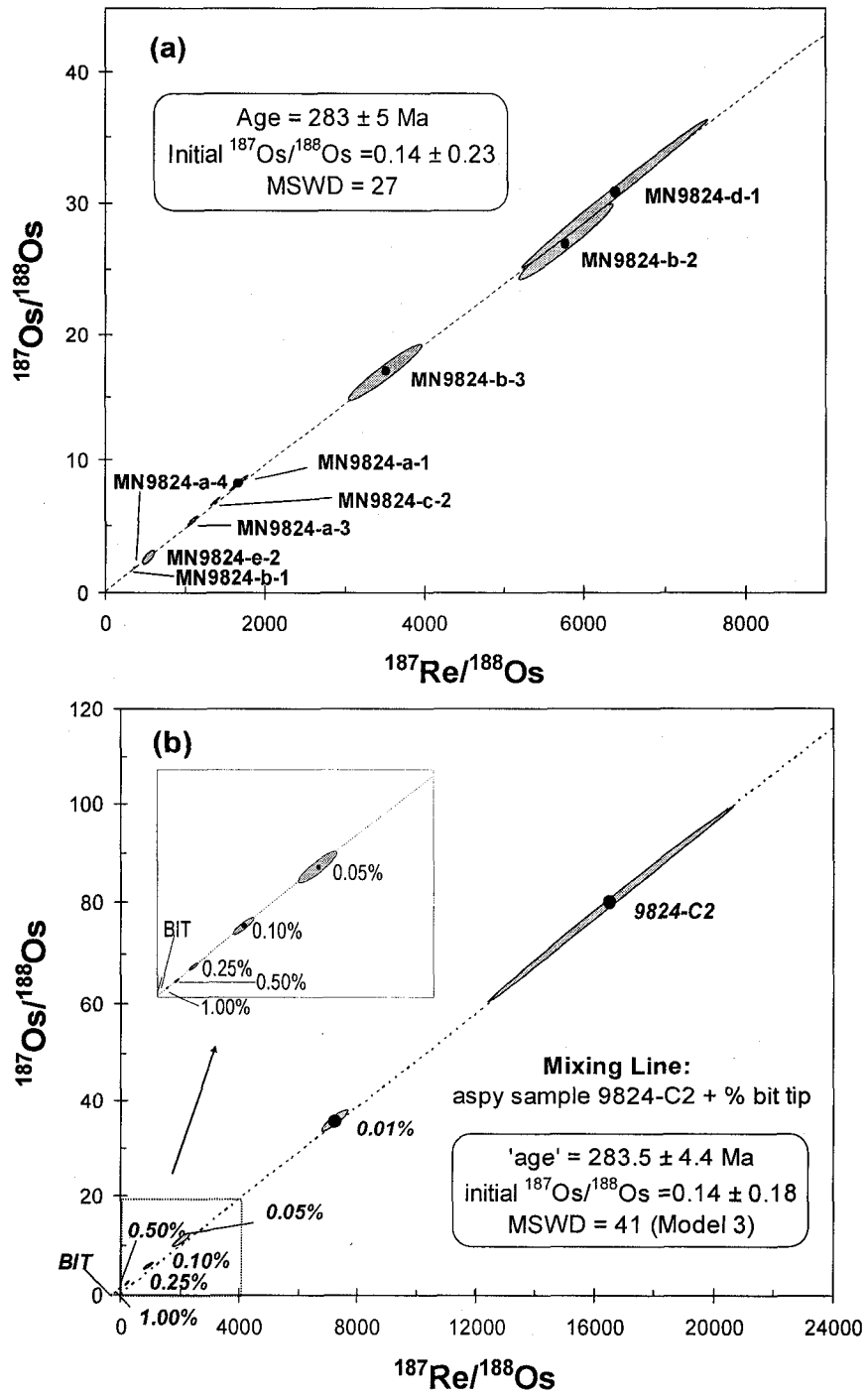


Figure 2.1: (a) Re-Os isochron diagram for Muruntau arsenopyrite 9824 from analyses of drilled samples only, (b) Re-Os mixing line for mixtures of different proportions of pure arsenopyrite (9824-C2) and pure drill bit ('BIT').

temperature, and was then placed in a steel jacket and into an oven for ~ 24 hours at 240°C, during which complete sample digestion and sample/spike equilibration takes place (i.e. the 'Carius tube method'; Creaser et al., 1993; Shirey and Walker, 1995).

Upon cooling, the exterior of the tube is cleaned with water and immersed in liquid nitrogen to completely freeze all liquids and gases contained within the tube. The tube is opened and 4 ml of chloroform (CHCl_3) is pumped into the tube along with the frozen contents, which are then emptied into a polypropylene 50 ml centrifuge vial and centrifuged for 1-2 minutes. Os partitions strongly into the chloroform, which is then extracted from the aqua regia and placed into a glass vial containing 3 ml of 9 N HBr (solvent extraction technique described by Cohen and Waters, 1996). This extraction is repeated twice more; the glass vial containing CHCl_3 , HBr and the Os fraction is then capped and placed on a 70°C hotplate overnight to reduce Os to the bromide form. The remaining aqua regia, which contains the Re fraction, is dried down in an uncovered glass vial overnight.

Once cooled, the HBr is extracted from the CHCl_3 and dried down on a watch glass covered with Teflon tape. Just prior to complete drying, the droplet is taken up in a thin disposable pipette and placed onto the lid of the glass vial that held the CHCl_3 /HBr mixture. The lid is covered with an inverted conical Savillex vial containing 20 μl of 9N HBr and Os oxidized with a CrVI+ H_2SO_4 mixture (30 μl) on a heating block at 80°C for ~ 3 hours. The droplet is then redried back onto the vial lid, the microdistillation (Birck et al., 1997) is repeated, and the droplet is dried down in the apex of the Savillex conical vial at 60°C and under nitrogen gas.

To recover Re, the aqua regia residue is redissolved in 3 ml of 0.2 N HNO_3 , placed in a centrifuge tube, and centrifuged at 5000 rpm for 5 minutes. The Re is removed from this solution via anion exchange column chromatography (Morgan et al., 1991) with Eichron analytical grade anion exchange resin (1 x 8, 100-200 mesh) in a modified disposable pipette. Once completed, the eluate is dried down in a PMP beaker at 70°C. The remaining Re-bearing solid is redissolved in 200 μl of 0.05 N HNO_3 and placed into a 1.5 ml polypropylene centrifuge tube, along with a single Dowex AGI-X8 (< 20 mesh) anion exchange bead. The bead is agitated in the solution for ~ 8 hours and

is then removed and placed into another centrifuge tube containing 1 ml of 6N HNO₃ for ~ 8 hours. The solution is extracted from the vial and dried down on a hotplate at ~ 70°C.

In preparation for spectrometry, the purified Os fraction is dissolved in ~ 0.3 µl of 9N HBr and deposited onto a crimped Pt filament using a micropipette. The Re fraction is dissolved in ~0.35 µl of 16N HNO₃ and is transferred from the watch glass onto a Ni wire filament that was previously crimped and glowed at ~2.5 A under atmospheric conditions. Once deposited onto the filament, the Re and Os samples are covered with Ba(NO₃)₂ and Ba(OH)₂ / NaOH activator solutions, respectively, which lower the electron work function of the filament metals and thereby promote ionization of Re and Os. Re and Os isotopic compositions are performed by NTIMS (Creaser et al., 1991; Völkening et al., 1991) using a Micromass Sector 54 thermal ionization mass spectrometer at the University of Alberta Radioisotope Facility. In preparation for Os isotopic analysis, a 20 minute warmup period is performed during which the current is slowly increased to ~ 1.4 A, followed by a static, ~ 20 minute warmup period at the first detection of Os emission. All Re isotopic analyses were measured by static Faraday collector analysis, whereas Os isotopic abundances were measured by an ETP electron multiplier in pulse counting mode. Data reduction is performed using Microsoft Excel, including Re and Os spike unmixing and corrections for instrument-induced fractionation of Os isotopes during spectrometry. Isochron regression is performed using Isoplot v.2.22 (Ludwig et al., 2000) using the ¹⁸⁷Re decay constant of Smoliar et al. (1996).

2.4. Re-Os Procedural Blanks

Due to the low Re and, especially, low Os concentrations (Os = commonly in the low ppt range) inherent to many sulfide minerals, it is imperative that all sources of blank Re and Os be identified, accurately quantified, and minimized. The reagents and other supplies used for Re and Os separation, purification, and analysis at the University of Alberta Radioisotope Facility have been tested for Re and Os contents. The main blank contributions are from 16N nitric acid, and from the Ni and Pt filament wire. At the outset of this PhD study, total procedural blanks were low, but significant, at ~ 3 – 5 pg for Re and ~ 1 pg for Os. The ultimate goal for work with low-level Re-Os sulfide analysis is to reduce these blank levels to the point where the impact on the true isotopic

composition of the sample is essentially negligible, and considerable effort was expended to achieve this objective.

To reduce Os blank derived from the filament Pt, a change was made from use of pre-flattened Pt ribbon (ESPI) to Pt wire that is crimped with precision pliers (Williams Advanced Materials). This has resulted in a 4 –10 fold decrease in the Os loading blank, now routinely at ~ 5 fg. The Ni wire used for Re analysis has not been changed (Johnson Matthey), as loading blanks are sufficiently low that they do not pose a problem for most Re isotopic analyses (~ 200 – 400 fg). Exceptions to this are samples with very low Re contents (< ~ 1 ppb), or for cases in which Re purification chemistry resulted in a poor yield. This was found to occur when the anion exchange resin begins to degrade, a problem easily prevented by careful tracking of Re blank levels, proper storage and cleaning protocol for resin, and limiting use of individual resin batches to < 6 months.

In attempt to reduce blank levels in the nitric acid, distillation of trace metal grade acid was attempted in a Teflon distillation apparatus at ~ 70°C. Although it was found that the earliest fraction to be distilled and to condensate had a marginally lower Re content than subsequent fractions, it was also characterized by a lower normality (from 15.5N initially down to ~ 10N) due to preferential condensation of H₂O in the early distillation stages. This is problematic, as it could potentially decrease the oxidizing power of the acid and prevent adequate sample-spike equilibration during dissolution in the Carius tube. Distillation had no effect on Os content, which is unsurprising given the volatility of Os under the oxidizing conditions of the stock acid. Considering these unfavourable results, distillation was not pursued further for decreasing reagent Re and Os blank levels. We have instead found that, when care is taken to maximize yield when performing Re blank analyses, more accurate total procedural Re blanks of 1 – 2 pg are determined with the use of Trace Metal grade stock nitric acid. Although this is an acceptable blank contribution for precise Re determinations of most low-level sulfides, future work should concentrate on further reductions.

To decrease Os blank abundances, another experiment was performed in which small amounts of hydrogen peroxide (H₂O₂), a powerful oxidizing agent, were added to heated nitric acid in an attempt to oxidize and remove existing Os in the acid as OsO₄. A specific proportion of 30% H₂O₂ was added to a known volume of nitric acid over

various temperatures in the range of 60 – 110°C, and the resulting solutions were tested for Os concentrations. It was found that the optimal results were obtained by addition of 5% H₂O₂ by volume to the nitric acid (e.g. 50 ml H₂O₂ per litre of HNO₃) in a 4L open glass beaker on a hotplate set at 100°C. Approximately ten to fifteen minutes after addition of the H₂O₂, a reaction occurs during which vigorous bubbling and instantaneous evolution of a brownish-coloured gas (NO₂?) is observed. Once the reaction has completed (< 1 minute), the beaker is left on the hot plate for two hours, resulting in the evaporation of some of the H₂O produced from the addition of the H₂O₂ (i.e. an increase in normality). This procedure has been found to produce a sufficiently concentrated acid (~ 14N) to digest the sample and achieve sample-spike equilibration, with a significantly decreased Os content (routinely < 0.2 pg per full Carius tube digestion, but as low as 0.08 pg). This treatment is now applied to all nitric acid used for Re-Os sample digestion at the University of Alberta Radioisotope Facility, and is among the lowest reported Os blank worldwide for full Carius tube analysis.

2.5. Re-Os Spike Solutions and Low-Level Sulfides

An important requirement for accurate Re-Os age determinations of low-level sulfide minerals is the proper calibration of spike solutions. For this study, all samples were spiked with mixed Re and Os spikes that have been precisely calibrated against gravimetric Re and Os standards. Two different types of Re-Os spikes were used: (1) a mixed ¹⁸⁵Re and ¹⁹⁰Os spike ('Re-Os spike #3'), most suitable for 400 mg samples containing > 1 ppb Re and common Os, and (2) a mixed ¹⁸⁵Re and isotopically normal Os spike ('SN1/SN2'), best suited for high concentration samples with negligible common Os (e.g. molybdenite).

Many low-level sulfides, including several samples used in this study, are characterized by Re concentrations below < 1 ppb, and even lower Os concentrations. For this reason, an attempt was made to gravimetrically dilute existing Re-Os tracer solutions with 1N HCl to better suit them for application to such sulfides. Gravimetric dilution was performed on both Re-Os spike #3 and a mixed double Re-Os spike containing ¹⁸⁵Re, ¹⁸⁸Os, and ¹⁹⁰Os, and which is used mainly for molybdenite analysis. The double spike is advantageous for highly radiogenic samples, since the two spike Os isotopes can be used

to correct for spectrometer-induced isotopic fractionation during Os analysis. Re-Os spike #3 was diluted approximately 100 times to produce 'Re-Os spike #4'. This dilute spike was tested on two arsenopyrite samples (18 and 20A) from the Muruntau orogenic gold deposit, Uzbekistan, which were previously dated at ca. 290 Ma using spike #3 (see chapter 4.2). Using the dilute spike #4, both samples yielded ages of 301 Ma, ~ 3 – 4 % older than the ages determined using spike #3. A similar phenomenon was observed when using the dilute mixed double spike, an approximately 300-fold dilution of the original double spike solution. This spike was tested on arsenopyrite samples from the Muruntau gold deposit (sample 9824, ~ 290 Ma) and the Homestake orogenic gold deposit, South Dakota (H-1a, ~ 1734 Ma), both previously dated using Re-Os mixed spike # 3 (see chapter 4). Use of the dilute mixed double spike resulted in calculated ages that are ~ 12 % (9824) and 4 % younger than the previously determined ages.

This experiment shows the importance of testing new Re-Os spike solutions, including gravimetric dilutions of existing spikes, against well-calibrated spikes. These results suggest that dilution of a Re-Os tracer solution by 1N HCl causes a chemical reaction involving either Re or Os that alters the concentration of the dilute spike from the original. It is therefore recommended that all diluted Re-Os spikes be directly calibrated against a gravimetric standard prior to use with samples.

2.6. Error Propagation for Re-Os Analyses of Low-Level Sulfides

A critical consideration for Re-Os dating of low-level sulfide minerals is the proper assignment of uncertainties to the determined Re and Os isotopic compositions. The method of uncertainty determination can have a significant impact on the precision of the determined age, and can vary widely depending on the isotopic characteristic of a particular sulfide sample. Nevertheless, the importance of proper error propagation has gone unrecognized in some published Re-Os low-level sulfide studies to date, leading to a problem of nonstandardization of techniques amongst existing Re-Os laboratories worldwide.

For low-level Re-Os sulfide studies, proper assignment of uncertainties must include all potential sources of analytical error for each Re and Os isotopic determination. Common, but misrepresentative, practice in some recent Re-Os literature is to simply

assign fixed uncertainties to Re and Os isotopic compositions (e.g. to assign a 1% uncertainty to all $^{187}\text{Re}/^{188}\text{Os}$ ratios, etc.). In other cases, reported 2σ uncertainties are determined from only one or two potential sources of error, or the basis of uncertainty calculation are omitted altogether. Depending on the Re-Os isotopic compositions of the sulfide, this can lead to gross over- or underestimations of the actual 2σ uncertainty. An example of this problem is the aforementioned study of Kirk et al. (2001, 2002; see chapter 1.5), which describes the results of Re-Os geochronology of pyrite and gold from the Witwatersrand gold ores, South Africa. In this study, the authors state “*errors were determined by using the greater value of either the 2σ counting error ($2SD\sqrt{n}$) or by varying the Os blank between measured values of 1 to 2 pg*”. Clearly this arbitrary method of uncertainty determination is unacceptable and could potentially lead to gross underestimation of the true 2σ uncertainty for the gold and pyrite Re-Os isotopic compositions, and hence of the final 2σ uncertainty on the reported age.

Error propagation for Re-Os isotopic analyses performed at the University of Alberta Radioisotope Facility includes consideration of all relevant sources of analytical error. Initially propagated at 67% (1σ) confidence intervals, this includes uncertainty in Re and Os spike compositions, Re and Os blank levels and Os blank isotopic composition, monitored variations in Re and Os standards, and $^{18}\text{O}/^{16}\text{O}$ ratios of the measured Re and Os oxides. Although not relevant to this study, laboratories that do not use mixed Re-Os tracer solutions should also include the uncertainty in spike weights. Once calculated, the result of the numerical error propagation is multiplied by 2 to determine the 2σ uncertainty (95% confidence interval), which is that reported for all Re-Os isotopic compositions and ages. To remain consistent with common practice of geochronological studies utilizing other decay systems, the uncertainty in the ^{187}Re decay constant were excluded from uncertainty determinations, but strictly should be included when comparing Re-Os ages to ages derived from other isotope systems.

Many low-level sulfides contain highly radiogenic Os compositions, such that the majority of Os in the sample was produced by the *in situ* decay of ^{187}Re (i.e. negligible common Os). Such samples typically yield $^{187}\text{Re}/^{188}\text{Os}$ ratios in the thousands to hundreds of thousands, with the majority of measured ^{188}Os being blank-derived. The use of ^{188}Os as the normalizing isotope for both axes in a traditional ($^{187}\text{Re}/^{188}\text{Os}$ vs.

$^{187}\text{Os}/^{188}\text{Os}$) Re-Os isochron plot thus introduces a highly correlated uncertainty in both axes (Stein et al., 2000). To account for this source of highly correlated uncertainty, an error correlation function has been applied that effectively assesses the degree of correlation between the $^{187}\text{Re}/^{188}\text{Os}$ and $^{187}\text{Os}/^{188}\text{Os}$ ratios for a given analysis (ρ ; Ludwig, 1980):

$$\rho = \frac{\left(\frac{\sigma_{(^{187}\text{Re}/^{188}\text{Os})}}{^{187}\text{Re}/^{188}\text{Os}} \right)^2 + \left(\frac{\sigma_{(^{187}\text{Os}/^{188}\text{Os})}}{^{187}\text{Os}/^{188}\text{Os}} \right)^2 - \left(\frac{\sigma_{(^{187}\text{Os}/^{187}\text{Re})}}{^{187}\text{Os}/^{187}\text{Re}} \right)^2}{2 * \frac{\sigma_{(^{187}\text{Re}/^{188}\text{Os})}}{^{187}\text{Re}/^{188}\text{Os}} * \frac{\sigma_{(^{187}\text{Os}/^{188}\text{Os})}}{^{187}\text{Os}/^{188}\text{Os}}}$$

where σ denotes the 1σ uncertainty (67% confidence interval) of each ratio. This function yields a value that approaches unity (highly correlated uncertainties) for highly radiogenic samples, whereas unradiogenic samples without correlated uncertainties have ρ values closer to zero.

2.7. Conclusions

The Re-Os system applied to “LLHR” sulfides demands a highly rigorous approach to sampling and digestion techniques, chemical separation and purification, mass spectrometry, data treatment and uncertainty propagation. Failure to adopt such an approach can severely compromise the determined Re-Os results, and may result in incorrect geological interpretation of compromised analytical data.

Determination of Re-Os isotopic compositions of low-level sulfides did not become feasible until after the mid 1990’s, following the advent of several analytical advances that significantly improved chemical yield and instrument sensitivity. This also corresponded with improved accuracy and precision of accepted value of the ^{187}Re decay constant. In addition to these developments, this PhD thesis reports important advances in sampling and dissolution techniques, chemical separation and purification protocol, procedural blank reduction, and suitable uncertainty determination for low-level sulfide work. Collectively, these improvements have made possible the routine determination of accurate and precise Re-Os ages for low-level sulfide minerals.

2.8. References

Bazan, J.M., 1987, Enhancement of osmium detection in inductively coupled plasma atomic emission spectrometry: *Analytical Chemistry*, v. 59, p. 1066 – 1069.

Birck, J.L., RoyBarman, M., and Capmas, F., 1997, Re-Os measurements at the femtomole level in natural samples: *Geostandards Newsletter*, v. 20, p. 19-27.

Blum, J.D., Pellin, M.J., Calaway, W.F., Young, C.E., Gruen, D.M., Hutcheon, I.D., and Wasserburg, G.J., 1990, Resonance ionization mass spectrometry of sputtered osmium and rhenium atoms: *Analytical Chemistry*, v. 62, p. 209.

Carius, L., 1865, *Liebig's Annalen der Chemie.*, v. 136, p. 129.

Cohen, A.S., and Waters, F.G., 1996, Separation of osmium from geological materials by solvent extraction for analysis by TIMS: *Analytical Chimica Acta*, v. 332, p. 269-275.

Creaser, R.A., Papanastassiou, D.A., and Wasserburg, G.J., 1993, Rhenium-osmium isotope systematics of group IIA and group IVA iron meteorites [abs.]: Geological Association of Canada-Mineralogical Association of Canada Annual Meeting, Edmonton, Abstracts, p.A20.

Creaser, R.A., Papanastassiou, D.A., and Wasserburg, G.J., 1991, Negative thermal ion mass spectrometry of osmium, rhenium and iridium: *Geochimica et Cosmochimica Acta*, v. 55, p. 397 – 401.

England, J., Reisberg, L., Marcantonio, F., and Zindler, A., 1992, Comparison of one- and two-color ionization schemes for the analysis of osmium and rhenium isotopic ratios by sputter-induced resonance ionization mass spectrometry: *Analytical Chemistry*, v. 64, p. 2623 – 2627.

Fehn, U., Teng, R., Elmore, D., and Kubik, P.W., 1986, Isotopic composition of osmium in terrestrial samples determined by accelerator mass spectrometry: *Nature*, v. 323, p. 707-710.

Frei, R., Nägler, Th.F., Schönberg, R., and Kramers, J.D., 1998, Re-Os, Sm-Nd, U-Pb, and stepwise lead leaching isotope systematics in shear-zone hosted gold mineralization: genetic tracing and age constraints of crustal hydrothermal activity: *Geochimica et Cosmochimica Acta*, v. 62, p. 1925-1936.

Hirt, B., Tilton, G.R., Herr, W., and Hoffmeister, W., 1963, The half-life of ^{187}Re . In: Geiss, J. and Goldberg, E.D. (eds.): *Earth Science and Meteoritics*, North Holland Pub. P. 273 – 280.

Kirk, J., Ruiz, J., Chesley, J., Titley, Walshe, J., and England, G., 2002, A major Archean gold- and crust-forming event in the Kaapvaal craton, South Africa: *Science*, v. 297, p. 1856 – 1858.

Kirk, J., Ruiz, J., Chesley, J., Titley, and Walshe, J., 2001, A detrital model for the origin of gold and sulfides in the Witwatersrand basin based on Re-Os isotopes: *Geochimica et Cosmochimica Acta*, v. 65, p. 2149 – 2159.

Lichte, F.E., Wilson, S.M., Brooks, R.R., Reeves, R.D., Holzbecher, J., and Douglas, E.R., 1986, New method for the measurement of osmium isotopes applied to a New Zealand boundary shale: *Nature*, v. 322, p. 816 – 817.

Lindner, M., Leich, D.A., Russ, G.P., Bazan, J.M., and Borg, R.J., 1989, Direct determination of the half-life of ^{187}Re : *Geochimica et Cosmochimica Acta*, v. 53, p. 1597 – 1606.

Luck, J.M., and Turekian, K.K., 1983, Osmium-187 / Osmium-186 in manganese nodules and the Cretaceous-Tertiary boundary: *Science*, v. 222, p. 613-615.

Ludwig, K., 2000, Isoplot/Ex, version 2.22: A geochronological toolkit for Microsoft Excel: Geochronology Center Berkeley.

Ludwig, K., 1980, Calculation of uncertainties of U-Pb isotope data: *Earth and Planetary Science Letters*, v. 46, p. 212-220.

Meisel, T., Walker, R.J., and Morgan, J.W., 1996, The osmium isotopic composition of the Earth's primitive upper mantle: *Nature*, v. 383, p. 517-520.

Morelli, R.M., Creaser, R.A., Selby, D., Kontak, D.J., and Horne, R.J., 2005, Rhenium-osmium geochronology of arsenopyrite in Meguma Group gold deposits, Meguma Terrane, Nova Scotia, Canada; evidence for multiple gold-mineralizing events: *Economic Geology*, v. 100, p. 1229 – 1242.

Morgan, J.W., Horan, M.F., Walker, R.J., and Grossman, J.N., 1995, Rhenium-osmium concentration and isotope systematics in group IIAB iron meteorites: *Geochimica et Cosmochimica Acta*, v. 59, p. 2331-2344.

Morgan, J.W., Golightly, D.W., and Dorrzapf, A.F., 1991, Methods for the separation of rhenium, osmium and molybdenum applicable to isotope geochemistry: *Talanta*, v.38, p.259-265.

Peucker-Ehrenbrink, B., and Jahn, B., 2001, Rhenium-osmium isotope systematics and platinum group element concentrations: Loess and the upper continental crust: *Geochemistry, Geophysics, Geosystems*, v. 2, doi: 10.1029/2001GC000172.

Selby, D., and Creaser, R.A., 2001b, Late and Mid-Cretaceous mineralization in the northern Canadian Cordillera: constraints from Re-Os molybdenite dates: *Economic Geology*, v. 96, p. 1461-1467.

Selby, D., and Creaser, R.A., 2001a, Re-Os geochronology and systematics in molybdenite from the Endako porphyry molybdenum deposit, British Columbia, Canada: *Economic Geology*, v. 96, p. 197-204.

Selby, D., Creaser, R.A., Stein, H.J., Markey, R.J., and Hannah, J.L., 2007, Assessment of the ^{187}Re decay constant by cross calibration of Re-Os molybdenite and U-Pb zircon chronometers in magmatic ore systems: *Geochimica et Cosmochimica Acta*, v. 71, 1999 – 2013.

Shirey, S.B., and Walker, R.J., 1995, Carius tube digestion for low-blank rhenium-osmium analysis: *Analytical Chemistry*, v. 67, p. 2136-2141.

Smoliar, M.I., Walker, R.J., and Morgan, J.W., 1996, Re-Os ages of Group IIA, IIIA, IVA and IVB iron meteorites: *Science*, v. 271, p. 1099–1102.

Stein, H.J., Morgan, J.W., and Scherstén, A., 2000, Re-Os dating of low-level highly radiogenic (LLHR) sulfides: the Harnäs gold deposit, southwest Sweden, Records continental-scale tectonic events: *Economic Geology*, v. 95, p. 1657-1671.

Sun, W., Bennett, V.C., Eggins, S.M., Kamenetsky, V.S., and Arculus, R.J., 2003, Enhanced mantle-to-crust rhenium transfer in undegassed arc magmas: *Nature*, v. 422, p. 294–297.

Völkening, J., Walczyk, T., and Heumann, K., 1991, Osmium isotopic ratio determinations by negative thermal ionization mass spectrometry: *International Journal of Mass Spectrometry and Ion Physics*, v. 105, 147 – 159.

Walker, R.J., and Fassett, J.D., 1986, Isotopic measurement of subnanogram quantities of rhenium and osmium by resonance ionization mass spectrometry: *Analytical Chemistry* v. 5 p. 2923 – 2927.

Yu, G., Yang, G., Chen, J., Qu, W., Du, A., and He, W., Re-Os dating of gold-bearing arsenopyrite of the Maoling gold deposit, Liaoning Province, Northeast China and its geological significance: Chinese Science Bulletin, v. 50, p. 1509-1514.

3. Re-Os Low Level Sulfide Geochronology of Archean Orogenic Gold Deposits: A Feasibility Study

3.1. Introduction

The Late Archean was an important period in Earth history for the formation of new continental crust, with proposed crustal growth rates as high as 80-90% of the total present day volume during the interval 3200 to 2500 Ma (McLennan and Taylor, 1982). Concomitant with the formation of this new crust was the formation of hydrothermal gold deposits ('orogenic gold deposits', OGD; Groves et al., 1998) within many Late Archean granite-greenstone terranes worldwide (Hagemann and Cassidy, 2000; Goldfarb, 2001). Late Archean gold deposits include some of the largest individual deposits known on Earth and, to date, account for ~ 20% of total global gold production (Roberts, 1988). Despite their geologic and economic significance, the tectonothermal processes by which these deposits formed remain insufficiently understood. As reviewed by Kerrich and Cassidy (1994) and Hagemann and Cassidy (2000), the origin of Archean OGD has been attributed to an array of geologic processes.. Their common spatial association with specific rock types, such as felsic intrusions, mafic to ultramafic volcanic rocks, and mantle-derived lamprophyre dikes, has been interpreted to indicate a genetic relationship between each of these magmas and gold mineralization. In contrast, their presence in metamorphosed rocks and their broad temporal association with peak regional metamorphism has led to models invoking regional metamorphism as the driving force of gold mineralization, with metamorphic dehydration reactions providing a source of mineralizing fluids. Although the timing of magmatism and peak metamorphism are often clearly defined in well-studied Late Archean terranes, a lack of accurate and precise dates for gold mineralization has historically been problematic for accurate modeling of OGD genesis (see Kerrich and Cassidy, 1994).

As with most metalliferous ore deposits, this shortcoming largely stems from a lack of robust and/or paragenetically suitable silicate minerals that are common to orogenic gold deposits, and that are readily dateable with routinely used radioisotope systems, such as U-Pb, Ar-Ar, and Rb-Sr. In recent years there has been significant progress made in the application of the Re-Os geochronometer to 'low-level' sulfide

minerals (Stein et al., 2000) for dating ore deposition.. To this point, studies dealing directly with Archean OGD deposits have focused mainly on dating of molybdenite (Frei, 1998; Stein et al, 1998; Bucci et al., 2004; Marshik et al., 2005) due to its inherently high Re and low common Os contents (Stein et al., 2001). However, the lack of molybdenite in many Archean gold deposits requires dating of more common sulfide minerals by the Re-Os technique to assess the timing of ore formation. There is presently little information on the effectiveness of the Re-Os technique for dating of common sulfide minerals in Archean OGD. Initial attempts at Re-Os geochronology of Late Archean, low-level sulfide minerals were performed by Stein et al. (1998) and Frei et al. (1998). On the basis of a three point Re-Os pyrite regression, Stein et al. (1998) proposed the disturbance of primary Re-Os pyrite ages by millimeter-scale movement of Re and/or Os during upper greenschist to lower amphibolite grade regional metamorphism. Similarly, Frei et al. (1998) show that two Re-Os isotopic analyses of 'clastic arsenopyrite' plot on a 2600 Ma Re-Os molybdenite-scheelite isochron, and interpret this to record the timing of a Late Archean mineralizing event. However, the conclusions of both of these studies are compromised by the small data sets, and uncertain paragenesis of the sulfide minerals relative to the main mineralizing events. Kirk et al. (2001) subsequently reported relatively precise Re-Os isochron dates for gold from the enormous Witwatersrand deposits, South Africa, interpreted to reflect the crystallization age for gold and a presumed detrital origin for mineralization in the Witwatersrand Basin. However, the validity of this result has been challenged on both theoretical (Hannah et al, 2004) and statistical (section 2.6, this study) grounds. The conclusions of their study are controversial amongst researchers of the Witwatersrand deposits, and do not address the accuracy of the Re-Os technique for Archean gold deposits.

To date, there has not been a rigorous assessment of the utility of Re-Os low-level sulfide geochronology for dating Archean gold deposits. The objective of this study is to test the accuracy of the chronometer against Archean deposits with well-defined mineralization ages, as defined by other robust chronometers (e.g. U-Pb zircon dating of cross-cutting igneous rocks). In doing so, three worldclass gold deposits from three different Archean cratons were studied: 1) the Red Lake deposit, Superior Craton,

Canada 2) the Golden Mile deposit, Yilgarn Craton, Australia and 3) the Con deposit, Slave Craton, Canada (Fig. 3.1).

The results of this study indicate that, even with the best analytical methodologies currently available, there are limiting factors for Archean, OGD-hosted sulfide minerals that hinder the routine application of this technique. These relate mainly to the appropriateness of sample preparation and spiking procedures, and include the inherently low primary Re (and $^{187}\text{Os}^*$) contents, the negligible common Os contents, and the commonly very fine-grained, disseminated nature of these sulfides. Notwithstanding these limitations, we demonstrate that accurate and reasonably precise Re-Os mineralization ages can be obtained from some low-level sulfide minerals, and show that this technique has the potential to become a fundamental part of Archean metallogenic studies.

3.2. Deposit Geology and Age Constraints on Mineralization

i. Red Lake Deposit

The Red Lake gold deposit is one of the largest gold deposits in Canada, with reserves of 1.775 million tonnes at an average grade of 80.6 g/t Au in the 'high grade zone' (Goldcorp Inc., 2003). The deposit is situated within the Red Lake greenstone belt of the Uchi Subprovince, Ontario (Fig. 3.2), which comprises an array of Mesoarchean volcanic rocks ranging from ultramafic to felsic calc-alkaline in composition. The main host to gold mineralization is polydeformed tholeiitic basalt and komatiitic basalt of the ca. 2.99 to 2.96 Ga Balmer assemblage, though other rock types are locally present at the mine site (Dubé et al., 2004, and references therein).

Several periods of deformation have affected the mine rocks, and the deposit itself is strongly structurally controlled. The main ore zone is situated within a high strain zone defined by a steeply dipping foliation that developed regionally during D_2 folding. Both the host rocks and mineralization were affected by middle- to upper-greenschist peak metamorphism (Penczak and Mason, 1997), which was synchronous with D_2 deformation at ca. 2720 – 2715 Ma (Thompson, 2003). This timing also coincides with emplacement of the third of four main stages of felsic plutonism in the greenstone belt. Gold ore at Red Lake is associated with carbonate alteration and is present as five different mineralization

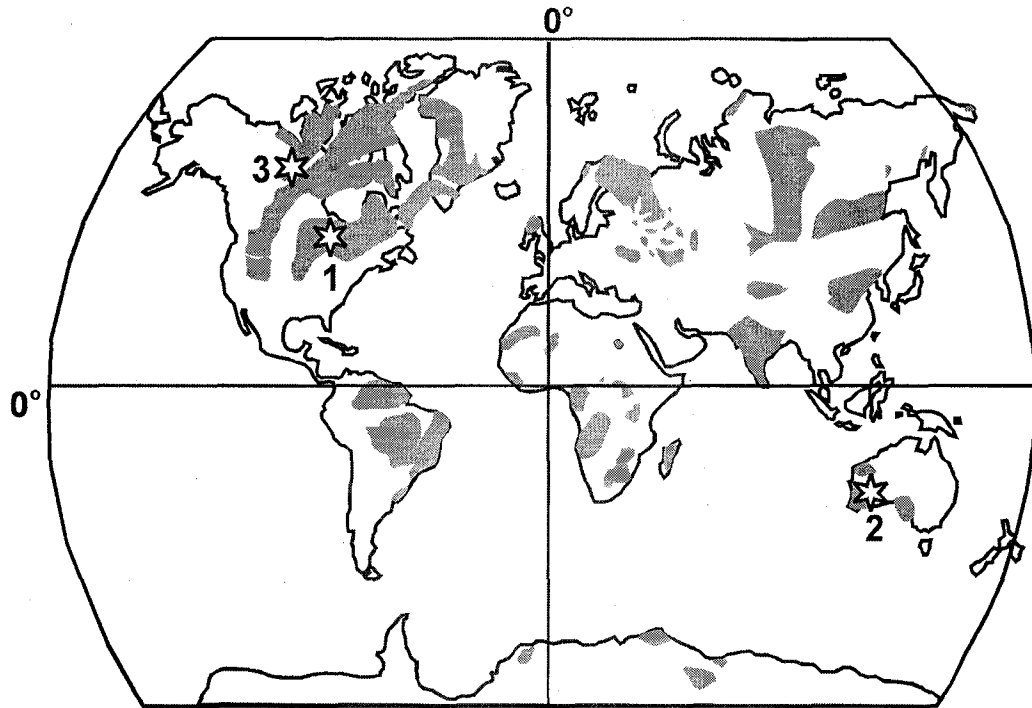


Figure 3.1: Location of Archean cratons worldwide, and of Late Archean orogenic gold deposits sampled for this study (stars). 1 = Red Lake deposit, Superior Province, Canada; 2 = Golden Mile deposit, Yilgarn Craton, Australia ; 3 = Con deposit, Slave Province, Canada. Modified from Kusky and Polat (1999).

styles (Dubé et al., 2004), though the high-grade arsenopyrite-rich silicification style was the focus of this study.

The timing of main stage gold mineralization is addressed in three comprehensive studies of Red Lake mineralization (Corfu and Andrews, 1987; Penczak and Mason, 1997; Dubé et al., 2004), which collectively provide a good framework by which to test the accuracy of the Re-Os results. The minimum age of gold mineralization is provided by a 2712 ± 2 Ma age from sensitive high resolution ion microprobe (SHRIMP) U-Pb zircon analysis of a feldspar porphyry granodiorite dike that cuts high-grade, arsenopyrite-rich carbonate/quartz veins (Dubé et al., 2004). This age corresponds well with the 2714 ± 4 Ma U-Pb TIMS (thermal ionization mass spectrometry) zircon age from a quartz porphyry dike from within the Red Lake mine (Corfu and Andrews, 1987), though a minimum gold mineralization age of 2700 Ma is suggested by these authors on the basis of a U-Pb zircon upper intercept age of 2701 ± 5 Ma from a late granodiorite dike that postdates gold mineralization. Moreover, Corfu and Andrews (1987) determined U-Pb TIMS ages of 2720 ± 2 Ma and 2718 ± 1 Ma for the McKenzie and Dome Stocks, respectively, both of which are located within ~ 10 km of the deposit (Fig. 3.2) and predate the main (D2) phase of deformation, thus providing a plausible maximum mineralization age of ca. 2720 Ma. This range is in accordance with the interpretation of Penczak and Mason (1997) and Dubé et al., (2004), who set the maximum age of D2 deformation and, hence, gold mineralization at 2723 Ma, based on the same McKenzie Stock results. The consensus age for main stage gold mineralization at Red Lake is thus bracketed between 2722 Ma and 2710 Ma.

ii. Golden Mile Deposit

The Golden Mile deposit, which has produced in excess of 1450 t gold, is situated within the Kalgoorlie gold camp of the Eastern Goldfields province, Yilgarn Craton, western Australia. This deposit is the largest of several that were formed within second order structures along the craton-scale Boulder Lefroy shear zone (Fig. 3.3). The majority of gold deposits in the Eastern Goldfields province are located in the Norseman-Wiluna greenstone belt, which consists predominately of ca. 2720 – 2660 Ma ultramafic to felsic volcanic rocks and subordinate clastic sedimentary and felsic plutonic rocks. Gold

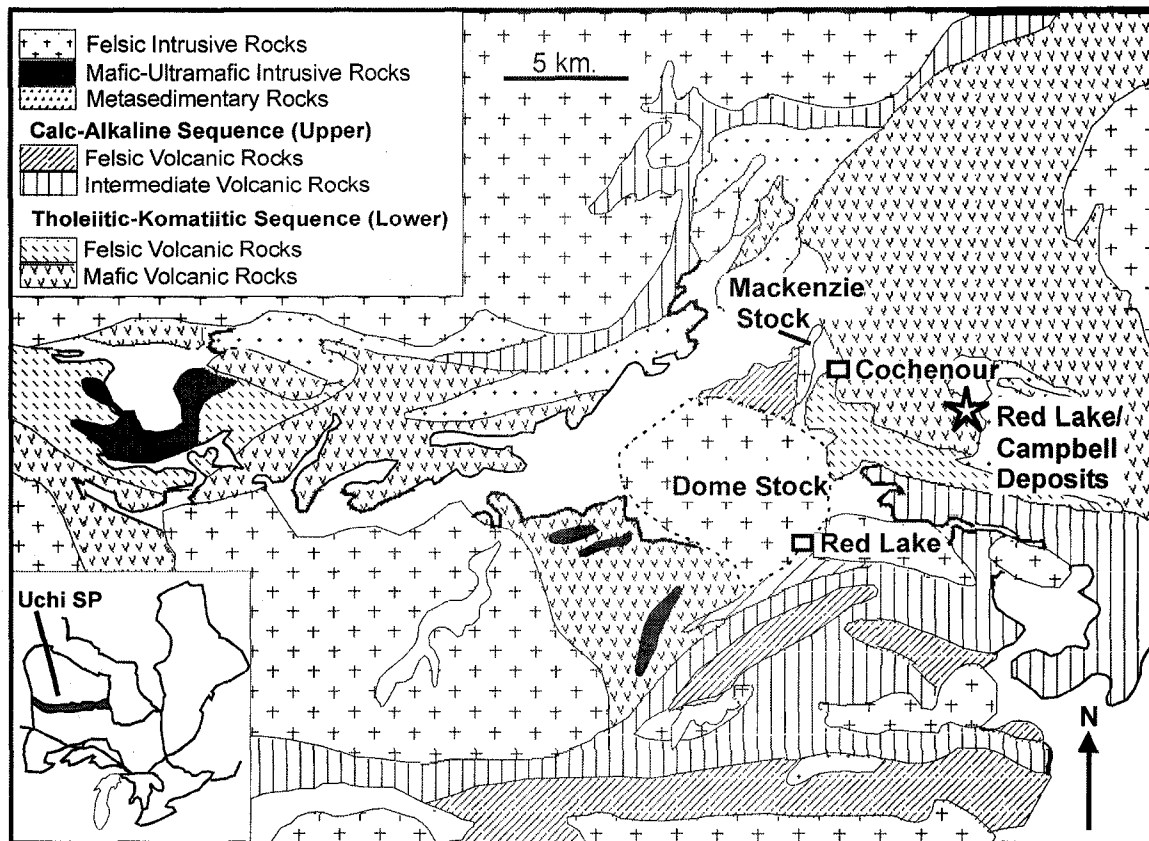


Figure 3.2: General geology of the Uchi Subprovince, Ontario, near the Red Lake gold deposit. Modified from Andrews et al. (1986).

mineralization at Golden Mile is hosted mainly within siliceous, iron-rich portions of an extensive differentiated dolerite sill ('Golden Mile sill') that was intruded into an unconformable contact between underlying mafic to ultramafic volcanic rocks of the Kambalda Group and volcanoclastic and clastic sedimentary rocks of the overlying Black Flag Group. This sequence, including the gold mineralization, was crosscut by a suite of felsic porphyritic dikes at ca. 2675 Ma, just after the cessation of peak metamorphism (Phillips, 1986).

A structural control on gold mineralization is apparent at Golden Mile, as gold-bearing veins have a strong association with zones of structural complexity. The host rocks to the deposit have been intensely folded and faulted during several periods of deformation. The deposit area is situated within an upright, northwest-trending anticline-syncline pair (the 'Kalgoorlie' anticline and syncline) and smaller parasitic folds on the main anticline's southwest limb. These folds are offset by major sinistral faults (e.g. Golden Mile and Boulder-Lefroy faults), which are themselves displaced by a series of brittle-ductile dextral faults that host gold-bearing quartz-carbonate veins. Rocks in the deposit area were metamorphosed to greenschist facies between ca. 2660 – 2630 Ma, and were subsequently chloritized upon introduction of hydrothermal fluids. Gold mineralization at Golden Mile is characterized by two different styles (Fimiston and Oroya lodes; Bateman et al., 2001) and is generally associated with pyrite, arsenopyrite, and tellurides hosted in quartz-carbonate-sericite veins.

Current constraints on the timing of gold mineralization in the Kalgoorlie camp are reviewed by Robert et al. (2005) and McNaughton et al. (2005). The best existing geochronological data indicate that gold mineralization may have been a protracted event in the district, and that different mineralization styles (e.g. Fimiston, Oroya lodes) represent emplacement in either two distinct, superimposed mineralization events or during a single, long-lived event. The age of Fimiston-style gold mineralization is bracketed by TIMS U-Pb zircon ages of ca. 2676 and 2663 Ma from pre- and post-ore feldspar porphyry dikes, respectively, though the possibility that these may be inherited zircons must be considered (Robert et al., 2005). The age of Oroya style mineralization appears to be younger, as indicated by recent U-Pb zircon and monazite dates by SHRIMP ion microprobe. Magmatic-hydrothermal zircon analyses from a

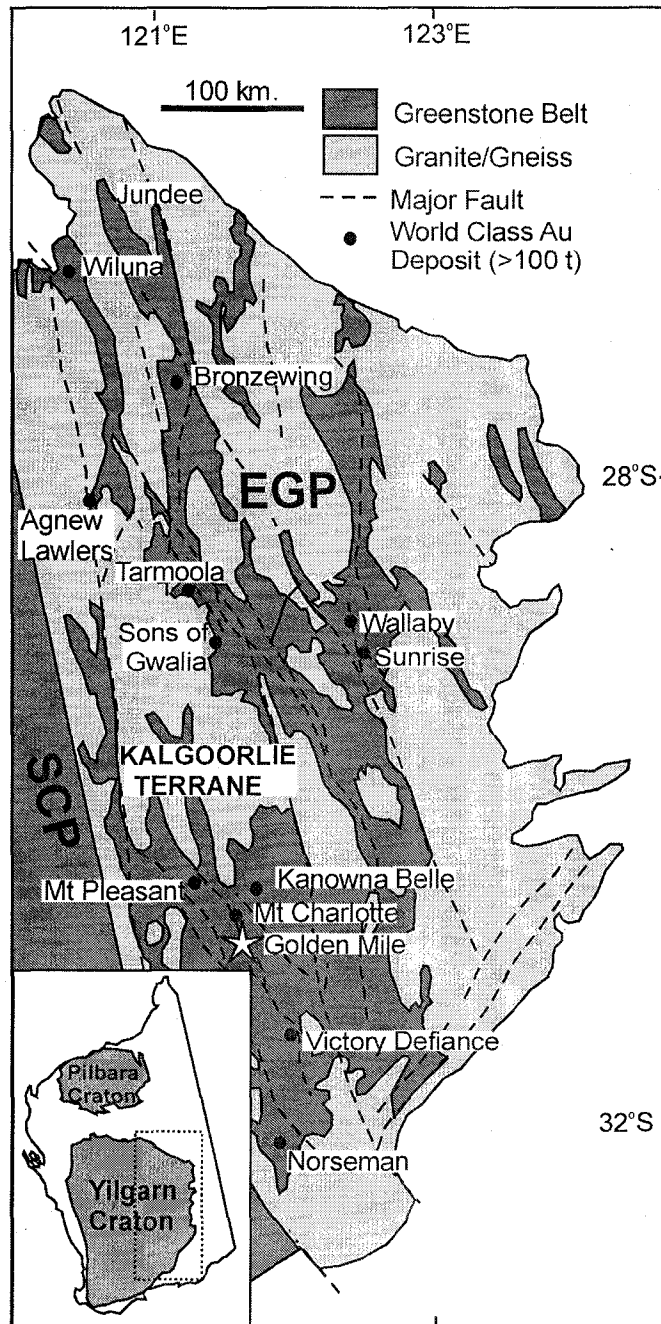


Figure 3.3: General geology of the Eastern Goldfields, Australia, near the Golden Mile gold deposit. EGP = eastern Goldfields Province; SCP = Southern Cross Province. After Hagemann and Cassidy (2000).

synmineralization lamprophyre dike yield a weighted mean $^{207}\text{Pb}/^{206}\text{Pb}$ age of 2642 ± 6 Ma, whereas cogenetic hydrothermal monazite yields a concordant $^{207}\text{Pb}/^{206}\text{Pb}$ age of 2637 ± 20 Ma. These data indicate that the gold-bearing hydrothermal system at Golden Mile was at least periodically active from approximately 2675 to 2640 Ma.

iii. Con Deposit

The Con gold deposit is located near the city of Yellowknife, Northwest Territories, Canada. The deposit is one of several Archean orogenic gold deposits in the Yellowknife area, including the nearby Giant, Crestauram, and Ptarmigan deposits (Fig. 3.4). By the time of the closure of the Miramar Con mine in 2003, the deposit had produced over 5.8 million ounces of gold and 180,000 ounces of silver (Hauser et al., 2006). It is situated within the north-south trending Yellowknife Greenstone Belt of the Yellowknife Domain, Slave Province, which consists predominantly of ca. 2.7 Ga Kam Group mafic volcanic rocks, ca. 2.66 Ga intermediate volcanic and intrusive Banting Group rocks, and clastic sedimentary rocks derived from these groups. Two main granitoid suites, known as the Defeat (~ 2630 – 2620 Ma; Davis and Bleeker, 1999) and Prosperous (~2600 – 2585 Ma; Davis and Bleeker, 1999) suites, were intruded into the greenstone belt contemporaneously with belt-wide metamorphism. The deformational history of the belt comprises four generations of structures (Martel et al., 2002), with a recognizable change from homogeneous to heterogenous strain that might be related to focusing of gold-bearing fluids along narrow high-strain zones (Thompson, 2006). Gold mineralization is hosted by quartz-carbonate-sericite veins or lenses within or proximal to two parallel north-striking, west-dipping shear zones known as the Con and Campbell shears.

Gold mineralization in the Con orebody comprises two distinct styles: refractory and free-milling ore (Falck, 1992). The relative timing relationships between the two styles is currently not well understood, though textural observation suggest that the refractory ore, characterized by extremely fine gold particles hosted within fine-grained pyrite, arsenopyrite, and sulfosalts, is the earlier of the two styles. The free-milling style is associated with quartz veins and includes coarse gold grains that can be independent of sulphide minerals or occur within late sulfide veins. These veinlets may contain one or

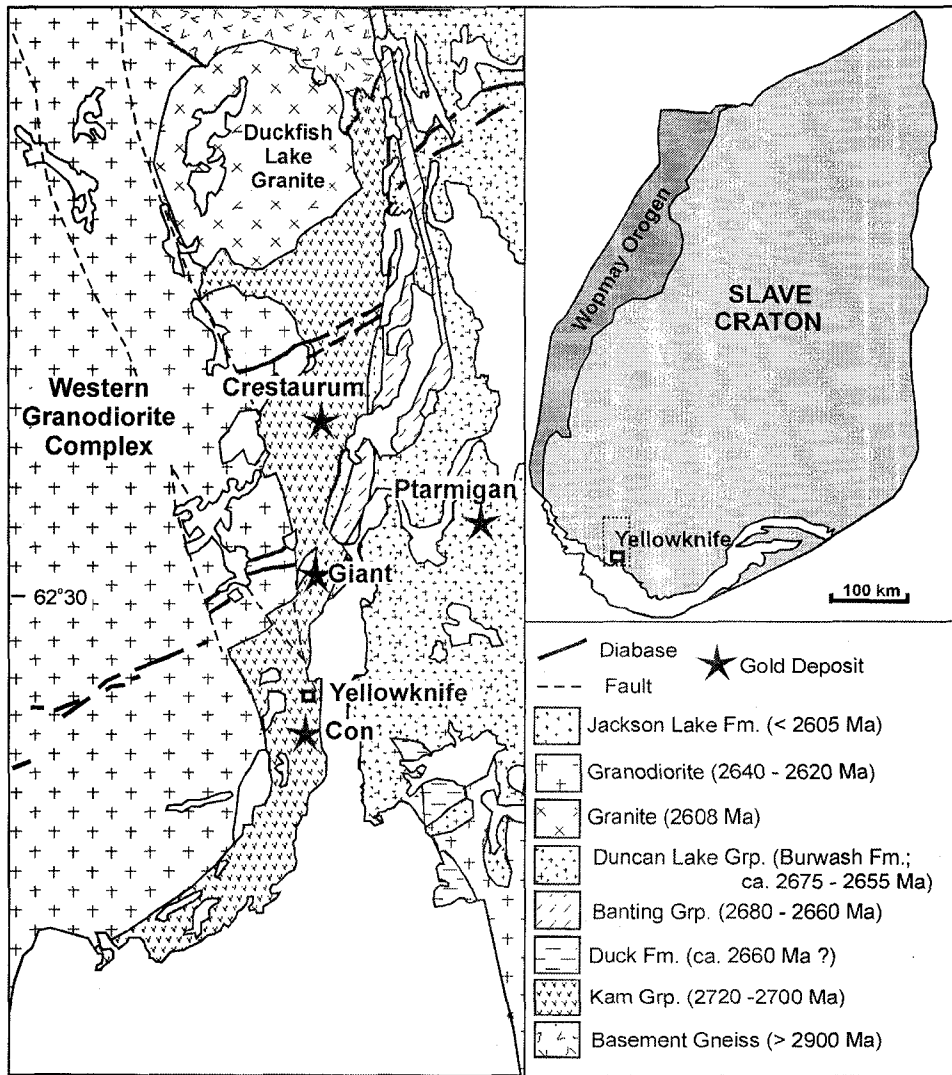


Figure 3.4: General geology of the Yellowknife Greenstone Belt, Northwest Territories, near the Con gold deposit. Modified from Cousens et al (2006a).

more of several sulfide minerals, including pyrite, arsenopyrite, sphalerite, galena, chalcopyrite, and/or molybdenite.

Of the three deposits examined in this study, the Con deposit is the least studied, and the age of main stage gold mineralization is thus the least well constrained. Ootes et al. (2007) obtained U-Pb zircon and Re-Os molybdenite ages of ca. 2670 Ma from the Ryan Lake stock, which predates main stage gold mineralization at the Crestauram deposit. The Re-Os molybdenite ages were attributed to an early mineralization event coincident with magmatic activity during emplacement of Banting Group igneous rocks, and that predated Yellowknife district gold mineralization. Refractory-style gold mineralization is interpreted to be synchronous with the development of the regional S₁ foliation prior to 2640 – 2620 Ma, though could possibly be related to early D₂ deformation at ca. 2600 Ma (Ootes et al., 2003). Shelton et al. (2004) suggest that the emplacement of quartz veins bearing free-milling ore occurred sometime after 2620 Ma during D₂ deformation, possibly at around 2580 Ma. This interpretation is generally consistent with recent U-Pb dates from ca. 2595 Ma from felsic intrusive rocks that texturally predate free-milling ore (H. Falck, pers. comm.). Together, these timing constraints indicate a protracted mineralization event in the Yellowknife greenstone belt, during which refractory gold was likely emplaced between 2640 and 2620 Ma (but possibly as late as 2600 Ma), followed by deposition of free-milling gold ore at or after ~ 2600 Ma.

3.3 Sampling and Mineral Separation

Sulfide samples for Re-Os analysis from Red Lake were taken from three different sources: surface outcrop exposure, drill core, and underground exposures (see Table 3.1). Surface-derived samples were taken from a stripped outcrop near the town of Cochenour, which was the focus of detailed mapping study by Williamson and Dubé (2003). Core samples were derived from drill holes that intersected mineralization, and were chosen on the basis of assay results that showed elevated values of both Au and As. Underground samples were derived from level 35 of the Red Lake mine, and were taken *in situ* from the mine wall. All Red Lake sulfide samples consisted of a single generation of fine-grained (~1 mm) disseminated needles of arsenopyrite in silicified basalt (Fig.

5a), a phase known to be paragenetically equivalent to main stage gold mineralization at Red Lake (G. Beakhouse, pers. comm.). In addition to arsenopyrite, samples D2 and D3 consisted of fine-grained gersdorffite (NiAsS) see Table 3.1).

All Red Lake samples were wrapped in plastic and broken by a hammer covered in duct tape to avoid contamination. The broken pieces were then crushed by hand with an agate mortar and pestle, and the resulting powder was then sieved. The 70-200-mesh fraction of each sample subsequently underwent density separation using methyl iodide in order to separate the sulfide and silicate fractions. The sulfide (heavy) fraction was put through a FrantzTM magnetic separator at consecutive amperages of 1.0, 1.25, 1.6, 1.8, 1.9 and 2.0 A. Arsenopyrite was purified as the non-magnetic fraction at > 2.0 A, whereas gersdorffite was removed as the magnetic fraction between 0.5 and 1.0 A. Hand picking was subsequently performed to attempt removal of remaining impurities.

The sample from the Golden Mile deposit consisted of a small (3 x 1.5 x 1 cm) portion of a carbonate-quartz vein and its contained components. The sample was composed entirely of coarse-grained, subhedral calcite, quartz, arsenopyrite, and scheelite, with individual crystal sizes ranging from ~ 0.5 - 2 cm across (Fig. 3.5b). The arsenopyrite is interpreted to be temporally equivalent to the gold mineralizing event at Golden Mile deposit (A. Mueller, pers. comm.). The sample was wrapped in plastic and broken into cm-sized fragments with a tape-covered hammer. Individual pieces of arsenopyrite and scheelite were picked out into separate ca. 500 mg aliquots for Re-Os analysis, and were crushed with an agate mortar and pestle. An oxidization tarnish noted on small fracture surfaces within all arsenopyrite crystals was avoided as much as possible.

Samples from the Con deposit were collected from mine workings of the former Miramar Con mine. The sample used for Re-Os analysis consisted of a quartz-vein hosted veinlet of pyrite of a single generation that was ~ 0.2 - 1.5 cm thick (Fig. 5c). Petrographic examination of this sample revealed no other sulfide mineral or metallic phases. The thickest portions of the veinlet were cut out by a rock saw into individual 3 x 2 x 0.5 cm pieces. These pieces were wrapped in plastic and broken with a tape-covered hammer, and then crushed in an agate shatterbox. The 70 - 200 mesh sieved fraction then

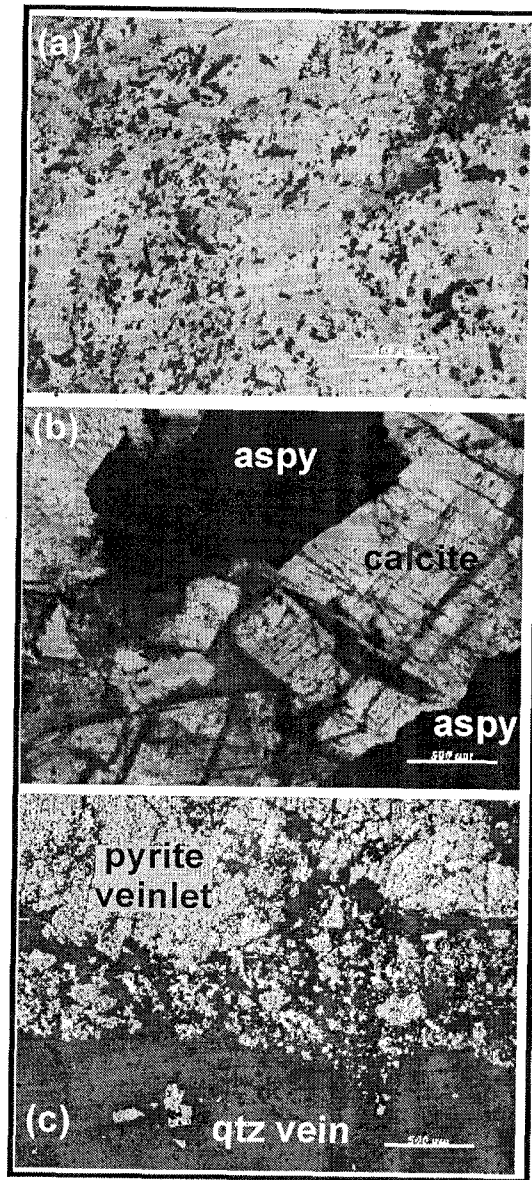


Figure 3.5: Photomicrographs of sulfide samples used for Re-Os isotopic analysis in this study, including (a) fine-grained sulfide minerals hosted by silicified basalt from the Red Lake deposit, (b) coarse-grained arsenopyrite in a carbonate-quartz vein from the Golden Mile deposit, and (c) a quartz vein-hosted pyrite veinlet from the Con deposit.

underwent density separation in methyl iodide, after which a pure pyrite fraction remained.

3.4 Results

The results of Re-Os isotopic analysis from all three deposits are shown in Table 3.1. In total, 15 Re-Os analyses of Red Lake sulfides were performed on either arsenopyrite (12) or gersdorffite (3). All samples fall within a range of total Re concentrations from 0.06 – 1.08 parts per billion (ppb), with the exception of arsenopyrite sample D10-1, which returned a result of 3.9 ppb. This range of Re concentrations resulted in the sulfides having a corresponding range in radiogenic ^{187}Os ($^{187}\text{Os}^*$) concentrations from ~ 6 – 88 ppt. These samples are characterized by quite variable common Os contents, as evident from ^{192}Os contents ranging between ~ 1 and 45, with the majority containing < 10 ppt. These Re and Os concentrations result in the Red Lake samples having significant spread along an isochron diagram, with $^{187}\text{Re}/^{188}\text{Os}$ ratios ranging from ~ 7.5 – 1570.

Collective regression of all arsenopyrite and gersdorffite samples yields a Model 3 (Ludwig et al., 2000) ‘errorchron’ age of 3040 ± 170 Ma on a $^{187}\text{Re}/^{188}\text{Os}$ vs. $^{187}\text{Os}/^{188}\text{Os}$ plot (MSWD = 216; Fig. 3.6). If only arsenopyrite analyses are included in the regression, the result is unchanged at 3028 ± 190 Ma (MSWD = 268; Fig. 3.6), whereas regression of only gersdorffite analyses yields a geologically impossible result. Regression of individual groups of samples (e.g. drillcore vs. underground) does not change the result. The initial $^{187}\text{Os}/^{188}\text{Os}$ composition (Os_i) derived from regression of all Red Lake analyses is -1.1 ± 2.6 , and that derived from regression of only arsenopyrite analyses is -1.6 ± 2.1 .

Arsenopyrite from the Golden Mile deposit contained consistently low Re contents (0.23 – 0.44 ppb) and $^{187}\text{Os}^*$ contents of between 6.2 and 12 ppt. The very low common Os contents of these sulfides (< 0.79 ppt ^{192}Os) results in their having very radiogenic Re-Os isotopic compositions, with $^{187}\text{Re}/^{188}\text{Os}$ ratios ranging from ~ 940 to 12,000. Regression of the seven Re-Os isotopic analyses for Golden Mile arsenopyrite yields a Model 3 age of 2542 ± 120 Ma (MSWD = 4.3; Fig. 3.7). If sample regression is instead performed using concentrations of ^{187}Re and $^{187}\text{Os}^*$ in order to compensate for

Table 3.1: Re-Os data for sulfides from select Archean orogenic gold deposits.

Sample	Sample wt. (g)	Re (ppb)	¹⁸⁷ Os* (ppt)	¹⁸⁷ Re/ ¹⁸⁸ Os	2σ unc. ²	¹⁸⁷ Os/ ¹⁸⁸ Os	2σ unc. ²	error corr. (ρ) ²	¹⁹² Os (ppt)	model age (Ma) ³
Red Lake¹:										
<i>U3b-1</i>	0.399	0.62	18	1300	760	60	35	0.993	1.1	—
<i>U3cd-2</i>	0.457	0.18	6.1	43.9	1.7	2.43	0.11	0.571	8.3	—
<i>U4-1</i>	0.403	1.08	32	48.64	0.55	2.37	0.04	0.549	44.3	—
<i>D1-1</i>	0.197	0.06	1.6	7.6	3	0.41	0.11	0.543	17.1	—
<i>D10-1</i>	0.344	3.9	132	1070	170	56.8	9.1	0.998	7.4	—
<i>D10-2</i>	0.583	0.48	88	891	26	46.2	1.6	0.853	6.0	—
<i>D10b-1</i>	0.402	0.56	10	343	22	9.71	0.7	0.891	3.3	—
<i>D10b-2</i>	0.521	0.55	14	161.6	4.4	6.93	0.21	0.825	6.7	—
<i>D10c-1</i>	0.405	1.2	37	355	11	17.2	0.57	0.920	6.8	—
<i>D10c-2</i>	0.502	1.2	45	54.93	0.47	3.46	0.04	0.557	42.3	—
<i>CO2-1</i>	0.396	1.6	53	1570	160	80.1	8.1	0.987	2.1	—
<i>CO2-2</i>	0.327	1.6	53	1510	180	77.7	9.2	0.982	2.2	—
<i>D2-1 (G)</i>	0.504	0.54	15	425	33	18.9	1.6	0.898	2.5	—
<i>D3-1 (G)</i>	0.553	0.48	14	405	29	18.7	1.4	0.898	2.3	—
<i>D3-2 (G)</i>	0.404	0.34	9.2	388	47	16.9	2.2	0.935	1.7	—
Golden Mile:										
<i>Ka-1</i>	0.413	0.37	0.0	940	470	39	20	0.999	0.79	—
<i>Ka-2</i>	0.412	0.28	0.0	990	700	45	32	0.999	0.55	—
<i>Kb-1</i>	0.477	0.42	0	4400	1200	186	51	0.997	0.19	2484
<i>Kb-3</i>	0.496	0.33	0.0	8500	5300	360	220	0.999	0.05	2467
<i>Kb-4</i>	0.501	0.44	0	6000	2000	268	89	0.997	0.15	2640
<i>Kb-5</i>	0.504	0.23	0.0	12000	16000	520	680	0.999	0.04	2461
<i>Kb-6</i>	0.512	0.44	0	1860	190	79.2	8.2	0.984	0.47	—
Con:										
<i>C-1a (P)</i>	0.400	0.22	6.0	332	16	15.44	0.79	0.944	1.3	—
<i>C-1c (P)</i>	0.409	0.22	6.0	428	26	19.6	1.2	0.969	1.0	—
<i>C-2c-a (P)</i>	0.392	0.20	5.6	171.3	4.9	8.35	0.25	0.928	2.3	—
<i>C-2c-c (P)</i>	0.393	0.18	5.0	206.7	7.9	9.81	0.39	0.924	1.7	—
<i>C-5b (P)</i>	0.406	0.36	10	468	19	21.61	0.91	0.953	1.5	—
<i>C-5c (P)</i>	0.406	0.33	8.7	443	19	20.1	0.90	0.949	1.4	—
<i>C-6a (P)</i>	0.395	0.37	10	276.4	7.2	13.1	0.40	0.839	2.7	—
<i>C-7a (P)</i>	0.411	0.17	4.8	241	11	11.5	0.60	0.876	1.4	—

¹U = underground samples, D = drill core samples, CO = samples derived from Cochenour outcrop; gersdorffite samples denoted by (G), pyrite samples denoted by (P); all other entries are arsenopyrite analyses.

²2σ uncertainties and the error correlation function are calculated according to the procedure described in Chapter 2.6; the large uncertainty in ¹⁸⁷Re/¹⁸⁸Os and ¹⁸⁷Os/¹⁸⁸Os in more radiogenic samples results primarily from propagation of the uncertainty in the blank ¹⁸⁸Os abundance.

³model ages are calculated only for samples with ¹⁸⁷Re/¹⁸⁸Os ratios of ~ 5000 or greater, and assume an Os_i of 0.10.

Note: raw ¹⁸⁷Os/¹⁸⁸Os NTIMS measurements typically have a precision of 0.1 - 0.8% in this study.

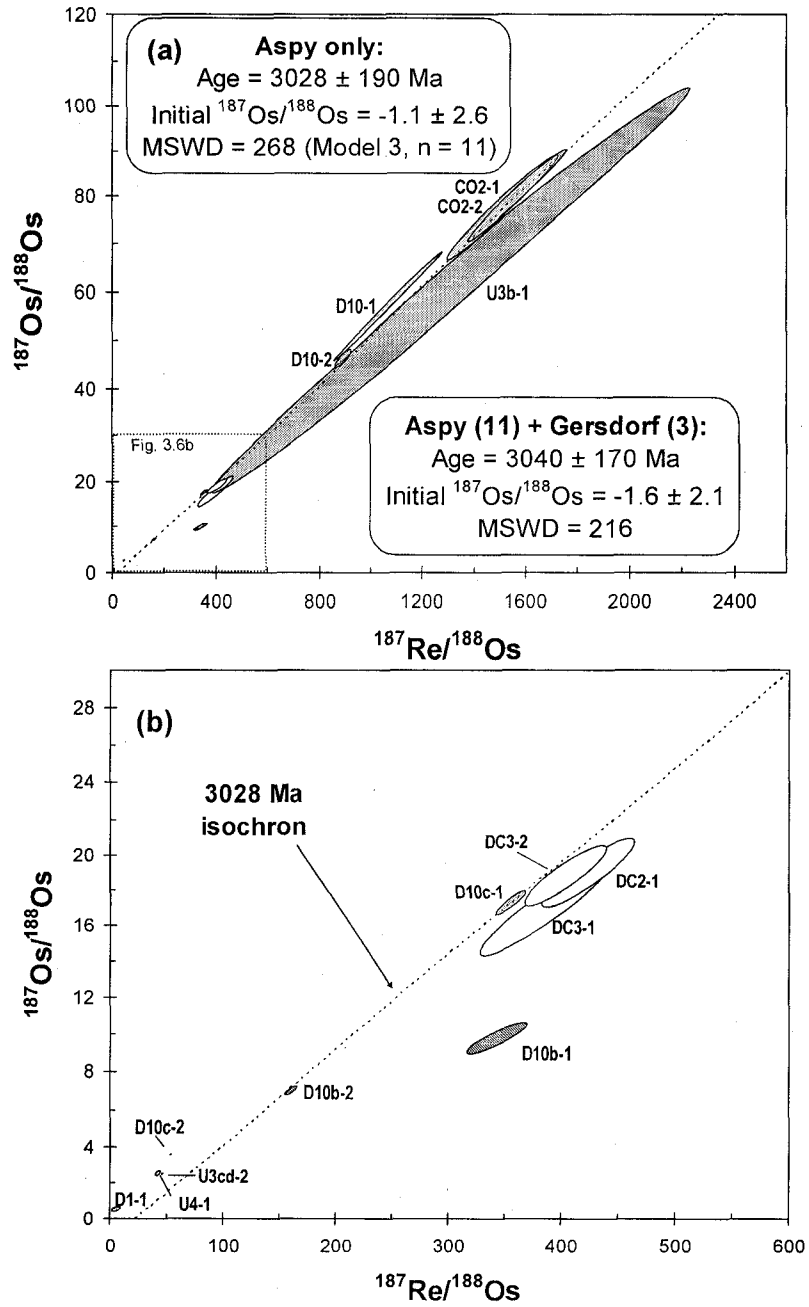


Figure 3.6: Results of linear regression of Re-Os analyses of Red Lake arsenopyrite and gersdorffite.

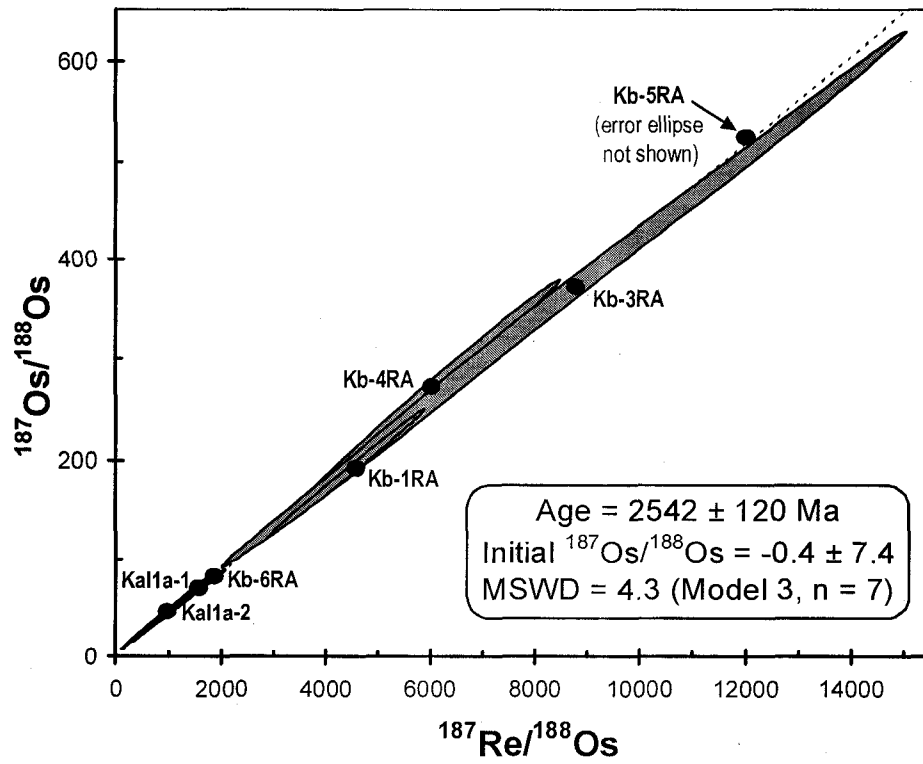


Figure 3.7: Results of linear regression of Re-Os analyses of Golden Mile arsenopyrite.

their highly radiogenic compositions (Stein et al., 2000), a similar but less precise result of 2581 ± 410 Ma (MSWD = 4.1) is determined. Additionally, the radiogenic character of four of the seven samples renders them suitable for model age calculation (Arne et al., 2001; Morelli et al., 2004), the results for which range from 2467 – 2640 Ma. The conventional ($^{187}\text{Re}/^{188}\text{Os}$ vs. $^{187}\text{Os}/^{188}\text{Os}$) isochron regression yielded a very imprecise Os_i of -0.4 ± 7.4 .

Of the three deposits investigated in this study, analyses of pyrite from the Con deposit returned the most promising result. Re-Os isotopic compositions of Con pyrite were relatively unradiogenic, yielding $^{187}\text{Re}/^{188}\text{Os}$ ratios between 170 and 470. The eight Re-Os analyses yield a well-defined Re-Os isochron with a slope corresponding to an age of 2591 ± 37 Ma (Model 1, MSWD = 1.3; Fig. 3.8). Their unradiogenic character allows determination of a reasonably precise Os_i of 0.78 ± 0.17 .

3.5. Discussion

Despite the potential advantages of Re-Os sulfide geochronology for dating hydrothermal ores, the youth of the technique requires implementation of a cautious and systematic approach to prospective applications. This is especially important for the case of Archean sulfide minerals, considering the paucity of existing work that characterizes the typical Re-Os contents and isotopic compositions of Archean sulfides, as well as the extensive time during which their original Re-Os isotopic compositions could be disturbed by younger geological events. Previous low-level sulfide Re-Os studies have disregarded the requirement to systematically prove the accuracy of the technique by testing it in deposits that have established age constraints. The following discussion provides an assessment of the Re-Os results from Archean orogenic gold deposits, and provides recommendations for the future application of the Re-Os sulfide technique for dating Archean ore deposits.

Re contents of Archean sulfides

The feasibility of this application hinges on whether Archean sulfide minerals typically contain enough Re for quality Re-Os isotopic analysis. This is not only important for determination of the amount of parent ^{187}Re in the sulfides, but also for the

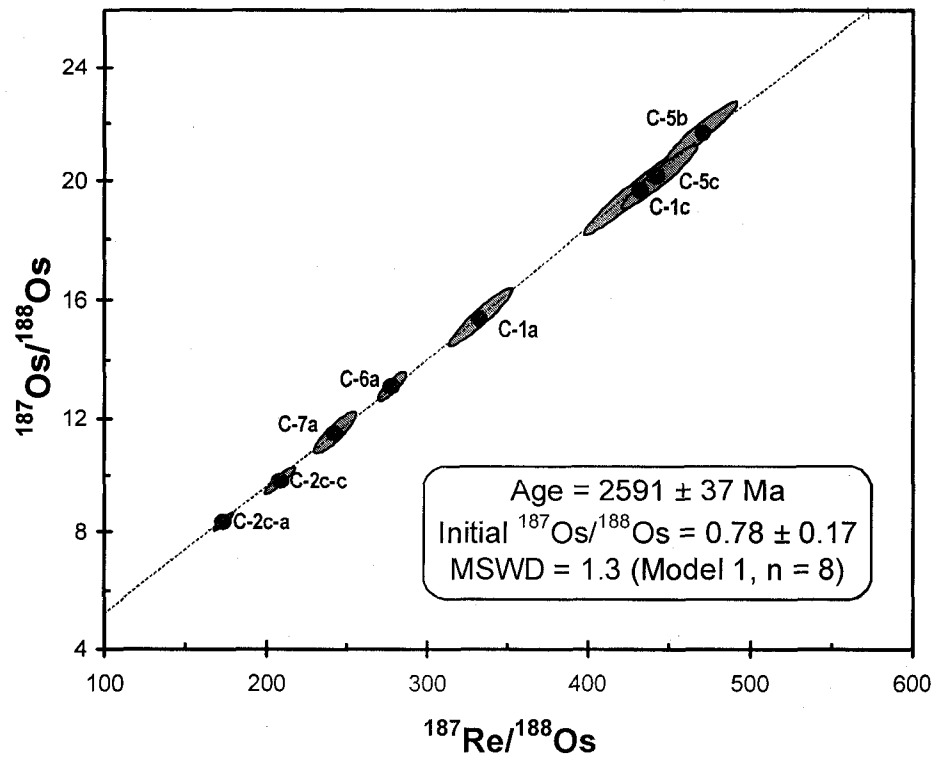


Figure 3.8: Re-Os pyrite isochron from the Con Deposit, Northwest Territories, Canada.

amount of daughter $^{187}\text{Os}^*$, which can be estimated if the approximate age of the sample is known. The data presented herein suggest that low concentrations of $^{187}\text{Os}^*$ appear to be a substantial impediment to the success of Archean Re-Os sulfide geochronology.

To assess the characteristic Re and ^{187}Os contents of sulfide minerals in Archean OGD, Re concentration data from pyrite and arsenopyrite are compiled (Fig. 3.9) and compared to Re contents of pyrite and arsenopyrite from post-Archean OGD. Such a comparison allows for detection of variation in Re content that does not result from a mineralogical control.

The minimum required amount of $^{187}\text{Os}^*$ separated from of a 400 mg sample to obtain a precise ($< 1\%$ SE) NTIMS measurement at the University of Alberta Radioisotope Facility is conservatively estimated to be 1.5 pg. This lower limit is depicted in Figure 3.9 as a dashed line, samples below which cannot confidently be dated using current Re-Os protocols. Samples that plot above this line should yield results with sufficiently precise results to calculate meaningful Re-Os ages. With the exception of one example (arsenopyrite from the Nicholas Lake deposit, NWT; 0.1 ppt Re), all tested Archean OGD sulfides plot above this lower limit, indicating that Re-Os geochronology of these samples is feasible. However, 70% of the tested Archean samples contain only 0.24 - 1.0 ppb Re, and lie just above the 1.5 ppt ^{187}Os hypothetical cutoff. In terms of overall Re and ^{187}Os contents, this compilation also reveals subtle trends that appear to differentiate Archean OGD sulfides from their post-Archean counterparts. Although based on a relatively small amount of data, these trends may hold important information on the source of Re to hydrothermal sulfide minerals.

It is possible to define two distinct fields for Re content of Archean OGD sulfides. Two sulfide samples from Archean OGD that are hosted in metasedimentary-dominated belts have an average Re content of ~ 22 ppb. This is in clear contrast to Archean OGD that are hosted by belts dominated by metavolcanic (greenstone) and felsic plutonic rocks, which have an average Re concentration of only 0.45 ppb. The two analyses of sulfides contained in Paleoproterozoic OGD (Homestake, Three Bluffs), both of which are iron formation-hosted, carry elevated average Re contents of between 35-100 ppb. Other analyzed post-Archean OGD include the Neoproterozoic Harnäs deposit in southwest Sweden, hosted by Mid-Proterozoic gneisses of tonalite-granodiorite to

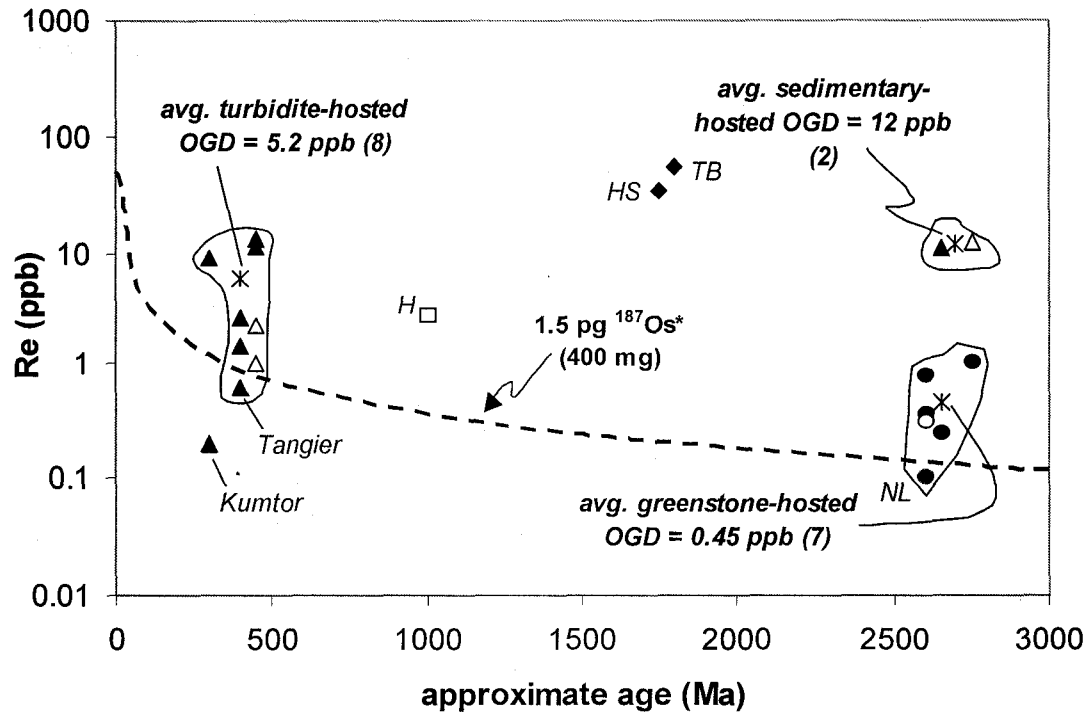


Figure 3.9: Plot of Re concentration of orogenic gold deposit-derived arsenopyrite and pyrite versus approximate deposit age. The dashed line represents a hypothetical lower threshold of $^{187}\text{Os}^* = 1.5 \text{ pg}$ for a 400 mg sample, required for precise Re-Os isotopic analysis; see text for details. H = Harnäs, Sweden; HS = Homestake, South Dakota, USA; NL = Nicholas Lake, Northwest Territories, Canada; TB = Three Bluffs, Nunavut, Canada. Data from this study, as well as Stein et al. (2000), Morelli et al. (2005), R. Creaser (pers. comm.), and T. Keith (pers. comm.).

granite-granodiorite composition (Stein et al., 2000), and a group of Paleozoic OGD that formed at different localities along the Paleo-Tethyan margin. The Paleozoic deposits, containing sulfides with an average 5.2 ppb Re, include examples produced during different orogenic episodes (e.g. Acadian, Lachlan, Tien Shan orogenises), but that are all hosted by turbiditic sequences. The only exception is pyrite from the Kumtor deposit in Kyrgyzstan, hosted by quartz veins in Vendian metasedimentary rocks in the Middle Tien Shan volcano-plutonic arc sequence, and which contains a much lower Re content of 0.2 ppb.

Based on structural, textural, and geochemical evidence, Archean and post-Archean OGD are thought to share a similar origin and fluid composition (Groves and Foster, 1993; Groves et al., 1998). Nevertheless, variation in the Re contents of OGD sulfides (pyrite and arsenopyrite) through time appears to reveal a difference between Archean and post-Archean deposits. An important parameter might be the observed secular change of the dominant host rock lithology at the ore depositional site (Groves et al., 1998). Largely a function of the proportion of dominant rock types present in gold-producing belts through time, combined with the capacity of a particular rock type to react with gold-bearing fluids, deposits in most Archean greenstone belts are hosted by ultramafic to mafic volcanic and felsic plutonic rocks (e.g. Colvine et al., 1988; Groves and Foster, 1993). This contrasts with Paleozoic OGD, which are commonly hosted by clastic sedimentary rocks in accretionary prisms that often contain black shales, a crustal Re (and Os) sink. Considering the patterns observed in Figure 3.9, the variation in Re content of OGD sulfides might not be a primary feature of the fluid/gold source, but rather reflects Re contents of the crustal lithologies within host terranes or ore depositional sites. With the exception of the Kumtor deposit, sulfides in OGD hosted by sedimentary rocks and/or in sedimentary rock-dominated belts have higher Re contents relative to OGD sulfides hosted in predominately volcano-plutonic belts (Figure 3.9). Assuming the presence shales in the host sedimentary sequences, this observation is broadly consistent with the typical Re concentrations for different rock types (Shirey and Walker, 1998), since Re contents of black shales (~ 517 ppb) greatly exceeds that of komatiites (<1.5 ppb) and basalts of all types (<2 ppb).

Hydrothermal transport of Re is greatly facilitated by an oxidizing fluid, even at high temperatures, since the solubility of ReS_2 is much less than that of ReO_2 (Xiong and Wood, 2002; Stein et al., 2003). If OGD hydrothermal fluids are sufficiently oxidizing to transport S, Au, and Re, it is reasonable to deduce that these fluids also have the capacity to interact with and leach Re from rocks encountered en route from the source to the depositional site, especially considering the presence of extensive wall rock alteration zones with most OGD.

Assessment and Implications of Re-Os results

i. Red Lake arsenopyrite and gersdorffite

To be a useful chronometer for dating ore mineralization events, any technique must provide sufficient accuracy and precision to resolve the ore-forming event from non-related geologic events. This is not the case for the determined Re-Os date from sulfides from the Red Lake deposit, for which the 3040 ± 170 Ma result is both imprecise and characterized by a large degree of data scatter (MSWD = 216). The derived age does not overlap the age brackets for mineralization at Red Lake, as they are currently understood. In this instance, the limitations of the Re-Os sulfide dating technique for dating Archean mineralizing events are apparent.

Three possible factors might have contributed to the inability to determine a meaningful Re-Os mineralization age for Red Lake sulfides. Firstly, disturbance of the Re-Os system in the sulfides might have occurred due to a younger thermal event. However, peak metamorphic conditions attained in the Red Lake area were only middle to upper greenschist facies (Christie, 1986; Thompson, 2003), which is probably insufficient to disturb the Re-Os arsenopyrite chronometer. This was shown by Morelli et al. (2005), who demonstrated that the Re-Os ages of arsenopyrite were undisturbed by temperatures that reset $^{40}\text{Ar}/^{39}\text{Ar}$ muscovite ages (i.e. $> 350^\circ\text{C}$), and is supported by Re-Os results in arsenopyrite from the Homestake deposit, South Dakota, which preserved primary age information through post mineralization temperatures of $400 - 500^\circ\text{C}$ (chapter 4, this study). Furthermore, there is considerable uncertainty as to whether peak metamorphism occurred before, during, or after ore deposition in the Red Lake belt (see Penczak and Mason, 1997).

It is considered more likely that the poor result from Red Lake sulfides is analytically-based. The two most obvious analytical issues to result in the observed discrepancies are (i) the low Re content of the Red Lake sulfides and (ii) the difficulty in acquiring a mineralogically pure sulfide separate for Re-Os analysis. The 15 Red Lake sulfide analyses used to perform the linear regression have an average Re content of ~ 1.1 ppb, which should permit sufficiently accurate and precise measurement of $^{187}\text{Os}^*$ (Figure 3.9). However, 7 of these 15 samples contain 0.56 ppb Re or less, with two samples containing < 0.2 ppb Re. These low Re contents not only make measurement of $^{187}\text{Os}^*$ challenging but also make these samples very sensitive to blank corrections. Impure mineral separates are probably a more important factor in this age discrepancy since regression of samples with higher Re contents (> 1 ppb) produces an equally inaccurate result (3018 ± 120 Ma, MSWD = 353). The fine-grained nature of arsenopyrite and gersdorffite related to main stage gold mineralization at Red Lake (see Fig. 3.5a) makes obtaining pure mineral separates problematic. Despite extensive efforts in mineral separation (e.g. sieving, methyl iodide, magnetic separation, hand-picking), the fine-grained, disseminated character of these sulfides makes it highly unlikely that a pure mineral separate was analyzed. This contention is supported by the observed presence of numerous unidentified minerals under binocular microscope in some Red Lake separates that were not readily removed during hand-picking. Any sulfide, oxide, or other Re- or Os-bearing mineral not removed from the separate and unrelated to the main stage of gold mineralization could potentially affect measured Re and/or Os isotopic composition of that separate, especially if the Re and Os contents of the OGD sulfides are very low. The determined Re-Os 'age' for the Red Lake sulfides (3040 ± 170 Ma) is significantly older than the current constraints on gold mineralization (2722 - 2710 Ma), but broadly overlaps the 2990 - 2960 Ma age range of the host Balmer Assemblage mafic volcanic rocks. This might suggest that Re and/or Os bearing minerals from the host rocks have been incorporated into some of the analyzed mineral separates, and influenced the determined isotopic compositions.

The determined Os_i of all analyzed Red Lake sulfides is -1.1 ± 2.6 . The inaccuracy in the Re-Os age and the gross imprecision in the measured ratio renders this value geologically meaningless, and no interpretation is provided.

ii. Golden Mile arsenopyrite

The determined Re-Os age for arsenopyrite from the Golden Mile deposit (2542 ± 120 Ma), although consistent within uncertainty with the 2675 – 2640 Ma age bracket for main stage gold mineralization in the Kalgoorlie district, is highly imprecise and the data exhibit minor scatter from the regression line (MSWD = 4.3). In contrast to the Red Lake result, the age derived from Golden Mile arsenopyrite is nominally younger than the true mineralization age. This could result from several natural or analytical issues. The observed internal fracturing of arsenopyrite and the ubiquitous oxidization staining of the fractured surfaces could represent zones of disturbed Re-Os isotopic composition, due to the flow of oxidizing fluids through the fractures subsequent to mineral crystallization. However, such surfaces were avoided as much as possible during mineral separation, or were ground off by a diamond-coated polishing surface when present. Another possibility, as considered with the Red Lake sulfides, is that the poor Re-Os result may be a consequence of post-crystallization thermal disturbance via open-system behaviour of Re and/or Os in the arsenopyrite. However, since peak metamorphic conditions attained in the immediate Kalgoorlie camp did not exceed upper greenschist facies (Robert et al., 2005) and due to the same lines of reasoning provided for the Red Lake sulfides, this possibility is again considered unlikely.

Analytical issues might explain the imprecision of the determined Re-Os ‘age’ for the Golden Mile arsenopyrite, but the coarsely crystalline nature of the Golden Mile arsenopyrite sample (Fig. 3.5b) means that mineral impurity is unlikely to be a problem in this case. The consistently low Re (0.28 – 0.44 ppb) and low $^{187}\text{Os}^*$ contents ($\sim 8 - 12$ ppt) of analyzed fractions might be problematic, due to sensitivity to procedural blank contributions and low signal strength during spectrometry. Another potential problem could be the extremely low common Os contents (0.4 – 0.8 ppt ^{192}Os), which could result in analytical uncertainties not captured by the conventional error propagation analysis. The very low common Os contents result in the Golden Mile arsenopyrite having a significantly more radiogenic Os isotopic composition than both the Red Lake and Con sulfides (Table 3.1), making the final Os isotopic composition very sensitive to both spike unmixing and fractionation correction procedures when using a monoisotopic (^{190}Os) spike. Even a small deviance of the true spike isotopic composition from that

measured and used during spike unmixing could potentially have a significant impact on determined Re-Os isotopic compositions for these low-level radiogenic sulfides. Additionally, the inability to accurately measure $^{192}\text{Os}/^{188}\text{Os}$ ratios for these arsenopyrites makes Os fractionation corrections of dubious value, since such corrections are made by normalization of the measured value to the natural Os isotopic composition ($^{192}\text{Os}/^{188}\text{Os} = 3.08271$). To better assess the effects of these factors, and to eliminate them from future studies on minerals with similar Re-Os isotopic characteristics, it is suggested that a dilute, mixed ^{185}Re - ^{188}Os - ^{190}Os spike be used (see Markey et al., 2002). Although Markey et al. (2002) claim that this double spike is also suitable for use with LLHR sulfides through a gravimetric dilution, our findings indicate that this is not a valid assumption due to apparent changes in Re and/or Os abundances of mixed Re-Os spikes (both mono- and double Os isotope) during gravimetric dilutions (see section 2.5). It is therefore suggested that future geochronological studies of Archean LLHR be performed using a dilute, mixed Re-double Os isotope spike solution that has been calibrated directly against gravimetric standards of well-characterized composition.

Linear regression of the seven Golden Mile arsenopyrite analyses yielded an Os_i of -0.4 ± 7.4 . As with the Red Lake sulfides, the imprecision of this value precludes a meaningful interpretation. It is noteworthy, however, that the maximum allowable Os_i for these arsenopyrites is 7.0 – considerably lower than the Os_i of ~ 925 determined by Lambert et al. (1998) for sulfides from the Revenge OGD deposit at Kambalda, western Australia. Considering that the Re-Os arsenopyrite age of 2542 ± 120 Ma for Golden Mile determined here is accurate within associated uncertainty, it is suggested that the Os_i determined by Lambert et al. (1998) is excessively high, and probably represents an analytical artifact.

iii. Con pyrite

The Re-Os pyrite age of 2591 ± 37 Ma for pyrite from the Con deposit is accurate within the confines of the existing age constraints (post-2640 to ~ 2580 Ma) for gold mineralization in the Yellowknife Greenstone Belt. The accuracy and relative precision ($<1.5\%$, 2σ) of this age is an excellent result, especially considering the very low Re contents (< 0.4 ppb) of the pyrite; the ~ 400 mg maximum sample weight for the pyrite

samples used for Re-Os analysis corresponds to total filament loads of as little as 45 pg Re and 2 pg $^{187}\text{Os}^*$ for the least concentrated sample (C-7a) assuming 100% chemical yield. In contrast to the Red Lake and Golden Mile sulfides, this favourable result is only achievable because of the physical and compositional characteristics of the pyrite itself. Concentration of the sulfide mineral within a sizeable veinlet, itself hosted in (and buffered from the host rock by) a quartz vein, facilitates the acquisition of a pure sulfide mineral separate and drastically reduces the risk of contamination by other Re and/or Os-bearing mineral phases. Importantly, the pyrite itself carries sufficiently high Re concentrations to make measurement of its $^{187}\text{Os}^*$ contents feasible. Moreover, the relatively unradiogenic Re/Os isotopic compositions of the Con pyrite ($^{187}\text{Re}/^{188}\text{Os} = < 500$, compared to ca. 1000 – 12,000 for Golden Mile) justifies the use of a mixed ^{185}Re - ^{190}Os spike solution, and validates the effectiveness of spike unmixing and Os isotope fractionation procedures for samples of this type.

The determined 2σ uncertainty for the Con pyrite Re-Os age is not low enough to confidently discriminate between the geologic processes that played a role in the mineralization process. This level of precision is also below that achieved in rare examples of Pb-Pb dating of Late Archean gold-related minerals, the only other radioisotope system currently capable of dating sulfide mineralization. For example, Wang et al. (1993) report a very precise and demonstrably accurate Pb-Pb isochron age of 2638 ± 4 Ma for alteration titanite and pyrite associated with orogenic gold mineralization in the Murchison Province, western Australia. Nevertheless, Kerrich and Cassidy (1994) point out that, as with the majority of chronometers applied to ore deposit dating, Pb-Pb dating of ore minerals often yields disparate mineralization ages due to issues such as mixing of Pb from multiple sources and post-crystallization isotopic disturbance of the dated minerals. The result from Con presented here reveals the potential of the Re-Os low-level sulfide chronometer for routinely and accurately dating Archean gold-mineralizing events. The reduced precision for Archean sulfide dates compared to that for Paleozoic examples (e.g. Morelli et al., 2005) likely results from the much lower $^{187}\text{Os}^*$ contents in the Archean sulfides, and the relative imprecision on the raw Os isotopic measurements. By this reasoning, analysis of appropriately spiked, pure mineral separates of Archean sulfides with higher Re contents (i.e. > 1 ppb) should yield

more precise mineralization ages. For extremely low-level sulfides, such as the Con pyrite, improvements to analytical protocol must be developed to increase ionization efficiency and sensitivity during spectrometry.

Significance for Late Archean Gold Metallogeny in the Yellowknife Greenstone Belt

As with Archean OGD in other greenstone belts globally, the ultimate origin of gold mineralization in the Yellowknife region is unknown. The introduction of gold-bearing fluids into the belt has been proposed to originate from both regional (Kerrick and Fyfe, 1987; van Hees et al., 1999) and contact (McDonald et al., 1993) metamorphic processes. Additionally, the presence of lamprophyre dikes in the Con-Giant deposit area, the intrusion of which were broadly contemporaneous with gold mineralization, is considered by some to indicate a possible mantle contribution to mineralization (Webb and Kerrich, 1988). Thompson (2006) further points out that the exsolution of fluids from crystallizing granitic magmas could also lead to the formation of hydrothermal gold deposits. In an attempt to synthesize these viable possibilities, Thompson (2006) proposed a 'preferred fluid-flow model', in which all four of these potential fluid sources (i.e. peak regional metamorphic dehydration, cooling of contact metamorphic aureoles, exsolution from crystallizing plutons, mantle fluids) contributed components to the mineralizing system simultaneously with a change from a penetrative to a focused strain regime at ca. 2610 Ma.

The demonstrably accurate Re-Os pyrite age, together with the determined initial Os ratio, provides new information on the origin of gold mineralization in the Yellowknife Greenstone Belt. The slight overlap between the 2591 ± 37 Ma Re-Os pyrite age and the timing of both Defeat Suite Plutonism and M₁ regional metamorphism does not clearly eliminate a possible relationship between any of these events and gold mineralization. The determined 2591 Ma age might more clearly point to a temporal relationship between an episode of gold mineralization and intrusion of the younger Prosperous plutonic suite, as well as M₂ regional metamorphism and D₂ deformation (Fig. 3.10). Although allowable within the uncertainty in the Re-Os age, this timing is inconsistent with the model of Thompson (2006), since the initiation of focused fluid flow resulting in gold mineralization in this model is proposed to have occurred at ca.

2610 Ma, some 20 m.y. earlier than the 2591 Ma timing determined here. It does not, however, preclude the possibility that an earlier phase of the gold mineralizing event was initiated through this process.

A model better suited to the determined 2591 Ma age is that of van Hees et al. (2006), in which the origin of gold mineralization at the Ptarmigan deposit, located ~ 13 km northeast of the Con deposit, is attributed to a combination of magmatic and contact metamorphic-derived fluids produced during the intrusion of the nearby Prosperous Granite. This peraluminous granite, emplaced at ca. 2596 Ma (Cousens et al., 2006a), is thought to have originated from melting of the Burwash Formation turbidite sequence, the host to both the granite and the Ptarmigan Au deposit. Based on fluid inclusion compositions of mineralized veins, this model proposes the occurrence of two distinct mineralizing events: the first derived from slow cooling of the Prosperous granite, and the second due to contact metamorphism of the Burwash sedimentary rocks surrounding the pluton.

Some support for this model might also be provided by the Con pyrite Os_i ratios. The Burwash sedimentary rocks are characterized by Pb (Cousens et al., 2006b) and Nd (Yamashita and Creaser, 1999) isotopic compositions that are inhomogeneous and that indicate detrital input from a variety of sources, ranging from isotopically enriched (> 2900 Ma) basement rocks to isotopically juvenile mafic and ultramafic igneous rocks. A similarly mixed composition is also reflected in the Prosperous granite since its Pb isotopic composition plots in the middle of the Burwash Formation Pb isotopic array, possibly indicating an average of the Burwash Pb compositions (Cousens et al., 2006b). Although the current lack of Os isotopic data for rocks of the Burwash Formation precludes a definitive comparison, the mixed juvenile - ancient Pb and Nd isotopic compositions of both the Burwash Formation and the Prosperous granite are generally compatible with the Os_i of the Con pyrite. The Con pyrite Os_i of 0.78 ± 0.17 is elevated above the mantle value at 2600 Ma of 0.109 (Meisel et al., 2001), showing a clear crustal contribution of Os to the pyrite. Assuming that the pyrite $^{187}Re/^{188}Os$ ratio of 321 (the average of the eight pyrite analyses used to construct the Re-Os isochron) was transferred unchanged into the hydrothermal fluid from its source, and assuming 71 m.y. of ^{187}Re decay prior to ore deposition (i.e. an average depositional age of 2662 Ma for Burwash

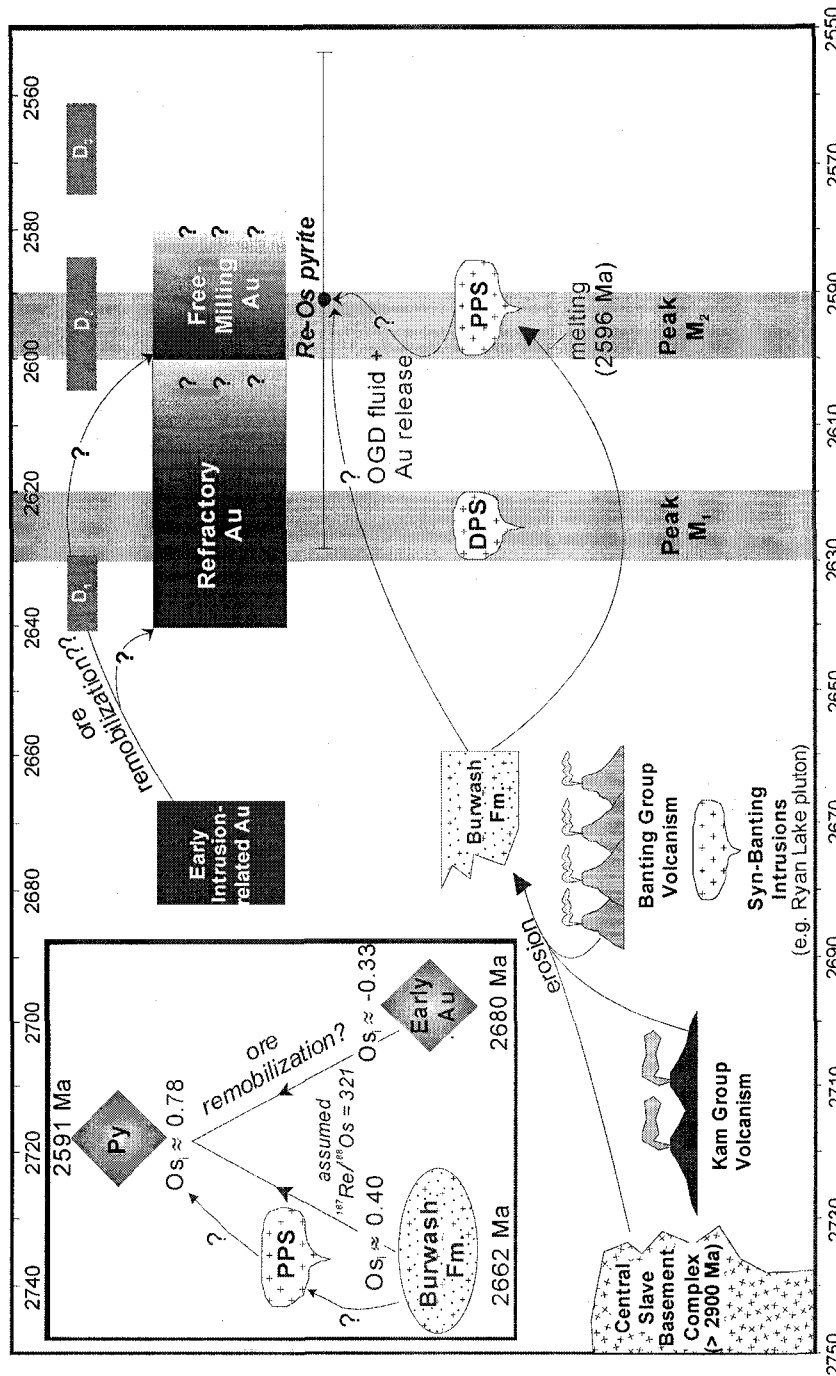


Figure 3.10: Chronological evolution of the Yellowknife greenstone belt, with proposed models for orogenic gold mineralization. Inset shows the isotopic evolution of Os to the determined Os_i from Con pyrite for models discussed in the text. DPS = Defeat Suite Plutons; PPS = Prosperous Suite Plutons; Py = Con pyrite. Geochronological data from Davis and Bleeker (1999), Ootes et al. (2007), and Cousens et al. (2006a).

turbidites; Bleeker and Villeneuve, 1995), it is possible to approximate a hypothetical Os_i of 0.40 for the Prosperous magmas. This value is generally consistent with a source contribution from both juvenile and ancient material, and could possibly reflect the mixed provenance of the Burwash Formation sediment.

Another intriguing possibility for the origin of gold in the Yellowknife area is that the ca. 2600 Ma gold and related sulfides formed as a result of remobilization and recrystallization of older ores (Ootes et al., 2007). The youngest of the suggested 'proto-ores' to the syn- to late- D2 gold mineralization is that associated with the Ryan Lake pluton near the Crestauram mine (Fig. 3.4). Molybdenite from this occurrence has been dated by the Re-Os method at ca. 2680 Ma (Ootes et al., 2007). Using the same approach as that described above for modeling of the Burwash Formation Os_i , a hypothetical Os_i of - 0.64 can be estimated for the 2680 Ma mineralization. If valid, this calculation of a negative Os_i (a geologically impossible result) would preclude remobilization of older ores as a viable model for the origin of the 2600 Ma gold-forming event. To be feasible, this model would require a much lower hydrothermal fluid $^{187}Re/^{188}Os$ ratio of < 150, a requirement that is atypical of crustal sulfide minerals in general. However, another way to assess the Con pyrite Os_i value is to calculate the maximum possible residence time that the Os could have resided in the crust to produce the determined $^{187}Os/^{188}Os$ ratio of 0.78. To do this, a chondritic initial Os_i at the time of crystallization is assumed, as is an average crustal $^{187}Re/^{188}Os$ value of 348 (Peucker-Ehrenbrink and Jahn, 2001; Sun et al., 2003). This approach yields a maximum Os crustal residence time of ~ 117 m.y., requiring that the Os might have been emplaced into the crust by ca. 2715 to 2710 Ma (assuming a pyrite crystallization age of 2596 Ma) and thus permitting the ore remobilization model. Further high quality Os isotopic data are clearly required to accurately interpret the source(s) of Os in gold deposits of the Yellowstone Greenstone Belt.

Although worthy of discussion, the validity of the above interpretation of the Re-Os pyrite results for Con deposit genesis is clearly compromised by both the uncertainty in the determined Re-Os age and the paucity of Os isotopic data for possible ore sources. More important at this stage in the development of the Re-Os low-level sulfide technique is the recognition that demonstrably accurate ages and unique tracer information can be

extracted directly from an Archean, ore-related sulfide mineral, thereby removing ambiguity surrounding the paragenesis of the chronometer in relation to the ore-forming event. This result exhibits the potential that this technique holds for future studies on Archean orogenic gold deposits.

3.6 Conclusions

This study provides a preliminary assessment of the ability of the Re-Os low-level sulfide chronometer to date Archean OGD. Pyrite and arsenopyrite from the majority of tested OGD are characterized by significantly lower Re contents than from post-Archean deposits. The significance of this is currently unclear, but may relate to the dominant host lithologies of OGD through geologic time. Despite their lower Re concentrations, late Archean OGD typically contain sufficient levels of ^{187}Re and $^{187}\text{Os}^*$ for precise ($< 1\%$) isotopic measurement using negative thermal ionization mass spectrometry.

Attempts at Re-Os geochronology of late Archean arsenopyrite, pyrite, and gersdorffite from three world-class OGD had mixed success. Arsenopyrite and gersdorffite from the Red Lake deposit (Superior Province) and arsenopyrite from the Golden Mile deposit (Yilgarn craton) yield scattered Re-Os data, and imprecise age results. In the case of Red Lake, the determined age is also inaccurate. Although post crystallization isotopic disturbance of the Re-Os systematics is a possible cause of this age disparity, a preferred interpretation is that it results from analytical issues. In particular, both rigorous mineral separation techniques and the use of spikes with appropriate Re-Os isotopic compositions and concentrations are considered critical for the determination of accurate and precise low-level sulfide Re-Os ages.

In contrast, pyrite from the Con deposit (Slave craton) yielded a demonstrably accurate and reasonably precise ($\pm 1.43\%$) Re-Os age of 2591 ± 37 Ma for gold mineralization in the Yellowknife Greenstone Belt. Together with the determined initial $^{187}\text{Os}/^{188}\text{Os}$ ratio of 0.78 ± 0.17 for the pyrite and combined with existing isotopic data for the deposit, this new age provides important new information on the origin of gold mineralization in this greenstone belt, and for other late Archean OGD worldwide. The results of this study indicate that, through continued and careful development of the

technique, the Re-Os low-level sulfide chronometer has the potential to become a powerful tool for improving our knowledge of the timing and genesis of Archean OGD.

3.7. References

Andrews, A.J., Hugon, H., Durocher, M., Corfu, F., and Lavigne, M.J., 1986, The anatomy of a gold-bearing greenstone belt: Red Lake, northwestern Ontario, Canada, in: MacDonald, A.J. [ed.], Gold '86, Willowdale, Ontario, Konsult International, p. 3-22.

Arne, D.C., Bierlein, F.P., Morgan, J.W., and Stein, H.J., 2001, Re-Os dating of sulfides associated with gold mineralization in central Victoria, Australia: *Economic Geology*, v. 96, p. 1455-1459.

Bateman, R.J., Hagemann, S.G., McCuaig, T.C., and Swager, C.P., 2001, Protracted gold mineralization throughout Archean orogenesis in the Kalgoorlie camp, Yilgarn craton Western Australia: Structural, mineralogical, and geochemical evolution: *Geological Survey of Western Australia Record 2001/17*, p. 63-98.

Bleeker, W. and Villeneuve, M., 1995, Structural studies along the Slave portion of the SNORCLE transect, in: Cook, F., and Erdmer, P. [comp.], Slave – Northern Cordillera Lithospheric experiment (SNORCLE) Transect Meeting, Calgary, AB, Lithoprobe Report 44, p. 8-13.

Bucci, L.A., McNaughton, N.J., Fletcher, I.R., Groves, D.I., Kositcin, N., Stein, H.J., and Hagemann, S.G., 2004, Timing and duration of high-temperature gold mineralization and spatially associated granitoid magmatism at Chalice, Yilgarn Craton, Western Australia: *Economic Geology*, v. 99, p. 1123-1144.

Christie, B.J., 1986, Alteration and gold mineralization associated with a sheeted veinlet zone at the Campbell Red Lake mine, Balmertown, Ontario: Unpublished M.Sc. thesis, Kingston, Ontario, Queen's University, 334 p.

Colvine, A.C., Fyon, J.A., Heather, K.B., Marmont, S., Smith, P.M., and Troop, D.G., 1988, Archean lode gold deposits in Ontario: Ontario Geological Survey, Miscellaneous Paper 139, 136 p.

Corfu, F., and Andrews, A.J., 1987, Geochronological constraints on the timing of magmatism, deformation, and gold mineralization in the Red Lake greenstone belt, northwestern Ontario: Canadian Journal of Earth Sciences, v. 24, p. 1302-1320.

Cousens, B., Falck, H., Ootes, L., Jackson, V., Mueller, W., Corcoran, P., Finnigan, C., van Hees, E., Facey, C., and Alcazar, A., 2006a, Regional correlations, tectonic settings, and stratigraphic solutions in the Yellowknife Greenstone Belt and adjacent areas from geochemical and Sm-Nd isotopic analyses of volcanic and plutonic rocks, *in*: Anglin, C.D., Falck, H., Wright, D.F., and Ambrose, E.J. [eds.], Gold in the Yellowknife Greenstone Belt, Northwest Territories: Results of the EXTECH III Multidisciplinary Research Project, Geological Association of Canada, Mineral Deposits Division, Special Publication No. 3, p. 70-93.

Cousens, B.L., Falck, H., van Hees, E.H., Farrell, S., and Ootes, L., 2006b, Pb isotopic compositions of sulphide minerals from the Yellowknife gold camp: Metal sources and timing of mineralization, *in*: Anglin, C.D., Falck, H., Wright, D.F., and Ambrose, E.J. [eds.], Gold in the Yellowknife Greenstone Belt, Northwest Territories: Results of the EXTECH III Multidisciplinary Research Project, Geological Association of Canada, Mineral Deposits Division, Special Publication No. 3, p. 286-300.

Davis, W.J. and Bleeker, W., 1999, Timing of plutonism, deformation, and metamorphism in the Yellowknife Domain, Slave Province, Canada: Canadian Journal of Earth Sciences, v. 36, p. 1169-1187.

Dubé, B., Williamson, K., McNicoll, V., Malo, M., Skuśki, T., Twomey, T., and Sanborn-Barrie, M., 2004, Timing of gold mineralization at Red Lake, Northwestern

Ontario, Canada: new constraints from U-Pb geochronology at the Goldcorp high-grade zone, Red Lake mine, and the Madsen mine: *Economic Geology*, v. 99, p.1611-1641.

Falck, H., 1992, Gold mineralization in the Yellowknife mining district, NWT (NTS 85J/7,8,9,16): Geological Survey of Canada Open File 2484, p. 31–36.

Frei, R., Nägler, Th.F., Schönberg, R., and Kramers, J.D., 1998, Re-Os, Sm-Nd, U-Pb, and stepwise lead leaching isotope systematics in shear-zone hosted gold mineralization: genetic tracing and age constraints of crustal hydrothermal activity: *Geochimica et Cosmochimica Acta*, v. 62, p. 1925-1936.

Goldcorp Incorporated, 2003, Annual Report: Toronto, Ontario, 36 p.

Goldfarb, R.J., Groves, D.I., and Gardoll, S., 2001, Orogenic gold and geologic time: a global synthesis: *Ore Geology Reviews*, v. 18, p. 1–75.

Groves, D.I., and Foster, R.P., 1993, Archean lode gold deposits, *in*: Foster, R.P. [ed.], *Gold Metallogeny and Exploration*, Chapman and Hall, London, U.K., p. 63-103.

Groves, D.I., Goldfarb, R.J., Gebre-Meriam, M., Hagemann, S.G., and Robert, F., 1998, Orogenic gold deposits: a proposed classification in the context of their crustal distribution and relationship to other gold deposit types: *Ore Geology Reviews*, v. 13, p. 7-27.

Hagemann, S.G. and Cassidy, K.F., 2000, Archean orogenic lode gold deposits, *in*: Hagemann, S.G., and Brown, P.E. [eds.]: *Gold in 2000*, Society of Economic Geologists, *Reviews in Economic Geology*, v. 13, p. 9-60.

Hannah, J.L., Stein, H.J., Markey, R.J., and Scherstén, A., 2004, Gold: A Re-Os geochronometer?: Supplement to *Geochimica et Cosmochimica Acta*, Abstracts of the 13th Annual V.M. Goldschmidt Conference, Copenhagen, Denmark, v. 68, p. A773.

Hauser, R.L., McDonald, D.W., and Siddorn, J.P., Geology of the Miramar Con Mine, *in*: Anglin, C.D., Falck, H., Wright, D.F., and Ambrose, E.J. [eds.], Gold in the Yellowknife Greenstone Belt, Northwest Territories: Results of the EXTECH III Multidisciplinary Research Project, Geological Association of Canada, Mineral Deposits Division, Special Publication No. 3, p. 173-187.

Kirk, J., Ruiz, J., Chesley, J., Titley, and Walshe, J., 2001, A detrital model for the origin of gold and sulfides in the Witwatersrand basin based on Re-Os isotopes: *Geochimica et Cosmochimica Acta*, v. 65, p. 2149 – 2159.

Lambert, D., Frick, L., Bateman, R., and Stone, W., 1998, Geochemistry and rock-fluid interactions in Archean lode gold systems: New insights from the Re-Os isotopic system, *in*: Woods, S.E. [ed.], Geodynamics and gold exploration in the Yilgarn, Nedlands, Western Australia, Australian Geodynamics Cooperative Research Centre, Workshop abstracts.

Ludwig, K., 2000, Isoplot/Ex, version 2.22: A geochronological toolkit for Microsoft Excel: Geochronology Center Berkeley.

Marshik, R., Mathur, R., Ruiz, J., Leveille, R.A., de Almeida, A.J., 2005, Late Archean Cu-Au-Mo mineralization at Gameleira and Sierra Verde, Carajas mineral province, Brazil; constraints from Re/Os molybdenite ages: *Mineralium Deposita*, vol.39, p.983-991.

Martel, E., Lin, S., and Bleeker, W., 2002, Kinematic observations in the Yellowknife River fault zone and structures in the Jackson Lake Formation, Yellowknife Greenstone Belt, Northwest Territories: Geological Society of Canada, Current Research 2002-E4, 10p.

McLennan, S.M., and Taylor, S.R., 1982, Geochemical constraints on the growth of the continental crust: *Journal of Geology*, v. 90, p. 347-361.

McNaughton, N.J., Mueller, A.G., and Groves, D.I., 2005, The age of the giant Golden Mile Deposit, Kalgoorlie, Western Australia: Ion-microprobe zircon and monazite U-Pb geochronology of a synmineralization lamprophyre dike: *Economic Geology*, v. 100, p. 1427-1440.

Meisel, T., Walker, R.J., Irving, A.J., and Lorand, J., 2001, Osmium isotopic compositions of mantle xenoliths: a global perspective: *Geochimica et Cosmochimica Acta*, v. 65, p. 1311-1323.

Morelli, R.M., Creaser, R.A., Selby, D., Kontak, D.J., and Horne, R.J., 2005, Rhenium-osmium geochronology of arsenopyrite in Meguma Group gold deposits, Meguma Terrane, Nova Scotia, Canada: Evidence for multiple gold-mineralizing events: *Economic Geology*, v. 100, p. 1229-1242.

Morelli, R.M., Creaser, R.A., Selby, D., Kelley, K.D., Leach, D.L., and King, A.R., 2004, Re-Os Sulfide Geochronology of the Red Dog Sediment-Hosted Zn-Pb-Ag Deposit, Brooks Range, Alaska, v. 99, p. 1569 – 1576.

Ootes, L., Lentz, D.R., Creaser, R.A., Ketchum, J.W., and Falck, H., 2007, Re-Os molybdenite ages from the Archean Yellowknife greenstone belt: Comparison to U-Pb ages and evidence for metal introduction at ~2675 Ma: *Economic Geology*, v. 102, p. 511-518.

Ootes, L., Lentz, D.R., and Creaser, R.A., 2002, Timing constraints and paragenesis of mineralizing events at the Crestauram gold deposit, Yellowknife greenstone belt, NWT, Canada, *in: Geological Association of Canada/Mineralogical Association of Canada Abstracts Volume*, v. 27, p. 85.

Penczak, R.S., and Mason, R., 1997, Metamorphosed Archean Epithermal Au-As-Sb-Zn-(Hg) vein mineralization at the Campbell Mine, northwestern Ontario: *Economic Geology*, v. 92, p. 696-719

Peucker-Ehrenbrink, B. and Jahn, B., 2001, Rhenium-osmium isotope systematics and platinum group element concentrations: Loess and the upper continental crust: *Geochemistry, Geophysics, Geosystems*, v. 2, doi: 10.1029/2001GC000172, doi: 10.1029/2001GC000172.

Phillips, G.N., 1986, Geology and alteration in the Golden Mile, Kalgoorlie: *Economic Geology*, v. 81, p. 779–808.

Ridley, J.R., and Diamond, L.W., 2000, Fluid chemistry of orogenic lode gold deposits and implications for genetic models, *in*: Hagemann, S.G., and Brown, P.E. [eds.]: *Gold in 2000*, Society of Economic Geologists, *Reviews in Economic Geology*, v. 13, p. 141-162.

Robert, F., Poulsen, K.H., Cassidy, K.F., and Hodgson, C.J., 2005, Gold metallogeny of the Superior and Yilgarn Cratons, *in*: Hedenquist, J.W., Thompson, J.F.H., Goldfarb, R.J., and Richards, J.P. [eds.], *Economic Geology 100th Anniversary Volume*, Society of Economic Geologists, Inc., p.1001-1033.

Roberts, R.G., 1988, Archean lode gold deposits, *in*: Roberts, R.G. and Sheahan, P.A. [eds.], *Ore Deposit Models: Geoscience Canada, Reprint Series 3*, p. 1-19.

Shelton, K.L., McMenemy, T.A., van Hees, E.H.P., and Falck, H., 2004, Deciphering the complex fluid history of a greenstone-hosted gold deposit: fluid inclusion and stable isotope studies of the giant mine, Yellowknife, Northwest Territories, Canada: *Economic Geology*, v. 99, p. 1643-1663.

Shirey, S.B., and Walker, R.J., 1998, The Re-Os isotope system in cosmochemistry and high-temperature geochemistry: *Annual Reviews of Earth and Planetary Science*, v. 26, p. 423-500.

Stein, H.J., Scherstén, A., Hannah, J.L., and Markey, R.J., 2003, Subgrain scale decoupling of Re and ^{187}Os and assessment of laser ablation ICP-MS spot dating in molybdenite: *Geochimica et Cosmochimica Acta*, v. 67, p. 3673 – 3686.

Stein, H.J., Markey, R.J., Morgan, J.W., Hannah, J.L., Schertén, A., 2001, The remarkable Re-Os chronometer in molybdenite: how and why it works: *Terra Nova*, v. 13, p. 479-486.

Stein, H.J., Morgan, J.W., and Scherstén, A., 2000, Re-Os dating of low-level highly radiogenic (LLHR) sulfides: the Harnäs gold deposit, southwest Sweden, Records continental-scale tectonic events: *Economic Geology*, v. 95, p. 1657-1671.

Stein, H. J., Sundblad, K., Markey, R. J., Morgan, J. W., and Motuza, G., 1998, Re-Os ages for Archean molybdenite and pyrite, Kuittila-Kivisuo, Finland and Proterozoic molybdenite, Kabeliai, Lithuania: testing the chronometer in a metamorphic and metasomatic setting, *Mineralium Deposita*, v. 33, p. 329 – 345.

Sun, W., Bennett, V.C., Eggins, S.M., Kamenetsky, V.S., and Arculus, R.J., 2003, Enhanced mantle-to-crust rhenium transfer in undegassed arc magmas: *Nature*, v. 422, p. 294–297.

Thompson, P.H., 2006, Metamorphic constraints on the geological setting, thermal regime, and timing of alteration in the Yellowknife Greenstone Belt, NWT, Canada, *in*: Anglin, C.D., Falck, H., Wright, D.F., and Ambrose, E.J. [eds.], *Gold in the Yellowknife Greenstone Belt, Northwest Territories: Results of the EXTECH III Multidisciplinary Research Project*, Geological Association of Canada, Mineral Deposits Division, Special Publication No. 3, p. 142-172.

Thompson, P.H., 2003, Toward a new metamorphic framework for gold exploration in the Red Lake greenstone belt: Ontario Geological Survey Open File Report 6122, 51 p.

van Hees, E.H., Kirkham, G.D., Sirbescu, M.L., Shelton, K.L., Hauser, R.L., and Falck, H., 2006, Large lithogeochemical alteration halos around Yellowknife gold deposits and implications for fluid pathways *in*: Anglin, C.D., Falck, H., Wright, D.F., and Ambrose, E.J. [eds.], Gold in the Yellowknife Greenstone Belt, Northwest Territories: Results of the EXTECH III Multidisciplinary Research Project, Geological Association of Canada, Mineral Deposits Division, Special Publication No. 3, p. 232-248.

van Hees, E.H.P., Shelton, K.L., McMenamy, T.A., Ross Jr., L.M., Cousens, B.L., Falck, H., Robb, M.E., and Canam, T.W., 1999, Metasedimentary influence on metavolcanic-rock-hosted greenstone gold deposits: Geochemistry of the Giant mine, Yellowknife, Northwest Territories, Canada: *Geology*, v. 27, p. 71-74.

Wang, L.G., McNaughton, N.J., and Groves, D.I., 1993, An overview of the relationship between granitoid intrusions and gold mineralization in the Archean Murchison Province, western Australia: *Mineralium Deposita*, v. 28, p.482-494.

Webb, D.R. and Kerrich, R., 1988, An Archean ultramafic lamprophyre, Yellowknife: implications for tectonics and source regions: *Contributions to Geology of the Northwest Territories*, v. 3, p.115-122.

Williamson, K. and Dubé, B., 2003, Detailed geology, hydrothermal alteration and gold mineralization of the Cochenour stripped outcrop, Red Lake gold district, Ontario: Open-File Report - Geological Survey of Canada, Report: 1673, 1 sheet.

Xiong, Y. and Wood, S., 2002, Experimental determination of the hydrothermal stability of ReS_2 and the Re-ReO_2 buffer assemblage and transport of rhenium under supercritical conditions: *Geochemical Transactions* 1, d.o.i. 10, 1039/b109002j.

Yamashita, K. and Creaser, R.A., 1999, Geochemical and Nd isotopic constraints for the origin of late Archean turbidites from the Yellowknife area, Northwest Territories, Canada: *Geochimica et Cosmochimica Acta*, v. 63, p. 2579-2598.

4. Re-Os Sulfide Geochronology of Post-Archean Orogenic Gold Deposits, and Implications for Deposit Genesis

4.1 Re-Os geochronology of arsenopyrite and pyrrhotite - a case study from the Paleoproterozoic Homestake Orogenic Au deposit, Black Hills, South Dakota

4.1.1. Introduction

The ability to measure absolute geologic time is critical for understanding geologic processes and their role in the development of the Earth. Formation of hydrothermal ore deposits is an important example of such a process, but is an event that has proven extremely difficult to directly date because of a lack of suitable minerals that crystallize contemporaneously with ore. Recently, use of rhenium-osmium (Re-Os) geochronology with sulfide minerals has emerged as a viable means of overcoming this impediment, since the parent element (Re) is chalcophile and partitions from a hydrothermal fluid directly into ore-related sulfide minerals. However, as with any geochronological technique, Re-Os sulfide chronometers must satisfy a number of fundamental parameters, including the requirement that no post-crystallization open system behavior of in Re and/or Os has occurred.

The Re-Os technique has been applied to a variety of sulfide minerals, including molybdenite (Stein et al., 2001, Selby and Creaser, 2001a, b), pyrite (Stein et al., 2000; Morelli et al., 2004), arsenopyrite (Arne et al., 2001; Morelli et al., 2005), pyrrhotite (Lambert et al., 2000; Frei et al., 1999), and chalcopyrite (Mathur et al., 2000). However, apart from molybdenite, which remains robust through granulite facies metamorphic conditions (Bingen and Stein, 2003), there is currently little information regarding the susceptibility of other sulfide minerals to post-crystallization disturbance of the Re-Os system, therefore obscuring the meaning of determined age results. In this chapter, two sulfide minerals, arsenopyrite (FeAsS) and pyrrhotite (Fe_{1-x}S), are tested for their ability to retain accurate Re-Os dates through post-crystallization thermal events. These two minerals occur widely in many ore deposit types, but are especially prevalent in orogenic

gold deposits (Groves et al., 1998). This class of gold deposit presents a classic case where the inability to determine the absolute age of mineralization has hindered successful modeling, and is therefore an ideal candidate for application of Re-Os sulfide geochronology. To test the reliability of these chronometers, the Re-Os isotopic compositions of sulfide specimens from the Paleoproterozoic Homestake gold deposit, Black Hills, South Dakota, were examined.

The Homestake deposit, having produced >1200 t Au during mining from 1876-2001, is currently the 5th largest of all known orogenic gold deposits (OGD) worldwide and the second largest of Paleoproterozoic age (Goldfarb et al., 2005). The deposit and its host rocks are well studied and, in contrast to many OGD, there exists reasonable control on both the timing of Au mineralization and the thermal history of the host terrane, making Homestake an exceptional natural setting for this study.

The results of this study establish the Re-Os arsenopyrite chronometer as a reliable geochronological tool for dating ore deposition, but indicate that pyrrhotite is unreliable, questioning the general results of Re-Os studies using pyrrhotite. Furthermore, determination of the precise age of gold deposition at Homestake by the Re-Os arsenopyrite method now allows a better understanding of processes that may have contributed to the deposit's origin. Development of the hydrothermal system that formed the deposit has most commonly been linked to either peak regional metamorphism, or intrusion of the proximal, late orogenic Harney Peak granite. New U-Pb monazite dates for the Harney Peak granite are also presented here that allow for a more accurate assessment of the relative timing between magmatism and gold mineralization. Together, these new Re-Os and U-Pb ages provide critical insight into the generation of a world-class orogenic gold deposit, and promote understanding of the genesis of orogenic gold deposits as a whole.

4.1.2. Regional and Deposit Geology

The Homestake deposit is situated within the northern Black Hills uplift in central South Dakota, U.S.A (Fig. 4.1.1). This uplift resulted from doming of the crust above Laramide-aged intrusions, and is exposed at the present erosional level as an inlier of predominantly Precambrian rocks surrounded by Phanerozoic cover. Precambrian rocks

in the uplift constitute the southernmost exposure of the Paleoproterozoic Trans-Hudson Orogen, and record opening of a siliciclastic-dominated basin and its subsequent closure during the collision between the Archean Wyoming and Superior Provinces (Dahl, 1999). The regional geology of the Black Hills is thoroughly described by Redden et al. (1990).

Although limited exposure of Archean basement occurs within the uplift (Zartman and Stern, 1967; Gosselin et al., 1988; McCombs et al., 2004), polydeformed and metamorphosed Paleoproterozoic sedimentary, volcanic and intrusive rocks dominate the geology. Regionally, there exists a progression from a basal assemblage of continentally-sourced, >2170 Ma conglomerate, quartzite and iron formation, into unconformably overlying shallow water deposits (ca. 2170 Ma - 1974). These younger rocks include a range of coarse- to fine-grained clastic sedimentary rocks, iron formation, minor carbonate and mafic volcanic flows, some of which have been intruded by metagabbro dikes and/or sills. Deeper water turbiditic and tuffaceous deposits, equivalent in age to shelf quartzites to the north (ca. 1974 Ma), exist in the central and southern Black Hills, whereas an extensive unconformable sequence of ca. 1870 Ma conglomerate, turbidites, and basalts is preserved in the east-central portion. This sequence of Paleoproterozoic sedimentary and volcanic rocks comprising the main basin is hypothesized to represent deposition in a long-lived intracontinental rift basin (Redden et al., 1990; Houston, 1992) or rather in a backarc basin succeeding earlier rifting (pre-2170 Ma) of Archean crust (Caddey et al., 1990).

Following deposition of the youngest sedimentary unit in the main basin, metamorphism and deformation of the Archean and Early Paleoproterozoic rocks resulted from convergence and the eventual collision between the flanking Wyoming and Superior Archean provinces (Dahl et al., 1999). This collision culminated with the intrusion of multiple dikes and sills comprising the Harney Peak granite, exposed in a circular dome in the south-central portion of the uplift (Fig. 4.1.1). The granitic intrusions are highly peraluminous and likely resulted from melting of Archean and Paleoproterozoic metapelitic rocks via shear heating during collisional orogeny (Nabelek and Liu, 1999). Intrusion of the granite, which post-dates all major Precambrian structural fabrics and regional metamorphism in the Black Hills, was previously dated by three U-Pb monazite TIMS analyses at 1715 ± 3 Ma (Redden et al., 1990).

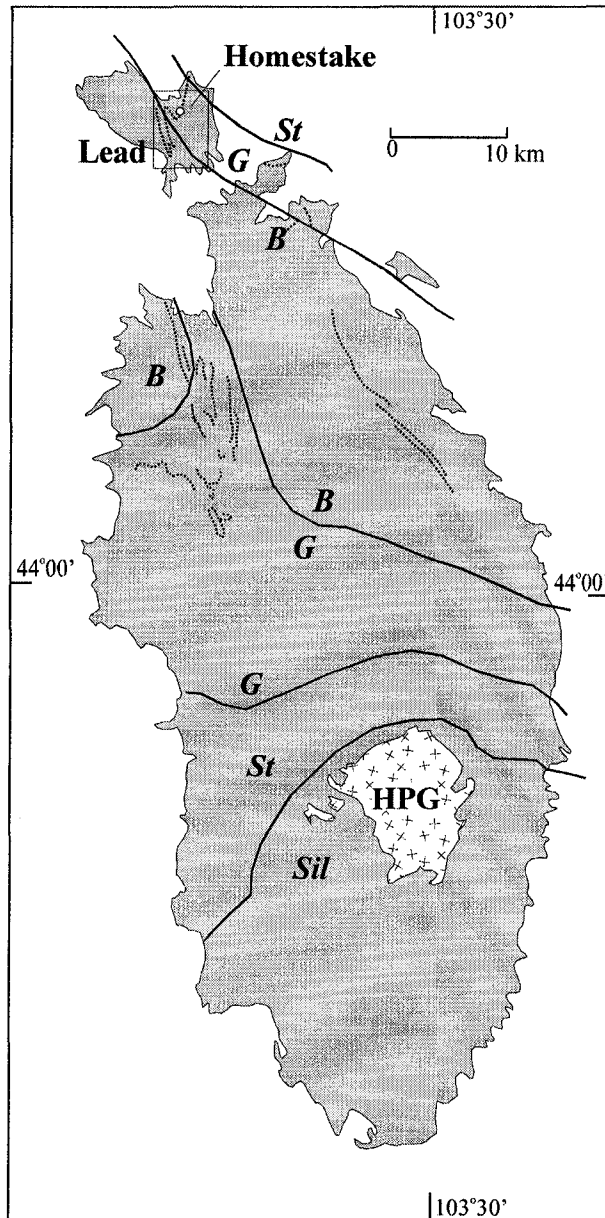
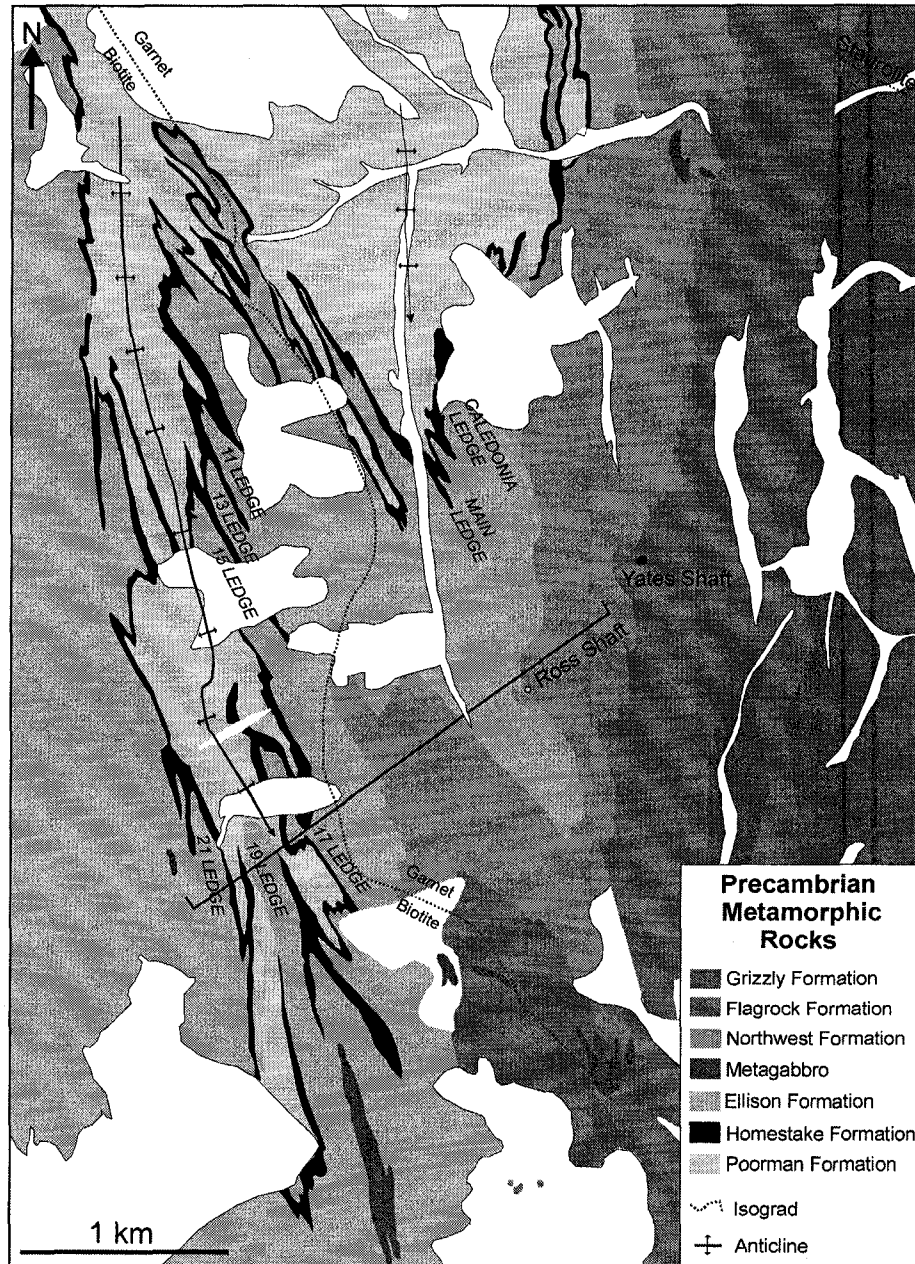


Figure 4.1.1: Geological setting of the Black Hills Uplift, South Dakota, USA. Box shows area covered in Figure 4.1.2; HPG = surface exposure of Harney Peak granite; B, G, St, and Sil indicate the positions of the biotite, garnet, staurolite, and sillimanite isograds, respectively. After Redden et al. (1990).

The Homestake deposit is exposed in an isolated window on the northern margin of the main Black Hills uplift known as the 'Lead window' (Fig. 4.1.1). Rocks within this small inlier are equivalent to Paleoproterozoic rocks situated elsewhere in the Black Hills, with the exception of Tertiary-aged intrusions exposed only in the extreme northern portion of the uplift. The Harney Peak granite is not exposed in the Lead window, though granite of equivalent age has been intersected by drill hole near the Homestake deposit (the 'Crook Mountain Granite'; Bachman et al., 1990).

Around the Homestake deposit, three folded and metamorphosed units - the Poorman, Homestake, and Ellison Formations - constitute the Paleoproterozoic stratigraphy (Fig. 4.1.2; Caddey et al., 1990). The Poorman Formation, having a thickness of up to ~ 1000 m, consists of a lower unit of metatholeiite of oceanic affinity ('Yates unit'; Caddey et al., 1990) overlain by carbonate bearing pelitic to semipelitic metasediments. Overlying the Poorman Formation, the Homestake Formation comprises a thin (0 – 125 m), metamorphosed, carbonate-facies iron formation, which hosts almost all gold mineralization at the Homestake deposit. The Homestake iron formation is dominated locally by Fe-carbonate (siderite) or Fe-silicate (grunerite) mineralogy, as well as quartz, biotite, and chlorite. Unconformably overlying the Homestake Formation is the Ellison Formation, a quartzite-dominated unit that marks regional uplift and a consequent transition from deep-water deposition of turbidites (Poorman Formation) and iron formation (Homestake Formation) into a shallow water environment. Zircons derived from a tuff bed at the base of the Ellison Formation yielded a U-Pb age of ca. 1974 Ma. Though strictly a minimum age, this is interpreted to reasonably approximate the depositional age of the Homestake iron formation (Redden et al., 1990).

Wyoming – Superior continental collision, beginning after ca. 1780 Ma (Dahl et al., 1999), initiated intense folding and thermal metamorphism that resulted in the N-NW trending upright, isoclinal folds present throughout the Black Hills. Specific to the Lead area, this event produced two large anticlinoriums (the 'Lead' and 'Poorman' anticlinoriums), visible in the map pattern of the Homestake Formation (Fig. 4.1.2). Prograde metamorphism in the Lead area reached upper greenschist to lower amphibolite facies, with the garnet isograd being situated within the Homestake deposit itself (Fig. 4.1.2). Prograde metamorphism and ductile deformation subsequently gave way to



retrograde metamorphism and development of widespread brittle structures. Gold mineralization was emplaced into dilated segments of shear zones during a period of 'retrogressive hydrothermal alteration' that overprints all other prograde and retrograde metamorphic fabrics but, based on textural relationships, is interpreted to pre-date intrusion of the ca. 1715 Ma Harney Peak (and related) granite (Caddey et al., 1991).

Gold mineralization at Homestake is associated with shear zone hosted quartz veining, and is concentrated within relatively undeformed ore bodies with an overall tabular morphology. Whereas ore bodies are strongly concentrated within smaller synclinal structures (equivalent to odd numbered ore 'ledges'; Fig. 4.1.3) on the anticlinorium limbs, the adjacent anticlinal structures (i.e. even-numbered ore ledges) are nearly devoid of gold mineralization. Gold has a cogenetic relationship with both pyrrhotite and arsenopyrite in the Homestake deposit (Caddey et al., 1991), and is typically concentrated within alteration zones containing any or all of chlorite, biotite, sericite, carbonate, and quartz.

4.1.3. Proposed Models for and Timing of Gold Mineralization

The age of the Homestake deposit has been debated since its discovery at the turn of the 20th century, a problem reflected in the evolution of proposed genetic models. It was regarded as Tertiary in age by many early researchers (e.g. Hosted and Wright, 1923; Noble, 1950), due in large part to observable cross-cutting relationships between sulfide-bearing veins and Tertiary-aged dikes at other ore occurrences in the Lead area. However, this relationship is not recognized at the Homestake deposit itself, leading many to conclude that the mineralization was more likely related to the Precambrian host rocks (e.g. Paige, 1924; Connolly, 1927; Gustafson, 1930; Slaughter, 1968). This debate was eventually resolved by a Pb isotope study of quartz vein hosted galena from the Homestake deposit (Rye et al., 1974), which concluded from common Pb Model Ages that gold mineralization was emplaced ca. 1600 Ma.

Recognition of a Precambrian mineralizing event, though critical in advancing understanding of deposit genesis, only initiated a new debate amongst researchers. The stratabound character of the Homestake OGD within the Homestake iron formation (so-called 'Homestake-style' mineralization) spurred a syngenetic sedimentary exhalative

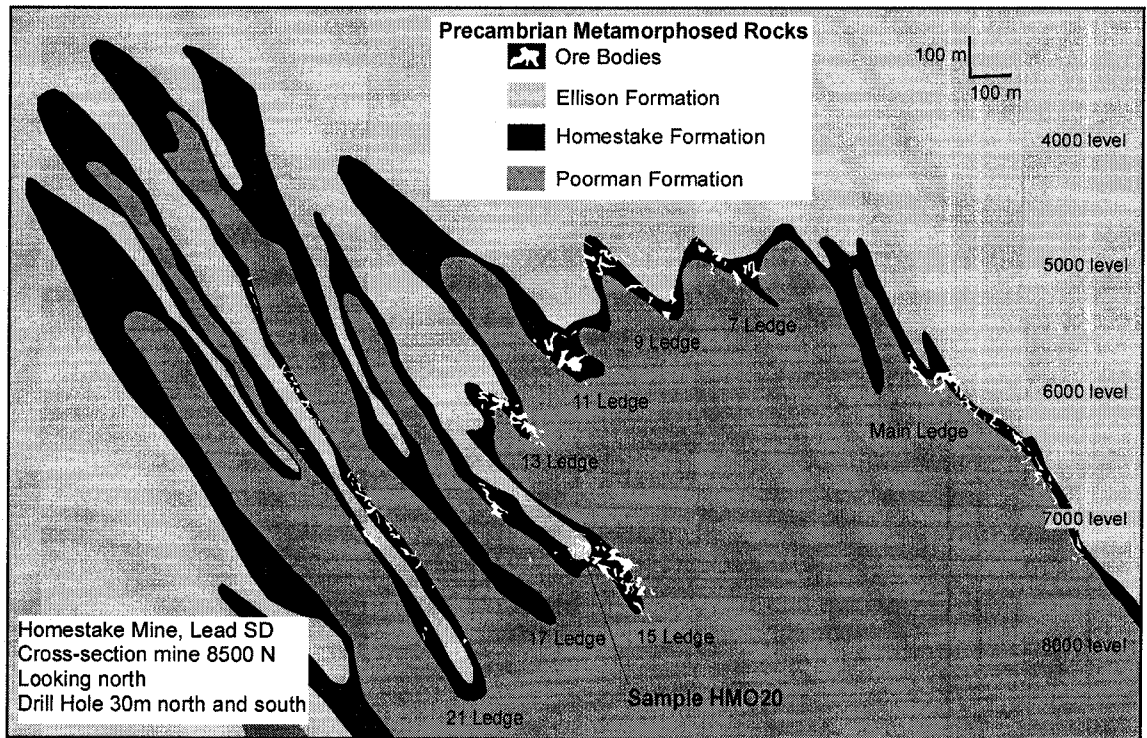


Figure 4.1.3: Cross section of the Homestake mine subsurface geology at the 8500 N level, showing sample HMO20 derivation location. Interpreted by C. Bell (pers. comm.).

model, supported by Rye et al. (1974) on the basis of the Pb and S isotopic data (Rye and Rye, 1974). Others subsequently adopted this syngenetic model (e.g. Redden and French, 1989), though the age of the Homestake Formation (and thus gold mineralization, according to this model) is now known to be at least 1774 Ma or older (Redden et al., 1990).

A more widely accepted model is that the deposit is epigenetic and that the stratabound character results from the iron formation being a favourable chemical trap for gold from a hydrothermal fluid (e.g. Caddey et al., 1990). Proponents of this model would classify Homestake as being a typical 'orogenic gold deposit' (Groves et al., 1998) and recognize both the structural control on mineralization and the introduction of gold-bearing fluid after the initiation of peak regional metamorphism, as indicated by mineral assemblages from vein selvages in the deposit (Terry et al., 2003). Pb-Pb stepwise leaching of allanite inclusions in prograde metamorphic garnet from the Homestake Formation provides a maximum age of 1746 ± 10 Ma for regional metamorphism in the northern Black Hills (Terry et al., 2003). This constraint is supported by a 1750 ± 10 Ma mean total-Pb age from a metapelite-hosted monazite crystal, interpreted to date the onset of east-west convergence and development of the main (S_2) regional foliation (Dahl et al., 2005). A minimum age for gold mineralization is provided by existing geochronology for intrusion of the ca. 1715 Ma (Redden et al., 1990) Harney Peak (and associated) granitic intrusions, which are late- to post-orogenic and overprint mineralization textures. These constraints provide a bracket for the timing of gold mineralization at Homestake between ca. 1746 and 1715 Ma.

4.1.4. Sample Locality and Description

Re-Os isotopic analyses were performed on arsenopyrite and pyrrhotite from a sulfide-rich hand specimen (HM020) from the Homestake underground mine. Specifically, the sample was retrieved from Ore Ledge #19 (Fig. 4.1.3), a synclinal structure on the eastern limb of the Poorman anticlinorium.

Sample HM020 comprises Homestake iron formation that was metamorphosed and then underwent hydrothermal alteration during the gold mineralizing event. The sample contains predominantly chlorite (~ 30 - 35%), Fe-carbonate (~ 20%), biotite (5 -

10%) and quartz (< 5%) in addition to ore-related pyrrhotite (~ 20%) and arsenopyrite (15%) and rare traces of graphite, chalcopyrite, and sphalerite. In detail, arsenopyrite forms large euhedral crystals, ~ 3 mm to 1 cm in size, dispersed throughout the sample (Fig. 4.1.4). Pyrrhotite occurs as coarse (~ 2 - 5 mm) anhedral grains or 'blebs' that are irregularly distributed within carbonate-rich ovoid bodies (possible remnants of carbonate-rich lithic fragments) and on the margins of coarse arsenopyrite crystals or, alternatively, as granular aggregates ('layers') elongated within the trend of the foliation (Fig. 4.1.4a). Pyrrhotite layers are intergrown with pyrrhotite blebs in sample HM020, both pyrrhotite occurrences and the coarse arsenopyrite are cogenetic with gold at Homestake (Caddey et al., 1991). Although two small individual grains of native gold are observed (i) at the margin of, and (ii) in a fracture within a large arsenopyrite crystal, most gold is observed as small (~ 1 to ~ 25 μm) angular inclusions within, but near the margins of, the coarse arsenopyrite crystals.

To determine the timing of intrusion of the Harney Peak Granite, hand samples were collected from outcrop of both the Calamity Peak satellite intrusion and the main mass of the Harney Peak intrusion. Polished petrographic thin sections were made from five of these samples, which were then scanned for Th by X-ray mapping using an electron microprobe to facilitate monazite identification. Only two of the five samples (SD-9A, -9B) contained monazite in sufficient quantity and of sufficient size to be useful for geochronology. Both samples were from an aplitic dike (1-2 mm grain size) situated in the main exposure of the Harney Peak pluton (Fig. 4.1.1), and consist primarily of equigranular K-feldspar, quartz, muscovite, and biotite.

4.1.5. Sample Separation and Analytical Procedures

Individual arsenopyrite crystals were isolated from sample HM020 using an agate pestle, and further crushed using an agate mortar and pestle. Pure pyrrhotite fractions were obtained by crushing portions of sample HM020 containing abundant pyrrhotite stringers using an agate shatterbox, followed by sieving (70-100 mesh), methylene iodide density separation, and FrantzTM magnetic separation. Total sample weights for individual samples depended on Re content, and ranged from ~ 58 – 170 mg for arsenopyrite and from ~ 225 – 425 mg for pyrrhotite. Total procedural blanks (n = 7) varied slightly

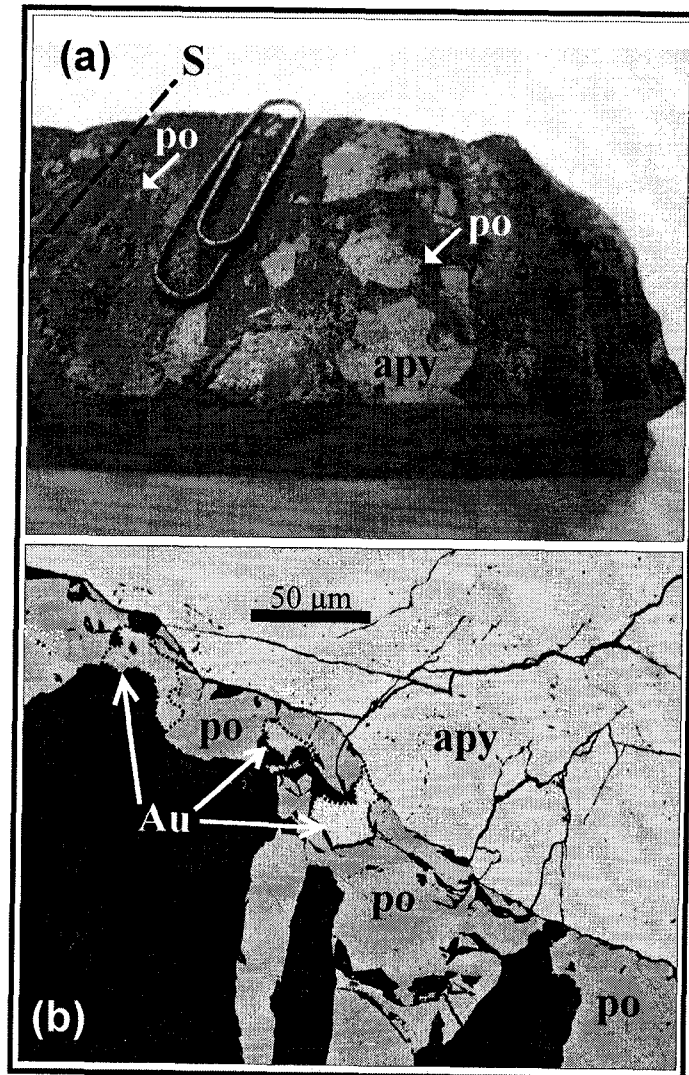


Figure 4.1.4: (a) Photo of sample HMO20, showing pyrrhotite (po) surrounding arsenopyrite (apy) crystals and parallel to the main foliation (S). (b) Photomicrograph of sample HMO20.

depending on the batch and volume of HNO₃ used (arsenopyrite: Re = 1.2 pg, Os = 0.3 pg, Os_{IC} = 0.27; pyrrhotite: Re = 1.6 pg, Os = 0.09 pg, Os_{IC} = 0.23). At these levels, blank contribution accounts for < 0.6 % (Re) and < 0.3% (¹⁸⁷Os) for arsenopyrite analyses and < 2.4 % (Re) and < 0.21 % (¹⁸⁷Os) for pyrrhotite analyses. Procedures for separation, purification, and isotopic analysis of Re and Os fractions and propagation of analytical uncertainties are described in Chapter 2.

Five individual monazite crystals, which ranged in diameter from ~ 20 to 250 μm (Fig. 4.1.5a-e), were used from the Harney Peak granite samples SD-9A and -9B for U-Pb geochronology. U-Pb isotopic analyses were performed by the *in situ* petrographic thin section technique described by Simonetti et al. (2006), using a New Wave Research UP213 laser ablation system coupled to a Nu Plasma multi-collector ICP-MS. Individual spot sizes for ablation analyses were 12 μm; all other instrument parameters and measurement protocol are identical to that described by Simonetti et al. (2006). Analysis of an external standard from the Eleys Creek region of western Australia (Simonetti et al, 2006) was performed using a 12 μm spot size both prior to and following all sample analyses, and a 30 s blank measurement was performed prior to laser ablation.

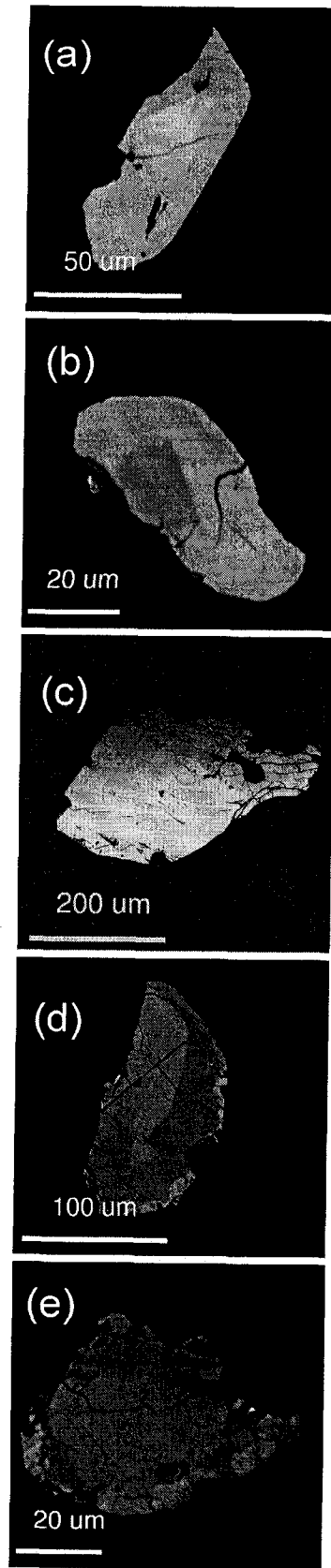
4.1.6. Results

Re-Os

Seven analyses of arsenopyrite and ten of pyrrhotite from sample HM020 were performed, and the results are reported in Table 4.1.1. These data reveal a strong contrast in both Re and common Os contents for the two minerals from this sample. Arsenopyrite shows relatively high but variable Re content (~ 3.5 to 63 ppb), whereas pyrrhotite Re contents are much lower and more consistent (~ 0.3 – 0.6 ppb). Common Os contents for both minerals were comparable, as indicated by ¹⁹²Os concentrations (arsenopyrite = 0.003 – 0.021 ppb; pyrrhotite = 0.009 – 0.032 ppb). The variation in total Re (and corresponding radiogenic ¹⁸⁷Os) and common Os contents between arsenopyrite and pyrrhotite results in a large range in ¹⁸⁷Re/¹⁸⁸Os and ¹⁸⁷Os/¹⁸⁸Os ratios.

Regression of all seven arsenopyrite analyses results in a Model 1 isochron with an age of 1736 ± 8 Ma (Fig. 4.1.6a; MSWD = 1.6, initial Os ratio (Os_i) = 0.28 ± 0.15). The high precision of the age and, to a lesser degree, in the Os_i is a function of the large

Figure 4.1.5: Electron microprobe photomicrographs of monazite crystals from Harney Peak granite thin sections used for laser ablation U-Pb geochronology. Samples are (a) 9A-1, (b) 9A-3, (c) 9B-1, (d) 9B-3, and (e) 9B-4.



spread between data points ($^{187}\text{Re}/^{188}\text{Os} = \sim 400 - 17,000$) and the excellent fit of data to the regression line. Five of the seven Homestake arsenopyrites qualify as ‘low-level highly radiogenic’ samples (i.e. $^{187}\text{Re}/^{188}\text{Os} > 5000$; Stein et al., 2000), and can be used to calculate single mineral model ages, assuming an initial $^{187}\text{Os}/^{188}\text{Os}$ ratio of $0.28 (\pm 0.15)$ as derived from the regression analysis (Arne et al., 2001; Morelli et al., 2005). Model ages for these five samples range from ca. 1715 Ma to 1741 Ma, identical (within associated 2σ uncertainties) to the Re-Os arsenopyrite isochron age.

In contrast, pyrrhotite analyses are highly scattered on a $^{187}\text{Re}/^{188}\text{Os}$ vs. $^{187}\text{Os}/^{188}\text{Os}$ plot (Fig. 4.1.6b). Owing to the consistency of Re and common Os concentrations, the spread between pyrrhotite data points is much more restricted than for arsenopyrite, with a range in $^{187}\text{Re}/^{188}\text{Os}$ from $\sim 20 - 80$. The collective regression of all ten pyrrhotite analyses yield a Model 3 ‘age’ of 1558 ± 680 Ma (MSWD = 2232, $\text{Os}_i = 0.4 \pm 0.6$ Ma). Only three of the pyrrhotite analyses plot on the arsenopyrite regression line, yielding a combined (arsenopyrite + pyrrhotite) Re-Os age of 1736.2 ± 6.6 Ma (MSWD = 1.2, $\text{Os}_i = 0.29 \pm 0.01$ Ma), whereas the seven remaining pyrrhotite data scatter both above and below the arsenopyrite isochron. Inclusion of these three pyrrhotite analyses with the seven Re-Os arsenopyrite analyses has a negligible effect on the determined Re-Os arsenopyrite isochron age, but does generate a slightly more precise Os_i ($= 0.29 \pm 0.01$). The lack of observable textural differences between these three pyrrhotite samples and those that show scattered Re-Os isotopic systematics obscures the significance of the variable pyrrhotite results.

Table 4.1.1: Re-Os isotopic data for Homestake arsenopyrite and pyrrhotite.

Sample	$^{187}\text{Re}/^{188}\text{Os}$	2σ	$^{187}\text{Os}/^{188}\text{Os}$	2σ	error. corr. (ρ)	model age (Ma)*
<i>arsenopyrite</i>						
H-1a	7860	280	231.2	8.4	0.978	1738
H-2a	513	50	15.3	1.5	0.994	—
H-2b	8100	2100	235	60	1.00	1723
H-2c	12400	2400	362	70	1.00	1724
H-2d	408	15	12.30	0.50	0.907	—
H-3b	7450	480	220	14	0.994	1741
H-3c	16700	2100	485	62	0.983	1715
<i>pyrrhotite</i>						
H-P1a	80.40	1.10	2.31	0.03	0.823	—
H-P1(ex)a	52.93	0.83	1.74	0.03	0.886	—
H-P2a	21.63	0.28	1.09	0.02	0.491	—
H-P1b	45.13	0.42	1.10	0.01	0.798	—
H-P2b	52.17	0.74	2.44	0.03	0.862	—
H-P1c	62.86	0.96	2.143	0.032	0.906	—
H-P2c	24.54	0.33	1.011	0.011	0.732	—
H-P1d	26.32	0.32	0.89	0.01	0.701	—
H-P1(ex)d	53.2	1.7	1.843	0.056	0.926	—
H-P2d	76.4	1.7	2.367	0.052	0.945	—

*assumes initial $^{187}\text{Os}/^{188}\text{Os}$ of 0.28 (from arsenopyrite isochron regression)

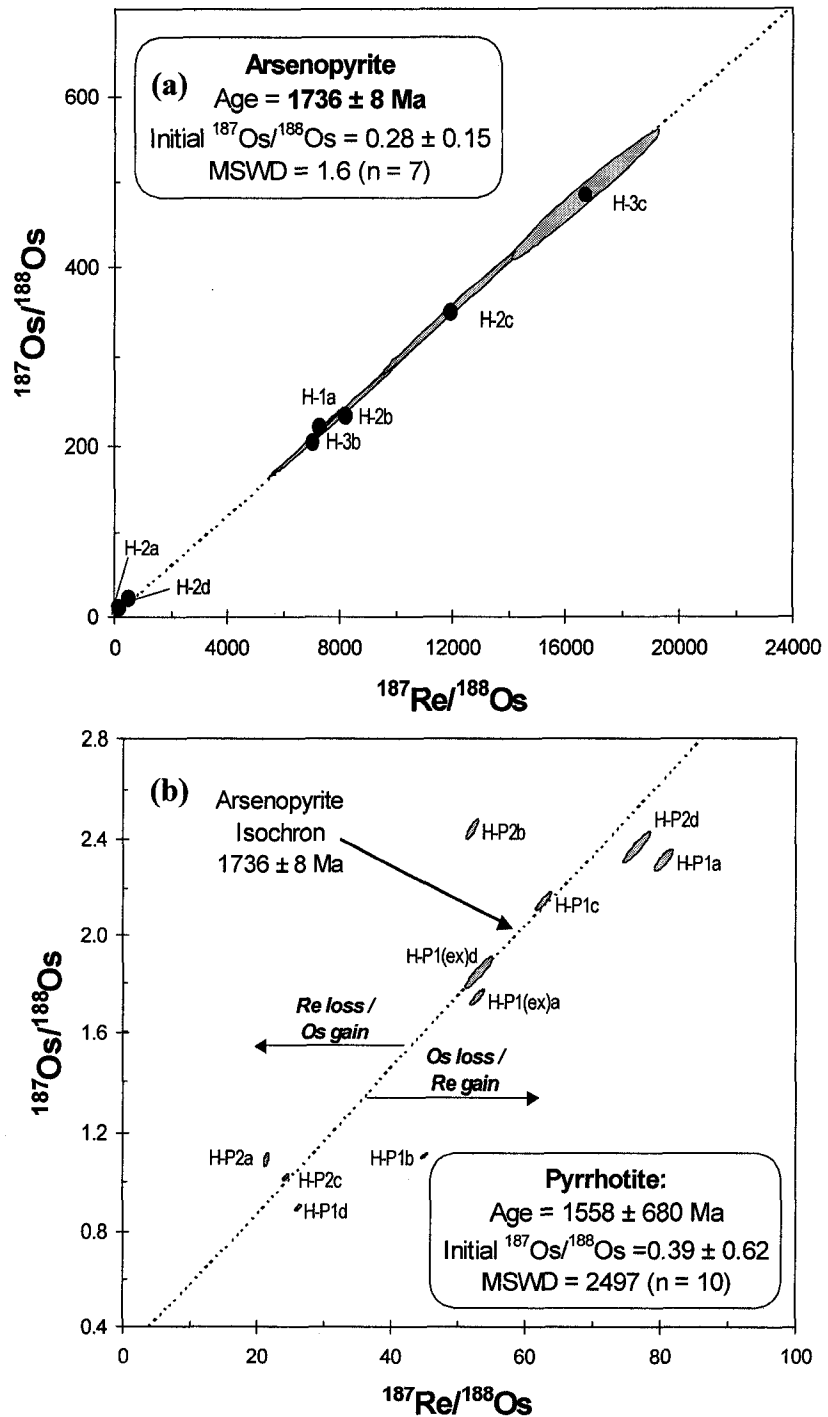


Figure 4.1.6: (a) Conventional Re-Os isochron from analyses of Homestake deposit arsenopyrite. (b) Results of linear regression of Re-Os analyses of Homestake deposit pyrrhotite, with reference to the Re-Os arsenopyrite isochron from (a).

U-Pb

In total, twenty-seven U-Pb isotopic analyses were performed using laser ablation mass spectrometry on two monazite crystals from thin section 9A and on three monazite crystals from thin section 9B (Table 4.1.2). All monazites analyzed have relatively high U, Th, and Pb concentrations and only four of the twenty-seven analyses yielded detectable common Pb. Though detectable, ^{204}Pb contents in these four analyses were low, and were corrected for prior to age calculation.

All monazite analyses are concordant within associated 2σ uncertainties. Inspection of $^{207}\text{Pb}/^{206}\text{Pb}$ ages from spatial groupings of each of the crystals apparently reveals two distinct age groupings. Nineteen analyses of samples 9A and 9B yield a weighted mean $^{207}\text{Pb}/^{206}\text{Pb}$ age of 1694.2 ± 2.4 Ma (2σ ; MSWD = 0.75, probability = 0.76; Fig. 4.1.7a). The remaining eight analyses, which includes all analyses of sample 9B-3 except for 9B-3-6, yield apparent $^{207}\text{Pb}/^{206}\text{Pb}$ ages between 1675 and 1686 Ma and a weighted mean $^{207}\text{Pb}/^{206}\text{Pb}$ age of 1682.5 ± 3.4 Ma (2σ ; MSWD = 0.62, probability = 0.74; Fig. 4.1.7). Analysis 9B-3-6, from the central region of monazite grain 9B-3 (Fig. 4.1.5d), yields an apparent $^{207}\text{Pb}/^{206}\text{Pb}$ age of 1699 ± 11 Ma, and is included within the first regression. However, a different interpretation of these data is possible. When plotted on a cumulative probability plot, the determined $^{207}\text{Pb}/^{206}\text{Pb}$ ages from all analyses resemble a normal distribution (Fig. 4.1.7b; 26 of 27 analyses) and define a weighted mean $^{207}\text{Pb}/^{206}\text{Pb}$ age of 1691.0 ± 2.6 (MSWD = 1.6; 26 of 27 analyses). The possible significance of each of these age interpretations is discussed further in the next section.

4.1.7. Discussion

Significance of Re-Os arsenopyrite and pyrrhotite results and assessment of apparent Re-Os chronometer closure temperatures

A mathematical concept originally defined by Dodson (1973), the closure temperature of a mineral chronometer is, “the temperature of the system at the time represented by its apparent age”. In other words, the closure temperature of a particular geochronometer reflects its ability to ‘see through’ geologic events, by retention of

Table 4.1.2: U-Pb isotopic data for Harney Peak granite monazite.

Grain/ Analysis #	²⁰⁶ Pb cps	²⁰⁷ Pb/ ²⁰⁶ Pb	²⁰⁷ Pb/ ²³⁵ U ±2σ	²⁰⁶ Pb/ ²³⁸ U ±2σ	rho	²⁰⁷ Pb/ ²⁰⁶ Pb apparent age (Ma)	²⁰⁶ Pb/ ²³⁸ U apparent age (Ma)	% discord.
9A-1								
-1	1846188	0.10410	0.00061	0.273	0.99	1698	1831	-8
-2	489646	0.10406	0.00060	0.179	0.99	1698	1870	-10
9A-3								
-1	813090	0.10433	0.00059	0.158	0.99	1703	1697	0
-2	1260174	0.10423	0.00074	0.142	0.98	1701	1706	0
-3	1514240	0.10389	0.00060	0.140	0.98	1695	1679	1
9B-1								
-1	1665346	0.10393	0.00053	0.283	0.99	1695	1745	-3
-2	1246611	0.10400	0.00054	0.295	0.99	1697	1798	-6
-3	2788506	0.10356	0.00053	0.310	0.99	1689	1807	-7
-4	2370122	0.10395	0.00066	0.275	0.99	1696	1795	-6
-5	1740174	0.10370	0.00054	0.287	0.99	1691	1826	-8
-6	1692077	0.10411	0.00061	0.281	0.99	1699	1795	-6
-7	2742664	0.10367	0.00054	0.282	0.99	1691	1798	-6
-8	1987878	0.10350	0.00055	0.259	0.99	1688	1848	-10
-9	1755524	0.10384	0.00057	0.250	0.99	1694	1787	-5
-10	2793019	0.10347	0.00056	0.302	0.99	1687	1837	-9
9B-3								
-1	1670799	0.10329	0.00053	0.135	0.99	1684	1640	3
-2	1231602	0.10336	0.00058	0.131	0.98	1685	1679	0
-3	1549173	0.10281	0.00052	0.134	0.99	1675	1653	1
-4	3052690	0.10339	0.00053	0.130	0.99	1686	1679	0
-5	3479083	0.10319	0.00053	0.128	0.99	1682	1669	1
-6	1587555	0.10412	0.00060	0.139	0.98	1699	1699	0
-7	3844246	0.10325	0.00054	0.136	0.99	1683	1691	0
-8	1711706	0.10296	0.00055	0.134	0.99	1678	1714	-2
-9	2742459	0.10337	0.00055	0.142	0.99	1686	1685	0
9B-4								
-1	994405	0.10398	0.00083	0.471	0.99	1696	1936	-14
-2	1093466	0.10357	0.00059	0.132	0.98	1689	1675	1
-3	1416950	0.10367	0.00059	0.129	0.98	1691	1665	2

Note: all analyses were corrected for measured ²⁰⁴Pb contents, which was negligible in most cases.

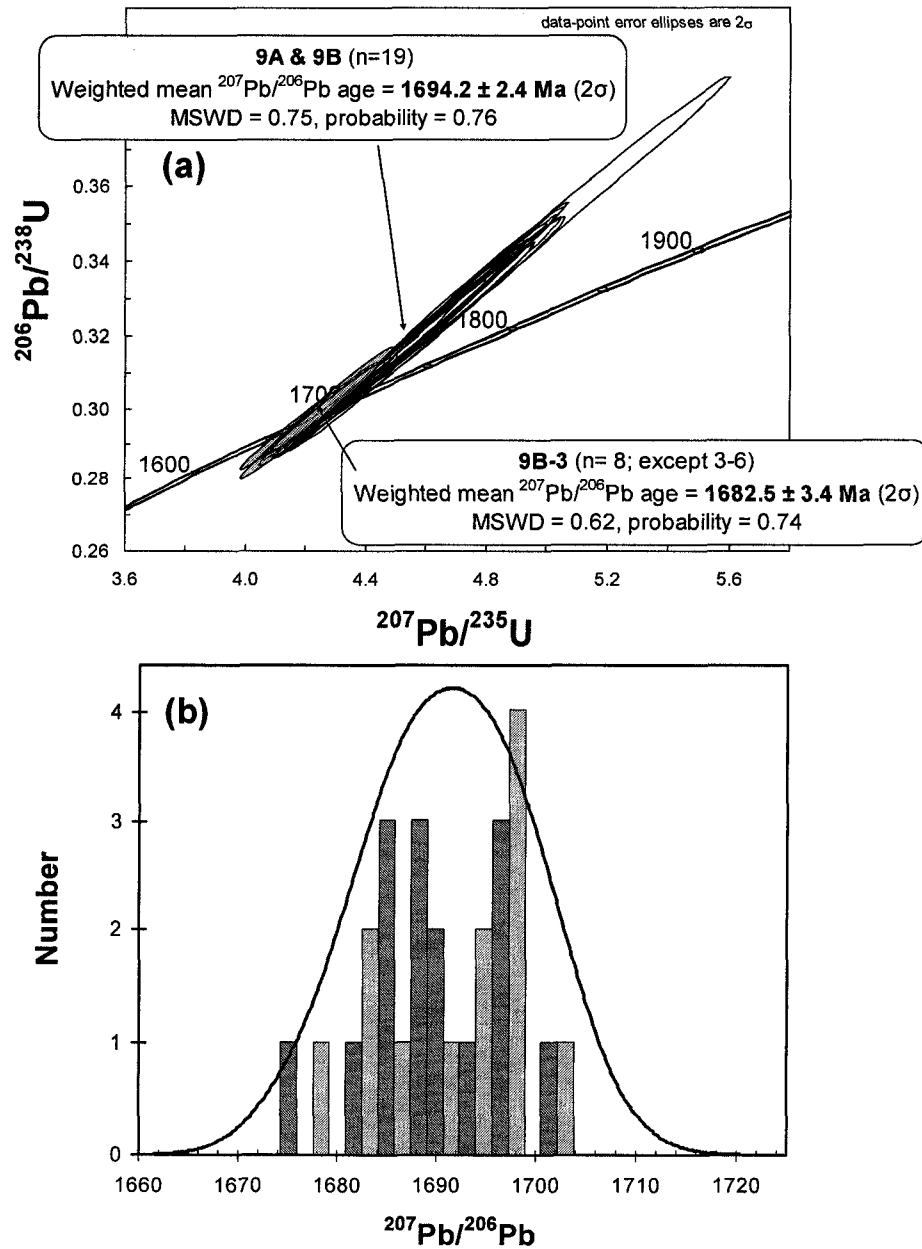


Figure 4.1.7: U-Pb isotopic data from laser ablation analyses of monazite from the Harney Peak granite: (a) U-Pb concordia plot, indicating two age domains at 1694 and 1683 Ma. (b) Cumulative distribution plot of determined $^{207}\text{Pb}/^{206}\text{Pb}$ ages approaching a normal distribution, with a weighted mean $^{207}\text{Pb}/^{206}\text{Pb}$ age of $1691.0 \pm 2.6 \text{ Ma}$.

primary age information. The new and existing age constraints for Homestake gold mineralization, coupled with knowledge of the syn- and post-mineralization thermal history of the region allow for estimations of apparent closure temperatures of the Re-Os arsenopyrite and pyrrhotite chronometers.

The timing of Homestake gold mineralization is bracketed between the onset of prograde regional metamorphism at ca. 1750 Ma and granite emplacement at ca. 1715 Ma. The Re-Os arsenopyrite age of 1736 ± 8 Ma is in excellent agreement with these constraints, and is interpreted as the age of gold mineralization at the Homestake deposit. The highly scattered Re-Os pyrrhotite analyses yield a very imprecise age result (1558 ± 680 Ma) that shows pyrrhotite to be unreliable for determination of mineralization ages. Given that the analyzed pyrrhotite contained negligible blank proportions, and that sufficiently high amounts of $^{187}\text{Os}^*$ were analyzed (1.2 – 4.2 picograms) to yield precision of better than 0.2% SE on raw measured $^{187}\text{Os}/^{188}\text{Os}$ ratios, both artificial contamination and spectrometric considerations can effectively be ruled out as the source of the observed scatter. An alternative possibility is the occurrence of the Claus process upon sample digestion, whereby Fe in the sample promotes oxidation of H_2S to elemental S and consequently inhibits the oxidation of Os required for sample-spike equilibration (Frei et al., 1998). However, if it has occurred, this reaction did not apparently affect Os isotopic compositions of Homestake pyrrhotite during digestion because, in contrast to the findings of Frei et al. (1998), no decrease in Os yield was observed between analyses of higher (> 400 mg) vs. lower (< 250 mg) sample weights. Moreover, even analyses of low sample weights (e.g. P1d, P2d; Table 4.1.1), in which the effects of the Claus process should be minimized, yielded erroneous results (Fig. 4.1.6b). Still another possibility is that an Os-bearing mineral phase(s) other than pyrrhotite was inadvertently included in the digested fraction, thereby causing scatter of the measured compositions. This possibility also seems unlikely since no such mineral phase was observed during petrographic or microprobe analysis of sample HM020, nor was any mineral phase other than quartz observed during binocular inspection of the final mineral separates.

The simplest interpretation of the Re-Os results is that the Re-Os system in Homestake pyrrhotite has been disturbed subsequent to its primary crystallization. This interpretation is consistent with experimental results that show measurable diffusion of

Os in pyrrhotite at temperatures as low as 400°C and on time scales less than 500,000 years (Brenan et al., 2000). In a study of Voisey's Bay magmatic nickel sulfide system, Lambert et al. (2000) provide further support for open-system behaviour of pyrrhotite. Regression of a six point multi-mineral isochron from the Voisey's Bay intrusion, including one pyrrhotite point, defines an age ~ 300 million years younger than the true mineralization age, a result attributed to mineral scale disturbance during a Grenvillian (1.0 Ga) hydrothermal overprint. Frei et al. (1998) also question the ability of pyrrhotite to retain primary Re-Os data in their study of shear zone hosted gold deposits in the Harare-Shamva Greenstone Belt, Zimbabwe. Two Re-Os analyses of pyrrhotite from the Kimberley mine plot well below a 1960 Ma Re-Os reference isochron defined by analyses of molybdenite-bearing scheelite, and are interpreted to reflect disturbance of pyrrhotite during post-crystallization, low temperature alteration.

Peak regional metamorphism in the Black Hills was contemporaneous with F₂ folding (Dahl et al., 1999) and resulted in the development of prominent S₂ regional foliation. This prolonged metamorphic event was initiated throughout the Black Hills at ca. 1760 - 1750 Ma (Dahl and Frei, 1998; Dahl et al., 2005), and resulted in prograde garnet growth at the Homestake deposit. Peak metamorphic temperatures were attained ~ 10 -15 m.y. after garnet growth (ca. 1745 Ma), just prior to the onset of gold mineralization (1736 ± 8 Ma, this study). Although there are currently no rigorous determinations of peak metamorphic temperatures in the immediate Homestake area, Helms and Labotka (1991) use Fe-Mg exchange equilibrium between garnet and biotite to estimate a temperature range from 469 – 500°C for garnet zone rocks in the central Black Hills. Nabelek et al. (2006) suggest that this temperature range is slightly overestimated, and establish a modified temperature range of ~ 400 – 480°C for garnet zone rocks. These temperature ranges are consistent, within error, with temperature determinations for peak metamorphic conditions attained in the Tinton area (500°C – 550°C; Dahl et al. 1999 and references therein) from Fe-Mg compositions of coexisting biotite and garnet in the Homestake host rocks (500°C; Chinn et al., 1969), and for the gold mineralizing event itself from arsenopyrite geothermometry (500°C; Sharp et al., 1985). This thermal regime was maintained in mid-crustal rocks of the Black Hills, including at the Homestake deposit, for a prolonged period of time, culminating in

regional unroofing, crustal melting, and emplacement of the Harney Peak granite beginning at ca. 1715 Ma (Helms and Labotka, 1991; Redden et al., 1991). Elevated temperature conditions prevailed in these rocks until 1500 – 1300 Ma, at which time regional temperatures finally cooled below the closure temperatures of the Ar/Ar muscovite (~ 350°C) and biotite (~ 300°C) chronometers (Holm et al., 1997; Dahl et al., 1999). Based on the determined Re-Os ages and on these existing temperature constraints, the minimum apparent closure temperature for the Re-Os arsenopyrite chronometer is conservatively estimated at 400°C, and likely exceeds 480°C. In contrast, the susceptibility of the Re-Os pyrrhotite chronometer to isotopic disturbance is confirmed, with a proposed apparent closure temperature of < 350°C.

Re-Os systematics of arsenopyrite and pyrrhotite

Textural relationships between ore-related minerals in the Homestake deposit indicate that arsenopyrite and pyrrhotite crystallized simultaneously during the hydrothermal event. This observation has important implications for the Re-Os systematics of these minerals by revealing information on both the fluid-mineral partitioning behaviour and post-crystallization mobility of Re and Os in fluid-mediated systems.

Homestake arsenopyrite has an average Re concentration of ~ 25 ppb, whereas pyrrhotite has a considerably lower average Re concentration of ~ 0.4 ppb. Although the difference is less than one order of magnitude, this variation is significant from an analytical perspective since the proportion of produced $^{187}\text{Os}^*$ is much higher in the arsenopyrite, allowing for easier and more precise spectrometric measurement of $^{187}\text{Os}^*$. In contrast, both arsenopyrite and pyrrhotite have similar average common Os contents, as indicated by ^{192}Os concentrations of ~ 11 and 19 ppt, respectively. At face value, these Re and Os concentrations suggest that Re has a slight preference for arsenopyrite over pyrrhotite, whereas Os partitioning is not controlled by these mineralogical variations.

A possible argument against this is that original Re-Os contents of pyrrhotite have been disturbed after crystallization, as shown by the isotopic data. This is consistent with the interpretation of Frei et al. (1998) that pyrrhotite acts as a Re ‘sink’ during post-crystallization alteration and/or weathering processes, whereby excess Re from the

alteration fluids is preferentially taken into the pyrrhotite structure. However, the Homestake pyrrhotite data do not support this view. It is evident from Figure 4.1.6b that no consistent pattern of scatter of individual pyrrhotite points exists either above or below the 1736 Ma arsenopyrite reference isochron. The most likely explanation for the observed random distribution is the occurrence of micron-scale movement of Re and/or $^{187}\text{Os}^*$ within pyrrhotite, such that some pyrrhotite experienced a net Re gain/ $^{187}\text{Os}^*$ loss, and some experienced a net Re loss/ $^{187}\text{Os}^*$ gain (Fig. 4.1.6b). Retention of the 1736 Ma age by three of the pyrrhotite analyses (H-P1c, -P2c, and -P1(ex)d; Fig. 4.1.6b) might indicate that these samples were sufficiently homogenized during sample preparation procedures so as to negate the effects of this small scale Re and/or ^{187}Os movement, a phenomenon similar to that observed for molybdenite (Stein et al., 1998, 2003; Selby and Creaser, 2004). Moreover, the fact that all pyrrhotite analyses generally conform to the trend of the arsenopyrite isochron suggests that there was not a significant change to the overall Re and Os contents of the pyrrhotite. Consequently, if pyrrhotite did behave as an open system for an extended period following its initial crystallization, the very low measured Re and Os contents suggest that it did not act as a significant sink for either element.

Another interesting feature of the Re-Os isotopic compositions of Homestake arsenopyrite is the large degree of spread between individual data points along the isochron, with $^{187}\text{Re}/^{188}\text{Os}$ ratios ranging from ~ 400 (H-2d) to 16,700 (H-3c). This large variation in isotopic composition could potentially be controlled by variation in Re contents, common Os contents, or both Re and common Os contents between the arsenopyrite specimens. The large range in arsenopyrite Re contents (3 – 63 ppb) compared to the more limited range of ^{192}Os contents (3 – 21 ppt), along with the correspondence of increasing Re concentrations with increasing $^{187}\text{Re}/^{188}\text{Os}$ ratios (Table 4.1.1) suggests that the overall isotopic character of low-level sulfide minerals (i.e. highly radiogenic vs. non-radiogenic) is governed primarily by Re content. If correct, this inference has the potential to simplify sampling and analytical protocols of Re-Os low-level sulfide minerals, since screening of samples that generate isochron spread could be performed by simply determining their Re contents.

If the variable Re-Os isotopic compositions in Homestake arsenopyrite are controlled mainly by differences in Re content, the actual source of these differences also becomes an important consideration. There are two possible explanations to account for this: (i) the arsenopyrite Re content is inherited directly from the hydrothermal fluid, with variations therefore reflecting slight changes in fluid chemistry over a short period of time, or (ii) the measured Re contents do not only reflect arsenopyrite compositions, but include variable proportions of input from other Re-bearing components. The first possibility seems unlikely, since there is no evidence for fluid compositional changes at Homestake. Considering the second possibility, an important observation is the recognition of significant proportions of pyrrhotite inclusions within individual arsenopyrite crystals (Fig. 4.1.8), which were not magnetically removed following isolation of arsenopyrite for Re-Os analysis. Because Homestake pyrrhotite has a much lower Re content than arsenopyrite, it is plausible that the variations in measured Re and Os contents and isotopic compositions of arsenopyrite actually reflect mixtures of variable proportions of arsenopyrite and pyrrhotite. In this scenario, arsenopyrite samples with the lowest Re contents (H-2a, -2d) originally contained the highest proportion of pyrrhotite inclusions, whereas the sample having the highest Re content (H-1a) would have had a lower proportions of inclusions. Importantly, preservation of isochronous behaviour by all arsenopyrite analyses, regardless of pyrrhotite content, requires the preservation of primary Re-Os isotopic compositions of the included pyrrhotite. If true, this implies that the pyrrhotite was effectively 'guarded' by the arsenopyrite, the latter preventing any Re and/or Os diffusion outside of pyrrhotite grain boundaries subsequent to mineral crystallization. Further work is required to confirm this interpretation.

U-Pb monazite geochronology of the Harney Peak granite

The close spatial and temporal association between late orogenic granitoid intrusions and emplacement of orogenic gold deposits is well documented (Groves et al., 1998; Goldfarb et al., 2001), but the genetic relationship, if any, remains unclear. Intrusion of the Harney Peak granite is widely accepted to have occurred ca. 1715 Ma, based on one slightly discordant U-Pb monazite analysis reported by Redden et al. (1991) with a $^{207}\text{Pb}/^{206}\text{Pb}$ age of 1715 ± 3 Ma. Two highly discordant U-Pb zircon analyses

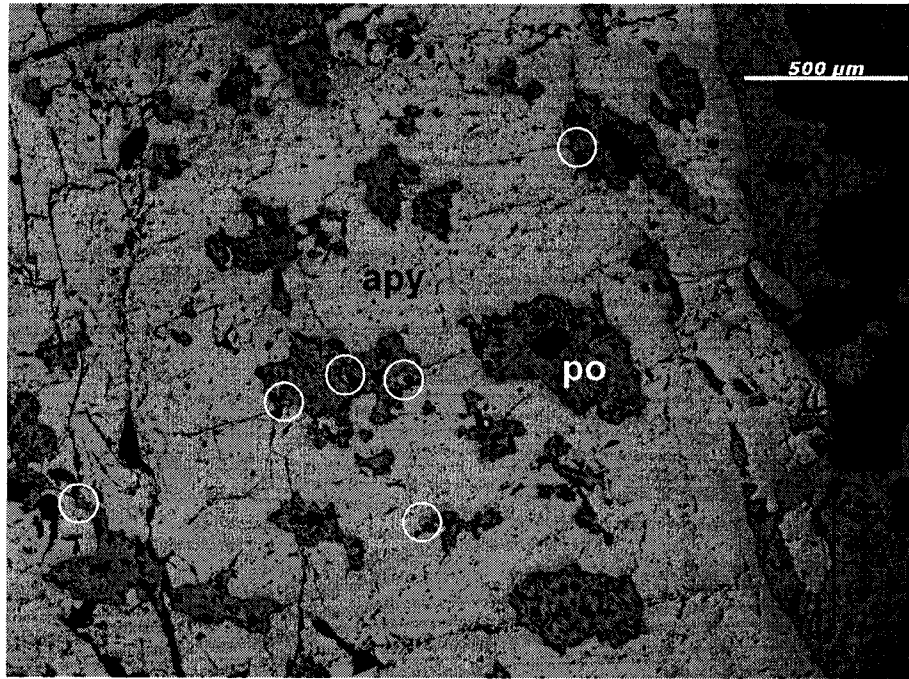


Figure 4.1.8: Photomicrograph of sample HMO20 showing inclusions of pyrrhotite (po) within arsenopyrite (apy). White circles surround visible gold inclusions.

reported in the same study yield an older upper intercept age of 1727.7 ± 4.3 Ma ($^{206}\text{Pb}/^{238}\text{U}$ ages of 274 and 767 Ma); however, this result is considered here to be an unreliable determination for the timing of Harney Peak magmatism due to the high degree of discordance, and to the significant potential for zircon inheritance in this S-type magma. Still, more recent studies suggest that the intrusion of the Harney Peak granite might, indeed, have been a protracted magmatic event (Dahl et al., 2005; Nabelek et al., 2006).

To further constrain the timing of granitic magmatism and to better assess a possible role for emplacement of granitic magmas in the genesis of the Homestake gold deposit, U-Pb monazite geochronology was performed. As discussed earlier, analyses of multiple monazite grains in the aplite samples yielded either (i) two, apparently distinct, age populations of 1694 and 1683 Ma, or (ii) a single age of 1691 Ma, depending on the method of data analysis. The petrogenetic significance of the age determinations for Harney Peak monazite can best be determined through examination of the compositional characteristics of the analyzed grains. Ten of the nineteen spot analyses that define the apparent 1694 Ma age are derived from the > 200 μm diameter 9B-1 grain. Careful inspection of the back-scattered electron image of this grain reveals a clear pattern of concentric zoning in the top left portion of the grain (Fig. 4.1.9). This concentric zoning is characteristic of monazite of igneous origin (Williams et al., 2007), likely reflecting an evolution in both the magma composition and the equilibrium composition of the monazite as it crystallized. Whether an age of 1694 or 1691 Ma age is accepted for this crystal, the observed zoning confirms that this represents the age of igneous crystallization age for the aplitic phase of the Harney Peak granite.

The validity and possible interpretation of the apparent 1683 Ma age is difficult to assess, but can be further explored using compositional variations within monazite 9B-3. This result is derived from 8 of 9 analyses of grain 9B-3, with the exception being a single spot analysis (9B-3-6) from the central region of the crystal that yields an apparent $^{207}\text{Pb}/^{206}\text{Pb}$ age of 1699 Ma (Fig. 4.1.10a). A possible explanation for the anomalous age variation in monazite crystal 9B-3 is that this crystal comprises a core that formed during magma crystallization at ca. 1694 Ma, and a younger rim that represents renewed monazite growth around the core at ca. 1683 (Fig. 4.1.10b). To test this idea, yttrium

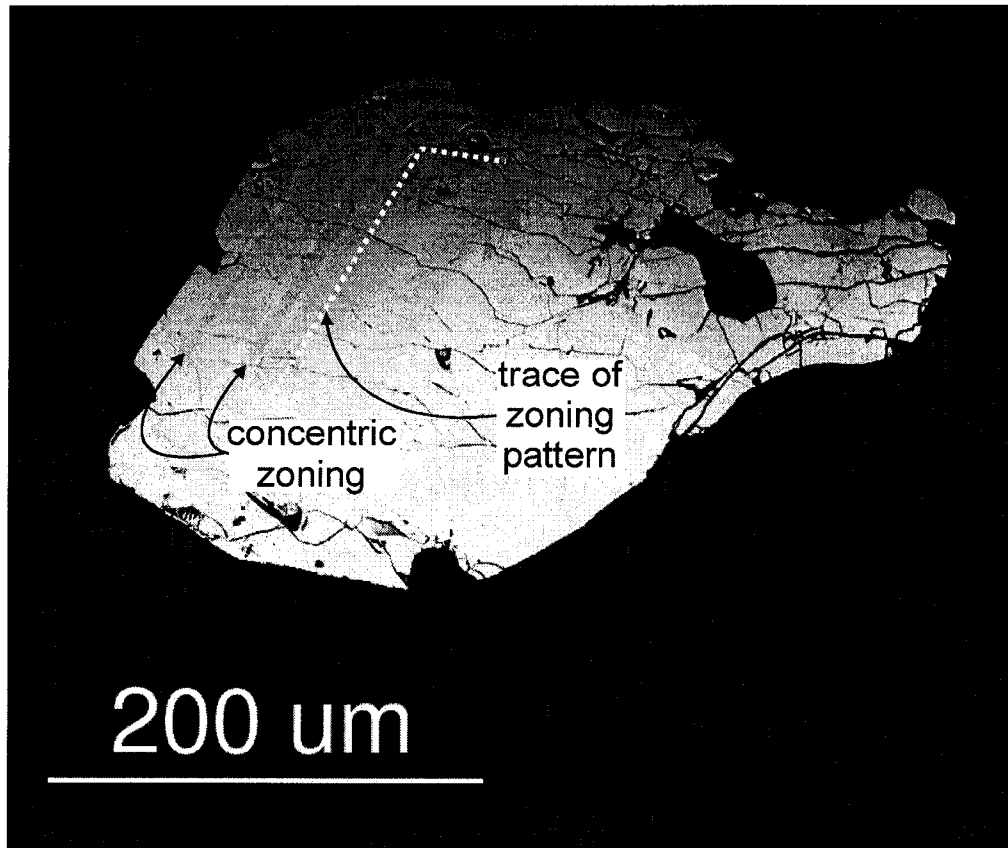


Figure 4.1.9: Electron microprobe photomicrograph showing magmatic zoning in monazite crystal from sample 9B-1 of Harney Peak Granite.

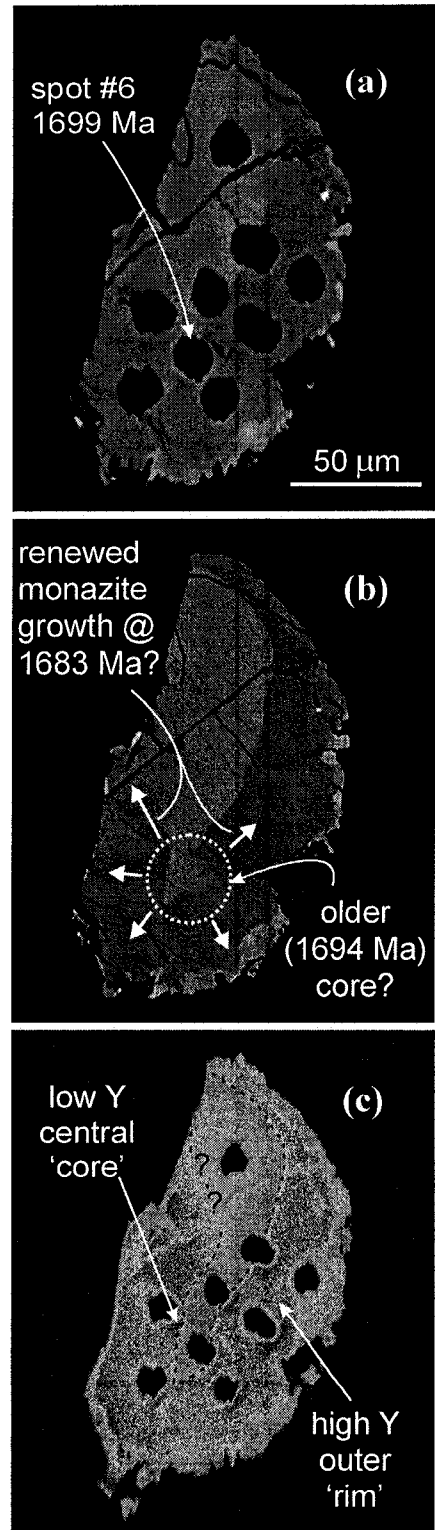
compositional mapping was performed by microprobe to reveal compositional zoning in the crystal (Dahl et al., 2005; Williams, 2007). The resulting yttrium distribution map of this grain does confirm the presence of intracrystal chemical zonation, showing a central region with a relatively low yttrium concentration surrounded by a high yttrium outer region (Fig. 4.1.10c). However, this low yttrium region encompasses an area beyond that of analysis 9B-3-6 and includes an area covered by spot analyses that yielded the apparently younger (1683 Ma) age. The existing monazite data are thus insufficient to conclusively determine whether monazite growth in this phase of the granite occurred only at 1691 Ma, or over a prolonged period from at least 1694 to 1683 Ma. Whatever the case, these results do confirm that the granite magmatism was a prolonged magmatic event. They also support the interpretation of Redden et al. (1991), that their 1715 ± 3 Ma U-Pb monazite date, derived from a foliated sample, represents the earliest phase of this magmatic event.

The younger ages presented here are interpreted to represent continued crustal melting and injection of aplite dikes, and directly constrains the timeframe for granite magmatism to between 1715 to ca. 1691 Ma, or possibly as late as 1683 Ma. This range is consistent with results from electron probe microchronometry of metamorphic monazite (Dahl et al., 2005), for which a 1715 to 1690 Ma timeframe was determined for the timing of the D₃ deformational event, resulting from localized doming related to granite magmatism. Importantly with respect to gold mineralization, the combined U-Pb monazite data indicate that the Harney Peak magmatic event significantly post-dated, and was thus unrelated to, the Homestake gold mineralizing event.

Implications for Paleoproterozoic gold metallogeny in the Black Hills

As reviewed by Patterson and Lisenbee (1990), various epigenetic models have been proposed for the origin of the Homestake deposit. These include a remobilized syngenetic model (Rye and Rye, 1974; Rogers, 1990; Redden and French, 1990), an intrusion-related model (Bachman and Caddey, 1990), and a metamorphic dehydration model (Patterson and Lisenbee, 1990). Even within the individual models, there is further debate as to the ultimate rock type that sourced the gold. The data presented here provide an excellent geochronological framework for clarifying temporal relationships between

Figure 4.1.10: Electron microprobe photomicrographs of Harney Peak monazite sample 9B-3, showing (a) location of laser ablation pits, (b) interpretation of grain history based on U-Pb results, and (c) yttrium map of grain in relation to pit location. Analyses were performed on polished thin sections using a JEOL JXA-8900R electron microprobe at the University of Alberta. Compositional (yttrium) mapping was done by scanning a focused beam using an accelerating potential voltage of 20.0 kV, a probe current of $1.016 \text{ e}^{-7} \text{ A}$, and a counting time of 50 ms.



Homestake gold mineralization and tectonic events that may have played a role in its origin. Moreover, Os_i from arsenopyrite provides valuable new information for the origin of ore-related metals at Homestake.

The combination of the new Re-Os arsenopyrite age of 1736 ± 8 Ma for gold mineralization and the established 1715 – 1690(?) Ma range for granite magmatism in the Black Hills effectively preclude models that relate these two events. Although development of orogenic gold deposits and regional granitoid magmatism might be eventual products of the same orogenic processes, these results demonstrate that, at Homestake, they were independent geologic events that did not share a cogenetic relationship.

The 1736 Ma timing for Homestake gold mineralization is consistent with a metamorphic origin, in which gold-bearing fluids were emplaced shortly after peak metamorphic conditions in the northern Black Hills. However, timing constraints alone do not distinguish which rock types / reservoirs may have contributed gold to the ore system. In this regard, initial Os isotopic compositions of the Homestake sulfides can provide unique insight into the ore-forming process, and can be used to directly test the feasibility of specific metamorphic models. For the remobilized syngenetic model, whereby the origin of Homestake epigenetic gold mineralization is attributed to dissolution, mobilization, and reconcentration of older syngenetic exhalative ore during regional metamorphism, evidence of the prior crustal prehistory should be evident in the sulfide initial Os ratio. The determined Os_i ratio for Homestake arsenopyrite (0.28 ± 0.17) does not support this model. This initial ratio is unradiogenic, meaning extensive input of Os from older ore is unlikely. Although difficult to precisely quantify, transfer of this Os isotopic signature to Homestake sulfides by a remobilizing fluid would only be feasible if the original syngenetic ore had a near chondritic Os_i and a very low Re content (i.e. a $^{187}Re/^{188}Os < 50$); such Re-Os isotopic compositions are atypical of Paleoproterozoic, syngenetic massive sulfide ores elsewhere in the Trans-Hudson Orogen (Chapter 5, this study). For example, sulfide ore with an age of 1974 Ma (the assumed depositional age of the Homestake iron formation) and with a conservatively low $^{187}Re/^{188}Os$ of 100 and a chondritic initial Os ratio, would evolve to a $^{187}Os/^{188}Os$ ratio of

~ 0.50 by 1736 Ma, distinctly more radiogenic than the Os_i determined from the arsenopyrite.

An alternative possibility, as forwarded by Caddey et al. (1990) on the basis of work on Archean greenstone-hosted gold by Groves et al. (1987), is that mafic igneous rocks ultimately sourced the gold in the Homestake deposit. The most voluminous sequence of mafic rocks known in the northern Black Hills is the Yates Unit (Poorman Fm.) of tholeiitic meta-basalts, which erupted ca. 2000 Ma (Redden et al., 1990) in a backarc basin setting. However, considering the new Os isotopic data presented here, this model suffers from the same issue as the remobilized syngenetic model, owing to the characteristically elevated $^{187}\text{Re}/^{188}\text{Os}$ ratios of mid-ocean ridge basalts (100 – 5000; Shirey and Walker, 1998). Osmium derived from these basalts during metamorphic dehydration at 1736 Ma would therefore be expected to have $^{187}\text{Os}/^{188}\text{Os}$ ratios considerably higher than the 0.28 value determined for the Homestake sulfides. A minimum $^{187}\text{Os}/^{188}\text{Os}$ ratio of ~ 0.54 for 1736 Ma sourced by 2000 Ma basalts can be calculated assuming a $^{187}\text{Re}/^{188}\text{Os}$ ratio = 100, and a chondritic Os_i . As with the syngenetic model, the Yates Unit basalts thus yield a calculated Os_i value that is too radiogenic to explain that determined for Homestake arsenopyrite.

In the absence of a more suitable explanation, the initial Os isotopic composition of the Homestake sulfides might best be attributed to the presence of mantle-derived osmium in the hydrothermal system. Considering the lack of ca. 1750 Ma rocks in the Black Hills, a plausible scenario is one in which the mantle supplied a component of heat for (ca. 1750 Ma) peak regional metamorphism in the Black Hills, and also contributed some fluids and metals to the Homestake mineralizing system. If a valid model, there are currently no data available to indicate whether this heat transfer was a conductive or advective process. The major implication of this interpretation is that the mantle may also supply some or all of the gold to the ore system, a potentially significant conclusion for improving our understanding of the genesis of OGD. Ultimately, the validity of this and other models for gold mineralization will hinge largely on the accurate characterization of Os isotope compositions of potential source rocks in the region, and procurement of supplementary data on ore component compositions from innovative geochemical techniques. These matters are considered in more detail in Chapter 4.2.

4.1.8. References

Arne, D. C., Bierlein, F. P., Morgan, J. W., and Stein, H. J., 2001, Re-Os dating of sulfides associated with gold mineralization in central Victoria, Australia: *Economic Geology*, v. 96, p. 1455-1459.

Bachman, R. L., Sneyd, D. S., and Campbell, T. J., 1990, The Crook Mountain Granite and its possible relation to Early Proterozoic gold mineralization, Homestake Mine, Black Hills, South Dakota: Geological Society of America, Rocky Mountain Section, Abstracts with Programs 22, p. A2.

Bingen, B., and Stein, H.J., 2003, Molybdenite Re-Os dating of biotite dehydration melting in the Rogaland high-temperature granulites, S Norway: *Earth and Planetary Science Letters*, v. 208, p. 181 - 195.

Brenan, J. M., Cherniak, D. J., and Rose, L. A., 2000, Diffusion of osmium in pyrrhotite and pyrite: implications for closure of the Re-Os isotopic system: *Earth and Planetary Science Letters*, v. 180, p. 399-413.

Caddey, S. W., Bachman, R. L., Campbell, T. J., Reid, R. R., and Otto, R. P., 1991, The Homestake gold mine, an early Proterozoic iron-formation-hosted gold deposit, Lawrence County, South Dakota: U. S. Geological Survey Bulletin 1857-J, 67 p.

Chinn, W., 1969, Structural and mineralogical studies at the Homestake mine, Lead, South Dakota. Ph.D. dissertation, Univ. California, Berkeley, California.

Connolly, J. P., 1927, The Tertiary mineralization of the northern Black Hills: South Dakota School of Mines and Technology Bulletin 15, 130 p.

Dahl, P.S., and Frei, R., 1998, Step-leach Pb-Pb dating of inclusion-bearing garnet and staurolite, with implications for Early Proterozoic tectonism in the Black Hills collisional orogen, South Dakota, United States: *Geology*, v. 26, p. 111-114.

Dahl, P.S., Terry, M.P., Jercinovic, M.J., Williams, M.L., Hamilton, M.A., Foland, K.A., Clement, S.M., and Friberg, L.M., 2005, Electron probe (Ultrachron) microchronometry of metamorphic monazite: unraveling the timing of polyphase thermotectonism in the easternmost Wyoming Craton (Black Hills, South Dakota): *American Mineralogist*, v. 90, p. 1712-1728.

Dahl, P. S., Holm, D. K., Gardner, E. T., Hubacher, F. A., and Foland, K. A., 1999, New constraints on the timing of Early Proterozoic tectonism in the Black Hills (South Dakota), with implications for docking of the Wyoming province with Laurentia: *Geological Society of America Bulletin*, v. 111, p. 1335-1349.

Frei, R., Nagler, Th. F., Schonberg, R., and Kramers, J. D., 1998, Re-Os, Sm-Nd, U-Pb, and stepwise leaching isotope systematics in shear-zone hosted gold mineralization: Genetic tracing and age constraints of crustal hydrothermal activity: *Geochimica et Cosmochimica Acta*, v. 62, p. 1925-1936.

Goldfarb, R.J., Groves, D.I., and Gardoll, S., 2001, Orogenic gold and geologic time: a global synthesis: *Ore Geology Reviews*, v. 18, p. 1-75.

Goldfarb, R. J., Baker, T., Dube, B., Groves, D. I., Hart, C. J. R., and Gosselin, P., 2005, Distribution, character, and genesis of gold deposits in metamorphic terranes, *in*: Hedenquist, J.W., Thompson, J.F.H., Goldfarb, R.J., and Richards, J.P., [eds.], *Economic Geology 100th Anniversary Volume*, Society of Economic Geologists, p. 407-451.

Gosselin D. C., Papike, J. J., Zartman, R. E., Peterman, Z. E., and Laul, J. C., 1988, Archean rocks of the Black Hills, South Dakota: reworked basement from the southern

extension of the Trans-Hudson Orogen: Geological Society of America Bulletin, v. 100, p. 1244-1249.

Groves, D. I., Goldfarb, R. J., Gebre-Mariam, M., Hagemann, S. G., and Robert, F., 1998, Orogenic gold deposits: A proposed classification in the context of their crustal distribution and relationship to other gold deposit types: Ore Geology Reviews, v. 13, p. 7-27.

Groves, D.I., Phillips, G.N., Ho, S.E., Houston, S.M, Standing, C.A., 1987, Craton-scale distribution of Archean greenstone gold deposits; predictive capacity of the metamorphic model: Economic Geology, v. 82, p. 2045-2058.

Gustafson, J. K., 1933, Metamorphism and hydrothermal alteration of the Homestake gold-bearing formation: Economic Geology, v. 28, p. 123-262.

Lambert, D. D., Frick, L. R., Foster, J. G., Li, C., and Naldrett, A. J., 2000, Re-Os isotope systematics of the Voisey's Bay Ni-Cu-Co magmatic sulfide system, Labrador, Canada: II. Implications for parental magma chemistry, ore genesis, and metal redistribution: Economic Geology, v. 95, p. 867-888.

Hosted, J. O. and Wright, L. B., 1923, Geology of the Homestake ore bodies and the Lead area of South Dakota: Engineering and Mining Journal Press, v. 115, p. 793-799.

Mathur, R., Ruiz, and Munizaga, F., 2000, Relationship between copper tonnage of Chilean base-metal porphyry deposits and Os isotope ratios: Geology, v. 28, p. 555-558.

McCombs, J. A., Dahl, P. S., and Hamilton, M. A., 2004, U-Pb ages of Neoproterozoic granitoids from the Black Hills, South Dakota, USA: implications for crustal evolution in the Archean Wyoming province: Precambrian Research, v. 130, p. 161-184.

Morelli, R. M., Creaser, R. A., Selby, D., Kontak, D. J., and Horne, R. J., 2005, Rhenium-osmium geochronology of arsenopyrite in Meguma Group gold deposits, Meguma Terrane, Nova Scotia, Canada: Evidence for multiple gold-mineralizing events: *Economic Geology*, v. 100, p. 1229-1242.

Morelli, R.M, Creaser, R.A., Selby, D., Kelley, K.D., Leach, D.L., and King, A.R., 2004, Re-Os Sulfide Geochronology of the Red Dog Sediment-Hosted Zn-Pb-Ag Deposit, Brooks Range, Alaska: *Economic Geology*, v. 99, p. 1569 – 1576.

Nabalek, P.I. and Liu, M., 1999, Leucogranites in the Black Hills of South Dakota: the consequence of shear heating during continental collision: *Geology*, v. 27, p., 523-526.

Nabalek, P.I., Labotka, T.C., Helms, T., and Wilke, M., 2006, Fluid-mediated polymetamorphism related to Proterozoic collision of Archean Wyoming and Superior provinces in the Black Hills, South Dakota: *American Mineralogist*, v. 91, p. 1473-1487.

Noble, J. A. (1950) Ore mineralization in the Homestake gold mine: *Geological Society of America Bulletins*, v. 61, p. 221-252.

Paige, S., 1924, *Geology of the region around Lead, South Dakota*: U. S. Geological Survey Bulletin 765, 56 p.

Redden, J. A., Peterman, Z. E., Zartman, R. E., and DeWitt, E., 1990, U-Th-Pb zircon and monazite ages and preliminary interpretation of the tectonic development of Precambrian rocks in the Black Hills, *in*: Lewry, J.F. and Stauffer, M.R. [eds.], *The Early Proterozoic Trans-Hudson Orogen of North America*, Geological Association of Canada Special Paper 37, p. 229-251.

Redden, J. A., and French, G., 1989, Geologic setting and potential exploration guides for gold deposits, Black Hills, South Dakota: U. S. Geological Survey Bulletin 1857-B, p. B45-B72.

Rye, D. M., Doe, B. R., and Delevaux, M. H., 1974, Homestake gold mine, South Dakota: II. Lead isotopes, mineralization ages, and source of lead in ores of the northern Black Hills: *Economic Geology*, v. 69, p. 814-822.

Rye, D. M., and Rye, R. O., 1974, Homestake gold mine, South Dakota: I. Stable isotope studies: *Economic Geology*, v. 69, p. 293-317.

Selby, D., and Creaser, R.A., 2004, Macroscale NTIMS and microscale LA-MC-ICP-MS Re-Os isotopic analysis of molybdenite: Testing spatial restrictions for reliable Re-Os age determinations, and implications for the decoupling of Re and Os within molybdenite: *Geochimica et Cosmochimica Acta*, v. 68, p. 3897 – 3908.

Selby, D., and Creaser, R.A., 2001b, Late and Mid-Cretaceous mineralization in the northern Canadian Cordillera: constraints from Re-Os molybdenite dates: *Economic Geology*, v. 96, p. 1461-1467.

Selby, D., and Creaser, R.A., 2001a, Re-Os geochronology and systematics in molybdenite from the Endako porphyry molybdenum deposit, British Columbia, Canada: *Economic Geology*, v. 96, p. 197-204.

Shirey, S., B. and Walker, R.J., 1998, The Re-Os isotope system in cosmochemistry and high-temperature geochemistry: *Annual Review of Earth and Planetary Sciences*, v. 26, p. 423-500.

Simonetti, A., Heaman, L.M., Chacko, T., and Banerjee, N.R., 2006, In situ petrographic thin section U-Pb dating of zircon, monazite, and titanite using laser ablation-MC-ICP-MS: *International Journal of Mass Spectrometry*, v. 253, p. 87-97.

Slaughter, A. L., 1968, The Homestake Mine, *in*: Ridge, J.D. [ed.], Ore Deposits of the United States, 1933-1967 (Volume II), New York, American Institute of Mining and Metallurgy, Petroleum Engineers, p. 1436–1459.

Stein, H.J., Markey, R.J., Morgan, J.W., Hannah, J.L., Schertén, A., 2001, The remarkable Re-Os chronometer in molybdenite: how and why it works: *Terra Nova*, v. 13, p. 479-486.

Stein, H. J., Morgan, J. W., and Scherstén, A., 2000, Re-Os dating of low-level highly radiogenic (LLHR) sulfides: The Harnäs gold deposit, southwest Sweden, records continental-scale tectonic events: *Economic Geology*, v. 95, p. 1657-1671.

Williams, M.L., Jercinovic, M.J., and Hetherington, C.J., 2007, Microprobe Monazite Geochronology: Understanding Geologic Processes by Integrating Composition and Chronology: *Annual Review of Earth and Planetary Sciences*, v. 35, p. 137-175.

Zartman R. E., and Stern, T. W., 1967, Isotopic age and geologic relationships of the Little Elk Granite, northern Black Hills, South Dakota: U. S. Geological Survey Professional Paper 575-D, p. D157-D163.

4.2 Age and source constraints for the giant Muruntau gold deposit, Uzbekistan, from coupled Re-Os-He isotopes in arsenopyrite*

4.2.1. Introduction

A major Phanerozoic crust-forming episode occurred during development of the Central Asian Altiid Tectonic Collage, involving volcano-plutonic island arc development and formation of multiple subduction-accretion complexes (Yakubchuk et al., 2002) and emplacement of voluminous post-tectonic granitoid intrusions of predominately juvenile character (Jahn et al., 2000). Concomitant with development of this tectonic collage was the generation a vast metallogenic wealth, including one of the richest gold provinces on Earth, the late Paleozoic Tien Shan Orogen. In terms of endowment, the Tien Shan ranks as the second largest gold province globally, behind only the Witwatersrand deposits of South Africa. The orogen is made up of three tectonic entities, designated the Northern, Middle, and Southern Tien Shan (Fig. 4.2.1), each separated by terrane-scale faults and containing distinctive styles of ore mineralization. The Northern Tien Shan comprises the early Paleozoic Kipchak magmatic arc and its Precambrian basement, as well as late Paleozoic granitoids and associated rare metal and rare earth element mineral deposits. The Middle Tien Shan encompasses magmatic rocks of the late Paleozoic Valerianov-Beltau-Kurama arc and contains large epizonal Cu-Mo porphyry deposits, epithermal gold stockworks, polymetallic veins, epithermal gold stockworks, and Mo-W and Pb-Zn skarns. Multiple world-class 'orogenic gold deposits' (Groves et al., 1998; 'OGD') occur within the Southern Tien Shan Orogen, which represents an extensive accretionary complex that formed after early-mid Carboniferous backarc basin closure (Yakubchuk et al., 2002).

The origin of the gold endowment of the Tien Shan is obscured by a lack of reliable age information on the mineralizing events, and conflicting interpretations for the source of gold. These problems result, in part, from the use of chronometers and chemical tracers that have an uncertain genetic relationship with the ore. The purpose of this study is to accurately place the Tien Shan gold mineralizing events into a tectonic context by

* A version of this chapter has been published in *Geology* (2007, v.35, no.9, p. 795-798).

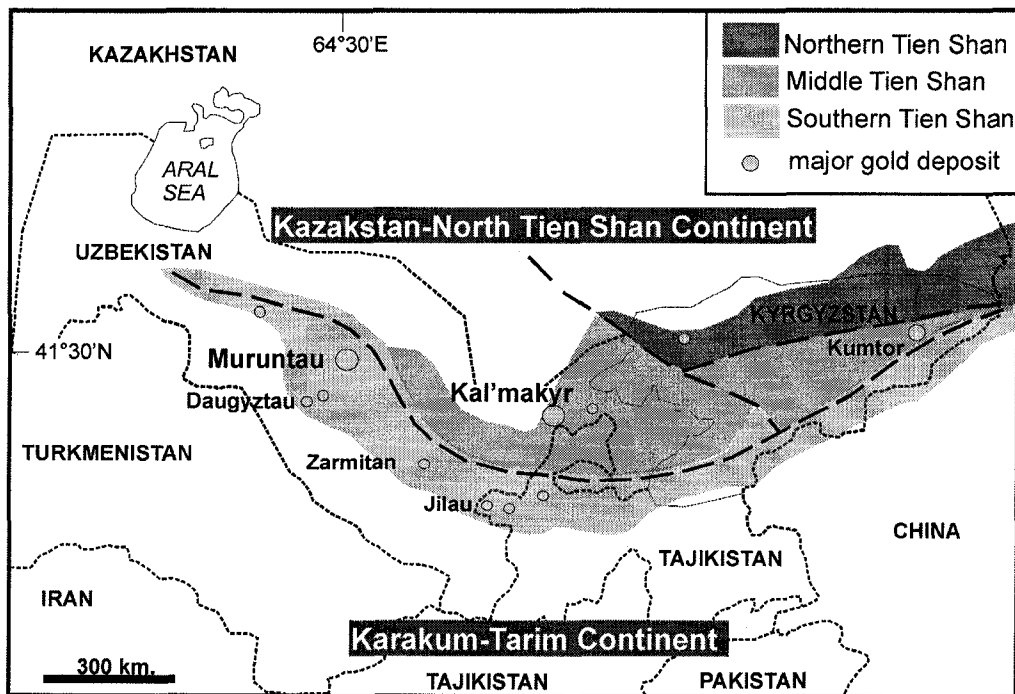


Figure 4.2.1: Tectonic subdivisions of the Tien Shan Orogen, with location of the Kal'makyr and Muruntau deposits. After Cole (2001).

using Re-Os sulfide geochronology to resolve the age of the two largest gold deposits in the Tien Shan, the Kal'makyr (Middle Tien Shan) and Muruntau (Southern Tien Shan) deposits. Furthermore, because Muruntau is the largest known OGD on Earth, it provides a spectacular opportunity to investigate the origin of this important style of gold mineralization. Orogenic gold deposits are a class of deposit represented episodically in the geologic record since ~ 3.2 Ga, occurring in broad coincidence with the production of juvenile continental crust (Goldfarb et al., 2001; Groves et al., 2005). The exact nature of this association is unknown, though mantle-to-crust heat transfer in crust-forming environments is considered necessary for driving gold-bearing hydrothermal systems (Goldfarb et al., 2001). Here, the possibility of a relationship between juvenile crust production and orogenic gold mineralization is evaluated for the Muruntau deposit. In addition to precisely determining the timing of the gold mineralization, the use of rare earth element and isotopic constraints on the source of metal (Os) and fluid (He) components to the ore system are explored by analysis of ore-related sulfide minerals.

4.2.2. Kal'makyr and Muruntau: Geology and Existing Geochronology

Together with the Dalnee deposit, the Kal'makyr deposit (2.5 Gt @ 0.5 g/t Au) makes up the giant Almalyk porphyry Cu-Au system of eastern Uzbekistan (Fig. 4.2.2), containing > 1980 t of gold. This porphyry system is situated within the southeastern portion of a 1500 km long volcano-plutonic belt comprising the Devonian-Carboniferous Valerianov-Beltau-Kurama magmatic arc. Fragmented blocks of Siluro-Devonian granitoid rocks as well as Devonian bimodal volcanic sequences and terrigenous sedimentary rocks represent the earliest development of the arc, which was built on the passive southern margin of the Kyrgyz-Kazakh microcontinent (Golovanov et al., 2005). Following deposition of thick carbonate and terrigenous sequences in the early Carboniferous, magmatic activity was renewed within the arc due to subduction beneath the margin of the Kyrgyz-Kazakh microcontinent. The initial stage of this magmatic event was characterized by andesitic volcanism and the widespread emplacement of mid-Carboniferous monzonitic, gabbroic, and dioritic plutons, as well as slightly younger granitoid magmas. This was followed by the intrusion of a gabbrodiorite-diorite-monzonite-quartz monzonite porphyry series beginning in the late Carboniferous,

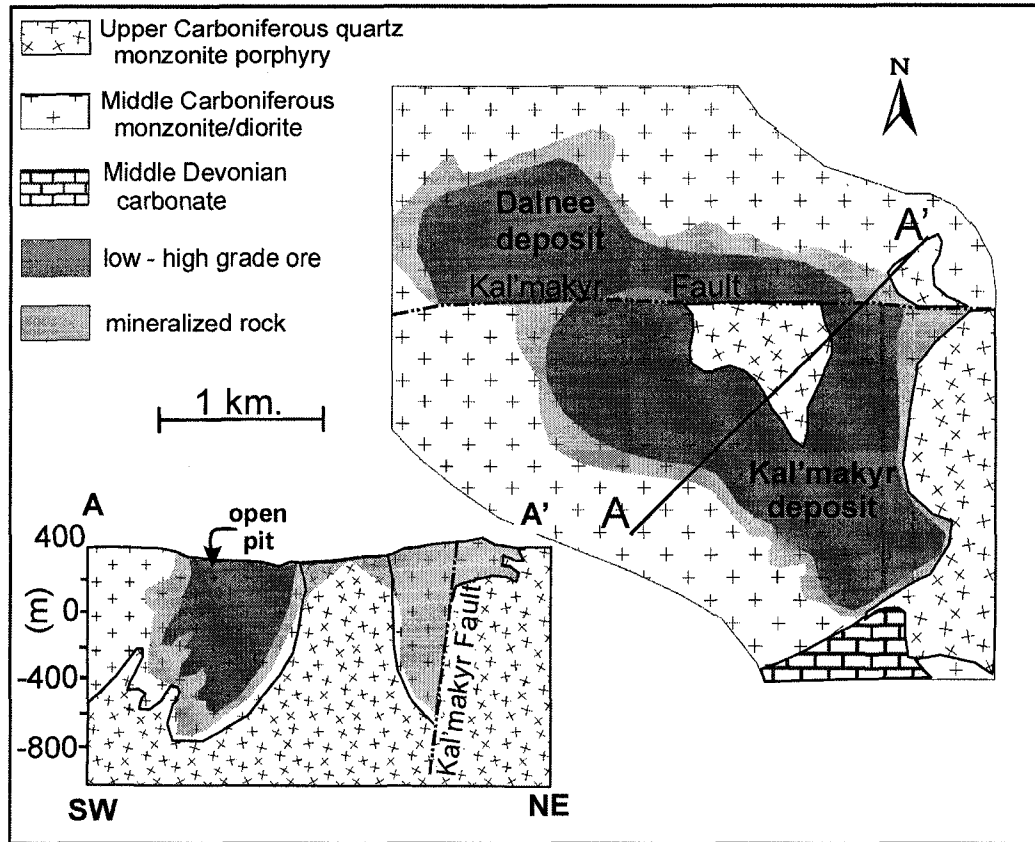


Figure 4.2.2: Geology of the Kal'makyr deposit, Middle Tien Shan Orogen, Uzbekistan. Modified from Golovanov et al. (2005).

believed to be concurrent with the porphyry-style mineralization at Almalyk. However, reliable absolute age determinations are lacking for both arc magmatism and the porphyry mineralization, the latter constrained only to a late Carboniferous to early Permian timeframe. Previous attempts at dating the mineralizing event have yielded ages of (i) 280 to 320 Ma from K-Ar whole rock dating of altered host rocks (Golovanov et al., 1988), (ii) 273 to 309 Ma from K-Ar dating of hydrothermal micas (Golovanov et al., 1988), and (iii) 270 Ma from preliminary Re-Os molybdenite dates (Badalov, 1970). Although broadly consistent with Rb-Sr ages of 320 to 290 Ma for porphyritic plutons (Golovanov et al., 2005), there remains an inadequate understanding of the temporal relationship between these events.

The giant Muruntau gold deposit has immense gold reserves (>5100 metric tons), and exhibits characteristics typical of most orogenic gold deposits, being hosted in a metamorphosed terrane, structurally controlled (Drew et al., 1996) and derived from aqueous-carbonic, low-salinity fluids (Graupner et al., 2001). Gold mineralization and associated hydrothermal alteration is confined to deformed and metamorphosed Cambro-Ordovician shales and carbonaceous siltstones of the 'Variegated Besapan Unit' (Drew et al., 1996), but also exhibits a close spatial relationship to granitoid plutons (e.g. the Murun granite and Saradin granodiorite; Kostitsyn, 1996), quartz dioritic to syenitic dikes, and lamprophyre dikes (Drew et al., 1996; Graupner et al., 2006; Fig. 4.2.3). The location of the Muruntau deposit in the thermal aureole of an unexposed pluton (Drew et al., 1996) and the presence of hydrothermally altered dikes along fault zones within the ore field (Kostitsyn et al., 1996) imply a relationship between granitoid magmatism and the ore-forming process (e.g., Drew et al., 1996; Yakubchuk et al., 2002). Ages of 286 - 293 Ma likely represent the main stage of granitoid magmatism in the vicinity of Muruntau, as defined by Rb-Sr whole rock + mineral isochron (Sardarin and Murun plutons; Kostitsyn, 1996) and reversely discordant U-Pb SHRIMP zircon analyses from the North Tamdinskii granite, located 31 km northwest of Muruntau (Kempe et al., 2004). Existing constraints for the timing of gold mineralization (Kostitsyn, 1994; Kempe et al., 2001; Wilde et al., 2001) indicate a hiatus of at least ten m.y. between cessation of the main period of granitoid magmatism and the onset of gold mineralization. These age

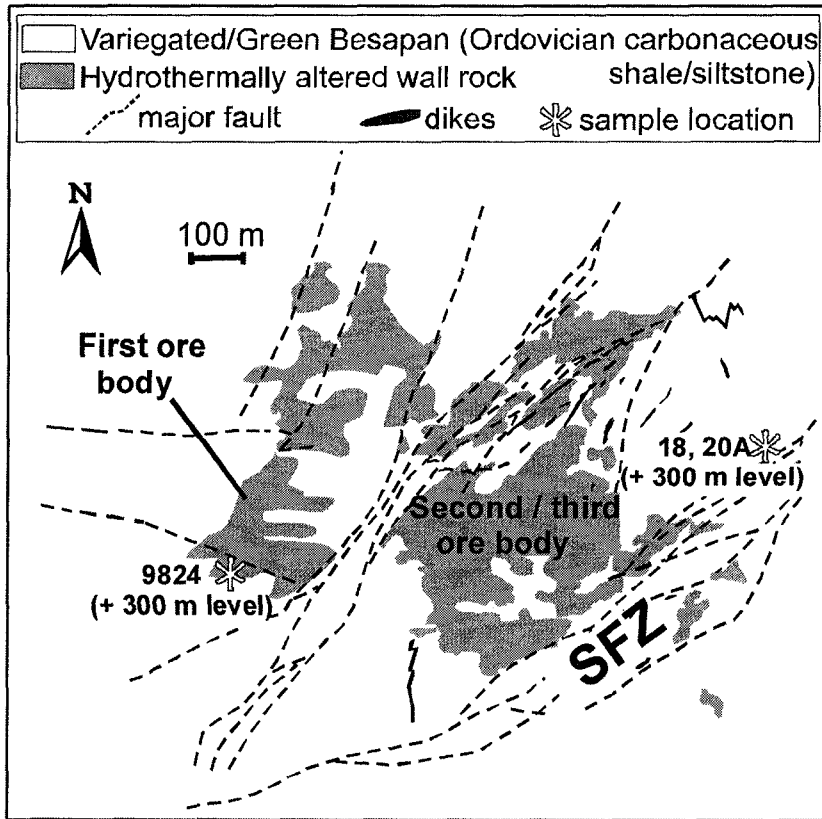


Figure 4.2.3: Geology of the Muruntau gold deposit, Southern Tien Shan Orogen, Uzbekistan.. SFZ = Southern Fault Zone. Figure provided by T. Graupner

data have, in part, resulted in diverse explanations for the origin of the Muruntau deposit (e.g., Wilde et al., 2001, Graupner et al., 2006).

In this study, Re-Os sulfide geochronology was used to clarify the temporal relationships between ore formation and other geologic processes in the Middle and Southern Tien Shan. Fine-grained molybdenite was sampled from Kal'makyr at four different locations and in three different host rocks (Table 4.2.1), and was subsequently separated by crushing and sieving and then by both heavy liquid (methylene iodide) and magnetic (FrantzTM) separations (see chapter 2.2). The molybdenite was chemically processed using the protocol described by Selby and Creaser (2001) and in chapter 2.3 of this study, with the distinction that three different spike solutions were used. Whereas four initial Re-Os molybdenite analyses were performed using a mixed ¹⁸⁵Re + double Os isotope (¹⁸⁸⁺¹⁹⁰Os) spike, additional individual analyses were performed using mixed ¹⁸⁵Re + isotopically 'normal' Os spikes (SN1 and SN2; see chapter 2.5) for verification of results (Table 4.2.1).

To determine the timing of gold mineralization at the Muruntau deposit, Re-Os isotopic analyses were performed on three coarsely crystalline arsenopyrite samples derived from the open pit. The samples comprise one (9824, donated by Natural History Museum, London) from a subvertical stockwork quartz veinlet from the first ore body, and two (18 and 20A, donated by T. Graupner) from steeply dipping quartz-arsenopyrite veinlets from the 'Southern Fault Zone' (Fig. 4.2.3). Arsenopyrite crystallization is, at least in part, genetically related to gold mineralization at Muruntau, as evidenced by the presence of gold inclusions within arsenopyrite in sample 9824. Rare Bi-Te phases constitute the only other inclusions detected by optical and electron microscopy. All analyzed arsenopyrite was mechanically separated and crushed using only agate tools, and Re-Os isotopic measurements were performed using isotope dilution negative thermal ionization mass spectrometry with a mixed ¹⁸⁵Re + ¹⁹⁰Os tracer solution (see chapter 2.3 for a full description of Re-Os analytical protocols). Isotopic analysis of fluid inclusion hosted He in arsenopyrite was performed by a Mass Analyser Products[®]215 gas-source mass spectrometer, according to the procedure of Stuart et al. (1995), following release/extraction of sample-hosted He into a gas processing line via crushing of ~200 mg of arsenopyrite with online, screw-type crushers.

4.2.3. Re-Os Results

4.2.3.1 *Kal'makyr*

The results of six Re-Os analyses of Kal'makyr molybdenites are shown in Table 4.2.1. Contents of Re for the molybdenite range between ~ 53 and 835 ppm, radiogenic Os ($^{187}\text{Os}^*$) range between ~ 263 and 2759 ppb, and, though detectable, common Os contents of all molybdenites are negligible with respect to $^{187}\text{Os}^*$ contents. Consequently, Model Age calculation was performed for all analyses, whereby the assumption of no initial Os is adopted (Stein et al., 2001). Calculated model ages from individual analyses of two samples (K-1, K-2) and two analyses of sample K-4 collectively define a restricted age range of between 313.3 and 314.6 Ma, regardless of the spike solution utilized. Together, these four analyses yield a Model 1 Re-Os isochron age of 314.0 ± 2.2 Ma (Fig. 4.2.4) and a Weighted Average age of 313.9 ± 0.6 (2σ , MSWD = 0.79; not shown). In contrast, two analyses of sample K-3 yield significantly older Re-Os model ages of 466.7 ± 2.7 Ma and 467.6 ± 1.7 Ma.

4.2.3.2 *Muruntau*

In total, sixteen Re-Os analyses were performed on the three arsenopyrite samples from Muruntau (Table 4.2.2). Measured Re contents for sample 9824 ranged consistently between 20 - 25 ppb, whereas samples 18 and 20A had much lower Re concentrations of 0.5 - 3.5 ppb. All three samples are characterized as being highly radiogenic (i.e. low common Os contents), although measured ^{192}Os contents are marginally lower for sample 9824 (1.4 - 2.8 ppt) compared to samples 20A (2.1 - 10.0 ppt) and 18 (2.0 - 12.3). Linear regression of data for individual samples yields well-fitted Re-Os isochrons and precise Model 1 ages: 288.6 ± 5.6 Ma (9824; MSWD = 1.1, initial $^{187}\text{Os}/^{188}\text{Os} = -0.2 \pm 1.9$ (Os_i), 290.4 ± 4.5 Ma (18; MSWD = 0.81, $\text{Os}_i = 0.14 \pm 0.41$), and 296.4 ± 6.1 Ma (20A; MSWD = 1.5, $\text{Os}_i = 0.07 \pm 0.59$; Fig. 4.2.5a). Moreover, the age for 9824 is confirmed by an additional analysis of this sample (9824-C6) performed using a mixed ^{185}Re + isotopically normal Os spike (SN1, see chapter 2.5),

Table 4.2.1: Re-Os isotopic data for molybdenite from the Kal'makyr deposit, Uzbekistan.

Sample	Description	Sample spike wt. (g)	sol ¹	Total Re (ppm)	¹⁸⁷ Re (ppm)	2σ unc.	¹⁸⁷ Os* (ppb)	2σ unc.	¹⁸⁷ Os*/ ¹⁸⁷ Re	2σ unc.	Model Age (Ma)	2σ unc. ²	
K-1	moly veinlet in monzonite (syenodiorite)	0.011	MD	835.5	4.0	525.1	2.5	2759	2	0.005255	0.000025	314.6	1.8
K-2	qtz-moly-opy veinlet in rhyolite (qtz porphyry)	0.021	MD	563.2	2.7	354.0	1.7	1852	1	0.005232	0.000025	313.3	1.8
K-3a	qtz-moly-py veinlet in monzonite (syenodiorite)	0.021	MD	54.18	0.26	34.06	0.16	265.8	0.2	0.007806	0.000038	466.7	2.7
K-3b	qtz-moly-py veinlet in monzonite (syenodiorite)	0.033	SN1	53.64	0.08	33.72	0.05	263.7	0.4	0.007821	0.000016	467.6	1.7
K-4a	qtz-moly veinlet in monzonite (syenodiorite)	0.022	MD	406.8	1.9	255.7	1.2	1338	1	0.005233	0.000025	313.3	1.8
K-4b	qtz-moly veinlet in monzonite (syenodiorite)	0.020	SN2	344.41	0.76	216.47	0.48	1136	2	0.005246	0.000014	314.1	1.3

¹MD = mixed double (i.e. ¹⁸⁵Re, ¹⁸⁶+¹⁸⁷Os), SN2 = mixed ¹⁸⁵Re + isotopically normal Os; SN1 = dilute SN2 (see chapter 2.5)

²calculated 2σ uncertainty for molybdenite model ages includes the uncertainty in λ of ¹⁸⁷Re.

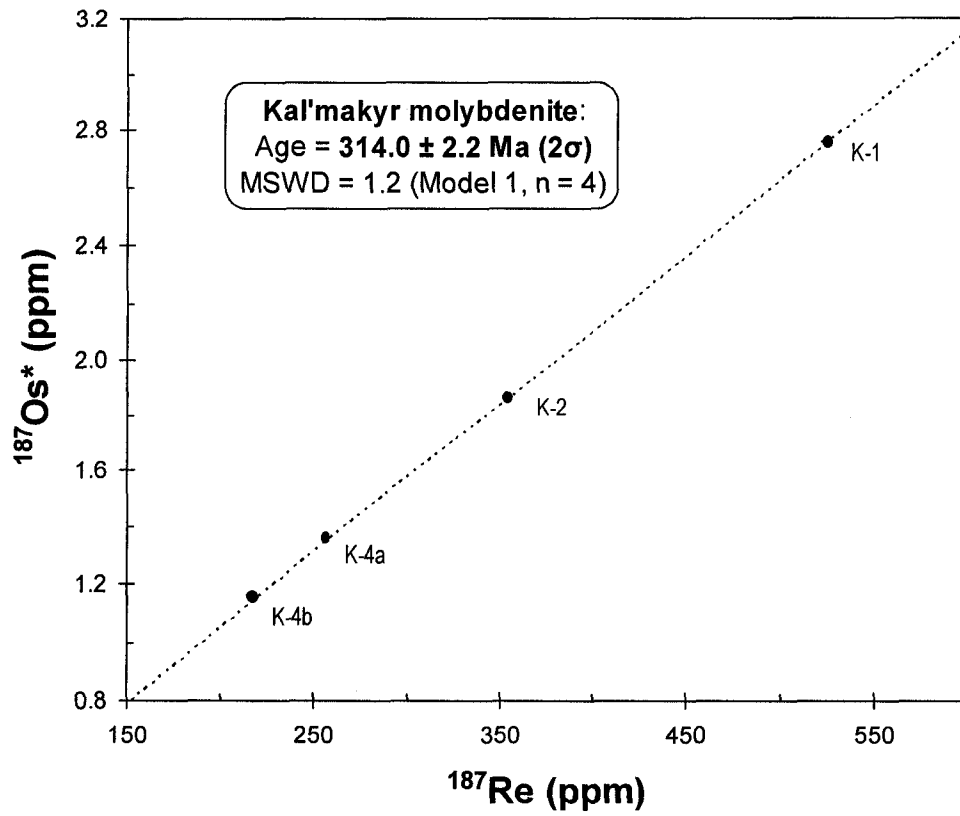


Figure 4.2.4: ^{187}Re - ^{187}Os (ppm) isochron diagram from four molybdenite analyses from the Kal'makyr porphyry Au-Cu deposit, Uzbekistan.

Table 4.2.2: Re-Os and He isotopic data for arsenopyrite from the Muruntau deposit, Uzbekistan.

	$^{187}\text{Re}/^{188}\text{Os}$	$\pm 2\sigma^2$	$^{187}\text{Os}/^{188}\text{Os}$	$\pm 2\sigma^2$	ρ	^{187}Re (ppt)	$\pm 2\sigma$	$^{187}\text{Os}^*$ (ppt)	$\pm 2\sigma$	R/R_a^4 (He)	$\pm 2\sigma$
sample 18¹	—	—	—	—	—	—	—	—	—	0.30, 0.30	0.04
18-1	3650	1400	17.6	7.0	0.999	296.3	1.9	1.403	0.033		
18-2	10300	3600	50	17	0.9995	973.8	3.9	4.691	0.054		
18-3	4800	970	23.5	4.8	0.997	750.8	3.1	3.624	0.072		
18-4	3310	410	16.3	2.0	0.989	867.6	3.5	4.18	0.10		
18-5	7300	1200	35.3	6.0	0.992	1423.5	5.4	6.83	0.15		
18-6	10200	1600	49.8	7.6	0.997	2189.3	8.1	10.60	0.12		
sample 9824¹	—	—	—	—	—	—	—	—	—	0.23, 0.29	0.03
9824-C1	16600	640	80.1	3.3	0.923	14652	54	70.37	0.09		
9824-C2	16540	600	79.8	3.0	0.964	14680	53	70.56	0.09		
9824-CB1-1	18210	750	87.3	3.7	0.977	15169	55	72.44	0.62		
9824-CB2-1	30800	2300	149	11	0.991	13746	50	66.21	0.63		
9824-C5	27400	1600	131.1	7.9	0.981	14799	54	70.51	0.80		
9824-C6 ³	—	—	—	—	—	—	—	—	—		
sample 20A¹	—	—	—	—	—	—	—	—	—	0.33, 0.33	0.04
20A-C1	5600	1000	28.1	5.1	0.997	979.9	3.9	4.855	0.082		
20A-C5	8200	1300	40.4	6.2	0.998	1706.4	6.4	8.336	0.088		
20A-C6	19300	9000	96	45	0.999	1360	150	6.74	0.15		
20A-C7	4970	990	24.7	4.9	0.998	789.9	3.3	3.873	0.065		
20A-C8	3600	1400	17.7	6.9	0.998	292.6	1.9	1.416	0.041		

¹ arsenopyrite samples for Re-Os analyses ranged from 0.391 to 0.415 grams.

² large uncertainties result primarily from the large blank correction applied to ^{188}Os (see Stein et al., 2000; Morelli et al., 2005).

³ analyzed using a mixed ^{185}Re - isotopically normal Os solution (Selby and Creaser, 2001).

⁴ R/R_a = ratio of sample $^3\text{He}/^4\text{He}$ to atmospheric $^3\text{He}/^4\text{He}$ ($=1.399 \times 10^{-6}$); contamination by atmospheric He during analysis monitored using $^{20}\text{Ne}/^4\text{He}$ ratios, was negligible. See Stuart et al. (1995) for full description of He methodologies.

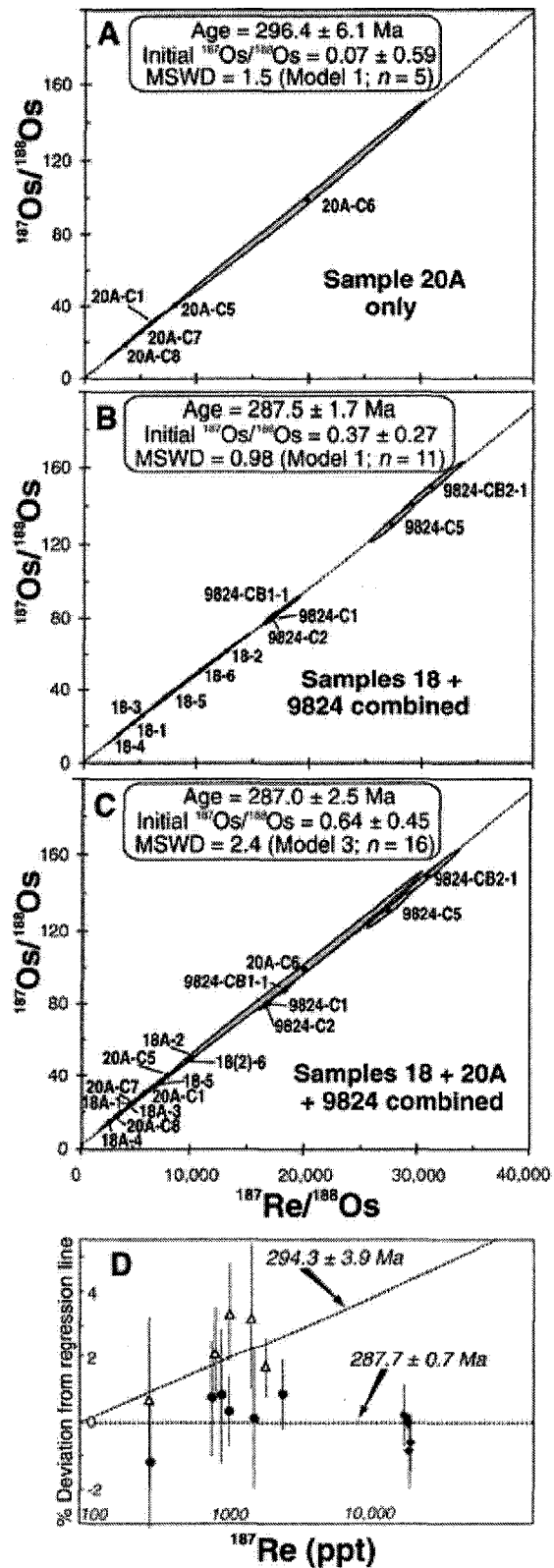
Re blank is 1.6 ± 0.3 pg and Os blank is 0.37 ± 0.05 pg (1 SD; n=4), blank $^{187}\text{Os}/^{188}\text{Os} = 0.21 \pm 0.07$ (1 SD; n=4),

Re-Os data for all samples were corrected using these values.

which yielded a single mineral model age of 286.9 ± 1.6 Ma¹. All ages overlap within 2σ uncertainties, clearly indicating arsenopyrite formation and associated gold mineralization occurred ca. 290 Ma. However, internal age structure may be revealed through collective regressions of multiple samples. Whereas collective regression of all analyses of samples 9824 and 18 yields a precise Model 1 isochron age (287.5 ± 1.7 Ma; MSWD = 0.98, $Os_i = 0.37 \pm 0.27$; Fig. 4.2.5b), addition of sample 20A fails to result in a Model 1 solution (Fig. 4.2.5c). This difference is evident when the data are plotted to avoid use of ^{188}Os , the precise quantification of which is challenging in these samples for which blank ^{188}Os contributes significantly to ^{188}Os (Stein et al., 2000; Morelli et al., 2005). Samples 9824 and 18 collectively yield a precise Model 1 age of 287.7 ± 0.7 Ma (MSWD = 1.0) on a plot of radiogenic ^{187}Os ($^{187}Os^*$) versus ^{187}Re (e.g., Stein et al., 2000), whereas sample 20A yields a distinguishable Model 1 age of 294.3 ± 3.9 Ma (MSWD = 0.82; Fig. 4.2.5d). This may suggest that arsenopyrite 20A crystallized at least two million years prior to samples 18 and 9824, but confirmation of this result will ultimately require additional high-precision Re-Os data.

¹ Single mineral model age of 286.9 ± 1.6 Ma for 9824-C6 is calculated using the measured ^{187}Re and ^{187}Os contents of 0.010408 ± 0.000003 ppm and 0.049861 ± 0.000211 ppb, respectively, and a resulting $^{187}Os^*/^{187}Re$ ratio of 0.004790 ± 0.000027 (all uncertainties reported at 2σ).

Figure 4.2.5: (A) Re-Os Model 1 isochron from regression of analyses of Muruntau arsenopyrite sample 20A, (B) Re-Os Model 1 isochron from regression of analyses of arsenopyrite samples 18 and 9824 from Muruntau. Age quoted is from $^{187}\text{Re}/^{188}\text{Os}$ vs. $^{187}\text{Os}/^{188}\text{Os}$ regression (C) Re-Os Model 3 ‘errorchron’ from regression of analyses of all arsenopyrite samples from Muruntau (9824 + 18 + 20A) (D) Re-Os ages derived from regression of analyses of independent arsenopyrite samples in ^{187}Re versus $^{187}\text{Os}^*$ (radiogenic Os) space. This plot reveals deviations outside 2σ uncertainties of analyses of sample 20A (open triangles), which individually yield a Model 1 age of 294.3 ± 3.9 Ma, from the regression line defined by samples 18 (filled circles) and 9824 (filled diamonds).



4.2.4. Discussion

Timing of Au(-Cu) Mineralization at Kal'makyr

The Re-Os results from Kal'makyr indicate two distinct periods of molybdenite crystallization at ~ 467 and 314 Ma. The younger Re-Os age of 313.9 ± 0.6 Ma, derived from a Weighted Mean age of four molybdenite analyses, is interpreted to date main stage porphyry style mineralization associated with Carboniferous magmatism in the Valerianov-Beltau-Kurama arc. This interpretation is consistent with a recently determined U-Pb sensitive high-resolution ion microprobe (SHRIMP) zircon age from a mineralized porphyry stock in the Almalyk open pit, for which an age of 316 ± 1.5 Ma was determined (R. Seltmann, pers. comm.). Thus, the main stage of Au (and Cu) mineralization at Kal'makyr was contemporaneous with the emplacement of porphyritic intrusions late in the developmental stages of the volcano-plutonic arc.

The significance of the 467 Ma age is uncertain, and several possibilities warrant consideration. This date may represent an early mineralization event, whereby the molybdenite comprising sample K-3, from which the dates are derived, reveals cryptic, previously unidentified mineralization that was overprinted by the late Carboniferous porphyry-related event. This possibility is permissible, given the absence of absolute age determinations on the immediate host rock. Although plausible, especially considering the presence of Ordovician rocks at base of the Valerianov-Beltau-Kurama arc sequence (Golovanov, 2005), there is currently no supporting evidence for the presence of older porphyry intrusions or related mineralization.. Another possibility is that this sample uniquely records an isotopic mixture between two or more different Re-Os sources. Although isotopic mixing between two or more sources is a feasible explanation, the purely radiogenic Os isotopic composition of sample K-3 requires that all contributing sources contained negligible common Os. Alternately, it is possible that this date reflects the disturbance of the Re-Os isotopic systematics of the late Carboniferous molybdenite. This is considered an unlikely explanation, however, since molybdenite has been established as an extremely robust Re-Os chronometer (Bingen and Stein, 2003). A final possibility is that the 467 Ma age reflects sampling issues, such that the small scale decoupling of Re and ^{187}Os known to occur within individual molybdenite crystals (Stein et al., 2003; Selby and Creaser, 2004) is manifested in analyses of sample K-3 as a

geologically meaningless age. This possibility is also considered unlikely, since (i) the sample was relatively fine-grained, (ii) the two analyses of the sample produced the exact same result, despite using different isotopic tracer solutions, and (iii) the second analysis (K-3b) used a sample size of 33 mg (Table 4.2.1), which should be sufficient to eliminate decoupling effects (Selby and Creaser, 2004). Based on the above arguments, and in the absence of other possible explanations, it is proposed that the 467 Ma age determined for analyses of sample K-3 represents either an older, as of yet unidentified mineralization event, or the effects of isotopic mixing from two or more Re-Os sources.

Timing of Gold Mineralization at Muruntau

A major problem in understanding the generation of orogenic gold deposits is the lack of reliable age determinations for mineralization (Groves et al., 2003). The new dates presented here, which are the completed data set of a previously reported preliminary age (Morelli et al., 2004), clearly demonstrate the utility of the Re-Os method for directly dating low-level sulfide minerals associated with gold mineralization, and also reveal the shortcomings of other methods. Gold mineralization at Muruntau was previously determined to be 272.6 ± 3.8 Ma (recalculated for consistency to 272.8 ± 4.5 Ma using the regression algorithm of Ludwig et al., 2003) based on Rb-Sr data from hydrothermal alteration minerals (Kostitsyn, 1994), 279 ± 18 Ma (279 ± 27 Ma; MSWD = 7.7, Model 3; using Ludwig et al., 2003) from Sm-Nd scheelite analyses (Kempe et al., 2001), or as young as ca. 245 Ma from $^{40}\text{Ar}/^{39}\text{Ar}$ dates of vein selvage sericite (Wilde et al., 2001). The Re-Os arsenopyrite ages show that sulfide and gold mineralization occurred ca. 290 Ma, 15 – 20 m.y. earlier than indicated by age determinations based on hydrothermal silicate/tungstate gangue minerals, and that it temporally overlaps regional late-tectonic magmatism (Fig. 4.2.6). The small but statistically significant Re-Os age difference between arsenopyrite samples might also indicate that hydrothermal activity occurred over at least two million years, suggesting a protracted or multi-stage hydrothermal event for formation of this very large deposit.

The ca. 290 Ma Re-Os age determination for Muruntau arsenopyrite compares favourably to $^{40}\text{Ar}/^{39}\text{Ar}$ whole rock and sericite ages reported by Mao et al. (2004) of 284 – 288 Ma for gold mineralization at the Kumtor deposit in Kyrgyzstan (Fig. 4.2.3),

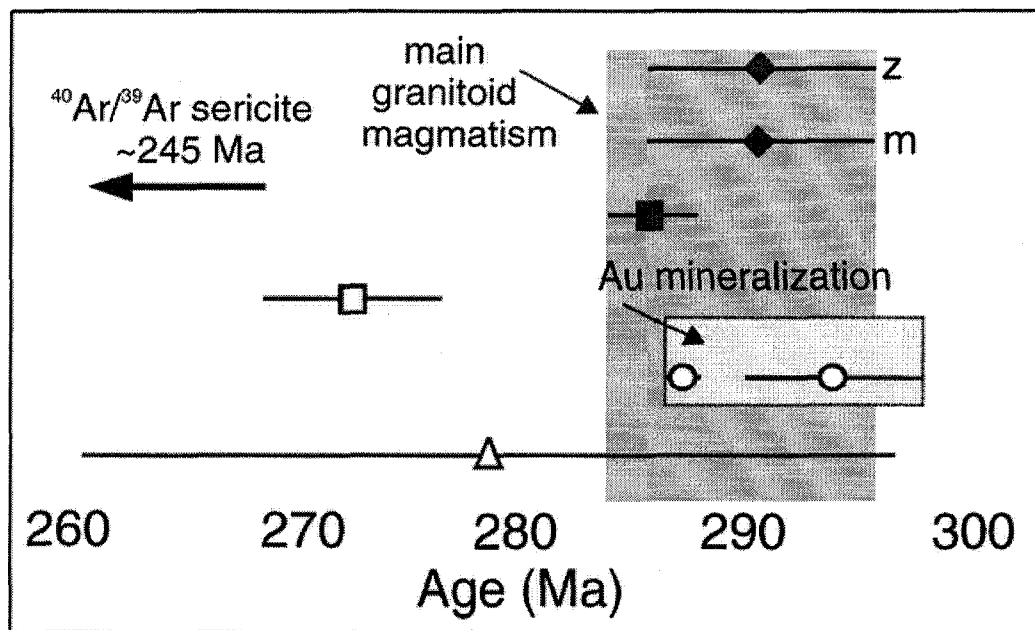


Figure 4.2.6: Comparison of Re-Os arsenopyrite isochron ages (with associated 2σ uncertainties; open circles) to existing ages for Muruntau gold mineralization. Open symbols represent inferred mineralization ages; filled symbols represent minimum crystallization ages for local felsic intrusives. Square—Rb-Sr whole rock (Kostitsyn, 1994); triangle—Sm-Nd scheelite (Kempe et al., 2001); diamonds—U-Pb zircon (z) and monazite (m) (Kempe et al., 2004).

another world class (18 Moz) orogenic gold deposit in the Tien Shan Orogen. Kumtor is hypothesized (Cole, 2000) to have formed at shallower crustal depths (~ 4.5 km) than the Muruntau deposit (~ 8 km) and, consequently, at a lower temperature and with increased potential for preservation of primary $^{40}\text{Ar}/^{39}\text{Ar}$ age information than at Muruntau. The new Re-Os ages for gold mineralization clarify the temporal relationship between mineralization at the Muruntau and Kumtor deposits, and may provide the first conclusive evidence for a short, but concentrated, terrane-scale mineralizing event at ca. 285 – 290 Ma in the Tien Shan. The duration and scale of gold emplacement events in the Tien Shan will become clearer as additional reliable dates from other large orogenic gold deposits in the belt become available.

Implications of Os_i and He Isotopes for Metal and Fluid Sources at Muruntau

The ultimate origin of the gold and the ore fluids at Muruntau is controversial, and has been attributed to several sources, including upper crustal/host rocks (Marakushev and Khokhlov, 1992; Kostitsyn, 1994; Wilde et al., 2001), granitoid intrusions (Kotov and Poritskaya, 1992; Sillitoe, 1993; Wall et al., 2004), and the mantle (Rusinova and Rusinov, 2003; Graupner et al., 2006). Information about metal sources in ore systems is carried by the Os_i ratios of sulfide minerals (e.g., Mathur et al., 2000; Arne et al., 2001; Levresse et al., 2004; Morelli et al., 2005), and He isotopes in fluid inclusions hosted by ore minerals are a powerful tracing tool for detection of mantle-derived volatiles (Turner and Stuart, 1992; Stuart et al., 1995; Levresse et al., 2004). The most precise determination of Os_i , identical (within uncertainty) to the Os_i of each individual regression, results from the conventional regression of samples 18 and 9824 (Fig. 4.2.5b; $\text{Os}_i = 0.37 \pm 0.27$) and allows contributions from potential Os sources to be assessed, despite the large uncertainty that results from the very radiogenic Os isotopic compositions of the arsenopyrite. Figure 4.2.7 compares Os_i of Muruntau arsenopyrite to reservoirs that may have contributed Os to the hydrothermal system, including upper (Peucker-Ehrenbrink and Jahn, 2001; Sun et al., 2003; Hattori et al., 2003) and lower (Saal et al., 1998) continental crust, and primitive upper mantle (Meisel et al., 2001). These data indicate that regional metamorphism of crustal rocks is unlikely to be the only source of Os in the Muruntau hydrothermal fluids, as Os_i values of upper continental

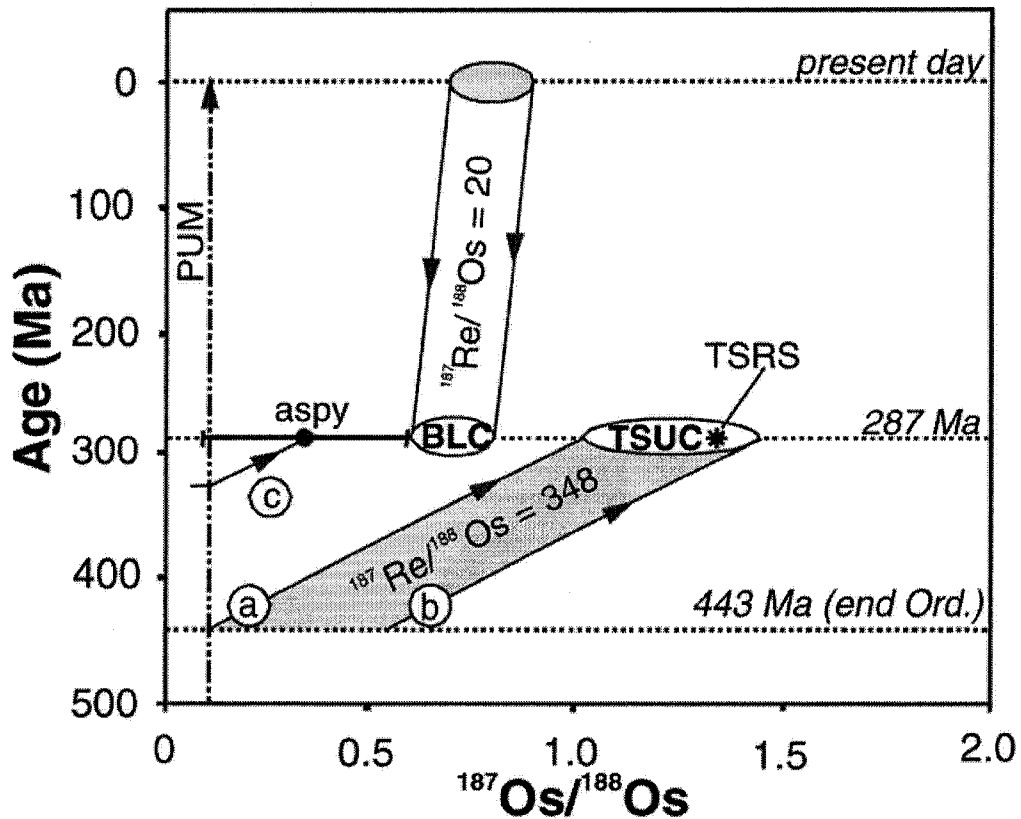


Figure 4.2.7: Comparison of Os_i from arsenopyrite to terrestrial Os reservoirs that may have contributed Os to the Muruntau hydrothermal system. PUM - Primitive Upper Mantle (Meisel et al., 2001). TSUC - Tien Shan Upper Crust is a minimum estimate of $^{187}\text{Os}/^{188}\text{Os}$ for Cambro-Ordovician host sediments at Muruntau, made by using mantle (a) and Ordovician seawater (Widom et al., 2004) (b) initial $^{187}\text{Os}/^{188}\text{Os}$ ratios and a $^{187}\text{Re}/^{188}\text{Os}$ ratio of 348 (Peucker-Ehrenbrink and Jahn, 2001; Sun et al., 2003). TSRS - Os isotopic composition of riverine sediment from the Tien Shan mountains calculated at 287 Ma (Hattori et al., 2003), which agrees with TSUC estimates. Also shown is the estimate of Os isotopic composition of bulk lower continental crust (BLC; Saal et al., 1998) at 287 Ma. The nominal Os_i from arsenopyrite at Muruntau of 0.37 could have a crustal prehistory of only ~ 40 m.y., based on typical crustal and mantle Re-Os characteristics (c).

crust are too radiogenic (Fig. 4.2.7). Similarly, a lack of overlap between Muruntau Os_i and the calculated range for lower continental crustal $^{187}Os/^{188}Os$ values (0.65 – 0.79) at 287 Ma suggests that a solely lower crustal origin for Os is also unlikely. A plausible explanation for the Muruntau arsenopyrite Os_i value of 0.37 ± 0.27 is one that requires contribution of Os from both older crust and contemporaneous mantle-derived magmas. Alternately, the Os_i could be explained solely from crust formed shortly before ca. 290 Ma – assuming typical crustal and mantle Re-Os values, only ~ 40 m.y. of prehistory is required to evolve from mantle Os values to the Muruntau arsenopyrite value of 0.37 (Fig 4.2.6).

Assuming He followed a similar premineralization pathway to Os, the presence of an unradiogenic Os component is supported by He isotopes from fluid inclusions in arsenopyrite. The $^3He/^4He$ ratios of fluid inclusions determined here show a narrow range (0.23–0.33 R_a ; table 4.2.2), consistent with other He isotope data from Muruntau arsenopyrite, quartz, and scheelite (Graupner et al., 2006). These values are an order of magnitude higher than continental crust-derived He ($^3He/^4He < 0.01 R_a$; Stuart et al., 1995), and require a contribution of mantle-derived ('primordial') 3He . Assuming a depleted mantle R_a value (~ 8 modern day, Stuart et al., 1995), at least a few percent of He in Muruntau ore fluids must be from a mantle source. A similar conclusion was reached by Graupner et al. (2006).

The Os and He isotope data do require a major crustal component in the ore system, but they also reveal input from an unradiogenic source, presumably the mantle, suggesting mantle-to-crust metal and volatile transfer was important in the formation of the Muruntau deposit. This signature, which is heavily masked via interaction with crust, is undetected by other isotope systems, including Nd (Kempe et al., 2001), Sr (Kostitsyn, 1994), and Pb (Chiaradia et al., 2006). As such, a juvenile source for gold at Muruntau (Graupner, 2006) must be considered. If a valid interpretation, emplacement of granitoid rocks proximal to Muruntau, now shown to overlap with the timing gold mineralization, may evidence this influx of juvenile material to the crust. Some intrusions have relatively unradiogenic initial Sr isotope ratios (e.g. Sardarin granodiorite, $^{87}Sr/^{86}Sr = 0.7079$; Kostitsyn, 1996) and are interpreted to have formed during interaction of mantle-derived magmas with lower crustal rocks on a regional scale (Kostitsyn, 1996). The juvenile Os

and He components in the ore fluids might then originate by exsolution of fluids from the granitoid magmas, or alternately may originate directly from mafic magmas emplaced into the crust. The latter scenario supports the interpretation of Graupner et al. (2006), who invoke a relationship between the generation of gold-bearing fluids and the emplacement of local lamprophyre dikes on the basis of noble gas, C isotope and halogen data from Muruntau. Robust isotopic ages are required for lamprophyre emplacement to further evaluate this hypothesis, as current dates (ca. 273 Ma) are based on Rb-Sr analyses of hydrothermally altered whole rock samples (Kostitsyn, 1996) that may reflect disturbance of true crystallization ages by later events.

Sulfide Os_i for Modeling of Orogenic Gold Systems

Successfully understanding the origin of orogenic gold deposits is an ongoing challenge that requires the input of multiple geological, geochemical, and geophysical data streams. Unfortunately, clarification of important components is not provided by all techniques, with some yielding information that is unrelated to the actual ore-forming event and, hence, that encumber accurate interpretation of ore genesis (see Ridley and Diamond, 2000). To avoid influence from potentially irrelevant data, the ability of Os isotopic compositions of ore-related sulfide minerals to differentiate genetic processes will be assessed here in isolation, without consideration of other geologic data and with the intention that, if pertinent, this new information will be incorporated into future comprehensive models.

The significance of the Os isotopic composition in relation to the origin of gold at Muruntau and other orogenic gold deposits remains uncertain due to a limited understanding of the exact relationship between Os and gold in terms of source(s) and transport in hydrothermal systems. It has been proposed that Os may be well suited as a tracer for gold, a monoisotopic element, since they exhibit geochemical similarities not shared by other tracer isotope systems (Shirey and Walker, 1998; Mathur et al., 2000). Importantly for hydrothermal ore deposit studies, both elements are known to be soluble in CO₂-rich hydrothermal solutions (Wood, 1987; Seward, 1991), such as those responsible for deposition of orogenic gold deposits. Furthermore, Pan and Wood (1994) demonstrated that, albeit at much lower concentrations relative to gold, platinum group

elements are soluble as bisulfide complexes, considered the primary ligand responsible for hydrothermal gold transport in orogenic deposits (Seward, 1991). Although more work is required for a conclusive determination, these available criteria suggest that Os isotopic compositions can act as a reasonable proxy for determining the source and/or transport history of gold in hydrothermal solutions, perhaps much more so than other lithophile isotopic tracers like Pb, Sr and Nd.

The new initial Os isotopic compositions reported in this thesis, combined with the limited sulfide Os isotopic data for orogenic gold deposits in the literature (Table 4.2.3), may be synthesized for preliminary interpretations of the genesis of OGD based on Os isotopic compositions. As with the Muruntau deposit, there is significant debate surrounding the origin of this deposit type generally. There is widespread agreement, however, that these deposits are generated relatively late (i.e. syn- to post-peak regional metamorphism) during orogenesis at continental margins (Goldfarb et al., 2001; Groves et al., 2003). Within this context, a variety of causative geologic processes have been proposed. Currently, the most widely invoked models include (i) leaching of mid- to upper-crustal rocks during regional metamorphic dehydration, with no specific source lithology required (Fyfe and Kerrich, 1984; Hodgson et al., 1989; Phillips et al., 1987), (ii) introduction of gold to crust via mantle-derived alkalic melts (Rock and Groves, 1988a, 1988b), (iii) fluid and gold sourced from and driven by contemporaneous felsic magmatism ('magmatic model'; MacDonald and Hodgson, 1986; Burrows and Spooner, 1987; McCoy et al., 1997); (iv) prograde metamorphic dehydration and derivation of gold from underplated, hydrated marine sedimentary rocks and oceanic crust, beneath continental margins (Wyman and Kerrich, 1988; Kerrich and Wyman, 1990; Titley, 1991; Hutchinson, 1993; Goldfarb et al., 2001), and (v) dehydration and derivation of gold specifically from primitive oceanic crust (Keays, 1987; Bierlein et al., 2001, 2005).

The existing Os_i data for orogenic gold-derived sulfides reveal a considerable range of values (Table 4.2.3, uncertainties excluded for simplicity), from a low of 0.28 for Homestake arsenopyrite, to a high of 1.04 for pyrite and arsenopyrite from the Bendigo deposit. Although based on only six available determinations, the range exhibited by these data significantly limits the possible models if a common origin for all

Table 4.2.3: Existing Os isotopic data for sulfides from orogenic gold deposits.

Deposit	Host Terrane	Mineral	Re-Os age (Ma)	Os _i	reference	host rock age (Ma)	T ₀ [†] (Ma)
*1 Witwatersrand	Witwatersrand Supergroup, Kaapvaal Craton, South Africa	gold	3033 ± 21 Ma	0.1079 ± 0.0001	Kirk et al., 2002	?	?
2 Con	Yellowknife Greenstone Belt, Slave Province, Canada	py	2591 ± 37	0.78 ± 0.17	chapter 3, this study	2760	169
3 Homestake	southern Trans-Hudson Orogen, South Dakota, USA	aspy	1736 ± 8 Ma	0.29 ± 0.1	chapter 4.1, this study	1970	234
4 Bendigo	western Lachlan fold belt, eastern Australia	aspy + py	438 ± 6 Ma	1.04 ± 0.16	Ame et al., 2001	500	62
5 The Ovens	Meguma Terrane, Nova Scotia, Canada	aspy	407 ± 4 Ma	0.83 ± 0.16	Morelli et al., 2005	500	93
6 Dufferin	Meguma Terrane, Nova Scotia, Canada	aspy	380 ± 3 Ma	0.38 ± 0.16	Morelli et al., 2006	500	120
7 Munttau	southern Tien Shan orogen, Uzbekistan	aspy	287.5 ± 1.7 Ma	0.37 ± 0.27	chapter 4.2, this study	443	155

*because the interpreted derivation of the Witwatersrand ores from an orogenic gold deposit(s) remains controversial.

Os isotopic data from this deposit are not considered in the genetic models discussed herein.

[†]T₀ = age of host rock - age of gold mineralization

orogenic gold deposits is assumed. The key to interpretation of these data lies in the recognition that the relatively unradiogenic Os_i values from three of the deposits (Homestake, 0.29; Dufferin, 0.38; Muruntau, 0.37) require an osmium source that was extracted from the mantle shortly before the gold mineralizing event. The reasoning behind this inference, also discussed specifically for Muruntau in section 4.2.4.2, is displayed in Figure 4.2.8, which compares the existing Os_i sulfide data to current constraints for the Os isotopic compositions of possible source reservoirs over the relevant periods of Earth history.

This modeling shows that any genetic model invoking derivation of gold exclusively from mid- to upper-crustal rocks is unlikely because the increased incompatibility of Re over Os during mantle melting results in high Re/Os for all crustal rocks, and thus in rapidly evolving crustal Os isotopic compositions over short periods of geologic time. If the immediate host rocks to an individual deposit are taken to be the youngest possible source rock in the hosting stratigraphy, the time difference between host rock deposition and gold mineralization (T_D) provides a hypothetical timeframe over which Os isotopic ratios can evolve through Re decay. For the deposits listed in Table 4.2.3, T_D values range from 62 m.y. (Bendigo) to 234 m.y. (Homestake) which, assuming a crustal $^{187}Re/^{188}Os$ ratio of 348 and a mantle initial Os_i for the host lithology, translates into a range of projected Os_i from 0.48 to 1.49, respectively, for gold-related sulfide minerals. Of all six deposits, only Bendigo and The Ovens (0.66) yield calculated $^{187}Os/^{188}Os$ ratios below the actual measured sulfide Os_i , whereas sulfide Os_i from the other four deposits are all significantly lower than the Os compositions calculated using T_D values. This discrepancy clearly shows that the Os initially incorporated into gold-related sulfide minerals cannot feasibly originate entirely from upper continental crustal rocks, including marine sedimentary rocks comprising accretionary prisms - common hosts to many orogenic gold deposits (i.e. Paleozoic 'turbidite-hosted' deposits). Current constraints for the composition of ancient lower continental crust (Esperança et al., 1997; Saal et al., 1998) also preclude this reservoir as a universal gold source to orogenic deposits. Since its hypothesized separation from the mantle at 2300 Ma, the $^{187}Os/^{188}Os$ compositions of the lower mafic crust has progressively increased from an upper mantle composition to a present day value of 0.7 to 0.9 (Saal et al., 1998). Although not evident

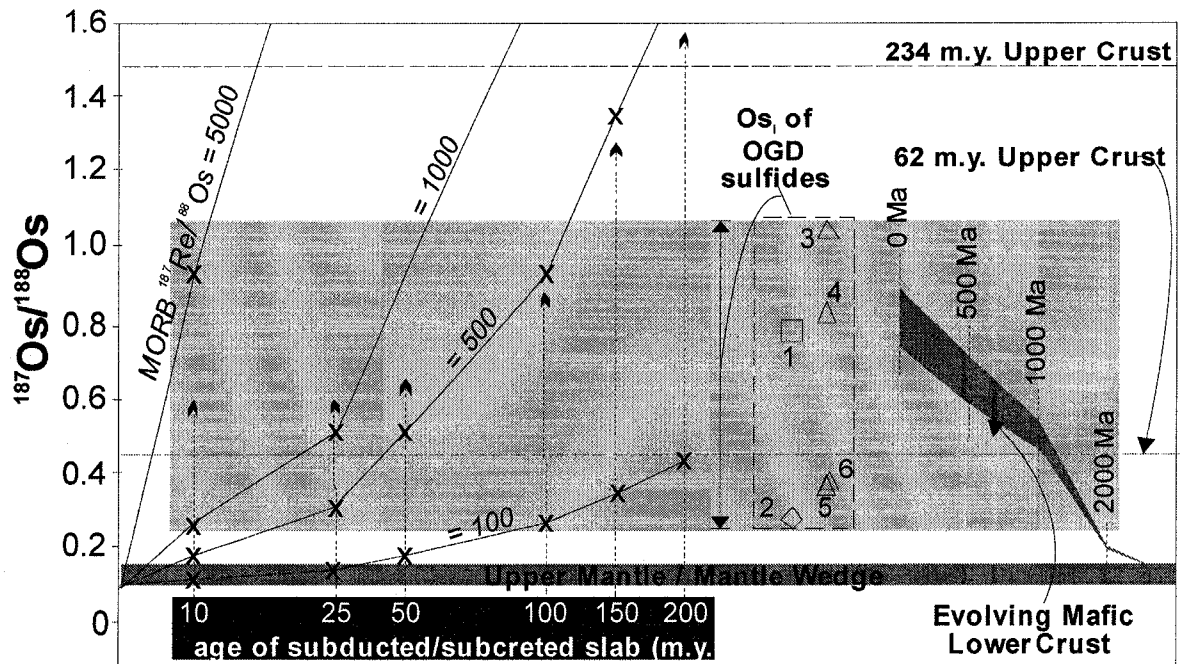


Figure 4.2.8: Evolution of Os isotopic compositions in potential metal source reservoirs to orogenic gold deposits over time. Ranges of Re and Os isotopic composition of primitive upper mantle is from Meisel et al. (2001), upper crust from Peucker-Ehrenbrink and Jahn (2001) and Sun et al. (2003), and mafic lower crust from Saal et al. (1998). Isotopic composition of Os for variably aged MORB is calculated assuming a mantle Os_i and $^{187}\text{Re}/^{188}\text{Os}$ ratios ranging from 100 – 5000. The indicated range of sulfide Os_i values shown (grey band) comes from compositions of pyrite (square) from the Con deposit (1) and arsenopyrite (triangles) from Homestake (2), Bendigo (3; Arne et al., 2001), The Ovens (4), Muruntau (5), and Dufferin (6) deposits. See text for discussion.

in Precambrian deposits due to the corresponding unevolved lower crustal Os isotopic compositions, some Paleozoic deposits have distinctively less radiogenic Os compositions than the lower crust. As shown on Figure 4.2.8, the Os_i of sulfides from both the Dufferin and Muruntau deposit are substantially below contemporaneous lower crustal compositions, effectively eliminating this as a possible source to orogenic gold deposits.

Despite the close spatial and temporal relationship between the intrusion of granitoid magmas and formation of orogenic gold deposits (Goldfarb et al., 2001; Groves et al., 2003), a genetic relationship between these events is not supported by the collective Re-Os isotopic data. As discussed earlier in this thesis, determined Re-Os sulfide ages and Os_i for both the Con (section 3) and the Muruntau (this chapter) deposits are compatible with derivation from proximal granitoid intrusions. However, geochronological constraints from the Homestake deposit (section 4.1.7) now eliminate this as a possible model for the origin of these deposits. The new Re-Os arsenopyrite age of 1736 ± 8 Ma for Homestake gold mineralization definitively predates intrusion of the Harney Peak granite (1715 to <1694 Ma), negating a genetic relationship between these geologic events. A similar temporal discrepancy exists between granitoid magmatism and main stage orogenic gold mineralization at the Bendigo (Arne et al., 2001) and Ovens (Morelli et al., 2005) deposits.

Of the comprehensive models proposed for the origin of orogenic gold deposits, only two can satisfy the requirements of the Re-Os isotopic compositions: derivation of gold from (a) metamorphic dehydration of oceanic crust, or (b) directly from mantle melts (e.g. lamprophyres) emplaced at the base of the crust (Fig 4.2.8). These two models are distinct from the others because, importantly in relation to the sulfide Os_i values, they both permit the input of juvenile Os into the ore system. Derivation of gold and ore-related metals from primitive oceanic crust can conceivably explain the observed range of sulfide Os_i compositions, since such crust can vary widely in both age (<10 to 250 m.y.) and Re concentration (0.36 – 2.3 ppb; Schiano et al., 1997). As shown in Figure 4.2.8, variation in either of these parameters can result in large variations in the $^{187}Os/^{188}Os$ ratio, which would eventually be transferred to the mineralizing system. Local variations in age or, more likely, Re content may also explain the range of sulfide Os_i values from

gold deposits within the same host terrane, such as with The Ovens (0.83) and Dufferin (0.38) deposits of the Meguma Terrane. A potential shortcoming of this model is that, given that such age and compositional variations are common in ocean crust, a much larger than observed range in sulfide Os_i should be evident. For example, assuming an age of 50 m.y. and a $^{187}Re/^{188}Os$ composition of 5000, both reasonable parameters for typical oceanic crust, a resulting $^{187}Os/^{188}Os$ ratio of 4.3 can be calculated, significantly greater than any measured sulfide Os_i (Fig. 4.2.9). If this model is valid, the sulfide Os_i values therefore demand that the average Re content of oceanic crust is actually lower than currently proposed, or that only very young oceanic crust (< 25 m.y.) is capable of sourcing orogenic gold deposits. The latter argument may be supported by studies suggesting that subduction of an oceanic spreading center can be an important component in deposit genesis (e.g. Haeussler et al., 1995).

Mantle-derived melts that impinge on the base of the crust and propagate towards shallower crustal levels as mafic dike swarms could potentially represent the source of juvenile Os in orogenic gold systems. This model for development of orogenic gold deposits stems from the observation that mafic alkaline dikes are commonly observed near, and have a broadly contemporaneous relationship with, these deposits. The Os_i of orogenic gold sulfides could feasibly be a product of mixing between these mafic magmas and assimilated crustal rocks at the base of the continental crust, similar to the scenario proposed for the generation of porphyry intrusions that host Cu-Au-Mo mineralization in magmatic arcs (Richards, 2003). Along similar lines, another possible process to produce this range of Os isotopic compositions might be the direct derivation of a gold-bearing hydrothermal fluid from an underplated mafic melt, followed by leaching of metals (Os, Au?) from more evolved crustal rocks en route to the depositional site. Central to either scenario is the emplacement of mantle-derived melts at the base of the existing crust. Some researchers have recognized that the introduction of asthenospheric melts late in orogenesis may be critical for providing the necessary heat for generation of orogenic gold deposits (Haeussler et al., 1995; Goldfarb et al., 2001). The Os_i compositions of gold-related sulfide minerals suggest that such processes might also provide an influx of gold and other metals into the ore system.

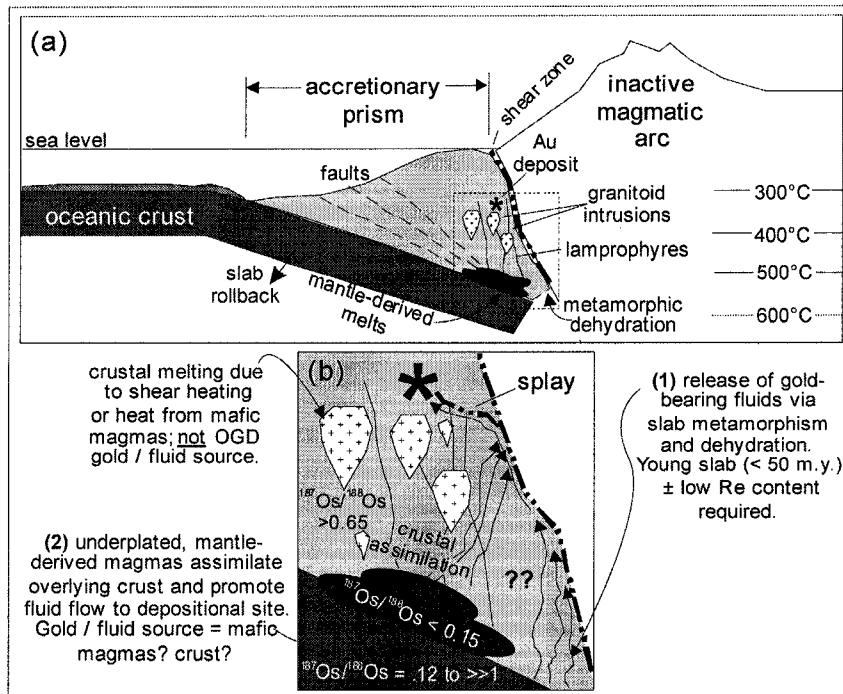


Figure 4.2.9: (a) Schematic cross section of an active continental margin, including close-up of orogenic gold mineralizing zone (b), showing possible fluid/metal sources that are compatible with the Os, and He data for Muruntau, and other orogenic gold deposits. See text for details. Modified from Kerrich et al. (2000).

Another possibility that must be considered is that there is no single model that can explain the origin of orogenic gold deposits, and that the observed range of sulfide O_s reflects the operation of multiple processes that are capable of producing gold deposits with very similar characteristics. Groves et al. (2003) support this assertion by stating, based on consideration of all the data derived from different deposits, that “no single model for the fluid and metal sources explains all observations from the orogenic gold deposits.” Similarly, Goldfarb et al. (2001) emphasize the possibility that no specific tectonic process is required to generate orogenic gold deposits: “Any thermal event within hydrous and sulfur-bearing juvenile crust, whether it be initiated by Precambrian plume-like events, or younger, more-typical subduction collision type processes, can form the same type of gold deposit”. The validity of this claim will become apparent with the acquisition of additional high-precision gold mineralization ages and source tracing data from deposits worldwide.

Sulfide Rare Earth Element Compositions: A Possible Tracing Tool?

The use of rare earth element (REE) contents of ore-related sulfide minerals is an essentially unexplored approach to ore deposit modeling, with only a handful of studies having considered this topic. This likely has to do with a preconceived notion that REE are immobile in hydrothermal fluids, and should not therefore be concentrated significantly within sulfide minerals that precipitated from such fluids. However, several conditions actually facilitate the partitioning of REE into aqueous phases (Lottermoser, 1992; Wood, 2004) including increased temperature, increased fluid CO_2 concentrations, low fluid pH, high fluid concentrations of REE complexing agents (CO_3^{2-} , F^- , Cl^- , PO_4^{3-}), and high water/rock ratios.

REE contents of arsenopyrite and pyrite from several orogenic gold deposits were measured, including the three from Muruntau and from other deposits for which O_s have been determined, to assess the significance of REE abundances with respect to ore genesis. Sulfide minerals from ten different deposits were dissolved in ~ 4.5 ml of inverse aqua regia and subsequently dried down and redissolved in 2% HNO_3 prior to analysis by quadrupole ICP-MS. Of the ten deposits, sulfides from nine yielded measurable REE concentrations (Table 4.2.4); arsenopyrite from The Ovens was the only to yield REE

Table 4.2.4: Rare earth element data for arsenopyrite (-A) and pyrite (-P) from Muruntau (MN) and other orogenic gold deposits worldwide. Duff = Dufferin, GM = Golden Mile, HS = Homestake, Kum = Kumtor, OV = The Ovens, NL = Nicholas Lake, RL = Red Lake; TQ = Touquoy.

	<i>MN-18-A</i>	<i>MN-20-A</i>	<i>MN-9824-A</i>	<i>Kum-P</i>	<i>Duff-A</i>	<i>TQ-A</i>	<i>OV-A</i>	<i>HS-A</i>	<i>GM-A</i>	<i>Con-P</i>	<i>NL-A</i>	<i>RL-A</i>
<i>La</i>	0.342	0.696	0.946	0.162	1.616	47.054	0.023	1.179	0.150	0.124	0.172	0.964
<i>Ce</i>	0.618	1.313	1.728	0.350	3.290	106.909	0.016	2.014	0.362	0.190	0.344	2.552
<i>Nd</i>	0.239	0.516	0.694	0.254	1.523	46.753	0.010	0.901	0.281	0.100	0.151	1.892
<i>Sm</i>	0.043	0.116	0.126	0.076	0.329	9.143	<i>bd</i>	0.146	0.094	0.022	0.026	0.552
<i>Eu</i>	0.014	0.025	0.026	0.037	0.087	1.826	<i>bd</i>	0.032	0.023	0.012	0.004	0.171
<i>Gd</i>	0.048	0.122	0.088	0.112	0.267	6.181	0.001	0.081	0.078	0.025	0.015	0.496
<i>Tb</i>	0.008	0.021	0.009	0.016	0.030	0.564	<i>bd</i>	0.006	0.009	0.004	0.002	0.060
<i>Dy</i>	0.091	0.174	0.104	0.088	0.264	2.871	0.058	0.095	0.124	0.034	0.063	0.298
<i>Ho</i>	0.013	0.029	0.010	0.015	0.028	0.400	<i>bd</i>	0.005	0.012	0.007	0.002	0.040
<i>Er</i>	0.059	0.093	0.053	0.037	0.081	0.869	0.001	0.017	0.038	0.022	0.006	0.076
<i>Yb</i>	0.041	0.077	0.024	0.024	0.086	0.662	<i>bd</i>	0.016	0.047	0.031	0.005	0.060
<i>Lu</i>	0.007	0.012	0.004	0.002	0.013	0.083	<i>bd</i>	0.002	0.008	0.005	0.001	0.008

all values are ppb

bd = below detection limits

contents beneath instrumentation detection limits. Chondrite-normalized REE patterns of the tested sulfides (Fig. 4.2.10) exhibit quite similar characteristics, with overall near chondritic light rare earth element (LREE) enrichment contents, and with an overall enrichment of the LREE relative to heavy rare earth elements (HREE). In detail, however, there exists a significant variation in the degree of REE fractionation between intra- (Muruntau) and interdeposit orogenic gold sulfide samples. This is most apparent from the large range of La/Yb_N ratios for these samples (~ 2 – 49, Fig. 4.2.11a), which shows fractionation of the LREE from the HREE, and to a lesser degree from the range in La/Sm_N (~ 1 – 5; Fig. 4.2.11b) and Gd/Yb_N ratios (~ 0.65 – 7.5; Fig.4.2.11c), which show fractionation of the LREE from the middle rare earth elements (MREE) and the MREE from the HREE, respectively.

With the exception of Eu, the abundance of which can be modified by crystallographic effects, the REE patterns of sulfide minerals have been interpreted to generally reflect those of the hydrothermal fluid from which they were precipitated, albeit at lower overall concentrations (Rimskaya-Korsakova and Dubinin, 2002). The degree to which these patterns reflect that of the original source is not known. In consideration, the REE compositions of the Earth's major geochemical reservoirs have been plotted along with the determined orogenic gold sulfide compositions. Comparison of these chondrite-normalized REE patterns and LREE/MREE/HREE ratios reveal no consistent similarities, though the upper continental crustal pattern shows a broadly similar LREE-enriched signature to the sulfides (Fig. 4.2.10). Likewise, the upper crust is the only reservoir that can approximate the observed sulfide REE fractionation trends (Figs. 4.2.10a-c), especially for the MREE/HREE (La/Sm_N) ratios. This is not unexpected since the ore fluids experienced definite interaction with upper crustal rocks during transport to the depositional site, thus potentially causing variable amounts of alteration of fluid (and rock) REE compositions during fluid-rock interactions (Lottermoser, 1992). A further complication is that preferential partitioning of LREEs from the source into the fluid can occur in fluids with elevated Cl contents due to the increased stability of chloride complexes of LREEs compared to MREE and HREE (Rimskaya-Korsakova and Dubinin, 2002). The net result of all these variables is that it becomes very difficult to elucidate sulfides (if any) that contain primary source REE compositional information

from those that largely reflect transport processes. Though further work on the possibility of interpreting ore petrogenesis from sulfide REE compositions is clearly required, the measurable REE contents and broadly similar compositions of sulfides studied herein are encouraging in this regard.

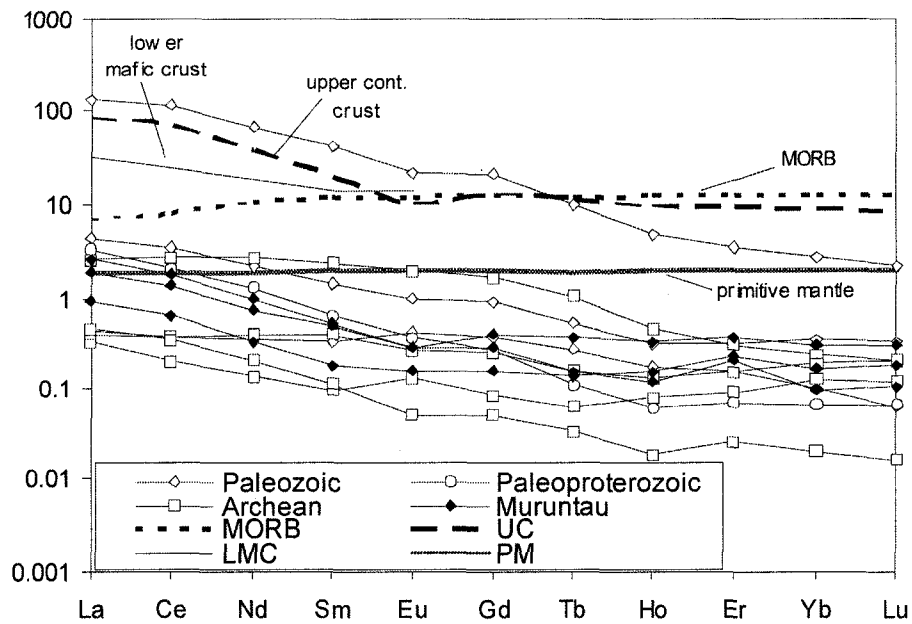


Figure 4.2.10: Chondrite-normalized rare earth element patterns for pyrite and arsenopyrite from global examples of orogenic gold deposits. Chondrite and upper and lower crust values from Taylor and McLennan (1985); MORB and primitive mantle values from Sun and McDonough (1989).

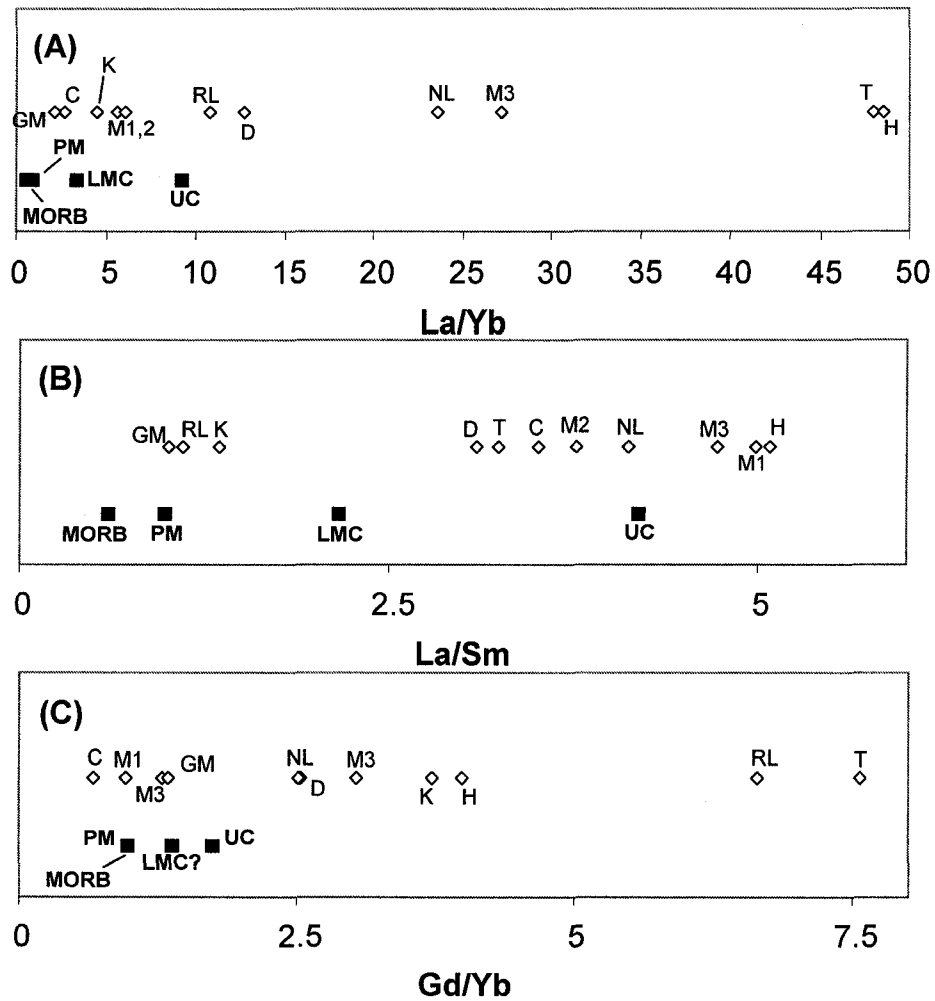


Figure 4.2.11: Chondrite-normalized rare earth element ratios for sulfides from global examples of orogenic gold deposits. M1, M2, M3 = Muruntau , respectively; C = Con; D = Dufferin; GM = Golden Mile; H = Homestake; Km = Kumtor; NL = Nicholas Lake; RL = Red Lake; T = Touquoy. For potential reservoirs, MORB = mid-ocean ridge basalt; PM = primitive mantle; LMC = lower mafic crust; UC = upper crust. References for REE reservoirs are same as in Fig. 4.2.10.

4.2.5 References

Arne, D.C., Bierlein, F.P., Morgan, J.W., and Stein, H.J., 2001, Re-Os dating of sulfides associated with gold mineralization in central Victoria, Australia: *Economic Geology and the Bulletin of the Society of Economic Geologists*, v. 6, p. 1455–1459.

Badalov, S.T., 1970, The provenance of some components in endogenic sulphate-sulphide and quartz-gold deposits in the Kurama Mountains, *in: Provenance of Matter in Endogenic Ore Deposits*, Alma-Ata, p. 36-54 (*in Russian*).

Bierlein, F.P., Groves, D.I., Goldfarb, R.J., and Dubé, B., 2006, Lithospheric controls on the formation of provinces hosting giant orogenic gold deposits: *Mineralium Deposita*, v. 40, p. 874–886.

Bierlein, F.P., Hughes, M., Dunphy, J., McKnight, S., Reynolds, P., and Waldron, H., 2001, Tectonic and economic implications of trace element, $^{40}\text{Ar}/^{39}\text{Ar}$ and Sm-Nd data from mafic dykes associated with orogenic gold mineralisation in central Victoria, Australia: *Lithos*, v. 58, p. 1-31.

Bingen, B. and Stein, H.J., 2003, Molybdenite Re-Os dating of biotite dehydration melting in the Rogaland high-temperature granulites, S Norway: *Earth and Planetary Science Letters*, v. 208, p. 181 - 195.

Burrows, D.R. and Spooner, E.T.C., 1987, Generation of a magmatic H₂O – CO₂ fluid enriched in Au, Mo and W within an Archean sodic granodiorite stock, Mink Lake, northwestern Ontario: *Economic Geology*, v. 82, p. 1931-1957.

Cameron, E.M., 1988, Archean gold: relation to granulite formation and redox zoning in the crust: *Geology*, v. 16, p. 109-112.

Card, K.D., Poulsen, K.H., and Robert, F., 1989, The Archean Superior Province and its lode gold deposits: *Economic Geology Monograph 6*, p. 19-36.

Chiaradia, M., Konopelko, D., Seltmann, R., and Cliff, R.A., 2006, Lead isotope variations across terrane boundaries of the Tien Shan and Chinese Altay: *Mineralium Deposita*, v. 41, p. 411-428.

Cole, A., 2001, Gold mineralization in the southern Tien Shan, central Asia: Tectonic setting, characteristics, exploration criteria, *in*: Seltmann, R. and Jenchuraeva [eds.], *Excursion Guidebook: IGCP-373 Field Conference in Bishkek and the Kyrgyz Tien Shan*, 6th Biennian SGA-SEG Meeting, Krakow, Poland, p. 71-81.

Dodson, M., 1973, Closure temperature in cooling geochronological and petrological systems: *Contributions to Mineralogy and Petrology*, v. 40, p. 259-274.

Drew, L.J., Berger, B.R., and Kurbanov, N.K., 1996, Geology and structural evolution of the Muruntau gold deposit, Kyzulkum desert, Uzbekistan: *Ore Geology Reviews*, v. 11, p. 175-196.

Fyfe, W.S., and Kerrich, R., 1984, Gold: natural concentration processes, *in*: Foster, R.P. [ed.], *Gold '82: The Geology, Geochemistry, and Genesis of Gold Deposits*, Rotterdam, A.A. Balkema, p. 99-127,

Goldfarb, R.J., Groves, D.I., and Gardoll, S., 2001, Orogenic gold and geologic time: a global synthesis: *Ore Geology Reviews*, v. 18, p. 1-75.

Golovanov, I.M., Seltmann, R., and Kremenetsky, A.A., 2005, The porphyry Cu-Au/Mo deposits of central Eurasia 2. The Almalyk (Kal'makyr-Dalnee) and Saukbulak Cu-Au porphyry systems, Uzbekistan, *in*: Porter, T.M. [ed.], *Super Porphyry Copper and Gold Deposits: A Global Perspective*, PGC Publishing, Adelaide, v. 2, p. 513-523.

Golovanov, I.M., Nikolayaeva, E.I., and Kazhikhin, M.A., 1988, Integral model for the forecasting and prospecting of porphyry copper deposits), Tashkent: Fan, 197 p. (*in Russian*).

Graupner, T., Niedermann, S., Kempe, U., Klemd, R., and Bechtel, A., 2006, Origin of ore fluids in the Muruntau gold system: Constraints from noble gas, carbon isotope and halogen data: *Geochimica et Cosmochimica Acta*, v. 70, p. 5356–5370.

Groves, D.I., Condie, K.C., Goldfarb, R.J., Hronsky, J.M.A., and Vielreicher, R.M., 2005, Secular changes in global tectonic processes and their influence on the temporal distribution of gold-bearing mineral deposits: *Economic Geology and the Bulletin of the Society of Economic Geologists*, v. 100, p. 203–224.

Groves, D.I., Goldfarb, R.J., Robert, F., and Hart, C.J.R., 2003, Gold deposits in metamorphic belts: Overview of current understanding, outstanding problems, future research and exploration significance. *Economic Geology*, v. 98, p. 1-29.

Groves, D.I., Goldfarb, R.J., Gebre-Meriam, M., Hagemann, S.G., and Robert, F., 1998, Orogenic gold deposits: a proposed classification in the context of their crustal distribution and relationship to other gold deposit types: *Ore Geology Reviews*, v. 13, p. 7–27.

Haeussler, P.J., Bradley, D., Goldfarb, R., Snee, L., and Taylor, C., 1995, Link between ridge subduction and gold mineralization in southern Alaska: *Geology*, v. 23, p. 995-998.

Hattori, Y., Suzuki, K., Honda, M., and Shimizu, H., 2003, Re-Os isotope systematics of the Taklimakan Desert sands, moraines and river sediments around the Taklimakan Desert, and of Tibetan soils: *Geochimica et Cosmochimica Acta*, v. 67, p. 1203–1213.

Hodgson, C.J., Hamilton, J.V., and Hanes, J.A., 1989, The late emplacement of gold in the Archean Abitibi greenstone belt: a consequence of thermal equilibration following

collisional orogeny: Geological Association of Canada / Mineralogical Association of Canada Annual Meeting, Program with Abstracts, v. 14, p. A45.

Hutchinson, R.W., 1993, A multi-stage, multi-process genetic hypothesis for greenstone-hosted lode gold lodes: *Ore Geology Reviews*, v. 8, p. 349-382.

Jahn, B., Wu, F., and Chen, B., 2000, Granitoids of the Central Asian Orogenic Belt and continental growth in the Phanerozoic: *Transactions of the Royal Society of Edinburgh: Earth Sciences*, v. 91, p. 181–193.

Keays, R.R., 1987, Principles of mobilization (dissolution) of metals in mafic and ultramafic rocks – the role of immiscible magmatic sulphides in the generation of hydrothermal gold and volcanogenic massive sulphide deposits: *Ore Geology Reviews*, v. 2, p. 47-63.

Kempe, U., Seltmann, R., Graupner, T., Wall, V.J., Matukov, D., and Sergeev, S., 2004, SHRIMP U-Pb zircon dating of Hercynian granite magmatism in the Muruntau gold district (Uzbekistan): *Proceedings of the Interim IAGOD Conference Abstracts, Vladivostok, Russia, Abstracts*, p. 210–213.

Kempe, U., Belyatsky, B.V., Krymsky, R.S., Kremenetsky, A.A., and Ivanov, P.A., 2001, Sm-Nd and Sr isotope systematics of scheelite from the giant Au(-W) deposit Muruntau (Uzbekistan): implications for the age and sources of gold mineralization: *Mineralium Deposita*, v. 36, p. 379–392.

Kerrich, R. and Wyman, D., 1990, Geodynamic setting of mesothermal gold deposits: An association with accretionary tectonic regimes: *Geology*, v. 18, p. 882-885.

Kerrich, R., Goldfarb, R., Groves, D., and Garwin, S., 2000, The geodynamics of world-class gold deposits: characteristics, space-time distribution, and origins *in*: Hagemann,

S.G., and Brown, P.E. [eds.]: Gold in 2000, Society of Economic Geologists, Reviews in Economic Geology, v. 13, p. 501-551.

Kirk, J., Ruiz, J., Chesley, J., Titley, Walshe, J., and England, G., 2002, A major Archean gold- and crust-forming event in the Kaapvaal craton, South Africa: Science, v. 297, p. 1856 – 1858.

Kostitsyn, Y.A., 1996, Rb-Sr isotopic study of the Muruntau deposit: magmatism, metamorphism, and mineralization: Geochemistry International, v. 34, p. 1009–1023.

Kostitsyn, Y.A., 1994, Rb-Sr studies on the Muruntau deposit: mineralized metasomatites: Geochemistry International, v. 31, p. 21–34.

Kotov, N.V. and Poritskaya, L.G., 1992, The Muruntau gold deposit: its geologic structure, metasomatic mineral associations and origin: International Geology Review, v. 34, p. 77-87.

Levresse, G., Cheilletz, A., Gasquet, D., Reisberg, L., Deloule, E., Marty, B., and Kyser, K., 2004, Osmium, sulphur, and helium isotopic results from the giant Neoproterozoic epithermal Imiter silver deposit, Morocco: evidence for a mantle source: Chemical Geology, v. 207, p. 59–79.

Lottermoser, B.G., 1992, Rare earth elements and hydrothermal ore formation processes: Ore Geology Reviews, v. 7, p. 25-41.

Ludwig, K.R., 2003, Isoplot/Ex, version 3; A geochronological toolkit for Microsoft Excel: Berkeley, California, Geochronology Center Berkeley.

MacDonald, A.J. and Hodgson, C.J., 1986, The case for the magmatic-hydrothermal origin of Archean lode gold deposits (abs.), *in*: Chater, A.M. [ed.], Gold '86, An

International Symposium on the Geology of Gold Deposits – Poster Paper Abstracts, Geological Association of Canada, Toronto, p. 98-99.

Marakushev, A.A. and Khokhlov, V.A., 1992, A petrological model for the genesis of the Muruntau gold deposit: *International Geology Review*, v. 34, p. 59-76.

McCoy, D., Newberry, R.J., Layer, P.W., DiMarchi, J.J., Bakke, A.A., Masterman, J.S., and Minehane, D.L., 1997, Plutonic-related gold deposits of interior Alaska: *Economic Geology Monograph* 9, p. 191-241.

Meisel, T., Walker, R.J., Irving, A.J., and Lorand, J., 2001, Osmium isotopic compositions of mantle xenoliths: a global perspective: *Geochimica et Cosmochimica Acta*, v. 65, p. 1311–1323.

Morelli, R.M., Creaser, R.A., Selby, D., Kontak, D.J., and Horne, R.J., 2005, Rhenium-osmium arsenopyrite geochronology of Meguma Group gold deposits, Meguma Terrane, Nova Scotia, Canada: evidence for multiple mineralizing events: *Economic Geology and the Bulletin of the Society of Economic Geologists*, v. 100, p. 1229–1242.

Morelli, R.M., Creaser, R.A., and Seltmann, R., 2004, Rhenium-osmium geochronology of arsenopyrite from the giant Muruntau Au deposit, Uzbekistan: *Proceedings of the Interim IAGOD Conference Abstracts, Vladivostok, Russia*, p. 510-513.

Pan, P. and Wood, S.A., 1994, Solubility of Pt and Pd sulfides and Au metal in Aqueous bisulfide solutions, II. Results at 200° to 350°C and saturated vapor pressure: *Mineralium Deposita*, v. 29, p. 373-390.

Peucker-Ehrenbrink, B. and Jahn, B., 2001, Rhenium-osmium isotope systematics and platinum group element concentrations: Loess and the upper continental crust: *Geochemistry, Geophysics, Geosystems*, v. 2, doi: 10.1029/2001GC000172, doi: 10.1029/2001GC000172.

Richards, J.P., 2003, Tectono-magmatic precursors for porphyry Cu-(Mo-Au) deposit formation: *Economic Geology*, v. 98, p. 1515-1533.

Rimskaya-Korsakova, M.N. and Dubinin, A.V., 2002, Rare earth elements in sulfides of submarine hydrothermal vents of the Atlantic Ocean: *Doklady Earth Sciences*, v. 389A, p. 432-436.

Rock, N.M.S. and Groves, D.I., 1988a, Do lamprophyres carry gold as well as diamonds?: *Nature*, v. 332, p. 253-255.

Rock, N.M.S. and Groves, D.I., 1988b, Can lamprophyres resolve the genetic controversy over mesothermal gold deposits?: *Geology*, v. 16, p. 538-541.

Rusinova, O.V. and Rusinov, V.L., 2003, Metasomatism in the Muruntau ore field (western Uzbekistan): *Geology of Ore Deposits*, v. 45, p. 75-96.

Saal, A.E., Rudnick, R.L., Ravizza, G.E., and Hart, S.R., 1998, Re-Os isotope evidence for the composition, formation and age of the lower continental crust: *Nature*, v. 393, p. 58-61.

Selby, D. and Creaser, R.A., 2004, Macroscale NTIMS and microscale LA-MC-ICP-MS Re-Os isotopic analysis of molybdenite: Testing spatial restrictions for reliable Re-Os age determinations, and implications for the decoupling of Re and Os within molybdenite: *Geochimica et Cosmochimica Acta*, v. 68, p. 3897 – 3908.

Selby, D. and Creaser, R.A., 2001, Re-Os geochronology and systematics in molybdenite from the Endako porphyry molybdenum deposit, British Columbia, Canada: *Economic Geology*, v. 96, p. 197 – 204.

Seward, T.M., 1991, The hydrothermal geochemistry of gold, *in*: Foster, R.P. [ed.], *Gold Metallogeny and Exploration*, Blackie and Son, Glasgow, U.K., p. 37-62.

Sillitoe, R.H., 1993, Intrusion-related gold deposits, *in*: Foster, R.P. [ed.], *Gold Metallogeny and Exploration*, Chapman and Hall, London, U.K., p. 165-209.

Stein, H.J., Scherstén, A., Hannah, J.L., and Markey, R.J., 2003, Subgrain scale decoupling of Re and ^{187}Os and assessment of laser ablation ICP-MS spot dating in molybdenite: *Geochimica et Cosmochimica Acta*, v. 67, p. 3673 – 3686.

Stein, H.J., Markey, R.J., Morgan, J.W., Hannah, J.L., and Scherstén, A., 2001, The remarkable Re-Os chronometer in molybdenite: how and why it works: *Terra Nova*, v. 13, p. 479 – 486.

Stein, H.J., Morgan, J.W., and Scherstén, A., 2000, Re-Os dating of low-level highly radiogenic (LLHR) sulfides: The Harnäs gold deposit, southwest Sweden, records continental-scale tectonic events: *Economic Geology and the Bulletin of the Society of Economic Geologists*, v. 95, p. 1657–1671.

Stein, H.J., Morgan, J.W., Markey, R.J., and Hannah, J.L., 1998, An introduction to Re-Os: what's in it for the mineral industry?: *Society of Economic Geologists Newsletter*, v. 32, p. 8 – 15.

Stuart, F.M., Burnard, P.G., Taylor, R.P., and Turner, G., 1995, Resolving mantle and crustal contributions to ancient hydrothermal fluids: He-Ar isotopes in fluid inclusions from Dae Hwa W-Mo mineralisation, South Korea: *Geochimica et Cosmochimica Acta*, v. 59, p. 4663–4673.

Sun, S.S. and McDonough, W.F., 1989, Chemical and isotopic systematics of oceanic basalts: implications for mantle compositions and processes, *in*: Saunders, A.D. and Norry, M.J. [eds.], *Magmatism in Ocean Basins*, Geological Society of London Special Publication 42, p. 313-345.

Sun, W., Bennett, V.C., Eggins, S.M., Kamenetsky, V.S., and Arculus, R.J., 2003, Enhanced mantle-to-crust rhenium transfer in undegassed arc magmas: *Nature*, v. 422, p. 294–297.

Taylor, S.R. and McLennan, S.M., 1985, *The Continental Crust: its Composition and Evolution*. Blackwell, Oxford, 312 pp.

Taylor, S.R. and McLennan, S.M., 1981, The composition and evolution of the continental crust: rare earth element evidence from sedimentary rocks: *Philosophical Transactions of the Royal Society*, A301, p. 381-399.

Titley, S., 1991, Phanerozoic ocean cycles and sedimentary-rock-hosted gold ores: *Geology*, v. 19, p. 645-648.

Turner, G. and Stuart, F.M., 1992, He/heat ratios and the deposition temperature of ocean floor sulphides: *Nature*, v. 357, p. 581–583.

Wall, V.J., Graupner, T., Yantsen, V., Seltmann, R., and Hall, G.C., 2004, Muruntau, Uzbekistan: A giant thermal aureole gold (TAG) system: *Society of Economic Geologists 2004 Predictive Mineral Discovery Under Cover*, Perth, Western Australia, Extended Abstracts, p 199-203.

Widom, E., Gaddis, S.J., and Wells, N.E., Jr., 2004, Re-Os isotope systematics in carbonates from Serpent Mound, Ohio: Implications for Re-Os dating of crustal rocks and the osmium isotopic composition of Ordovician seawater: *Geochemistry, Geophysics, Geosystems*, v. 5, doi: 10.1029/2002GC000444, doi: 10.1029/2002GC000444.

Wilde, A.R., Layer, P., Mernagh, T., and Foster, J., 2001, The giant Muruntau gold deposit: geologic, geochronologic, and fluid inclusion constraints on ore genesis:

Economic Geology and the Bulletin of the Society of Economic Geologists, v. 96, p. 633–644.

Wood, S.A., 2004, The hydrothermal geochemistry of the rare earth elements: ‘The Gangue’, Geological Association of Canada Mineral Deposits Division, v. 81, p.1, 5-7.

Wood, S.A., 1987, Thermodynamic calculations of the platinum-group elements (PGE): the PGE content of fluids at magmatic temperatures: *Geochimica et Cosmochimica Acta*, v. 51, p. 3041-3050.

Wyman, D. and Kerrich, R., 1988, Alkaline magmatism, major, structures, and gold deposits: Implications for greenstone belt gold metallogeny, *Economic Geology*, v. 83, p. 451-458.

Yakubchuk, A., Cole, A., Seltmann, R., and Shatov, V., 2002, Tectonic setting, and regional exploration criteria for gold mineralization in the Altaid Orogenic Collage: the Tien Shan province as a key example: *Society of Economic Geologists Special Publication*, v. 9, p. 177–201.

4.3 Conclusions

The results of this chapter demonstrate the tremendous potential that Re-Os sulfide geochronology holds for resolving the age and origin of post-Archean orogenic gold deposits. Seemingly higher Re contents in Proterozoic and Paleozoic orogenic gold deposits relative to their Archean counterparts results in much improved age precision (0.4 % or better) on determined ages.

Determination of a Re-Os arsenopyrite age of 1736 ± 8 Ma from the Homestake gold deposit in the southern Trans Hudson Orogen conclusively shows the reliability of this technique, as this age falls directly within existing age brackets for mineralization. Moreover, retention of this mineralization age through post-crystallization exposure to elevated temperatures (400-480°C) provides a minimum estimate of the apparent closure temperature of the Re-Os arsenopyrite chronometer. In contrast, pyrrhotite from

Homestake yields a scattered Re-Os isochron, resulting from Re-Os disturbance at these conditions. Scatter of individual pyrrhotite data points both above and below the 1736 Ma arsenopyrite reference isochron may reveal small scale movement of Re and/or Os between pyrrhotite crystals.

New U-Pb monazite ages derived from laser ablation analyses of thin sections from the Harney Peak Granite indicate that this was a protracted magmatic event from 1715 Ma to ca. 1690 Ma, or possibly even as late as 1683 Ma. The relative temporal relationship between the newly determined Homestake mineralization and Harney Peak magmatic ages eliminate the possibility of a cogenetic association between these events. Combined with the very unradiogenic (0.28) initial $^{187}\text{Os}/^{188}\text{Os}$ ratio derived from the arsenopyrite isochron, these timing constraints indicate that Homestake may have a broadly metamorphic origin, providing that gold was derived from the metamorphism of juvenile rocks, or rather was produced during the influx of mantle melts at depth in the crust.

Re-Os sulfide geochronology was also used to resolve the timing of metallogenic events in the Tien Shan Orogen of central Asia. Re-Os single mineral model ages from three of four analyzed molybdenite indicate that porphyry-style mineralization at the giant Kal'makyr (Almalyk) Cu-Au deposit occurred at ca. 314 Ma, contemporaneously with the intrusion of proximal porphyry intrusions in the host Valerianov-Beltau-Kurama magmatic arc. The significance of two determined 467 Ma ages from replicate analyses of the fourth molybdenite sample is unclear. They likely either represent an earlier phase of molybdenite crystallization or are the result of mixing between two or more Re-Os sources. Porphyry-related mineralization in the Northern Tien Shan gave way to extensive formation of orogenic gold deposits in the southern Tien Shan following terrane accretion in the late Permian. High-precision Re-Os arsenopyrite geochronology, coupled with Os and He isotopic tracing, provide new constraints for the origin of the giant Muruntau OGD, from which the timing of mineralization was determined to be ca. 290 Ma, not ca. 275 – 245 Ma as previously determined by other methods. The Os_i and He isotope data show that formation of the Muruntau deposit included a component of mantle-derived and/or juvenile metals and fluids. These data are incompatible with models that invoke a purely crustal source for fluids and metals at Muruntau (e.g., Wilde

et al., 2001), or those that require mineralization younger than ca. 290 Ma (Kostitsyn, 1996; Wilde et al., 2001). The new Re-Os dates for ore formation overlap the timing of proximal granitoid magmatism, so “intrusion-related” models for ore formation are permitted by these data (e.g., Wall et al., 2004), although a mantle component is required at some stage in magma genesis. Alternatively, if Os, He and Au in the hydrothermal system have different origins, more complex models involving the coincidence of mantle and crustal magmatism, juvenile and crustal fluids and favorable structural conditions at ca. 290 Ma, are possible. The use of coupled Re-Os-He isotopes in arsenopyrite should provide valuable constraints for the origin of orogenic gold deposits worldwide. In contrast, rare earth element abundances of ore-related sulfide minerals are ambiguous with respect to a gold source.

5. Generation of a World Class Volcanogenic Massive Sulfide Camp: Constraints from Re-Os Sulfide Geochronology in the Flin Flon and Kisseynew Domains, Trans-Hudson Orogen

5.1. Introduction

A technique in its developmental stages, the full potential of Re-Os sulfide geochronology is unclear because the ability of sulfide minerals to retain original Re-Os isotope compositions through subsequent geologic events remains unresolved. This theoretical requirement has generally been ignored in previous attempts at Re-Os sulfide dating, with the only detailed studies of this sort focusing on the Re-Os molybdenite chronometer. Some important studies (Stein et al., 1998; Raith and Stein, 2000; Bingen and Stein, 2003) have shown that the Re-Os molybdenite chronometer can be extremely reliable, even through intense deformation and high grade metamorphism (> 710°C; Bingen and Stein, 2003), although this might be controlled, to some extent, by the particular mineral assemblage with which it is associated (see Stein et al., 2001; Stein et al., 2003).

Though speculative, some studies have also commented on the capacity of other sulfide minerals to retain primary Re-Os age information. Stein et al. (2003) proposed that these 'low-level' sulfide minerals (Stein et al., 2001) are susceptible to disturbance if they share grain boundaries with molybdenite, demonstrated by geologically impossible ages for chalcopyrite in direct contact with molybdenite from the Pitkäranta district of western Russia. Other studies of sulfide minerals (e.g. pyrite - Mathur et al., 1999; Stein et al., 2000; pyrrhotite - Frei et al., 1998; Lambert et al. 2000; sphalerite - Morelli et al., 2004), suggest that chemical interaction with molybdenite is not necessarily a prerequisite for disturbing low-level sulfide Re-Os isotopic compositions, and that this can be accomplished solely through tectonothermal/hydrothermal effects. Notwithstanding these preliminary studies, a more focused and systematic assessment is required using sulfide samples with well constrained crystallization ages and metamorphic histories.

This study focuses on Re-Os isotopic geochronology of sulfide minerals from metamorphosed volcanogenic massive sulfide (VMS) deposits in the Paleoproterozoic Trans-Hudson Orogen of Manitoba and Saskatchewan, Canada. Specifically, sulfide

samples are derived from the Konuto Lake (chalcopyrite) and Trout Lake (pyrite, pyrrhotite) deposits in the Flin Flon belt, the Harmin deposit (pyrite) in the Snow Lake belt, and the Sherritt Gordon deposit (pyrite) in the Kisseynew Domain (Fig. 5.1). All sampled sulfide minerals within the individual VMS deposits are considered paragenetic equivalents that represent a single mineralizing event. These deposits collectively provide an excellent study area with which to assess the robustness of Re-Os sulfide chronometers because (a) the host belts are well studied, and the deposits generally have well constrained mineralization ages, (b) the deposits have been variably metamorphosed, thus providing a range of T-P conditions over which to test the chronometers, and (c) the timing of peak metamorphism is well established. Results of this work indicate that sphalerite and, less certainly, chalcopyrite, are readily disturbed during thermal events and are poor choices for Re-Os geochronology, whereas pyrite is a very robust Re-Os chronometer, remaining isotopically closed to ~ 700°C.

5.2. Geology

5.2a. Flin Flon, Kisseynew Domain Geology

The northern (Canadian) segment of the Trans-Hudson Orogen (THO) is a product of the collision of three Archean cratons (Hearne, Sask, and Superior) and the accretion of intervening juvenile terranes during closure of a Pacific-scale ocean from ca. 1.9 – 1.8 Ga. Exposed rock in the internal zone of the orogen comprises the ‘Reindeer Zone’ (Stauffer, 1984), which consists predominantly of metamorphosed Paleoproterozoic volcano-plutonic island arc rocks and flanking sedimentary belts. The rocks have been delineated into five distinct lithotectonic domains, including (from SE to NW; Fig. 5.1) the Flin Flon, Glennie, Kisseynew, LaRonge-Lynn Lake, and Rottenstone Domains, in addition to the Wathaman Batholith at the western margin of the zone. The Flin Flon and Kisseynew Domains, the focus of this study, respectively overlie the Archean Sask craton in a three component, NE-dipping structural ‘stack’ that formed during ca. 1.84 – 1.80 Ga collisional orogenesis (Lucas et al., 1997).

The Flin Flon Domain hosts one of the world’s most economically important Paleoproterozoic VMS districts, including three of the four VMS deposits sampled for

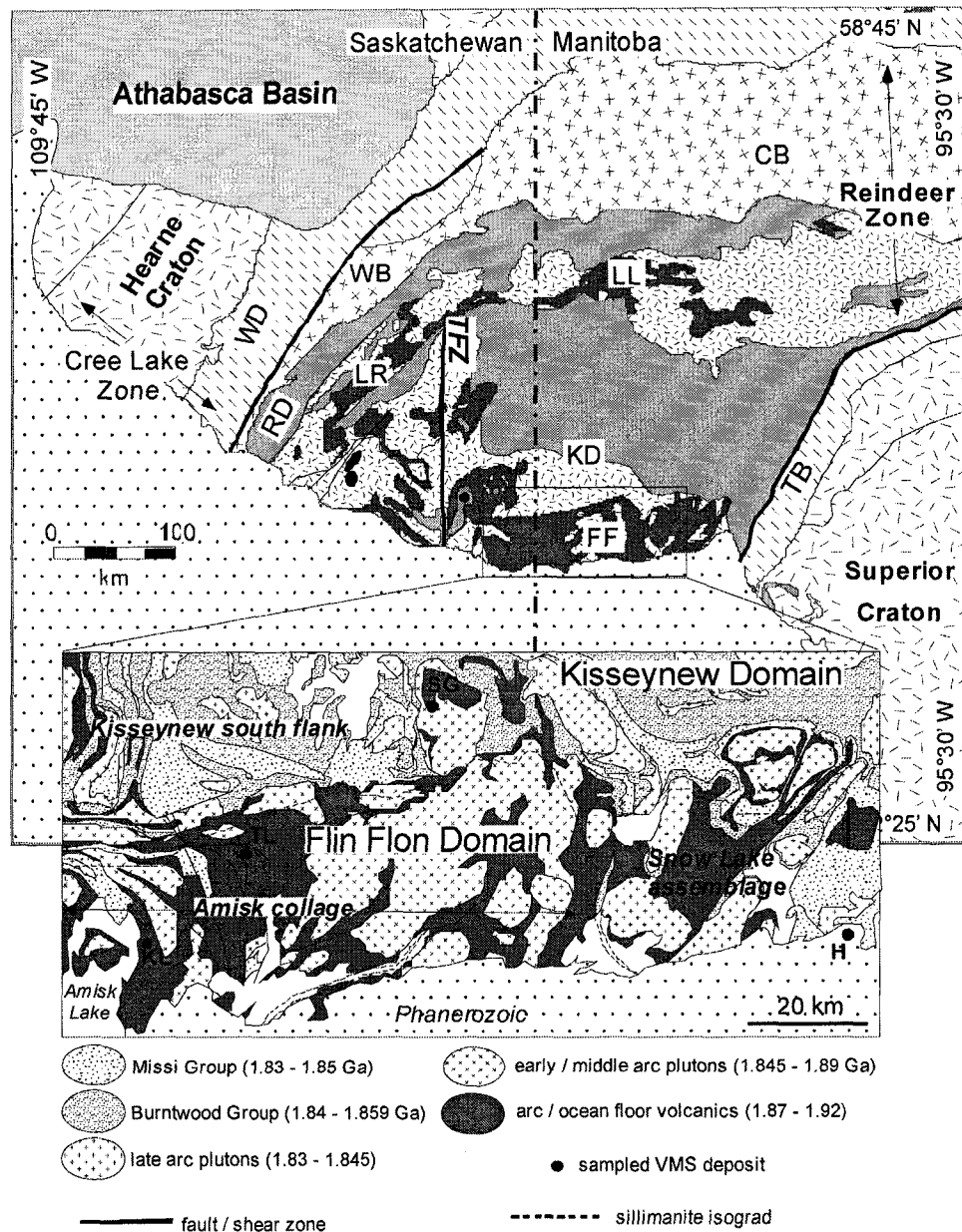


Figure 5.1: Lithotectonic Domains of the Reindeer Zone, with detailed geology of the Flin Flon and Kisseynew Domains. Individual domains are: WD = Wollaston, RD = Rottenstone, LR = LaRonge, LL = Lynn Lake, KD = Kisseynew, FF = Flin Flon, and WB and CB represent the Wathaman/Chipewan Batholith. TFZ = Tabbornor Fault Zone. Black dots show the location of VMS deposits sampled for this study (KL = Konuto Lake, TL = Trout Lake, H = Harmin, SG = Sherritt Gordon). Modified from Hoffman (1989) and Zwanzig (1999).

this study. It is believed that the Flin Flon Domain is one remnant of a larger intraoceanic island arc system that included the adjacent Glennie Domain, but that was dismembered during subsequent continental collision. The domain comprises several separate juvenile arc assemblages, including the Flin Flon and Snow Lake assemblages, which are fault-bounded or separated by ocean-floor rocks, and can range considerably in metamorphic grade. The geology of the Flin Flon belt, covered in detail by Syme et al. (1999), consists predominantly of 1.92 – 1.87 Ga, coeval juvenile arc and ocean floor (back arc) assemblages. The arc assemblage is dominated by bimodal (basalt – basaltic andesite, dacite – rhyolite) volcanic rocks erupted in arc or arc-rift settings, compositionally ranging from calc-alkaline to tholeiitic. Other common arc assemblage lithologies include orthogneiss, mafic to felsic volcanoclastic rocks, synvolcanic tonalitic and ultramafic/mafic intrusions, and subsidiary turbidite sequences. Economic VMS mineralization in the Flin Flon Domain is hosted almost exclusively by tholeiitic or calc-alkaline arc assemblage rocks, and has a strong genetic association with magmatic and structural elements characteristic of arc-rifting events (Syme et al., 1999; Bailes and Galley, 1999). The individual arc assemblages have been ‘stitched’ together by felsic, intermediate, and mafic intrusive rocks that were emplaced during the development of an overprinting successor arc from 1.87 – 1.84 Ga (Stern et al., 1999).

Arc assemblages in the Flin Flon Domain have been metamorphosed and experienced multiple episodes of deformation, resulting from collisions between the juvenile Paleoproterozoic terranes and the three Archean cratons during development of the THO (Ansdell, 2005a, and references therein). The first recognized deformational episode (D₁) occurred ca. 1.89 – 1.88 Ga and records the intraoceanic accretion and amalgamation/dismembering of individual arc assemblages, resulting in the formation of the so-called ‘Amisk Collage’ (Lucas et al., 1996). Underthrusting of the Archean Sask craton beneath the Amisk Collage at ca. 1.85 Ga caused the second deformational event (D₂), followed by the onset of the terminal collision between the Hearne and Superior cratons (D₃) ca. 1.83 – 1.82 Ga. This continental collision also coincides with the onset of regional metamorphism throughout the THO, with peak metamorphic conditions considered to have been attained at ca. 1.820 – 1.815 Ga (Gordon, 1989; Machado et al., 1999; Schneider et al., 2007). Peak metamorphic grade varies throughout the Flin Flon

Domain, with generally lower grade (sub-greenschist to upper greenschist facies) rocks occurring in the western portion (e.g. Flin Flon belt) and higher grade (upper amphibolite to lower granulite facies) rocks in the eastern portion of the domain (e.g. Snow Lake belt). Elevated thermal conditions and concomitant ductile (D₄, ca. 1.785 Ga) to brittle (D₅, ca. 1.72 Ga) deformation persisted in portions of the Reindeer zone, including the Flin Flon domain, through to ~ 1.7 Ga, at which time ambient crustal temperatures cooled through Ar-Ar mica blocking temperatures of ~ 300 - 350°C (Schneider et al., 2007).

Concurrent with (D₂) collision of the Sask craton with juvenile terranes ca. 1.85 was the deposition of voluminous turbidites in an extensive back-arc (Ansdell et al., 1995) or interarc/forearc (Zwanzig, 1990; Gordon et al., 1990) basin. These sedimentary deposits, derived principally from unroofing of the 1.92 – 1.87 Ga juvenile arc sequences (David et al., 1995), comprise the Burntwood and Missi Groups of the Kisseynew Domain. Deposition of the Burntwood Group turbidites commenced ca. 1860 - 1850 Ma in submarine fans in a deep water environment (David et al., 1996), whereas the Missi Group, deposited between ca. 1848 to 1840 Ma (Machado et al., 1999), is interpreted to represent equivalent near-shore deposits. The present day structure of the Kisseynew Domain, generally exhibiting an inwardly increasing metamorphic grade from greenschist facies at the basin margin to granulite facies in its interior (Bailes and McRitchie, 1978), reflects the structural inversion of the basin ca. 1.82 -1.81 Ga due to exhumation of tectonically thickened crust in the central portion of the basin (Ansdell et al., 1995). Rocks in the interior of the basin typically comprise high metamorphic grade quartzofeldspathic gneisses that were traditionally interpreted to derive from Missi Group sedimentary rocks, but were later reinterpreted to have Amisk Group-equivalent felsic volcanic protoliths (Ashton et al., 1996). These gneisses are commonly interleaved with amphibolitic rocks of uncertain paragenesis.

5.2b. Deposit Geology

The sulfides sampled for Re-Os analysis in this study are from four separate VMS deposits located in different regions of the Reindeer Zone (Fig. 5.1). The salient characteristics of each deposit are described below.

i. Trout Lake deposit, Flin Flon Assemblage

The Trout Lake deposit, located approximately 5 km northeast of Flin Flon, Manitoba, contains ~ 20,000,000 t of ore grading 1.83 % Cu, 5.59 % Zn, 1.73 g/t Au, and 17.37 g/t Ag. The deposit is hosted by hydrothermally altered pyroclastic quartz porphyritic rocks of the ca. 1.92 – 1.87 Ga Amisk Group, which have been metamorphosed to middle greenschist facies (estimated at ~ 450°C). Mineralization consists of both massive and disseminated sulfide minerals, and is present in a series of structurally stacked lenses that dip steeply (60 – 70°) to the northeast (Ko, 1986).

ii. Konuto Lake deposit, Flin Flon Assemblage

The Konuto Lake deposit is located in east-central Saskatchewan, approximately 16 km west of Flin Flon, and contains ~ 2,035,000 t of ore grading 4.4 % Cu, 1.6 % Zn, 2.16 g/t Au, and 8.98 g/t Ag. The deposit is hosted within a north-trending sequence of mafic volcanic rocks of the Birch Lake Assemblage (Amisk Group), which includes predominantly massive and pillowed tholeiitic basalts and intercalated mafic – ultramafic intrusions. Along with the host rocks, the mineralization has been metamorphosed to lower amphibolite facies (estimated at ~ 500 - 550°C) and consists of sulphide breccias and stockwork ore in a series of ore lenses that are bound by overprinting brittle-ductile shear zones (Tourigny et al., 2002).

iii. Harmin prospect, Snow Lake Assemblage

The Harmin prospect, situated beneath the Phanerozoic cover in Fenton Creek area of northern Manitoba, is presumed to belong to the Snow Lake arc assemblage. The prospect contains ~ 3,700,000 t of ore, grading 2.25% Cu, 2.32% Zn, 0.22 g/t Au, and 22.39 g/t Ag. Because the mineralization has only been intersected by drill core, little is known about the host rocks or mineralization style(s), except that the original stratigraphy contained some proportion of greywacke, siltstone, shale, and quartzite that is interbedded with or intruded by basaltic andesite, rhyolite, and gabbro (Polito et al., 2007). Further, perthitic feldspars, myrmekitic intergrowths, and metamorphic mineral assemblages in metasedimentary drill samples indicate that peak metamorphic conditions

attained uppermost amphibolite to granulite facies conditions (Polito et al., 2007), perhaps to a temperature $> 700^{\circ}\text{C}$.

iv. Sherritt Gordon deposit, Kisseynew Domain

The Sherritt Gordon deposit, located near Sherridon, Manitoba, contains 7,739,506 t of ore in two zones (East and West ore bodies) with an average grade of 2.46% Cu, 2.84% Zn, 0.58 g/t Au, and 33.3 g/t Ag. The mineralization is hosted by quartzofeldspathic gneisses of the Sherridon Group, which also contains discontinuous lenses of amphibolite that typically parallel the ore bodies. The ore bodies comprise ~ 5m thick tabular masses of sulphide minerals, consisting mainly of pyrite, pyrrhotite, sphalerite, and chalcopyrite. Several features of the local geology, including the presence of cordierite – anthophyllite rocks proximal to the deposit, the presence of leucosome in the host rocks, the metamorphic mineral assemblage of the host rocks and the sulfide mineral assemblage of the ore, and small zones of remobilized ore, indicate that the rocks (including the ore) have been metamorphosed to a relatively high metamorphic grade during ca. 1818 - 1785 Ma peak regional metamorphism (Machado et al., 1999), estimated by Froese and Goetz (1980) to have reached upper amphibolite facies (660°C , 5 kbar).

5.3. Sampling Protocol

Sulfide samples from the three Flin Flon domain deposits used for Re-Os analysis are derived from mineralized drill core fragments and typically consisted of intermingled combinations of two or more sulfide minerals. Separations of pure mineral fractions from each deposit were performed using slightly different methods, depending on the specific sulfide mineralogy. Core from all three deposits was initially broken inside of a plastic bag with a hammer covered with duct tape, and the pieces containing the highest proportion of the desired mineral were then isolated and further crushed using an agate shatterbox. The crushed material was subsequently sieved, and the 70 – 200 mesh fractions were magnetically separated using a FrantzTM separator.

Drill core from the Trout Lake deposit (sample J15943, hole TX 1399: 1456.5 – 1457.5 m) consisted of ~ 60 % subhedral pyrite crystals surrounded by sphalerite (30 %)

and pyrrhotite (5-10%; Fig. 5.2a). After sieving, the first six samples used for Re-Os analyses were magnetically separated at consecutive amperages of 0.2, 0.5, 1.0, and 1.3 A to attempt isolation of pure pyrite by removal of pyrrhotite and sphalerite. Following the first batch of Re-Os analysis (denoted with an 'a' in Table 5.1), it was observed that not all sphalerite had been removed. Therefore, all existing and subsequent samples from Trout Lake (denoted by 'b' in Table 5.1) were magnetically separated at 2.0 A, which resulted in the removal of a large magnetic fraction consisting predominantly of sphalerite. This is consistent with the lower extraction range for sphalerite (0.35 – 1.7 A) relative to pyrite (1.4 – 1.7 A) during magnetic separation (Rosenblum, 1958).

The sample from the Konuto Lake deposit (sample J15942, hole Ner 94: 478.57 – 479.57 m) contained approximately 50% chalcopyrite, 10% pyrrhotite, 10% sphalerite, and <5% pyrite, as well as 25-30% quartz/carbonate gangue (Fig. 5.2b). Pure pyrrhotite was magnetically removed at ~ 0.2 A, the majority of sphalerite was removed by 0.4 A, chalcopyrite was found in the magnetic fraction between 0.5 - 0.6 A, and pyrite remained in the nonmagnetic fraction at 2.0 A. To attempt retrieval of a pure chalcopyrite separate for Re-Os analysis, the Konuto Lake mineral separate was magnetically separated at amperages of 0.2, 0.4, and then three times at 0.5 A. Visual inspection of the sample following FrantzTM separation revealed no pyrite, sphalerite, or pyrrhotite grains, although it is possible that pyrrhotite and/or sphalerite remained as inclusions within chalcopyrite grains. It is estimated that the final Konuto Lake sulfide mineral separate consisted of at least 90% pure chalcopyrite.

Although drill core from the Harmin deposit (sample J15941, hole Nim-048: 293 – 294 m) consists predominantly of coarse-grained pyrrhotite, there are individual portions of 5 – 10 cm in length that consist of > 99% pure coarse-grained pyrite (Fig. 5.2c). Two such sections were used to obtain a crushed pyrite separate, which was subjected to a FrantzTM magnetic separation at 2.0 A to ensure the complete removal of pyrrhotite.

Pyrite from the Sherritt Gordon deposit is derived from a hand sample from the mine that was donated for this study by the Royal Ontario Museum in Toronto, Ontario, Canada (catalogue #M19674). The specimen consists of coarse (0.3 to 1.5 cm) pyrite crystals with anhedral to subhedral, pentagonal-dodecahedron morphologies (Fig. 5.2d),

with interstitial sphalerite and chalcopyrite. Individual pyrite crystals were separated from the matrix, and the entire crystal or portions thereof were used for Re-Os analysis. Inspection by scanning electron microscope revealed rare, micron-scale inclusions of sphalerite, chalcopyrite, and quartz within pyrite crystals. Though impossible to separate, these inclusions were unlikely to have any effect on the determined Re-Os isotopic compositions of the pyrite, since both sphalerite and chalcopyrite were determined to have significantly lower Re and Os contents than pyrite.

5.4. Results

Results of all Re-Os analyses performed in this study are given in Table 5.1. The Re concentrations for sulfides from the Flin Flon belt (Trout Lake pyrite, Konuto Lake chalcopyrite) are very low ($\sim 0.155 - 1.1$ ppb), but are sufficiently high to allow for precise measurement of Re and radiogenic Os ($^{187}\text{Os}^*$) isotopic compositions. Pyrite from the higher metamorphic grade Sherritt Gordon and Harmin deposits had marginally higher Re concentrations, ranging from $0.037 - 8.629$ ppb. In accord, $^{187}\text{Os}^*$ concentrations for the determined range of Re concentrations were between 0.2 and 45.1 ppt. Common Os contents for the measured sulfides ($^{192}\text{Os} = 0.01$ to 22.1 ppb) had a similar distribution to Re, in that the Flin Flon belt sulfides are generally characterized by lower common Os contents than the two higher grade deposits.

As discussed above, the first batch of analyzed samples from the Trout Lake deposit consisted of a mixture of pyrite and sphalerite, whereas the second batch contained only pyrite. Linear regression (Ludwig, 2000) of all twelve analyses from both batches yields a very inaccurate and imprecise Model 3 result of 1168 ± 470 Ma (MSWD = 673; Fig. 5.3). Using only the six analyses of pyrite + sphalerite from the first batch, an equally poor Model 3 result of 967 ± 860 Ma (MSWD = 657) is determined. However, the second batch of analyses of only pure pyrite yields a much improved, albeit somewhat imprecise, Model 1 result of 1892 ± 28 Ma ($\text{Os}_i = 0.32 \pm 0.10$, MSWD = 0.98; Fig. 5.3).

Analyses of chalcopyrite from the Konuto Lake deposit distinguish two distinct, highly variable groups of Re-Os compositions. These include (i) one group of radiogenic samples, characterized by $^{187}\text{Re}/^{188}\text{Os}$ ratios of $\geq \sim 5000$ (samples 942-1b and -8), and

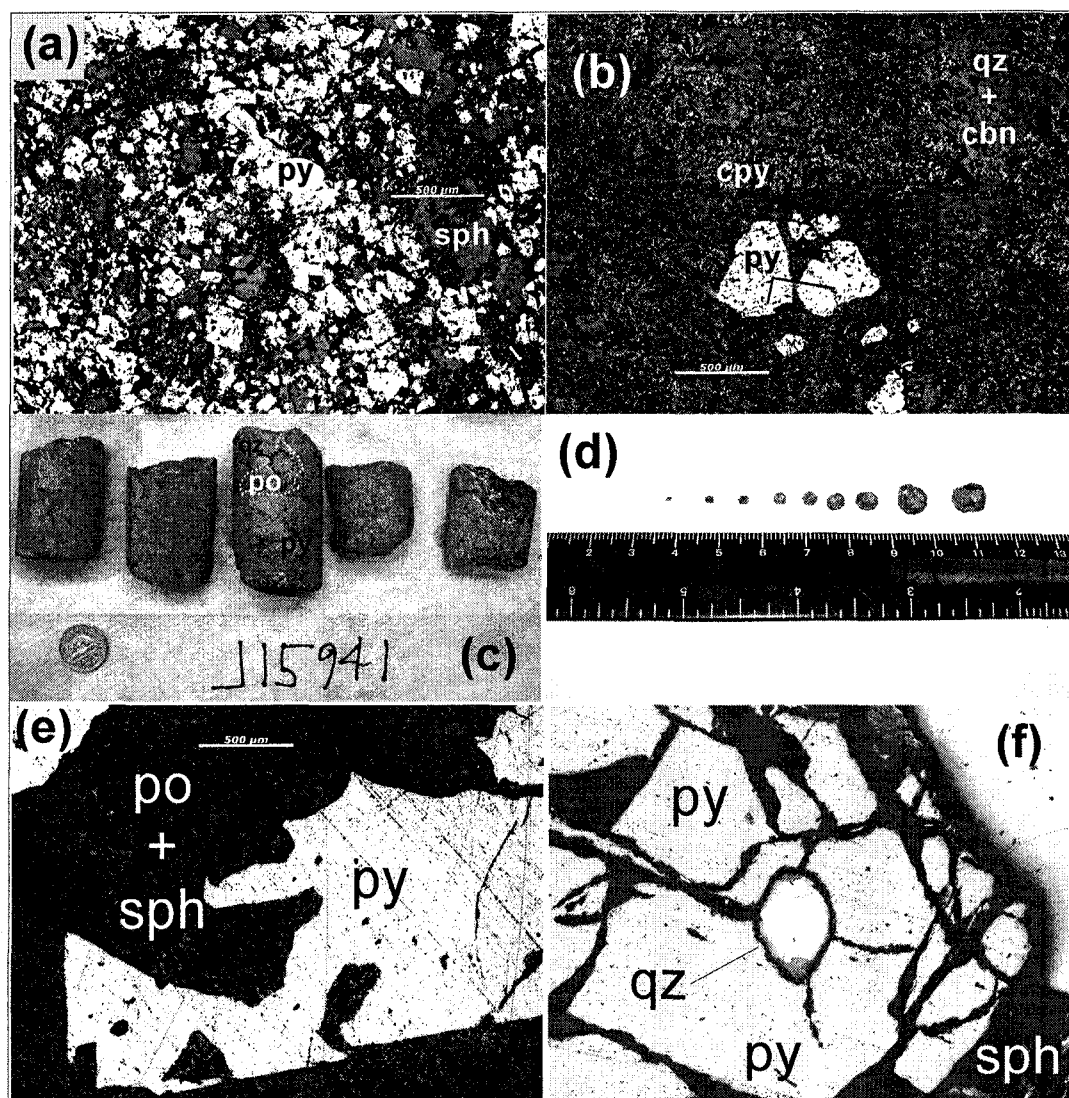


Figure 5.2: Sample photos of sulfides used for Re-Os analysis in this study; (a) photomicrograph of Trout Lake ore, (b) photomicrograph of Konuto Lake ore, (c) pyrite-rich drill core from the Harmin deposit, (d) individual pyrite crystals from the Sherritt Gordon deposit, (e) photomicrograph of Harmin sulfides, and (f) photomicrograph of Sherritt Gordon sulfides, showing pyrite cataclasis. Mineral abbreviations: py = pyrite, sph = sphalerite, po = pyrrhotite, qz = quartz, cbn = carbonate.

Table 5.1: Re-Os isotopic data for VMS-hosted sulfides in the northern Trans-Hudson Orogen.

	mineral	$^{187}\text{Re}/^{188}\text{Os}$	$\pm 2\sigma^2$	$^{187}\text{Os}/^{188}\text{Os}$	$\pm 2\sigma^2$	ρ	Re (ppb)	$^{187}\text{Os}^*$ (ppt)	^{192}Os (ppt)	
Trout Lake (J15943)										
	943-A(a)	py, sph, po	144.1	5.9	4.94	0.18	0.851	0.16	3.1	2.14
	943-B(a)	py, sph, po	121.8	2.7	4.31	0.09	0.785	0.26	5.4	4.26
	943-C(a)	py, sph, po	255.4	3.0	7.68	0.09	0.851	0.95	17.2	7.40
	943-D(a)	py, sph, po	291.8	4.0	8.69	0.15	0.736	1.13	20.4	7.71
	943-E(a)	py, sph, po	275.8	4.8	9.16	0.21	0.722	0.86	17.4	6.22
	943-F(a)	py, sph, po	412.9	7.0	8.41	0.15	0.887	1.05	1052	5.07
	943-A2(b)	py	128.4	3.6	4.40	0.12	0.775	0.22	219	3.39
	943-B2(b)	py	108.6	3.1	3.80	0.09	0.730	0.19	3.9	3.51
	943-Cb(b)	py	222.5	5.5	7.57	0.28	0.634	0.77	773	6.91
	943-Db(b)	py	269.0	3.3	8.91	0.12	0.816	1.03	1030	7.62
	943-F2(b)	py	244.9	4.6	8.15	0.15	0.889	0.53	529	4.30
	943-F3(b)	py	230.0	4.2	7.73	0.15	0.834	0.56	563	4.87
Konuto (J15942)										
	942-1b	cpy	4660	830	147	26	0.995	0.76	15.0	0.32
	942-2	cpy (+sph?)	695	26	23	0.86	0.980	0.81	15.8	2.32
	942-4	cpy (+sph?)	806	28	26	0.93	0.971	0.71	13.9	1.76
	942-5	cpy (+sph?)	664	13	22	0.46	0.923	1.09	21.7	3.27
	942-6	cpy (+sph?)	552	10	19	0.37	0.876	1.00	19.5	3.61
	942-1,6	cpy (+sph?)	496.5	8.9	17	0.32	0.905	0.95	18.4	3.81
	942-6b	cpy (+sph?)	523	11	18	0.40	0.739	0.97	19.0	3.69
	942-7	cpy (+sph?)	138.9	8.3	6	0.32	0.850	0.09	1.8	1.22
	942-8	cpy	19900	1600	635	48	0.937	0.10	2.0	0.01
	942-9	cpy (+sph?)	125.1	6.4	5	0.23	0.826	0.09	1.7	1.39
Harmin (J15941)										
	945-1	py	62.06	0.68	2.75	0.03	0.521	0.5	7.5	14.5
	945-1b	py	54.1	5.8	2.66	0.16	0.548	0.04	0.7	1.4
	945-2	py	526.0	5.1	16.45	0.19	0.770	2.8	52.0	10.7
	945-2b	py	1254	68	37.8	2.1	0.985	0.9	17.2	1.5
	945-3	py	137.0	1.1	5.46	0.05	0.638	1.0	20.2	14.7
	945-3b	py	130.8	9.8	4.98	0.32	0.841	0.09	1.6	1.3
	945-4	py	778.2	5.0	21.10	0.18	0.643	8.6	139	22.1
Sherritt Gordon (M19674)										
	Sh-CG-1	py	233.4	1.1	7.808	0.044	0.549	3.81	75.3	32.5
	Sh-CG-3	py	135.57	0.81	4.746	0.043	0.535	2.13	42.3	31.3
	Sh-CG-4	py	186.24	0.89	6.338	0.038	0.568	2.66	52.6	28.4
	Sh-CG-5	py	218.91	0.72	7.343	0.019	0.495	4.08	80.5	37.0
	Sh-CG-6	py	149.2	1.7	5.174	0.094	0.583	2.33	46.1	31.0
	Sh-CG-7	py	168.6	1.0	5.755	0.046	0.628	2.84	56.0	33.5
	Sh-CG-8	py	94.86	0.47	3.450	0.016	0.648	1.66	32.8	34.8
	Sh-CG-9	py	136.2	1.1	4.739	0.051	0.649	1.96	75.3	28.7
	Sh-CG-10	py	211.5	1.5	7.124	0.052	0.782	2.34	46.3	31.0
	Sh-CG-11	py	169.32	0.83	5.762	0.027	0.707	2.87	56.5	33.8
	Sh-CG-12	py	147.62	0.87	5.095	0.031	0.730	2.02	39.9	27.3

¹arsenopyrite samples for Re-Os analyses ranged from 0.391 to 0.415 grams.

Re blank is 1.6 ± 0.3 pg and Os blank is 0.37 ± 0.05 pg (1 SD; n=4), blank $^{187}\text{Os}/^{188}\text{Os} = 0.21 \pm 0.07$ (1 SD; n=4);

Re-Os data for all samples were corrected using these values.

(ii) one group of relatively unradiogenic samples, with compositions similar to Trout Lake pyrite ($^{187}\text{Re}/^{188}\text{Os}$ ratios ≤ 800 ; remaining 6 samples). It is unclear what is controlling this variation, though it is noteworthy that the two radiogenic samples contain the lowest common Os (^{192}Os) content of all samples (Table 5.1). When regressed together, all samples of the two groupings combined yield a Model 3 result of 1846 ± 27 Ma ($\text{Os}_i = 1.38 \pm 0.30$, MSWD = 5.0; not shown). However, if analyses of the two compositional groups are regressed separately, two distinct ages are apparent. Whereas the eight 'unradiogenic' samples yield an age of 1824 ± 42 Ma ($\text{Os}_i = 1.56 \pm 0.40$, MSWD = 5.8; Fig. 5.4a), the two radiogenic samples yield a result (albeit derived from only two points) of 1892 ± 68 Ma (Fig. 4b), identical to that of Trout Lake pyrite.

Seven analyses were performed on pyrite from the Harmin deposit (Table 5.1), which exhibited significant variability in Re-Os isotopic composition ($^{187}\text{Re}/^{188}\text{Os}$ ratios $\approx 54 - 1250$). Regression of all seven analyses generates a highly imprecise result of 1682 ± 150 Ma ($\text{Os}_i = 1.1 \pm 1.5$, MSWD = 305; Fig. 5.5). It is noteworthy, however, that four of the seven points yield a precise Model 1 age of 1729 ± 16 Ma ($\text{Os}_i = 1.1 \pm 0.12$, MSWD = 0.37; Fig. 5.5).

Pyrite from the Sherritt Gordon deposit is characterized by quite restricted, unradiogenic Re-Os isotopic compositions (Table 5.1; $^{187}\text{Re}/^{188}\text{Os}$ ratios $\approx 95 - 233$) due to the small variations in observed Re and common Os (^{192}Os) contents (Table 5.1). Notwithstanding this small variation, the Sherritt Gordon pyrite had the highest overall Re and common Os (^{192}Os) concentrations of all sulfides measured in this study. Regression of all twelve analyses of Sherritt Gordon pyrite yield a well constrained, precise Model 1 age of 1855.9 ± 9.1 Ma ($\text{Os}_i = 0.47 \pm 0.02$, MSWD = 1.2; Fig. 5.6).

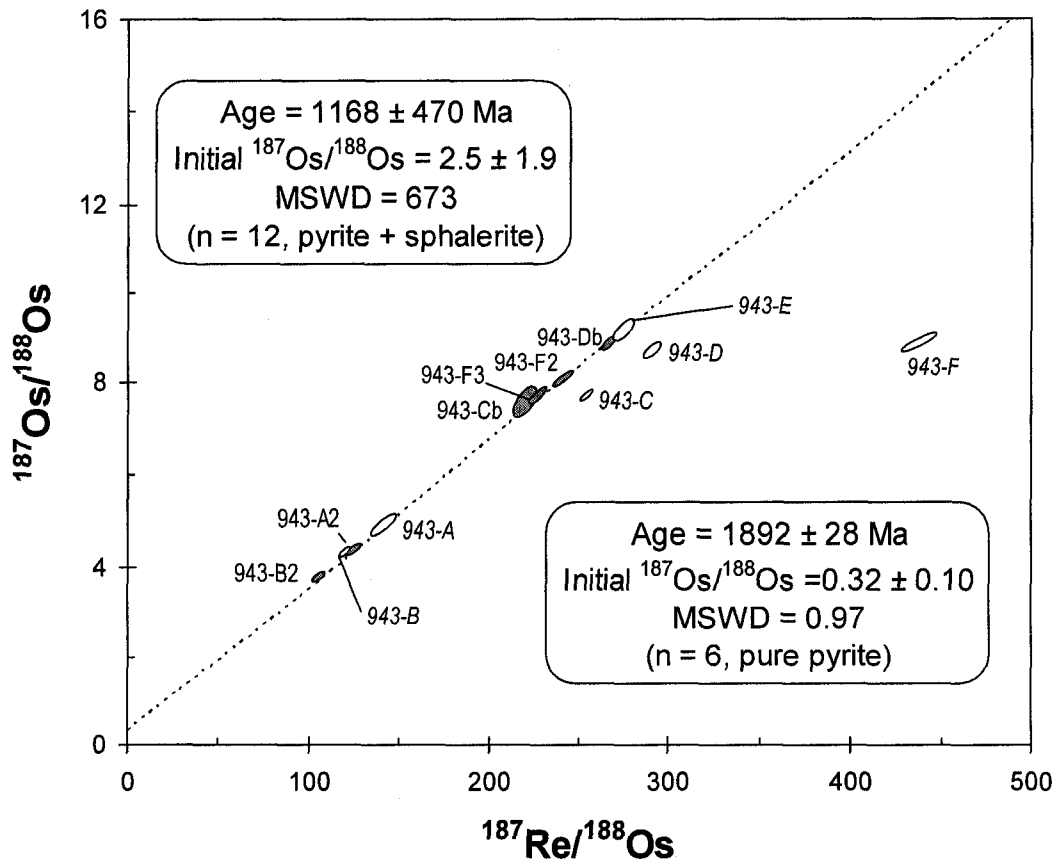


Figure 5.3: Regression of Re-Os isotopic data from Trout Lake sulfides. Upper left result derives from all analyses, including those of both pure pyrite (filled circles) and pyrite + sphalerite (open circles, italicized labels), whereas lower right result derives from analyses of pure pyrite only.

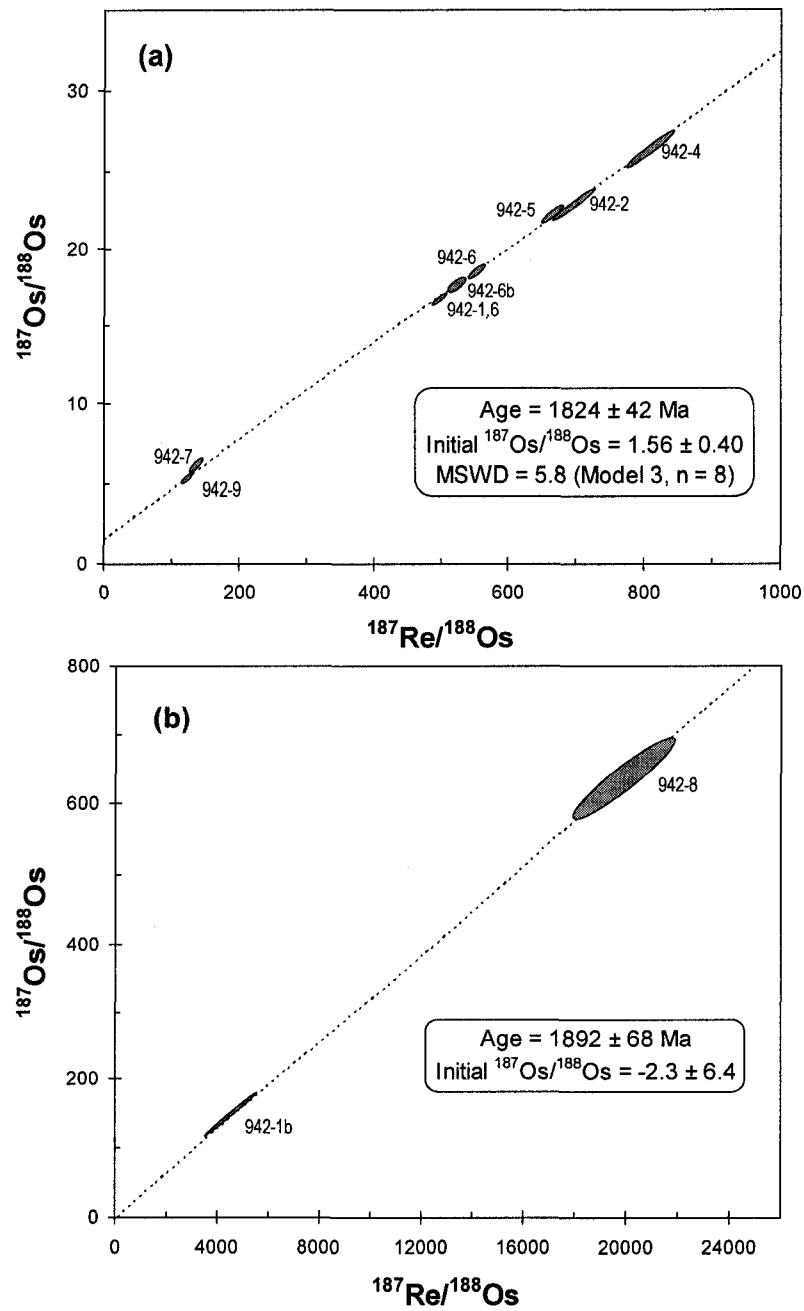


Figure 5.4: Results of linear regression of Re-Os isotopic analyses of Konuto Lake chalcopyrite. Result in (a) is from regression of all 'unradiogenic' chalcopyrite analyses, whereas the result in (b) is from two more distinctly radiogenic chalcopyrite analyses. Regression of all ten analyses combined yields a result of 1846 ± 27 Ma ($\text{Os}_i = 1.38 \pm 0.30$, MSWD = 5.0).

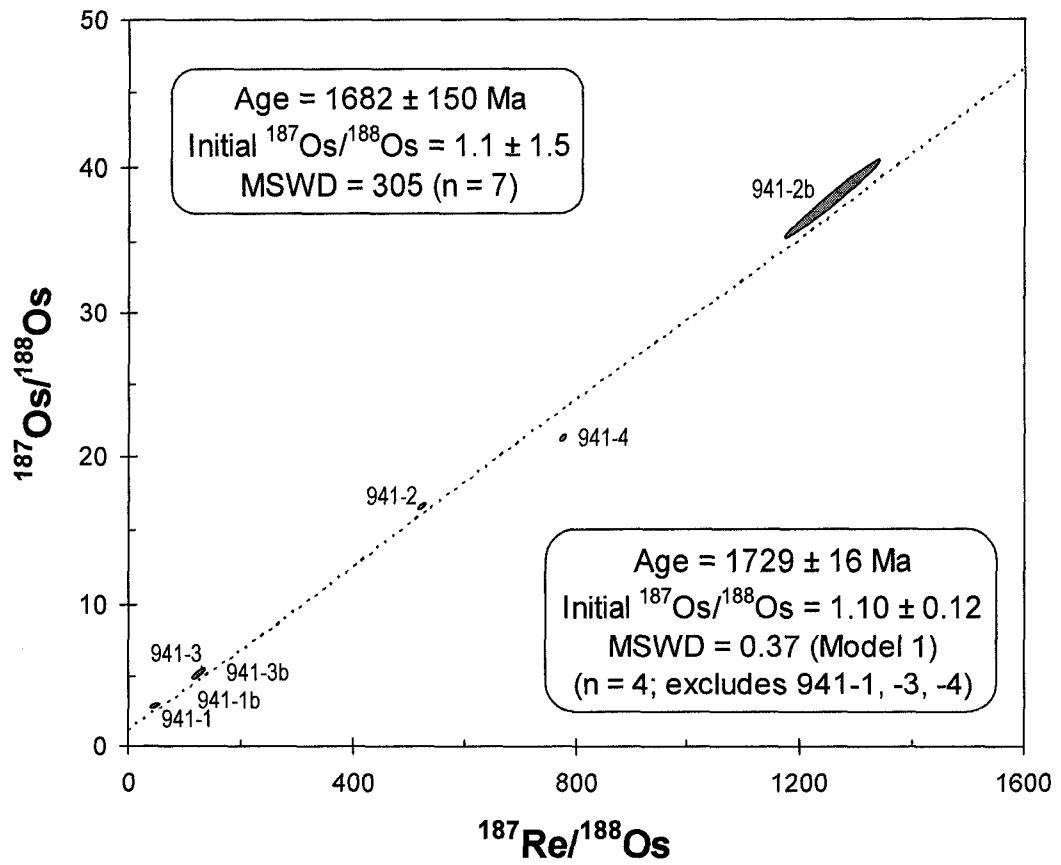


Figure 5.5: Linear regression of Re-Os isotopic analyses of pyrite from the Harmin deposit. Analyses 941-1b, -2, -2b, and -3b yield the 1729 ± 16 Ma result.

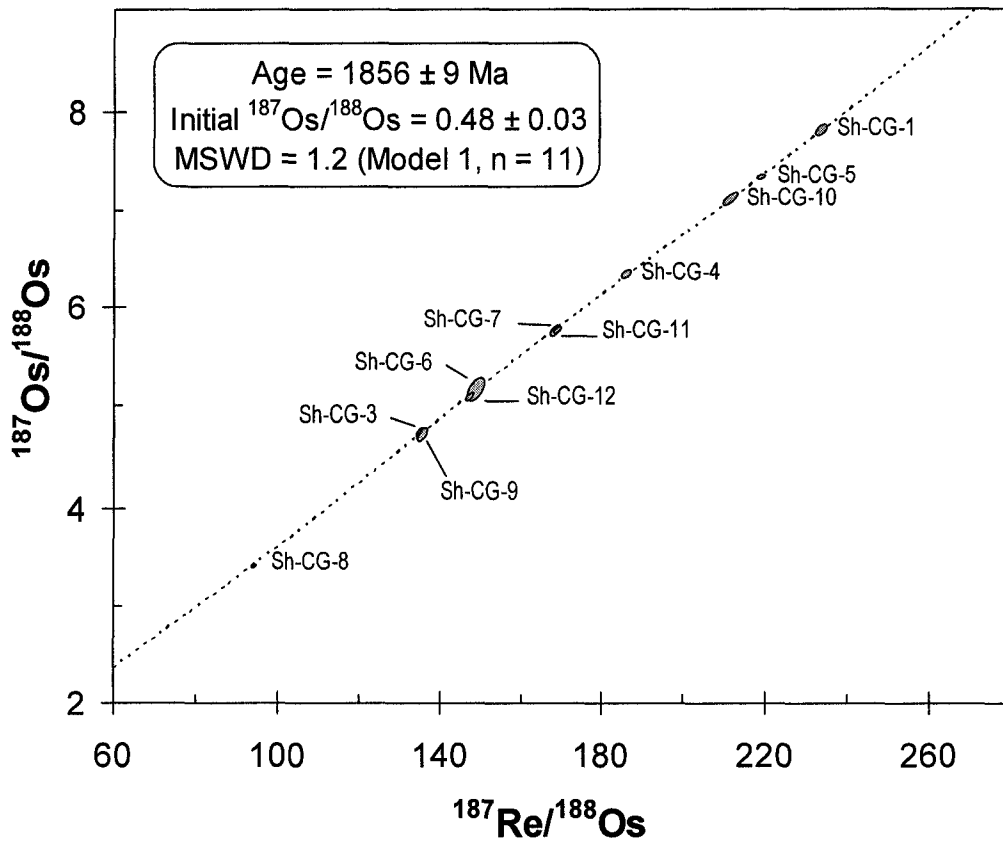


Figure 5.6: Re-Os isochron from analyses of the Sherritt Gordon deposit, Kisseynew Domain.

5.5. Discussion

Implications of Re-Os results

i. Trout Lake deposit

The Re-Os results from the Trout Lake sulfide minerals help to understand the susceptibility of different sulfide mineral chronometers to disturbance by thermal effects, and also demonstrate the need for obtaining pure sulfide mineral separates for Re-Os analysis. The true age of the Trout Lake sulfide deposit is not known, but can be approximated from existing age data for the deposit and other deposits nearby in the Flin Flon assemblage. The only reported age for rocks at the Trout Lake deposit is on the rhyolitic unit that hosts the deposit, determined to have erupted at 1869 Ma (Syme et al., 2001). This age, based on U-Pb zircon analysis by thermal ionization mass spectrometry (C. Böhm, pers. comm.), is interpreted to indicate that the Trout Lake deposit formed during post-accretion (post-D₁) magmatism. By implication, this interpretation makes the Trout unique amongst VMS deposits in the Flin Flon Domain, which are collectively believed to have formed during rifting of juvenile arc assemblages prior to the ca. 1.88 Ga arc accretion event (Syme et al., 1999). By comparison, existing dates for formation of other VMS deposits in the belt range from ca. 1903 Ma (e.g. Flin Flon - Callinan - Triple 7 deposits) to 1881 Ma (Syme et al., 1999, and references therein). Although the Trout Lake Re-Os age from pure pyrite (1892 ± 28 Ma) does allow for a younger mineralization age within uncertainty, it points more directly towards an older (pre-1.88 Ga) crystallization age that implies a belt-wide VMS mineralization episode from ca. 1.90 to 1.88 Ga. In any case, it is clear that the Trout Lake pyrite has preserved a primary mineralization age, thus confirming the robustness of this mineral through subsequent (1.82 Ga) middle greenschist facies peak metamorphic conditions. The minimum apparent closure temperature of the Re-Os pyrite chronometer for the assemblage pyrite + sphalerite + pyrrhotite is thus established to exceed $\sim 450^\circ\text{C}$.

In contrast to pure pyrite, the sample mixture of pyrite and sphalerite (\pm pyrrhotite) from Trout Lake yielded a highly scattered result, likely with a geologically meaningless 'age' (1168 ± 470 Ma). Because pyrite in isolation has been shown to retain primary Re-Os age information, this disparity can be attributed solely to the presence of sphalerite in the sample. The apparent closure temperature of the Re-Os sphalerite

chronometer, when associated with pyrite (\pm pyrrhotite), is consequently determined to be $< 450^{\circ}\text{C}$. This conclusion is in general agreement with the findings of Morelli et al. (2004), who determined that the Re-Os isotope systematics of sphalerite (in grain contact with pyrite) at the Red Dog Zn-Pb deposit in Alaska had been disturbed at temperatures as low as $\sim 200^{\circ}\text{C}$. The inability of sphalerite to retain primary Re-Os isotopic compositions is perhaps surprising when the highly refractory nature of this mineral is considered. However, it is also noteworthy that changes in FeS of sphalerite can cause this mineral to re-equilibrate at low temperatures (Vaughn and Craig, 1997), a phenomenon that diminishes its usefulness as a reliable geobarometer (Lusk et al., 1993). The Trout Lake Re-Os pyrite data require that the occurrence of any post-crystallization sphalerite disequilibrium had a negligible effect on the original pyrite chemical composition.

ii. Konuto Lake deposit

The most intriguing aspect of chalcopyrite from the Konuto deposit is its highly variable Re-Os isotopic compositions, ranging from moderately unradiogenic to highly radiogenic, and the small apparent Re-Os age variation between the two compositional groups. The first group of samples, with $^{187}\text{Re}/^{188}\text{Os}$ ratios of ~ 800 or less, yields a Re-Os age (1824 ± 42 Ma) that overlaps peak regional metamorphism in the THO. This, in addition to the slight scatter of these data (MSWD = 5.8), indicate that the Re-Os chalcopyrite chronometer was disturbed (and nearly completely reset) during (ca. 500°C) upper greenschist facies regional metamorphism of the Birch Lake Assemblage at ca. 1.82 – 1.81 Ga. This conclusion is supported by the highly radiogenic Os_i of 1.56 for these chalcopyrite (compared to an Os_i of 0.32 for the Trout Lake pyrite), indicating that the Os incorporated into the chalcopyrite at 1824 Ma had already resided in a crustal environment for an extended period of time. However, a disturbed Re-Os isotopic composition seems to be at odds with the results from the two more radiogenic chalcopyrite samples. If the Trout Lake pyrite Os_i of 0.32 is assumed for primary chalcopyrite mineralization at Konuto Lake, single mineral model ages of ca. 1860 ± 25 Ma (942-1b) and 1881 ± 50 Ma (942-8) can be calculated for these samples (see Stein et al., 2000; Morelli et al., 2005). Furthermore, regression of these two samples yields a 2-

point result of 1892 ± 68 Ma. These results point to the retention of an older, perhaps primary Re-Os age recorded in some chalcopyrite samples. This apparent age is broadly consistent with existing age constraints for the timing of VMS mineralization in the Flin Flon domain, including the Trout Lake Re-Os result.

These results might indicate either (i) variable disturbance of the Re-Os system of spatially proximal chalcopyrite samples, or (ii) variable proportions of chalcopyrite ‘contamination’ by other sulfide minerals, likely either sphalerite or pyrrhotite. The latter scenario is plausible, since sphalerite separation occurred at only a slightly lower setting ($\sim 0.3 - 0.5$ A) than for extraction of chalcopyrite (> 0.5 A). Still, this possibility seems unlikely because there was no obvious difference in relative sphalerite or pyrrhotite proportions in the initial sample fractions, and because all samples were subsequently prepared for Re-Os analysis in an identical manner. Variable (incomplete) resetting of the Re-Os system in chalcopyrite crystals originally situated < 5 cm apart is also difficult to envisage, but is possible at temperatures that overlap the “closure temperature” because of chalcopyrite grain size variations. Although further work is clearly required, the Konuto Lake data chalcopyrite data is sufficient to warrant caution in interpreting other Re-Os chalcopyrite results when the ore has been subjected to, at least, lower amphibolite facies metamorphism.

iii. Harmin deposit

Currently, no constraints exist on the primary age for mineralization at the Harmin deposit. As a minimum constraint, it can be assumed that sulfide mineralization occurred prior to the ca. 1.82 – 1.81 Ga peak metamorphic event, since the ore itself has been metamorphosed to upper amphibolite – lower granulite facies (Polito et al., 2007). The Re-Os pyrite result from Harmin therefore likely reveals isotopically reset pyrite compositions, as the 1682 ± 150 Ma Re-Os “age” postdates this metamorphism. As discussed for the Konuto Lake sulfides, the radiogenic Harmin pyrite Os_i (~ 1.1) also argues for disturbance of primary Re-Os compositions. Further, if the Model 1 age derived from 4 of the 6 pyrite analyses (1729 ± 16 Ma) is considered, one possible interpretation is that the ambient crustal temperature decreased through the Re-Os pyrite chronometer closure temperature at this time. This timing is similar to that (1.74 – 1.72

Ga) determined from total-Pb monazite age domains and overall apparent $^{40}\text{Ar}/^{39}\text{Ar}$ muscovite and biotite plateau ages (Schneider et al., 2007) determined for rocks from every lithotectonic domain of the THO west of the Tabbemor/Sturgen-Weir (TSW) strike-slip fault system (Fig. 5.1). The same general age distribution was not observed in the THO east of the TSW, which is overall characterized by slightly older apparent $^{40}\text{Ar}/^{39}\text{Ar}$ mica ages (> 1775 Ma), though individual apparent ages for multiple eastern locations do fall into this 1.74 – 1.72 Ga age bracket (Schneider et al., 2007). This general age distribution was interpreted by the authors to reflect temporally distinct periods of craton stabilization ('cratonization') for individual blocks east and west of the TSW, respectively. The Re-Os pyrite result presented here for the Harmin VMS deposit (ca. 1729 Ma), located east of the TSW, might indicate rapid cooling through moderate to high ($> 700^\circ\text{C}$?) crustal temperatures at this time, therefore providing evidence against tectonically discrete crustal blocks on either side of the TSW.

iv. Sherritt Gordon deposit

The origin of the Sherritt Gordon deposit is poorly understood, due primarily to its spatial separation from other VMS deposits in the THO and to the masking of primary geologic features in the host rocks by the effects of upper amphibolite facies prograde metamorphism. The host rocks, which comprise Sherridon Group felsic gneisses interleaved with amphibolitic rocks, were originally thought to be metamorphosed sedimentary rocks of the Burntwood or Missi suites. However, on geochemical grounds, Ashton et al., (1996) concluded that these felsic gneisses were actually metamorphosed felsic igneous rocks, and proposed that they were correlative with volcanic rocks of the Amisk Group.

The Re-Os age of 1855.9 ± 9.1 Ma determined here for Sherritt Gordon pyrite is at odds with this interpretation, as it is significantly younger than the ca. 1.92 – 1.88 Ga timeframe for Amisk Group magmatism in the Flin Flon belt. Assuming that the host rocks do have an igneous protolith, the Re-Os age can be interpreted in three ways: the ca. 1856 Ma age might represent the original pyrite crystallization (and hence, VMS mineralization) age, or could otherwise reflect either a partial or complete resetting of the primary crystallization age. A complete resetting at 1856 Ma is unlikely, considering that

Kisseynew basin subsidence and Burntwood Group sedimentation was ongoing at this time, and because the earliest metamorphic event known to affect these rocks did not occur until ca. 1830 Ma (Ansdell and Norman, 1995; Fig. 5.7). Furthermore, even if primary Re-Os compositions were reset at ca. 1856 Ma, they would almost certainly have been reset again during peak metamorphism ca. 1.82 – 1.81 Ga, which is not observed. Although partial resetting of Re-Os isotopic compositions of Sherritt Gordon pyrite is, perhaps, a more plausible scenario than complete resetting, it is also considered unlikely. In this scenario, a later metamorphic event, likely the ca. 1.82 – 1.81 Ga peak event, would have ubiquitously adjusted primary Amisk-age (1.92 – 1.88 Ga) Re-Os isotopic compositions of the Sherritt Gordon pyrite to the determined 1856 Ma ‘age’, which would have no actual geologic significance. This interpretation poses major difficulties, however, specifically related to characteristics of the sampled pyrite, the Re-Os isotopic compositions of the pyrite, and the excellent fit of all eleven data to the regression line (MSWD = 1.2; Fig. 5.6). The pyrite samples analyzed to obtain this result consisted of both mixed fragments of, and entire crystals of individual pyrite crystals that ranged in diameter from < 2 mm to > 1cm (Fig. 5.2d). If partial resetting had occurred, the effect on individual pyrite crystals would be expected to vary depending on crystal size, which is not observed. Using this reasoning, and in the absence of other reasonable explanations, the 1855.9 ± 9.1 Ma Re-Os age determined here is considered to represent the primary age of pyrite and VMS mineralization at the Sherritt Gordon deposit.

A significant consequence of this interpretation is the occurrence of a younger VMS mineralization event in the THO that is associated with post-arc accretion extensional magmatism during the development of the Kisseynew basin.

A new model for generation of the Sherritt Gordon deposit is proposed whereby the VMS-style mineralization was cogenetic with rift-related magmatism associated with opening of the Kisseynew basin. With reference to existing age constraints for geologic events in the Kisseynew Domain (Fig. 5.7), this model fits well into the tectonic framework of the internal THO. Commencement of deposition of Burntwood Group turbiditic rocks at ca. 1860 Ma reasonably approximates the earliest extensional phase of backarc (interarc?) Kisseynew basin development, which also overlaps with determined ages of interleaved orthogneisses in the domain, some of which derive from a volcanic

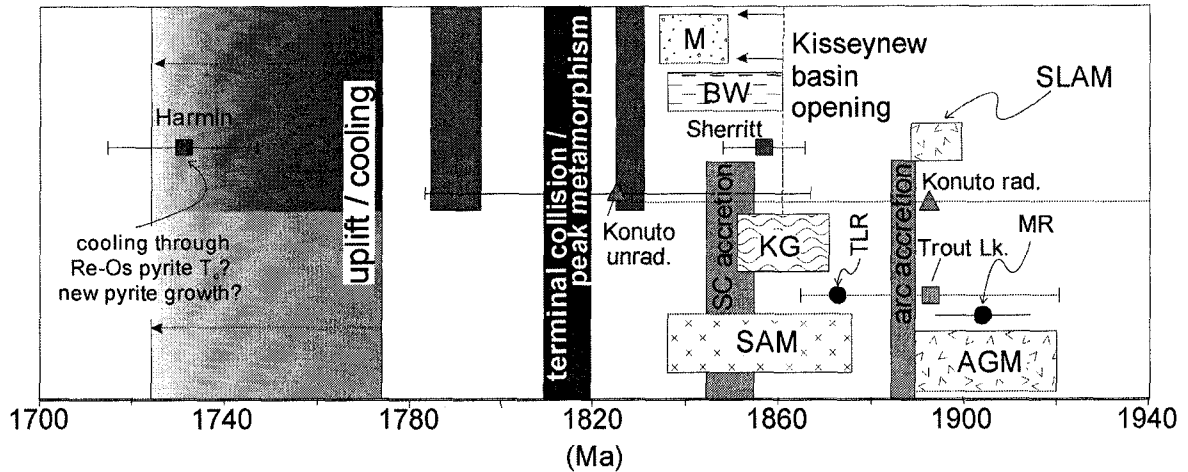


Figure 5.7: Synthesis of Re-Os sulfide geochronology for VMS mineralization at the Trout Lake (T), Konuto Lake (K), Harmin (H), and Sherritt Gordon (S) deposits, with reference to existing geochronology in the Flin Flon and Kiseynew Domains. See text for discussion. Results are shown for both compositional groups (K1, K2) at Konuto Lake. AGM = Amisk Group magmatism, MR = Mine Rhyolite U-Pb zircon age, SAM = successor arc magmatism, TLR = Trout Lake Rhyolite U-Pb zircon age, SLAM = Snow Lake arc magmatism, KG = Kiseynew orthogneisses, BW = Burntwood Group turbidites, M = Missi Group. Vertical grey bars show thermal/metamorphic events in the Flin Flon (bottom) and Kiseynew (top) domains. Geochronological data from Syme et al. (1998), Stern et al. (1999), Syme et al. (2001), and Ansdell (2005b), and Schneider et al. (2007).

protolith (Ansdell and Norman, 1995; Zwanzig and Schledewitz, 1992). Evidence for ca. 1860 Ma volcanism in the eastern Reindeer Zone is also provided by a handful of U-Pb zircon ages, including 1858 Ma dates from both a shoshonite and a rhyolite located near Schist Lake (~ 10 km south of Flin Flon; Stern et al., 1999) and an 1856 Ma date from a rhyolite at Wekusko Lake, in the Snow Lake assemblage (Ansdell et al., 1999). In the Kisseynew Domain itself, David et al. (1996) report ages in the range 1874 – 1859 Ma for Burntwood suite detrital zircons which they interpret to originate, at least in part, from successor arc volcanic rocks based on the presence of felsic volcanic rock fragments in Burntwood suite turbidites. Collectively, these data indicate the presence of arc-related volcanism in the eastern Reindeer Zone at the time of Sherritt Gordon VMS deposition. It is suggested, therefore, that the felsic gneisses and amphibolites associated with the Sherritt Gordon deposit are tectonic slivers of ca. 1860 – 1855 Ma volcanic rocks that were erupted during or just prior to the onset of extension that resulted in the opening of the Kisseynew basin. This scenario is somewhat analogous to the interpreted genesis of the Flin Flon belt VMS deposits in an intra-arc extensional environment (Syme et al., 1999).

Pyrite stability – inferences from Re-Os pyrite geochronology

In addition to being the most abundant sulfide mineral in the Earth's crust, pyrite is considered to be one of the most refractory of all sulfide minerals (Barton, 1970). Kullerud and Yoder (1959) determined its upper thermal stability at atmospheric pressures to be 742°C, increasing ~ 14°C /kbar of confining pressure. Nevertheless, Craig and Vokes (1993) emphasize that, notwithstanding its substantial hardness and its highly refractory nature, pyrite will typically begin to dynamically recrystallize when subjected to greenschist grade or higher metamorphic temperatures. General morphological consequences of this recrystallization is the development of annealed textures in metamorphosed pyrite, an increase in grain size, and development of ~120° dihedral angles (Ixer, 1990; Craig et al., 1998). However, the occurrence and/or extent of recrystallization can depend strongly on which, if any, sulfide minerals are spatially associated with the pyrite, pyrrhotite being an important phase in this regard.

Pyrite samples from three of the deposits investigated in this study have been metamorphosed to greenschist facies (Trout Lake) or above (Sherritt Gordon - upper amphibolite; Harmin – upper amphibolite to lower granulite). The preservation or disturbance of primary Re-Os data in these samples can thus provide important information on the stability of the Re-Os system in pyrite at increasing metamorphic grades.

Pyrite from Trout Lake ore comprises fine-grained ($\leq 100 \mu\text{m}$) crystals interspersed within equigranular sphalerite and pyrrhotite (Fig. 5.2a). This pyrite, metamorphosed to lower greenschist facies conditions, shows no obvious sign of recrystallization or annealing, consistent with preservation of the primary 1892 Ma Re-Os age.

The morphological characteristics of Sherritt Gordon pyrite, which has been metamorphosed to upper amphibolite facies conditions (660°C, 5 kbar; Froese and Goetz, 1980), are consistent with possible recrystallization textures, due to its relatively coarser grain size (up to 1 cm) and the presence of some dihedral angles that approximate 120°. However, petrographic inspection of the Sherritt Gordon samples reveals extensive internal fracturing (cataclasis) of pyrite crystals (Fig. 5.2f). If an effect of deformation during prograde metamorphism, this might suggest that the highest metamorphic temperature attained was insufficient to cause ductile deformation and full recrystallization. Primary Re-Os age information in the pyrite might not survive any recrystallization effects, as any new grain growth at the expense of preexisting pyrite would likely result in resetting of the Re-Os chronometer and homogenization of Os_i to more radiogenic values. The Sherritt Gordon pyrite Os_i (0.47) is distinctly less radiogenic than that of Harmin pyrite (~ 1.1) and Konuto Lake chalcopyrite (~ 1.5), both of which are interpreted to reflect reset Os isotopic compositions, and is more consistent with that determined for primary VMS mineralization elsewhere (Trout Lake = 0.32, this study; Iberian Pyrite Belt deposits: Tharsis = 0.38, Mathur et al., 1999; Neves-Corvo = 0.49, Munhá et al., 2005).

Pyrite from the Harmin deposit has clearly been affected, in terms of its Re-Os isotopic chronometer, by upper amphibolite – lower granulite facies peak metamorphic temperatures. Morphologically, this pyrite forms coarse irregular masses lacking any

regular crystal form. Although rare, well defined dihedral angles ranging from $\sim 40^\circ$, 65° , and 90° are evident in thin section (Fig. 5.2e). Brittle deformation features in Harmin pyrite are uncommon. The coarse nature of and lack of brittle structures in the pyrite, combined with its post-peak metamorphic Re-Os age, strongly suggest that the Harmin pyrite underwent dynamic recrystallization in response to the elevated temperature regime. The abundance of pyrrhotite in the Harmin ore probably also has significance in the determined pyrite Re-Os age, since the occurrence of sulfur exchange between pyrite and pyrrhotite can have a drastic influence on the proportion of each mineral in the metamorphosed ore (Vaughan and Craig, 1997). This phenomenon presents an intriguing alternative to dynamic recrystallization of pyrite during prograde metamorphism that may more readily explain the determined 1729 Ma Re-Os age. It is possible that the Harmin pyrite actually grew at the expense of pyrrhotite upon slow cooling of the latter following peak metamorphism, in which case the Re-Os age actually dates the crystallization of this pyrite, rather than a “cooling age” of previously formed pyrite. While further work is clearly required to distinguish the history of these pyrite occurrences and the effects by heat and pressure, it is clear that Re-Os dates and Os_i ratios are valuable tracers of the origin of sulphide minerals in VMS ores.

Metal sources to VMS deposits in the THO from primary sulfide Os_i

An important development from this study is the determination of two new Os_i values for primary Paleoproterozoic sulphide mineralization; 0.32 ± 0.10 for Trout Lake pyrite and 0.47 ± 0.02 for Sherritt Gordon pyrite. This information can be used to directly interpret metal sources to the ore system (e.g. Mathur et al., 2000; Levrresse et al., 2004; Chapter 4, this study) or, alternatively, can characterize the Os isotopic composition of a known metal source. As a deposit class, the metal and fluid source of VMS deposits is well understood. In brief, VMS mineralization is hypothesized to accumulate from circulation of heated seawater through subseafloor magmatic rocks, from which the metals are leached, followed by discharge of the metal-rich hydrothermal fluid through near-axis fractures and fault zones and back into the ocean (Franklin et al., 2005). To a lesser extent, metals and fluids may also be contributed during devolatilization of the subvolcanic intrusion(s) responsible for the heating and circulation of seawater (Yang

and Scott, 2003; Hannington et al., 2005). Osmium in the VMS mineralizing system can therefore originate from one (or more) of three sources: (i) seawater, (ii) sub-seafloor igneous rocks, or, less significantly, (iii) subvolcanic magmas.

Although there has been no geochemical characterization of the Sherritt Gordon host rocks to date, the majority of arc magmatism in the Flin Flon belt was of juvenile character, with ϵNd values ranging from +2 to +5. Although Archean rocks are known to exist within Amisk collage island arcs (David and Syme, 1994), the overall proportion of evolved crust is thought to be quite low. However, the Os_i range of 0.32 – 0.47 for pyrite from the VMS deposits indicate the input of some evolved crustal material into the ore system, and argues against osmium derivation either solely from the sub-seafloor strata or from the subvolcanic intrusion, both of which would be expected to carry Os_i values similar to that of contemporaneous upper mantle (~ 0.117 ; Meisel et al., 2001). The new Os isotopic data might then point to a genetic link between the presence of evolved crust and the generation of VMS mineralization in the THO, though supporting evidence is currently lacking.

Another possible explanation for the moderately radiogenic Os isotopic signatures is that they were inherited from seafloor sedimentary rocks during fluid leaching, or else directly from seawater that was transported through, and leached metals from, the oceanic rocks. Both possibilities are difficult to assess given the lack of Os isotopic data from sedimentary rocks (shales) or seawater at ca. 1900 Ma. It is noteworthy, however, that seawater Os inheritance is consistent with a proposed explanation for the moderately radiogenic Os isotopic compositions ($= 0.49 \pm 0.07$) of Devonian pyrite from the Neves-Corvo VMS deposit, Iberian Pyrite Belt (Munhá et al., 2005), which overlaps the determined Os_i for Late Devonian seawater ($= 0.59 \pm 0.05$; Creaser et al., 2002). On the other hand, the extremely low concentrations of Os in modern seawater (~ 55 fmol / kg; Sharma et al., 2000) does not support a substantial contribution of Os from seawater. More work needs to be done to determine the relative contributions of Os from seawater, seafloor sediments, and host igneous rocks into the VMS ore systems before the Os isotopic compositions of VMS-hosted sulfide minerals can be conclusively interpreted.

5.6. Conclusions

Metamorphosed VMS deposits represent an ideal opportunity to test the capabilities of various Re-Os sulfide chronometers to retain primary age information from ore mineralizing events. Through Re-Os isotopic analysis of sulfide samples from four spatially separated VMS deposits in the Flin Flon and Kisseynew Domains, Trans-Hudson Orogen, apparent closure temperatures of the Re-Os sphalerite, chalcopyrite, and pyrite chronometers have been constrained. Pure pyrite from the Trout Lake deposit yields a primary VMS mineralization age of 1892 ± 28 Ma, whereas pyrite mixed with sphalerite from this deposit yields a highly spurious result. These results indicate that Re-Os isotopic compositions of sphalerite are re-equilibrated by middle greenschist facies metamorphic conditions and that this mineral is generally unreliable as a Re-Os chronometer (see also Morelli et al., 2004). In contrast, pyrite remains a stable Re-Os chronometer to temperatures of at least 660°C (~ 5 kbar pressure), as revealed by retention of a primary crystallization age by pyrite from the upper amphibolite facies Sherritt Gordon deposit, Kisseynew Domain. A post-peak metamorphic age for pyrite from the upper amphibolite – lower granulite facies Harmin deposit indicates either that the Re-Os pyrite blocking temperature was surpassed during peak metamorphism and the ~ 1.74 Ga age reflects cooling, or that new pyrite crystallized during post-metamorphic cooling due to sulfur release during pyrrhotite degradation. In either case, these results suggest that pyrite is a very reliable Re-Os chronometer, with an apparent closure temperature broadly estimated at $\sim 700^{\circ}\text{C}$. Re-Os results for chalcopyrite from the Konuto Lake deposits are ambiguous, with apparent full resetting of some samples during metamorphism, but no clear disturbance to others in the same drill core. Although a clear interpretation for these results is elusive, the data are sufficient to necessitate caution when using Re-Os chalcopyrite geochronology to date primary ore events under conditions of lower amphibolite facies metamorphism.

The Trout Lake and Sherritt Gordon Re-Os pyrite results indicate the occurrence of at least two periods of VMS mineralization in the eastern THO. The first occurred during rifting of island arcs between ca. 1920 and 1880 Ma, whereas the other event was initiated during a rifting event that marked the opening of the Kisseynew basin ca. 1860 Ma. Initial Os isotopic compositions of these primary sulfides indicate the presence of

evolved Os in the ore systems, either due to input from older crustal rocks, from ocean floor sediments, or directly from seawater.

5.7. References

Ansdell, K.A., 2005b, Correlation chart of the evolution of the Trans-Hudson Orogen – Manitoba-Saskatchewan segment: *Canadian Journal of Earth Sciences*, v. 42, p. 761.

Ansdell, K.A., 2005a, Tectonic evolution of the Manitoba-Saskatchewan segment of the Paleoproterozoic Trans-Hudson Orogen, Canada: *Canadian Journal of Earth Sciences*, v. 42, p. 741-759.

Ansdell, K.M. and Norman, A.R., 1995, U-Pb geochronology and tectonic development of the southern flank of the Kisseynew Domain, Trans-Hudson Orogen, Canada: *Precambrian Research*, v. 72, p. 147-167.

Ansdell, K.M., Connors, K.A., Stern, R.A., and Lucas, S.B., 1999, Coeval sedimentation, magmatism, and fold-thrust development in the Trans-Hudson Orogen: geochronological evidence from the Wekusko Lake area, Manitoba, Canada: *Canadian Journal of Earth Sciences*, v. 293-312.

Ansdell, K.M., Lucas, S.B., Connors, K., and Stern, R.A., 1995, Kisseynew metasedimentary gneiss belt, Trans-Hudson orogen (Canada): Back-arc origin and collisional inversion: *Geology*, v. 23, p.1039-1043.

Ashton, K.E., Froese, E., and Legault, A., 1996, Recognition of felsic volcanic rocks and hydrothermal alteration in moderately to highly metamorphosed parts of the Flin Flon volcanic belt, *in*: Ashton, K.E. and Harper, C.T. [eds.], *MinExpo '96 Symposium – Advances in Saskatchewan Geology and Mineral Exploration*, Saskatchewan Geological Society Special Publication 14, p.27-43.

Bailes, A.H. and Galley, A.G., 1999, Evolution of the Paleoproterozoic Snow Lake arc assemblage and geodynamic setting for associated volcanic-hosted massive sulphide

deposits, Flin Flon Belt, Manitoba, Canada: Canadian Journal of Earth Sciences, v. 36, p. 1789-1805.

Bailes, A.H. and McRitchie, W.D., 1978, The transition from low to high grade metamorphism in the Kisseynew sedimentary gneiss belt, Manitoba: Geological Survey of Canada Paper 78-10, 155-178.

Barton, P.B., 1970, Sulfide Petrology: Mineralogical Society of America Special Paper 3, p. 187-198.

Bingen, B., and Stein, H.J., 2003, Molybdenite Re-Os dating of biotite dehydration melting in the Rogaland high-temperature granulites, S Norway: Earth and Planetary Science Letters, v. 208, p. 181-195.

Craig, J.R., Vokes, and Solberg, T.N., 1998, Pyrite: physical and chemical textures: Mineralium Deposita, v. 34, p. 82-101.

Creaser, R.A., Sannigrahi, P., Chacko, T., and Selby, D., 2002, Further evaluation of the Re-Os geochronometer in organic-rich sedimentary rocks: a test of hydrocarbon maturation effects in the Exshaw Formation, Western Canada Sedimentary Basin: Geochimica et Cosmochimica Acta, v. 66, p. 3441-3452.

David, J. and Syme, E.C., 1994, U-Pb geochronology of late Neoproterozoic tonalites in the Flin Flon belt, Trans-Hudson Orogen: surprise at surface: Canadian Journal of Earth Sciences, v. 31, p. 1785-1790.

David, J., Bailes, A.H., and Machado, N., 1996, Evolution of the Snow Lake portion of the Paleoproterozoic Flin Flon and Kisseynew belts, Trans-Hudson Orogen, Manitoba, Canada: Precambrian Research, v. 80, 107-124.

Franklin, J.M., Gibson, H.L., Jonasson, I.R., and Galley, A.G., 2005, Volcanic massive sulfide deposits, *in*: Hedenquist, J.W., Thompson, J.F.H., Goldfarb, R.J., and Richards, J.P., [eds.], *Economic Geology 100th Anniversary Volume*, Society of Economic Geologists, p. 523-560.

Froese, E. and Goetz, P.A., 1980, Geology of the Sherridon Group in the vicinity of Sherridon, Manitoba: Geological Survey of Canada Paper 80-21, 20p.

Gordon, T.M., 1989, Thermal evolution of the Kisseynew sedimentary gneiss belt, Manitoba: metamorphism at an early Proterozoic accretionary margin, *in*: Daly, J.S., Cliff, R.A., and Yardley, B.W.D. [eds.], *Evolution of Metamorphic Belts*, Geological Society Special Publication No. 43, p. 233-243.

Hannington, M.D., de Ronde, C.E.J., and Petersen, S., 2005, Sea-floor tectonics and submarine hydrothermal systems, *in*: Hedenquist, J.W., Thompson, J.F.H., Goldfarb, R.J., and Richards, J.P., [eds.], *Economic Geology 100th Anniversary Volume*, Society of Economic Geologists, p. 111-141.

Hoffman, P.F., United Plates of America, the birth of a craton: early Proterozoic assembly and growth of Laurentia: *Annual Reviews of Earth and Planetary Science*, v. 16, p. 543-603.

Ixer, R.A., 1990, Atlas of opaque and ore minerals in their associations. Van Nostrand Reinhold, New York, U.S.A., 208 p.

Ko, C.B., 1986, Geology of the Trout Lake copper-zinc sulfide deposit: Hudson Bay Mining and Smelting, Internal Report.

Kullerud, G. and Yoder, H.S., 1959, Pyrite stability in the Fe-S system: *Economic Geology*, v. 54, p. 533-572.

Lambert, D. D., Frick, L. R., Foster, J. G., Li, C., and Naldrett, A. J., 2000, Re-Os isotope systematics of the Voisey's Bay Ni-Cu-Co magmatic sulfide system, Labrador, Canada: II. Implications for parental magma chemistry, ore genesis, and metal redistribution: *Economic Geology*, v. 95, p. 867-888.

Levresse, G., Cheilletz, A., Gasquet, D., Reisberg, L., Deloule, E., Marty, B., and Kyser, K., 2004, Osmium, sulphur, and helium isotopic results from the giant Neoproterozoic epithermal Imiter silver deposit, Morocco: evidence for a mantle source: *Chemical Geology*, v. 207, p. 59-79.

Lucas, S.B., Stern, R.A., Syme, E.C., Zwanzig, H., Bailes, A.H., Ashton, K.E., Maxeiner, R.O., Ansdell, K.M., Lewry, J.F., Ryan, J.J., and Kraus, J., 1997, Tectonics of the southeastern Reindeer Zone, Trans-Hudson Orogen (Manitoba and Saskatchewan): Geological Association of Canada – Mineralogical Association of Canada, Annual Meeting, Program with Abstracts, 22, p. A93.

Lucas, S.B., Stern R., A., Syme, E.C., Reilly, B.A., and Thomas, D.J., 1996, Intraoceanic tectonics and the development of continental crust: 1.92 – 1.84 Ga evolution of the Flin Flon Belt, (Canada): *Geological Society of America Bulletin*, v. 108, p. 602-629.

Lusk, J., Scott, S.D., Bryndzia, L.T., and Ford, C.E., 1993, Phase relations in the Fe-Zn-S system to 5 kbar and temperatures between 325°C and 150°C: *Economic Geology*, v. 80, p. 1880-1903.

Machado, N., Zwanzig, H., and Parent, M., 1999, U-Pb ages of plutonism, sedimentation, and metamorphism of the Paleoproterozoic Kisseynew metasedimentary belt, Trans-Hudson Orogen (Manitoba, Canada): *Canadian Journal of Earth Sciences*, v. 36, p. 1843-1857.

Mathur, R., Ruiz, J., Titley, S., Gibbins, S., Margotomo, W., 2000, Different crustal sources for Au-rich and Au-poor ores of the Grasberg Cu-Au porphyry deposit: *Earth and Planetary Science Letters*, v. 183, p. 7-14.

Mathur, R., Ruiz, J., and Tornos, F., 1999, Age and sources of the ore at Tharsis and Rio Tinto, Iberian Pyrite Belt, from Re-Os isotopes: *Mineralium Deposita*, v. 34, p. 790-793.

Meisel, T., Walker, R.J., Irving, A.J., and Lorand, J., 2001, Osmium isotopic compositions of mantle xenoliths: a global perspective: *Geochimica et Cosmochimica Acta*, v. 65, p. 1311–1323.

Morelli, R.M., 2003, Evaluation of rhenium-osmium geochronology of pyrite, sphalerite, and arsenopyrite: examples from the Red Dog Zn-Pb-Ag deposit, Alaska, and the Meguma Group Gold Deposits, Nova Scotia: unpublished M.Sc. Thesis, University of Alberta, 78p.

Morelli, R.M., Creaser, R.A., Selby, D., Kontak, D.J., and Horne, R.J., 2005, Rhenium-osmium geochronology of arsenopyrite in Meguma Group gold deposits, Meguma Terrane, Nova Scotia, Canada; evidence for multiple gold-mineralizing events: *Economic Geology*, v. 100, p. 1229 – 1242.

Morelli, R.M., Creaser, R.A., Selby, D., Kelley, K.D., Leach, D.L., and King, A.R., 2004, Re-Os Sulfide Geochronology of the Red Dog Sediment-Hosted Zn-Pb-Ag Deposit, Brooks Range, Alaska, v. 99, p. 1569 – 1576.

Munhá, J., Relvas, J.M.R.S., Barriga, F.J.A.S., Conceição, P., Jorge, R.C.G.S., Mathur, R., Ruiz, J., and Tassinari, C.C.G., 2005, Osmium isotope systematics in the Iberian pyrite belt, *in*: Mao, J. and Bierlein, F.P. [eds.], *Mineral Deposit Research: 'Meeting the Global Challenge'*, Proceedings of the Eighth Biennial SGA Meeting, p.663-666.

Polito, P., Kyser, K., Lawie, D., Cook, S., and Oates, C., 2007, Application of sulphur isotopes to discriminate Cu-Zn VHMS mineralization from barren Fe sulphide mineralization in the greenschist to granulite facies Flin Flon-Snow Lake-Hargrave River region, Manitoba, Canada: *Geochemistry: Exploration, Environment, Analysis*, v. 7, p. 129-138.

Raith, J.G., and Stein, H.J., 2000, Re-Os dating and sulfur isotope composition of molybdenite from tungsten deposits in western Namaqualand, South Africa: Implications for ore genesis and the timing of metamorphism: *Mineralium Deposita*, v. 35, p. 741-735.

Rosenblum, S., Magnetic susceptibilities of minerals in the Frantz isodynamic magnetic separator: *The American Mineralogist*, v. 43, p. 170-173.

Schneider, D.A., Heizler, M.T., Bickford, M.E., Wortman, G.L., Condie, K.C., and Perilli, S., 2007, Timing constraints of orogeny and cratonization: Thermochronology of the Paleoproterozoic Trans-Hudson Orogen, Manitoba and Saskatchewan, Canada: *Precambrian Research*, v. 153, p. 65-95.

Sharma, M., Wasserburg, G.J., Hofmann, A.W., and Butterfield, D.A., 2000, Osmium isotopes in hydrothermal fluids from the Juan de Fuca Ridge: *Earth and Planetary Science Letters*, v. 179, p. 139-152.

Stauffer, M.R., 1984, Manikewan: an early Proterozoic ocean in central Canada, its igneous history and orogenic closure: *Precambrian Research*, v. 25, p. 257-281.

Stein, H.J., Scherstén, A., Hannah, J.L., and Markey, R.J., 2003, Subgrain scale decoupling of Re and ^{187}Os and assessment of laser ablation ICP-MS spot dating in molybdenite: *Geochimica et Cosmochimica Acta*, v. 67, p. 3673 – 3686.

Stein, H.J., Markey, R.J., Morgan, J.W., Hannah, J.L., and Scherstén, A., 2001, The remarkable Re-Os chronometer in molybdenite: how and why it works: *Terra Nova*, v. 13, p. 479 – 486.

Stein, H.J., Morgan, J.W., and Scherstén, A., 2000, Re-Os dating of low-level highly radiogenic (LLHR) sulfides: The Harnäs gold deposit, southwest Sweden, records continental-scale tectonic events: *Economic Geology and the Bulletin of the Society of Economic Geologists*, v. 95, p. 1657–1671.

Syme, E.C., Stern, R.A., Bailes, A.H., and Zwanzig, H.V., and Gilmore, K.V., 2001. Evolution of the Paleoproterozoic Flin Flon belt, Trans-Hudson Orogen, Manitoba: Geological Association of Canada – Mineralogical Association of Canada, Annual Meeting, Program with Abstracts, 26, p. 147.

Syme, E.C., Lucas, S.B., Bailes, A.H., and Stern, R.A., 1999, Contrasting arc and MORB-like assemblages in the Paleoproterozoic Flin Flon Belt, Manitoba, and the role of intra-arc extension in localizing volcanic-hosted massive sulphide deposits: *Canadian Journal of Earth Sciences*, v. 36, p. 1767-1788.

Syme, E.C., Lucas, S.B., Zwanzig, H.V., Bailes, A.H., Ashton, K.E., and Haidl, F.M., 1998, Geology, NATMAP Shield Margin Project Area, Flin Flon Belt, Manitoba/Saskatchewan, accompanying notes. Geological Survey of Canada, Map 1968A.

Tourigny, G., Gilmore, K., Howland, L., and Levers, J., 2002, Relationships between ore and overprinting structures at the Konuto Lake VMS deposit, Flin Flon Domain, *in*: Summary of Investigations 2002, Volume 2, Saskatchewan Geological Survey, Saskatchewan Industry and Resources, Miscellaneous Report 2002-4.2, CD-ROM, Paper B-5, 14p.

Vaughan, D.J. and Craig, J.R., 1997, Sulfide ore mineral stabilities, morphologies, and intergrowth textures, *in*: Barnes, H.L. [ed.], *Geochemistry of Hydrothermal Ore Deposits*, 3rd. Ed., John Wiley & Sons, Inc., U.S.A., p. 367-429.

Yang, K. and Scott, S.D., 2003, Geochemical relationships of felsic magmas to ore metals in massive sulfide deposits of the Bathurst Mining Camp, Iberian Pyrite Belt, and Hokuroko district and the Abitibi belt: *Economic Geology Monograph 11*, p. 457-478.

Zwanzig, H.V., 1999, Structure and stratigraphy of the south flank of the Kisseynew Domain in the Trans-Hudson Orogen, Manitoba: implications for 1.845-1.77 Ga collision tectonics: *Canadian Journal of Earth Sciences*, v. 36, p. 1859-1880.

Zwanzig, H.V. and Schledewitz, D.C.P., 1992, Geology of the Kississing-Batty Lakes area: interim report, Manitoba Energy and Mines, Geological Services, Open File report OF92-, 87 pp.

Chapter 6: Thesis Conclusions

The results of this thesis fall into three main categories: the applications limitations and implications of Re-Os low-level sulfide geochronology, as pertinent to hydrothermal ore deposit geology. The most important conclusions for each category are provided below.

Applications

A primary objective of this project was to determine the overall utility of the Re-Os low level sulfide dating technique, in terms of accuracy and precision, for dating important ore deposit types, specifically orogenic gold deposits (OGD) and volcanogenic massive sulfide (VMS) deposits. The choice of these two deposit types reflects their widespread presence in the rock record through much of geologic time and over a range of metamorphic grades, and for their economic significance as primary sources of their contained metals (Au, Cu, Zn, Pb, Ag).

In practical terms, much of the progress made in this study concerning the overall utility of this technique results from development and/or improvement of sampling and analytical protocols. Ideal sulfide samples for Re-Os dating are coarse-grained (> 0.5 cm) and monomineralic, and comprise only one paragenetic stage of the ore-forming event. Except for uncommon examples of very old sulfide minerals with high Re concentrations, individual samples for Re-Os isotopic analysis should be ~ 400 mg each. Extraction of the mineral from the host should be performed using only agate tools, as the use of metallic sampling tools may readily contaminate the natural Re and/or Os characteristics of the specimen. Low-level sulfide samples can vary widely in both Re (and hence $^{187}\text{Os}^*$) and common Os contents, and care must be taken to ensure that the sample is spiked with a solution of the appropriate Re-Os composition; unradiogenic samples require use of a $^{185}\text{Re} + ^{190}\text{Os}$ mixed spike, whereas a mixed double ($^{185}\text{Re} + ^{190}\text{Os} + ^{188}\text{Os}$) or mixed isotopically normal Os spike ($^{185}\text{Re} + \text{natural Os}$) is more appropriate for highly radiogenic samples with little or no common Os. To ensure complete equilibration between sample and spike Os, digestion must be performed in a glass Carius tube and, for high quality results, should be performed using ultrapure reagents (ideally, negligible Re, Os contents; sub-pg). Elemental separation and

purification of Re and Os is most efficiently accomplished through solvent extraction using CHCl_3 , followed by further purification of Re by anion exchange column chromatography using relatively fresh resin and single bead anion exchange, and further Os purification by two microdistillations using a $\text{CrO}_3\text{-H}_2\text{SO}_4$ mixture and HBr. The purified Re and Os fractions are deposited on ultralow-blank Ni and Pt wire filaments, respectively, for isotopic analysis using negative thermal ionization mass spectrometry. Precise isotopic analysis of the extremely low Os contents typical of low-level sulfide minerals during mass spectrometry is facilitated by a prolonged (~ 20 minute) warmup period until the first detection of Os emission, followed by a 20-30 minute period at the same temperature. Error propagation must account for all potential sources of analytical error, and, for highly radiogenic samples, must include an error correlation function to account for the typically imprecise measurement of predominately blank ^{188}Os , as this isotope is used as a denominator on both axes of a conventional $^{187}\text{Re}/^{188}\text{Os}$ vs. $^{187}\text{Os}/^{188}\text{Os}$ isochron diagram.

Using these improved protocols, several new Model 1 Re-Os sulfide ages have been determined for OGD and VMS deposits which range from Late Archean to Late Paleozoic in age, and are accurate within existing mineralization age brackets based on other chronometers. The oldest material successfully dated herein is pyrite from the Late Archean Con gold deposit, located in the Slave Province of northern Canada, which yielded a Re-Os age of 2591 ± 37 Ma (MSWD = 1.3, $\text{Os}_i = 0.78 \pm 0.17$). Primary mineralization ages were also successfully determined for pyrite from Paleoproterozoic VMS deposits in the northern Trans-Hudson Orogen in Manitoba, Canada. This includes pyrite from the Trout Lake deposit, Flin Flon Domain, which yielded a Re-Os age of 1892 ± 28 Ma (MSWD = 0.97, $\text{Os}_i = 0.32 \pm 0.10$) and from the Sherritt Gordon deposit, Kiseynew Domain, which yielded an age of 1856 ± 9 Ma (MSWD = 1.3, $\text{Os}_i = 0.48 \pm 0.03$). Arsenopyrite from the Paleoproterozoic Homestake gold deposit, southern Trans-Hudson Orogen, USA, likewise yielded a precise Re-Os age of 1736 ± 8 Ma (MSWD = 1.6, $\text{Os}_i = 0.28 \pm 0.15$). Three arsenopyrite samples from the Muruntau gold deposit, Southern Tien Shan Orogen, Uzbekistan, were the youngest materials to be successfully dated in this study. Re-Os isotopic analyses of two of these samples combine to give a gold mineralization age of 287.5 ± 1.7 Ma (MSWD = 0.98, $\text{Os}_i = 0.37 \pm 0.27$), whereas,

statistically, the third gave a slightly different result of 296.4 ± 6.1 Ma (MSWD = 1.5, $\text{Os}_i = 0.07 \pm 0.59$).

Collectively, these results demonstrate that, using careful sampling, analytical, and data reduction protocols, the Re-Os pyrite and arsenopyrite chronometers can be extremely valuable chronometers of ore mineralization events, capable of generating accurate and reasonably precise (< 1.5%) mineralization ages.

Limitations:

There are several instances in this study in which Re-Os low-level sulfide chronometers were unable to generate meaningful mineralization ages. Nevertheless, crucial new information regarding the overall utility of the technique was gained in such cases.

The most obvious limitation of the technique is the ^{187}Re content of the studied sulfide mineral, since this also dictates its $^{187}\text{Os}^*$ content. Conservatively, it is here estimated that, for a 400 mg sample, 1.5 pg of $^{187}\text{Os}^*$ is required to obtain an Os signal strong enough to produce a sufficiently precise Os isotopic analysis during mass spectrometry at the University of Alberta Radiogenic Isotope Facility. Despite apparently lower overall Re contents of sulfides from Archean OGD and VMS deposits relative to post-Archean examples, the antiquity of these minerals makes their average Re content sufficiently high to surpass the 1.5 pg $^{187}\text{Os}^*$ threshold. In contrast, although post-Archean sulfides carry nominally higher average Re contents than Archean sulfides, some of those below the average are unsuitable for Re-Os dating because the decay time has been inadequate to generate a sufficient amount of $^{187}\text{Os}^*$ (e.g. pyrite from the ca. 285 Ma Kumtor gold deposit). Thus, Re concentration seems to be a primary limiting factor primarily for sulfide minerals from younger (Phanerozoic) deposits.

Analytical issues can, in some circumstances, be a source of disparity between determined Re-Os sulfide ages and true mineralization ages. This is likely shown in the Re-Os results for sulfides from the Late Archean Red Lake (Uchi Subprovince, Ontario) and Golden Mile (Eastern Goldfields, Western Australia) gold deposits. Arsenopyrite and gersdorffite from Red Lake yield a highly imprecise Re-Os 'age' that is older than the accepted mineralization age by > 200 m.y. and overlaps with the age of the host rock.

This is interpreted to reflect the very fine-grained nature of the analyzed sulfides, and a consequent inability to sufficiently isolate sulfides from a single paragenetic stage during mineral separation. This example highlights the need for isolation of pure, single generation sulfide mineral separates for Re-Os dating, and demonstrates the advantage of coarse-grained samples for this purpose. In contrast, arsenopyrite from Golden Mile yields an imprecise age, nominally younger than that of the known timing of gold mineralization. This discrepancy is interpreted to derive from the utilization of a single Os isotope spike with this arsenopyrite, which has a very low Re (and $^{187}\text{Os}^*$) content, but a radiogenic Os isotopic composition due to its lack of common Os. It is thus recommended that, for very low concentration, radiogenic sulfides, a dilute, well-calibrated, double Os isotopic or isotopically normal Os spike be developed, calibrated directly, and used for isotopic analysis.

Unreliable Re-Os sulfide mineral chronometers are identified in this study by deviation of the derived result from the actual mineralization age, as defined by various other geochronologic techniques. In addition to the examples of Red Lake and Golden Mile mentioned above, spurious ages were also shown to result from Re-Os isotopic analysis of pyrrhotite from the Homestake OGD, southern Trans-Hudson Orogen; of sphalerite from the Trout Lake deposit and chalcopyrite from the Konuto Lake VMS deposit, Flin Flon Assemblage, Flin Domain; and of pyrite from the Harmin VMS deposit, Snow Lake Assemblage, Flin Flon Domain. Together with existing information on the thermal histories of the respective host terranes, these results can be used to constrain the apparent closure/blocking temperature of the sulfide chronometers. Consistent with previous natural and experimental studies, pyrrhotite is determined here to be a poor choice for Re-Os geochronology of primary mineralization events. Based on similarities between the Re-Os pyrrhotite results and disturbed Ar-Ar ages from mica hosted in Homestake veins, the maximum Re-Os pyrrhotite closure temperature is inferred to be $< 350^\circ\text{C}$. Despite its refractory nature, sphalerite is also a readily disturbed Re-Os chronometer, with a proposed closure temperature below that of the ca. 450°C peak metamorphic temperature that affected the Trout Lake deposit. Analyses of chalcopyrite from Konuto Lake also provide sufficient evidence to suggest that this mineral is disturbed by ambient temperatures of $< 500^\circ\text{C}$. In contrast, arsenopyrite and

pyrite have been shown to be extremely robust Re-Os chronometers, probably characterized by apparent closure temperatures of $> 450^{\circ}\text{C}$ and $> 675^{\circ}\text{C}$, respectively. These results suggest that the chemical breakdown of the mineral itself might be required to disturb pyrite and arsenopyrite Re-Os geochronometers.

Implications:

Although developmental in nature, this study has nonetheless produced new data that hold important implications for the individual ore deposits studied, the metallogenic histories of the host terranes, and the origin of OGD and VMS deposits generally. In this respect, the most important conclusions from the new Re-Os sulfide ages and Os_i are as follows:

- gold mineralization in the Yellowknife Greenstone Belt was, in part, simultaneous with emplacement of the Prosperous granitoid suite at ca. 2695 Ma, though the uncertainty in the determined Re-Os age allows for a possible temporal association of gold mineralization with a range of geologic events. Initial Os isotopic compositions of pyrite from the Con deposit are consistent with proposals invoking metal derivation from the Burwash Fm turbidite suite (the presumed source of the Prosperous granites), but not as clearly with a model calling for remobilization of ca. 2680 Ma ore.
- emplacement of gold at the Homestake deposit was likely a metamorphic process, and is shown to predate regional granitoid magmatism by 20 - 50 m.y. Osmium in the ore system has an unradiogenic isotopic composition and likely derives, in part, from mantle fluids and/or melts, or very juvenile crust. The new Re-Os data can be used to refute the “remobilized sedimentary” model for the origin of Homestake gold
- the Muruntau gold deposit formed simultaneously with the emplacement of proximal granitoid intrusions at ca. 287 – 295 Ma, and could be the end product of a protracted hydrothermal event consisting of multiple fluxes of mineralizing fluid. Unradiogenic initial Os isotopic compositions of ore-related arsenopyrite and He isotopic compositions of arsenopyrite-hosted fluid inclusions suggest a mantle-derived fluid and metal component to the mineralizing system, possibly related to the generation or exsolution of granitoid or lamprophyric magmas.

- if forced into an all-encompassing model that satisfies these, and previously reported Re-Os and He isotopic data, as well as other geochemical data from OGD, the formation of these deposits globally and through geologic time must originate from a geochemically primitive source. This signature could then sometimes be masked by interaction with crustal rocks during transport of ore metals and fluids to the depositional site. Alternatively, the orogenic gold classification might actually represent a group of deposits that form as a result of different geologic processes, but that are ultimately manifested in the rock record in a similar way.
- Re-Os molybdenite analyses indicate that emplacement of the Kal'makyr porphyry Au-Cu deposit, Uzbekistan, occurred contemporaneously with magmatism in the host Valerianov-Beltau-Kurama arc at 314.0 ± 2.2 Ma. However, one anomalously older Re-Os molybdenite age of ca. 467 Ma might indicate the presence of a relict mineralization event that was largely overprinted by the 314 Ma event.
- although VMS deposits in the Flin Flon Domain were formed during rifting of island arcs between ~ 1910 and 1880 Ma, a later (ca. 1855 Ma) VMS mineralization event in the Kisseynew Domain is now potentially recognized, possibly related to magmatism associated with the earliest stages of Kisseynew backarc/interarc basin opening. Initial Os isotopic compositions of pyrite from VMS deposits in both the Flin Flon and Kisseynew Domains demand input from some isotopically evolved, crustal source during mineralization.

Concluding Remarks:

Regarding Re-Os geochronology, it has been said that, “if it was easy, then everyone would be doing it” (R. Creaser, pers. comm., 2001 – 2006, repeatedly). The validity of this statement has become more apparent to me with each passing day over the past six years. I have come to recognize that the difficulty in dealing with this system is not so much the generation of data, but the attention to detail required in all facets of sampling and analysis to generate meaningful geologic data. Looking back on the work presented in this thesis, I feel that its most important contribution is the recognition that when used properly, the Re-Os low-level sulfide chronometer is capable of producing quality results that are critical for ore deposit research, but that are not currently

obtainable through any other geochemical technique. I also contend that the importance of this technique, especially for ore deposit studies, is just beginning to be realized. As more and more 'good' Re-Os sulfide data are collected over time, my prediction is that this technique will become a staple of mineral deposit research and exploration, and that it will significantly improve our understanding of ore deposit generation in the context of plate tectonic processes.

Appendix 1: Thesis Collection List

Sample	Deposit/ Rock Type	Location	Mineral of Interest	Origin/Comment
DC-10, CO-2, U3, U4	Red Lake OGD	Ontario	apy (±gdf ±gold)	DC = drill core; CO = Cochenour stripped outcrop; U = Red Lake mine
109726	Golden Mile OGD	Australia	apy (+sch)	Univ. Western Australia museum specimen (A. Mueller PhD collection)
C-1 to -7 (vials)	Con OGD		py	waste rock pile near Con mine portal
HMO20	Homestake OGD	South Dakota	apy, po	ore ledge 15, 7400 level, Homestake Mine (C. Bell thesis collection)
HM82	Homestake OGD	South Dakota	apy, po	Homestake Mine, exact derivation unknown (C. Bell thesis collection)
SD-9	Harney Peak granite	South Dakota	mnz	aplitic dyke, roadside o/c along Hwy 87
K-1 to -4 (vials)	Kal'makyr porphyry	Uzbekistan	moly	various locations from veinlets in ore-related intrusions (see Table 4.2.1)
MN9824	Muruntau OGD	Uzbekistan	apy	open pit - Ore Body 1
MN18	Muruntau OGD	Uzbekistan	apy	open pit - Southern Fault Zone
MN20A	Muruntau OGD	Uzbekistan	apy	open pit - Southern Fault Zone
942	Konuto VMS	Manitoba	cpy (±sph, py)	HBMC drill hole J15942
943	Trout Lake VMS	Manitoba	py (±sph)	HBMC drill hole J15943
945	Harmin VMS	Manitoba	py (±po)	HBMC drill hole J15945
SG	Sherritt Gordon VMS	Manitoba	py	Royal Ontario Museum specimen #M19674

Also: miscellaneous sulfide samples (labelled vials) from various deposits worldwide; used for Re tests

¹OGD = orogenic gold deposit; VMS = volcanogenic massive sulfide deposit

²apy = arsenopyrite; cpy = chalcopyrite; gdf = gersdorffite; mnz = monazite; moly = molybdenite; po = pyrrhotite; py = pyrite; sch = scheelite; sph = sphalerite